UNIVERSITAT DE BARCELONA

Biomarkers and therapeutic targets based on bacterial “Quorum Sensing” system

Bárbara Rodriguez Urretavizcaya

UNIVERSITAT DE BARCELONA
FACULTAT DE FARMÀCIA I CIÈNCIES DE L'ALIMENTACIÓ

Biomarkers and therapeutic targets based on bacterial "Quorum Sensing" system

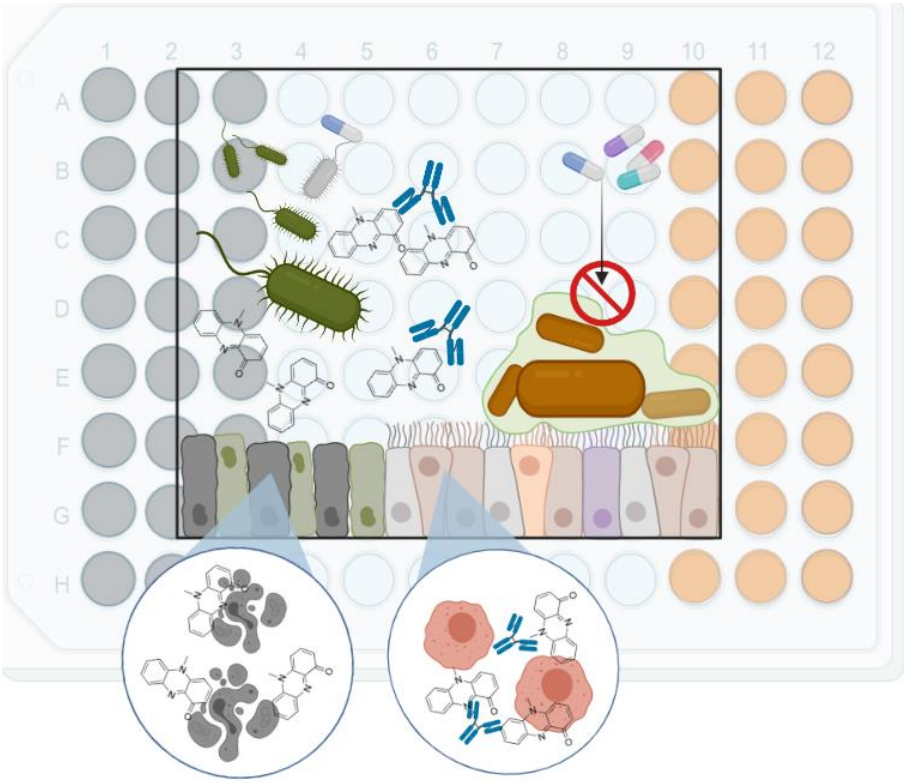

Supervisors:
Prof. Mª Pilar Marco Colás
Dr. Lluïsa Vilaplana Holgado

Bárbara Rodriguez Urretavizcaya

January 2022

UNIVERSITAT DE BARCELONA
Facultat de Farmàcia
i Ciències de l'Alimentació

Doctoral program: BIOTECHNOLOGY (HDK06)
Research line: biomedicine

BIOMARKERS AND THERAPEUTIC TARGETS BASED ON BACTERIAL "QUORUM SENSING" SYSTEM

"Dissertation presented by Bárbara Rodriguez Urretavizcaya in fulfillment of the requirements for the degree of doctor by Universitat de Barcelona"

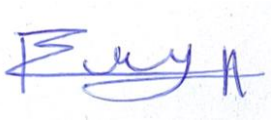

Bárbara Rodriguez Urretavizcaya

Supervisors:

Prof. Mª Pilar Marco Colás
(Dept. de Surfactantes y Nanobiotecnología Nb4D group, IQAC-CSIC)

Dr. Lluïsa Vilaplana Holgado
(Dept. de Surfactantes y Nanobiotecnología Nb4D group, IQAC-CSIC)

Tutor:

Dr. Laura Baldomà Llavinés
(Universidad de Barcelona)

January 2022

Agradecimientos

En primer lugar, quisiera empezar por agradecer a mis dos directoras de tesis Mª Pilar Marco y Lluïsa Vilaplana por haberme brindado la oportunidad de realizar esta tesis con ellas. Gracias por haberme guiado y ayudado a crecer a nivel científico. Gracias por haberme escuchado y haber tenido en cuenta mi opinión cuando teníamos discusiones científicas. Gracias. Y, sobre todo gracias por vuestra calidad humana para conmigo. Por haberme apoyado a lo largo de estos cuatro años tan intensos que me han tocado vivir. Gracias por haberme escuchado y aconsejado en todo momento. Siempre os estaré agradecida. Sin vosotras nada de esto hubiera sido posible.

En segundo lugar, me gustaría agradecer a todas las personas del grupo Nb4D por haber compartido su tiempo conmigo tanto para discutir cuestiones científicas como para reírnos del mundo. Gracias. Y por supuesto, quisiera hacer especial mención a aquellas personas con las que más tiempo he compartido. A mi rata de laboratorio David. Gracias por esas charlas interminables acompañadas de un buen cofins, gracias por los momentos "cocos locos" en el gym, gracias por haber reído y llorado conmigo, por haberme escuchado en todo momento… pero, sobre todo, gracias por haberme dejado conocerte. A mi querida Monsis por la ayuda científica y por el apoyo incondicional que me ha dado... A Juan y a Carla tanto por la ayuda científica como por las risas que nos hemos echado... Y a Julián por su buen rollo contagioso.

Por otro lado, quisiera agradecer a mis aitas por su apoyo tanto a nivel personal como profesional. Gracias aita por las clases de estadística y los skypes a cualquier hora del día, y gracias ama por las "masters class de Word" que me has dado. Y, claro está, gracias por haber estado los dos siempre ahí para ayudarme en todo. Porque sí, pase lo que pase, la familia siempre está ahí.

Y, finalmente, me gustaría dar las gracias a todas aquellas personas que me han apoyado a nivel emocional y, por supuesto, han tenido repercusión en esta tesis. Gracias a mi abueliska por esas llamadas interminables que solo ella y yo sabemos, por escucharme y estar siempre pendiente de mí. Gracias a mi niña por haberme apoyado siempre a pesar de la distancia… con ella las risas

están siempre aseguradas... Gracias también a mi Bb por haberme impulsado en esta última etapa de la tesis con su energía, sus risas y sus gritos. Y, como no, gracias a todos mis amig@s más cercanos por sacarme siempre una sonrisa, en especial, a mis niños gato y gorostidi.

Abstract

Infectious diseases are still one of the main leading causes of death worldwide mainly due the overuse and the lack of development of new antibiotics. This fact has increased the appearance of multidrug resistance (MDR) bacteria strains resulting in a growing number of infections difficult to treat with conventional drugs. In this context, *Pseudomonas aeruginosa* gram negative bacterium presents great interest since it is a MDR bacterium causing a high number of infections, especially nosocomial infections. Moreover, it is one of the most predominant pathogen in patients with cystic fibrosis. Usually, *P. aeruginosa* infections can be categorized as acute and chronic, but this classification is not always obvious. Acute infections are frequent during early stages of infection and associated with a planktonic lifestyle and with high levels of virulence factors (VFs) production. In contrast, chronic infections are characterized by a lower VF production and the formation of biofilms and persiter cells, which confer high resistance to antibiotics. The development of pathogenesis and the transition between acute and chronic infections are regulated by a bacterial communication system called Quorum Sensing (QS), which controls the expression of a myriad of genes in response to the presence of small signal molecules called autoinducers. In consequence, QS has attracted attention as a promising target to develop diagnostic and therapeutic approaches.

Although being a time-consuming technique, which delays treatment administration with the consequences that this entails, the gold standard technique used for *P. aeruginosa* detection is still based on plate culture. Thus, there is a clear need to obtain rapid and sensitive diagnostic techniques. Within this framework, a highly sensitive, specific and rapid immunochemical assay has been developed to detect one of the main VF of *P. aeruginosa*, pyocyanin (PYO), in less than 2 h using a high affinity monoclonal antibody (mAb) against it. The low limit of detection of the assay has allowed PYO detection in bacterial isolates from patients infected with *P. aeruginosa* and its validation as potential biomarker of these infections. In the light of the obtained results, further investigations have been assessed on analysing directly clinical samples, such as sputa and swab samples from patients infected with this pathogen. Furthermore, based on QS system and on the use of specific mAbs against key molecules of this system, a new therapeutical approach to treat *P. aeruginosa* infections has been studied. In this context, the quenching

activity of PYOmAb has been assessed using a developed cell based *in vitro* system. First, the cytotoxic effect caused by PYO has been evaluated on murine macrophages studying different hallmarks of viability since this VF is known to exert a large number of toxic effects in host cells. Subsequently, the protective effect of PYOmAb on the same cell line has been analysed obtaining a high increase of viability percentages (50 - 80 %). Apart from studying an effector molecule, the quenching of a signalling molecule, such as Pseudomonas Quinolone Signal (PQS), has been also adressed using the same *in vitro* system. In this case, the protection levels obtained have been even better reaching 80 - 100 % viability levels. Thus, the obtaines results has demonstrated the potential of these mAbs as therapeutic agents.

Resumen

Las enfermedades infecciosas siguen siendo una de las principales causas de muerte en todo el mundo debido principalmente al uso excesivo y la falta de desarrollo de nuevos antibióticos. Este hecho ha incrementado la aparición de cepas bacterianas resistentes a múltiples fármacos (multiresistentes), lo que ha dado lugar a un número creciente de infecciones difíciles de tratar con fármacos convencionales. En este contexto, la bacteria gram negativa *Pseudomonas aeruginosa* presenta gran interés al tratarse de un patógeno multiresitente causante de un elevado número de infecciones, especialmente infecciones nosocomiales. Además, es una de las bacterias más predominantes en pacientes con fibrosis quística. Por lo general, las infecciones por *P. aeruginosa* pueden clasificarse en agudas y crónicas, pero esta clasificación no siempre es obvia. Las infecciones agudas son frecuentes durante las primeras etapas de la infección y se asocian con un estilo de vida planctónico y con altos niveles de producción de factores de virulencia (FV). Por el contrario, las infecciones crónicas se caracterizan por una menor producción de FV y por la formación de biopelículas y células persitentes que confieren una alta resistencia a los antibióticos. El desarrollo de la infección y la transición entre infecciones agudas y crónicas están regulados por un sistema de comunicación bacteriano llamado sistema *Quorum Sensing* (QS), el cual controla la expresión genética en respuesta a la presencia de pequeñas moléculas señalizadoras llamadas autoinductores. Por ello, el sistema QS suscita gran interés en el desarrollo de herramientas tanto de diagnostico como de terapia.

A pesar de tratarse de una técnica larga que retrasa la administración del tratamiento con las consecuencias que esto conlleva, el cultivo en placa sigue siendo la técnica por excelencia utilizada para la detección de *P. aeruginosa*. Por esta razón, existe una clara necesidad de obtener técnicas de diagnóstico rápidas y sensibles. En este contexto, se ha desarrollado un ensayo inmunoquímico de alta sensibilidad, especificidad y rapidez para detectar uno de los principales FV de *P. aeruginosa*, la piocianina (PYO), en menos de 2 h utilizando un anticuerpo monoclonal (mAb). El bajo límite de detección del ensayo ha permitido la detección de PYO en aislados bacterianos de pacientes infectados con *P. aeruginosa* y su validación como potencial biomarcador de este tipo de infecciones. A la luz de los resultados obtenidos, se llevaron a cabo experimentos analizando directamente muestras clínicas como esputos e hisopos de pacientes infectados con este patógeno. Además, basándonos en el sistema QS y en el uso de mAbs

específicos contra moléculas clave de este sistema, se ha estudiado un nuevo enfoque terapéutico para tratar las infecciones causadas por *P. aeruginosa*. Así pues, la capacidad protectora del mAbPYO se evaluó utilizando un sistema *in vitro* basado en cultivo celular. Primero, se estudio el efecto citotóxico de la PYO en macrófagos murinos estudiando diferentes características de viabilidad debido a la gran cantidad de efectos tóxicos que ejerce este FV en las células huésped. Posteriormente, se ha analizado el efecto protector del mAbPYO sobre la misma línea celular obteniendo elevados porcentajes de viabilidad (50 - 80 %). Además de estudiar una molécula efectora, también se ha abordado el bloqueo de una molécula de señalización como la *Pseudomonas Quinolone Signal* (PQS) utilizando el mismo sistema *in vitro*. En este caso, los niveles de protección obtenidos han sido aún mejores alcanzando niveles de viabilidad del 80 - 100 %. Por lo tanto, los resultados obtenidos han demostrado el potencial de estos mAbs como agentes terapéuticos.

Abbreviations

β-GlcNAc-WTA	β-N-acetylglucosamine cell-wall teichoic acid
1-OHphz	1-hydroxiphenazine
2-AA	2'-aminoacetophenone
2D	bidimensional
2-HABA	2'-hydroxylaminobenzoylacetate
3oxoC_{12}-HSL	N-(3-oxododecanoyl)-L-homoserine lactone
AA	anthranilic acid
Ab	antibody
AB	AlamarBlue
ABA	aminobenzoylacetyl
AcoA	acetyl coenzyme A
ACP	acyl carrier protein
AE	active ester
Agr	accesory gene regulator
AHLs	acylated homoserine lactones
AI	autoinducer
AIE	antibiotic-inactivating enzymes
AiiA	autoinducer inactivation A
AiiK	AI inactivation from Kurthia huakui
AIP	autoinducer peptide
AM	acetoxymethyl
A_{max}	maximum absorbance
AMP	anthranilyl-adenosine monophosphate
AMR	antimicrobial resistance
AMS	anthranilyl-adeonsine-5'-O-monosulfamate
AMSN	sulfamide anthranilyl-5'-(aminodeoxy)adenosine-5'-N-monosulfamide
AQNO	alkylquinolones N-oxides
AQs	alkylquinolones
As	antiserum
ATP	adenosine triphosphate
BAL	bronchoalveolar lavage
BB	2-benzamidobenzoic acids
BM-DCs	bone marrow-derived dendritic cells
BSA	bovine serum albumin
BTK	Bruton's tyrosine kinase inhibitor
C_4-HSL	N-butyryl-L-homoserine lactone
Ca	calcein

CAR	chimeric antigen receptor
CF	Cystic fibrosis
cftr	Cystic fibrosis transmembrane conductance regulator
CFUs	colony forming units
Cif	Cystic fibrosis transmembrane conductance regulator inhibitory factor
CMV	Cytomegalovirus
CoA/CoASH	Coenzyme A
COPD	chronic obstructive pulmonary disease
CRS	cytokine-release syndrome
DCC	dicyclohexylcarbodiimide
DHQ	dihydroxyquinoline
DMEM	Dulbecco's Modified Eagle Medium
DMF	N,N-dimethylformamide
DMSO	dimethylsulfoxide
DPD	phenyl-4,5-dihydroxy-2,3-pentanedione
DTT	dithiothreitol
eDNA	extracellular DNA
ELISA	Enzyme-linked immunosorbent assay
ENR	enoyl-acyl carrier protein reductase
EPS	exopolysaccharides
ER	endoplasmic reticulum
ESKAPE	*Enterococcus faecium, Staphylococcus aureus, Klebsiella pneumoniae, Acinetobacter baumannii, Pseudomonas aeruginosa, and Enterobacter species*
FabH	β-ketoacyl-ACP synthase
FabI	enoyl-(acyl-carrier-protein) reductase
FBS	fetal bovine serum
FDA	Food and Drug Administration
FEDER	Fondo Europeo de Desarrollo Regional
FRET	Fluorescence Resonance Energy Transfer
H_2O_2	hydrogen peroxide
H_2SO_4	sulfuric acid
HAP	hospital-acquired pneumonia
HAQ	4-hydroxy-2-alkylquinoline
HAT	hypoxanthine-aminopterin-thymidine
HCAP	health care-associated pneumonia
HCH	Horseshoe-Crab Hemocyanin
HFCS	Hybridoma Fusion and Cloning Supplement
HHQ	2-heptyl-4-quinolone
Hod	2,4-dioxygenase
HPLC	High Performance Liquid Chromatography
HQNO	2-heptyl-4-hydroxyquinoline N-oxide
HRP	Horse Radish Peroxidise
HT	HAT medium without aminopterine
Htbe	primary tracheobronchial epithelial

HTS	hypertonic saline
HUVH	Hospital Universitari Vall d'Hebron
IC_{50}	half maximal inhibitory concentration
IL	interleukin
IM	inner membrane
IQS	integrated quorum sensing
IRequiv	immunoreactivity equivalents
LD_{50}	median lethal dosis
LoD	limit of detection
LPS	lipopolysaccharides
MA	Maleic acid
mAb	monoclonal antibody
MALDI	Matrix-Assisted Laser Desorption/Ionization
mBTL	meta-bromo thiolactone
MCoA	malonyl CoA
MC-ValCit-PABQ	maleimide and caproic acid-valine citrulline- p-aminobenzyl quaternary ammonium salt
MDR	multi-drug resistant
MH	Müeller Hinton
MH-S	Murine alveolar macrophages
MICIU	Ministerio de Ciencia, Innovación y Universidades
MINECO	Ministerio de Economía y Competitividad
MNP	magnetic nanoparticle
MS	Mass spectroscopy
MTT	3-(4,5-dimethylthiazol-2-yl)-2,5-diphenyltetrazolium bromide
n.d.	non detectable
n.s.	non significant
NAC	N-acetyl-L-cysteine
NADP/H	nicotinamide adenine dinucleotide phosphate
Nb	nanobody
NCFB	non–cystic fibrosis borchiectasis
NG	nanograss
NHBE	normal human epithelial cells
NP	nanoparticle
OD (600)	optical density at λ=600nm
OM	outer membrane
OMV	outer membrane vesicle
PAAI	*P. aeruginosa* acute infection
pAb	policlonal antibody
PACI	*P. aeruginos*a chronic infection
PASP	*P. aeruginos*a sputum
PASW	*P. aeruginos*a swab
PBS	Phosphate Buffered Saline solution
PBST	Phosphate Buffered Saline Tween-20 solution
PCA	phenazine-1-carboxylic acid

PCL	Pyochelin
PcvR	*P. aeruginosa* V-antigen
PI	propidium iodide
PoC	Point-of-Care
PQS	Pseudomonas quinolone signal
PVD	Pyoverdine
PYO	Pyocyanin
QQ	quorum quenchers
QS	Quorum Sensing
QSI	Quorum Sensing inhibitor
R^2	correlation coefficient
RNA	ribonucleic acid
ROS	Reactive Oxygen Species
RPMI	Roswell Park Memorial Institute Medium
RT	room temperature
rtPCR	Real time polymerase chain reaction
SAM	S-adenosyl methionine
SDR	short chain dehydrogenase/reductase
SERS	urface-Enhanced Raman Spectroscopy
SPR	surface plasmon resonance
sRNAs	small noncoding ribonucleic acids
SS	secretory system
STRC	Streptomycin
Tac	toxin-antitoxin-chaperone
T-CUAs	transparent carbon ultramicroelectrod arrays
TMB	3,3',5,5'- tetramethylbenzidine
TNF-α	Tumor Necrosis Factor alpha
TOF	time of fligth
UV-vis	ultraviolet-visible
VAP	ventilator-associated pneumonia
VF	virulence factor
VHUH	Vall d'Hebron University Hospital
WT	wild type
XTT	2,3-bis-(2-methoxy-4-nitro-5-sulfophenyl)-2H-tetrazolium-5-carboxanilide

Table of contents

Chapter 1

General introduction

The global impact of infectious diseases lies on two aspects that are explained in this chapter: the lack of rapid and sensitive diagnostic tools and the lack of new therapeutic methods due to the increase in antimicrobial resistance (AMR). In this sense, a special emphasis on *Pseudomonas aeruginosa* infections and impact is made. Furthermore, *P. aeruginosa* adaptability and its huge virulence factor (VF) arsenal will be analysed. In this sense, the reader will be introduced to some concepts used in this work, namely Quorum Sensing (QS) system, biofilm formation and pyocyanin (PYO), which is the main VF of *P. aeruginosa*. The chapter will conclude with the latest diagnostic tools used for detecting PYO, its levels found in clinical isolates and the necessity of developing new strategies.

1.1 Infectious diseases

Respiratory infections are among the three main leading causes of death worldwide together with Ischaemic hear disease and stroke, which are responsible for approximately 16 and 11 % of total deaths, respectively[1]. In 2019, chronic obstructive pulmonary disease (COPD), which refers to a group of pulmonary diseases that cause airflow blockage and breathing-related problems such as bronchitis, and lower respiratory infections accounted for a total of 3.23 and 2.49 million deaths[1-2], respectively. Furthermore, other respiratory infections such as tuberculosis and whooping cough (pertussis) triggered other 1.5 million (2020)[3-4] and 117000 (2019)[5] deaths worldwide. In the same line, 14 % of all deaths in children under 5 years were caused by pneumonia, resulting in more than 700,000 deaths[6]. In fact, the number of infectious disease outbreaks has increased significantly over the past 30 years and this scenario is unlikely to change due to the increase in global trade and travel, the population ageing and, specially, the increase in antimicrobial resistance (AMR)[7].

1.2 Antibiotic resistance troublesome appearance

The introduction of antibiotics more than 100 years ago to treat infectious diseases has drastically changed modern medicine being one of the most important medical breakthroughs of the 20th century[8-9]. However, antibiotic resistance genes have existed since ancient times in response to the presence of naturally occuring antibioics[10], thus its use is inevitably followed by resistance[11]. In addition, since the discovery of peniciline in 1928, a gradual decline of the duration of antibiotic effectiveness has been observed mainly as a consequence of the overuse and misuse of broad spectrum antibiotics[8]. In fact, more than 2 million people suffer multi-drug resistant (MDR) infections[12] and more than 700,000 people die by these infections worldwide anually[13]. Moreover, this number could rise to more than 10 million by 2050 if the problem is not addressed[7].

In a similar vein, in the last 30 years, no new antibiotics have been developed, being nearly all available antibiotics, variations of drugs discovered decades ago[14]. The lack of return in investment and the fact that antibiotics typically are short term treatments have been the main reasons for pharmaceutical companies to decline efforts in this direction[15]. In consequence, MDR microorganisms have emerged as a worldwide public health problem.

1.3 *Pseudomonas aeruginosa*

Pseudomonas aeruginosa is a rod-shape gram negative opportunistic bacterium that causes a wide variety of infections in both animals and human due to its high adaptability to diverse natural environments and its metabolic versatility[16]. This pathogen colonizes different parts of the body such as the skin, heart, urinary tract, ears, eyes, airways and lung tissues, causing urinary infections, burn infections, respiratory infections and septicemia[17-18]. Furthermore, it is associated with compromised host defences, which includes patients with diabetes, cancer, severe burns, organ transplants or other immunodeficiencies[19]. In the same context, *P. aeruginosa* is a MDR bacterium which uses different resistance mechanisms to counteract nearly all availabe antibiotics, such as β-lactams, aminoglycosides and quinolones[20-21]. These resistance mechanisms can be grouped as follows (see Figure 1. 1):

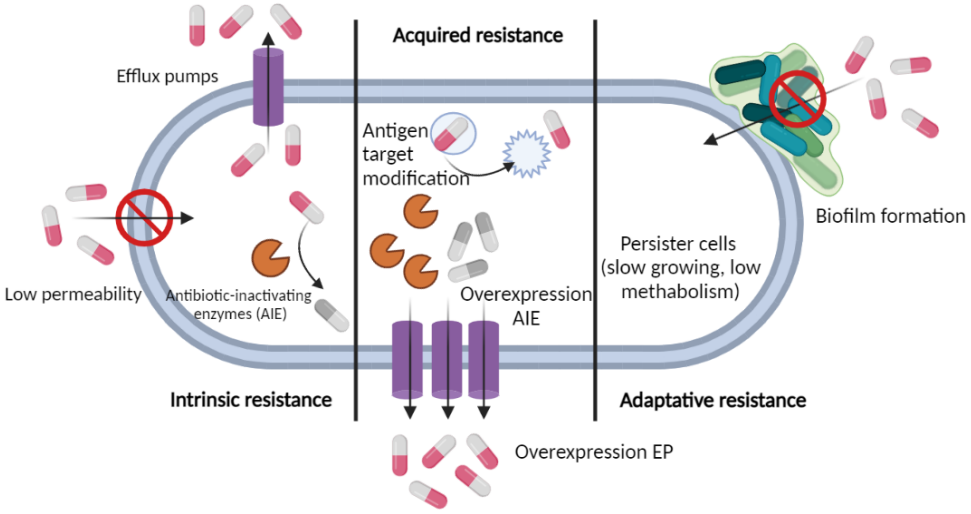

Figure 1. 1 *Antibiotic resistance mechanisms in P. aeruginosa bacterium*.

- Intrinsic resistance: includes low membrane permeability[20], increasing expression of efflux pumps that expel antibiotic outside the cell[22] and the expression of antibiotic-inactivating enzymes (AIE)[23].
- Acquired resistance: can be achieved via mutations in chromosomal genes or horizontal gene transfer of chromosomes or plasmids[20]. This resistance can result in the attenuation of antibiotic activity by post translational modifications of antibiotic target molecules that lead to conformational changes and in an ineffective target binding.
- Adaptative resistance: is a non-mutational resistance based on the formation of persister cells (slow growing and low metabolisms bacteria) and biofilms, especially as a consequence of the use of subinhibitory concentrations of antibiotics[16]. Biofilms are complex bacteria aggregates embedded in a matrix of extracellular polymeric

substances that functions as scaffold to protect bacteria against different environmental stresses, conferring the capacity for colonization and long-term persistence[24].

1.3.1 *P. aeruginosa* infections and impact

1.3.1.1 Nosocomial and Respiratory tract infections

P. aeruginosa belongs to the so-called "ESKAPE" (*Enterococcus faecium, Staphylococcus aureus, Klebsiella pneumoniae, Acinetobacter baumannii, Pseudomonas aeruginosa* and *Enterobacter* species) MDR pathogens[25-26] and it is the second most frequent pathogen causing nosocomial infections, such as hospital-acquired pneumonia (HAP), health care-associated pneumonia (HCAP), ventilator-associated pneumonia (VAP) and ventilator-associated tracheobronchitis, contributing to approximately 13 – 19 % of the total reported cases[27]. In fact, it is responsible for causing more than 51,000 HAP infections and 440 deaths anually in the USA[16] due to its ability to disrupt upper and lower airway homeostasis[19].

1.3.1.2 Cystic fibrosis

Furthermore, *P. aeruginosa* is one of the most predominant bacterium in the lungs of patients suffering cystic fibrosis (CF), especially among adult patients[28]. In fact, the majority of CF patients are chronically infected with this pathogen[29].

CF is a multisystemic autosomal recessive disorder, first recognized by Dorothy H. Andersen in 1938, that provokes damage in lungs, pancreas, gastrointestinal tract, liver and reproductive tract[30]. This life-threatening disease is common among Caucassian communities affecting to 1 in 3,000 people[31]. CF is caused by mutations in the *cystic fibrosis transmembrane conductance regulator (cftr)* gene which codes for CFTR ion channel protein, responsible of the transport of chloride and bicarbonate across epithelial cells. There are more than 2,000 different mutations of *cftr* gene that can be classified in 5 different groups according to the corresponding CFTR deficiency[31].

The defective expression of CFTR also affects sodium and calcium ion channels[32] causing abnormalities in the immune activation[33] and inducing mucus hypersecretion (Figure 1. 2), which favors the colonization and survival of *P. aeruginosa* stablishing chronic and persistent infections[34]. This can lead to airway obstruction and, ultimately, can trigger morbidity and mortality in CF patients. Moreover, although CF survival has been improving for the past 40 years, respiratory failure remains the leading cause of mortality in this patients[35].

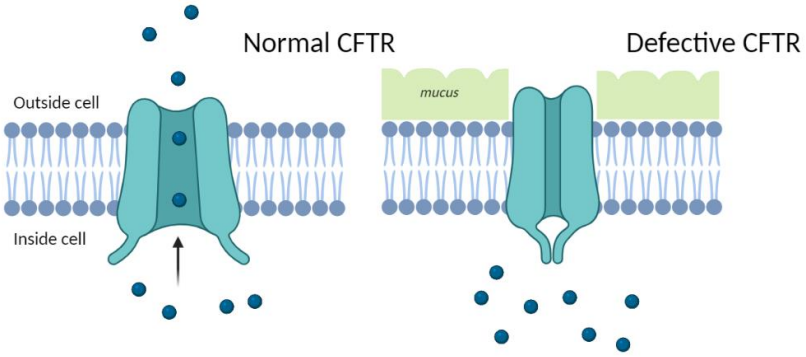

Figure 1. 2 *Normal (left) and defective (right) CFTR channel. When CFTR is defective, the flow of chloride ions and water in and out of cells is disrupted. In consequence, an abnormally thick and sticky mucus layer appears obstructing the airways.*

1.3.1.3 *P. aeruginosa* virulence

The adaptability of *P. aeruginosa* to different hostile environments, such as the respiratory tract of CF patients, is afforded by the vast number of virulence factors (VFs) it uses, which confers the ability of causing both acute and chronic infections[36]. In this sense, VFs can be categorized in cell-associated and secreted VFs.

1.3.1.3.1 Cell-associated virulence factors

1.3.1.3.1.1 The outer membrane

The *P. aeruginosa* outer membrane (OM) is an asymmetric bilayer composed of lipopolysaccharides (LPS), 3 major porins (OprF, OprH and OprD) and different lipoproteins (see Figure 1. 3). The main functions of these components are the capacity of decreasing permeability, limiting the entry of different compounds and inducing resistance to a wide variety of antibiotics, such as amynoglicosides, polymyxin and carbapenems and amiloglycans, the maintenance of cell integrity and the passive and active transport of extracellular molecules[19, 36].

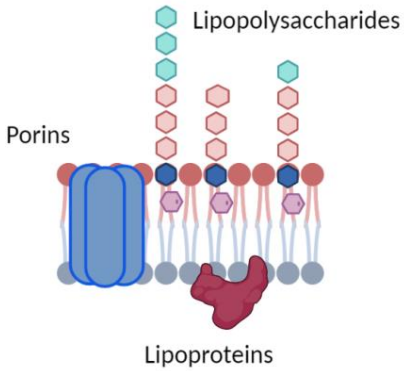

Figure 1. 3 *P. aeruginosa outer membrane (OM) structure and main components.*

1.3.1.3.1.2 Flagellum and type IV pili

P. aeruginosa possess a single polar flagellum, composed of different flagellins named FliC, FliD, FlgE, FlgKL, that is responsable for its swimming motility in both aqueous and/or low viscosity environments[24]. Thus, flagellum is crucial for bacteria colonization. At the same time, *P. aeruginosa* has hair-like filamentous appendages named type IV pilis that are essential for stablishing chronic infection as they control twitching motility and have extension and retraction capacity[24] (see Figure 1. 4).

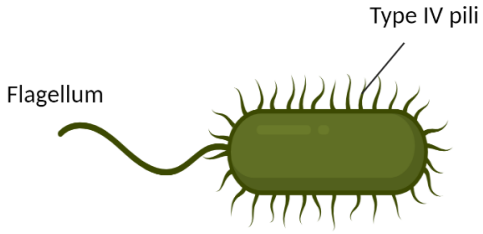

Figure 1. 4 *P. aeruginosa flagellum and type IV pili representation.*

1.3.1.3.2 Secreted virulence factors

1.3.1.3.2.1 Protein secretion systems

Protein secretion systems (SS) are used by a multitude of gram positive and negative bacteria to secrete different proteins across membranes promoting virulence and disrupting host immune systems[37]. In the case of *P. aeruginosa*, it uses 5 SS named type 1 SS (T1SS), T2SS, T3SS, T5SS and T6SS[36, 38]. Each of these SSs are composed of different structural proteins and are responsible of secreting different VFs. As illustrated in Figure 1. 5, T2SS and T5SS secrete proteins in a two-step mechanism where proteins first cross the inner membrane (IM) with the help of Sec or toxin-antitoxin-chaperone (Tac) secretion systems. In contrast, T1SS, T3SS and T6SS transport substrates in a one-step process making use of periplasm-spanning channels. Besides, T3SS and T6SS can also secrete proteins through host membrane directly delivering them to the cytosol of the host[37, 39].

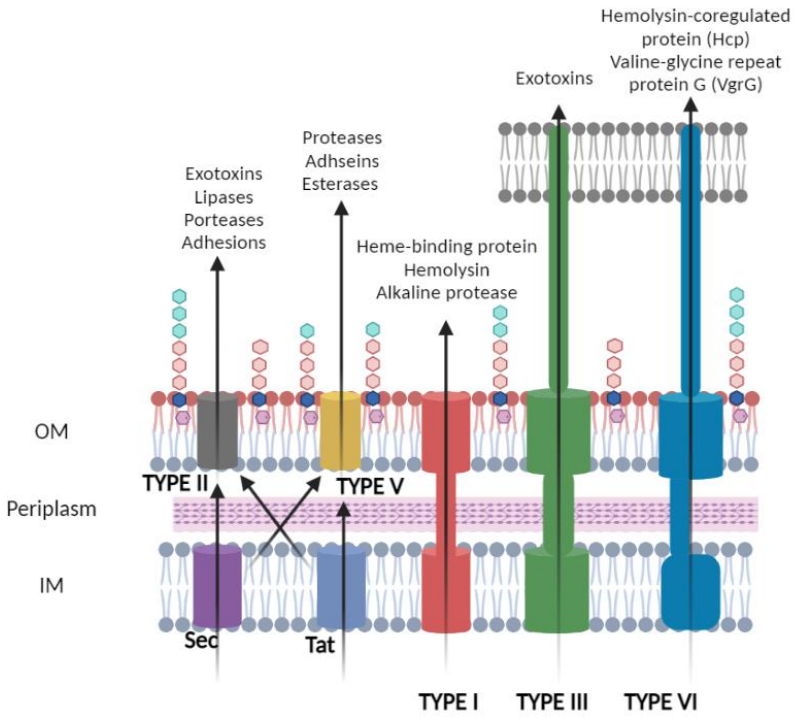

Figure 1. 5 *General structure of the 5 SS used by P. aeruginosa bacterium and the corresponding secreted VFs.*

1.3.1.3.2.2 Siderophores

Iron is essential for bacterial growth and virulence. However, it is mainly found in its oxidized state (Fe^{3+}) and it is insoluble at neutral and basic pHs. Hence, among other strategies, bacteria use secondary metabolites named siderophores to scavenge iron from the environment and to form soluble complexes that can be easily taken by specific receptors[40]. In the case of *P. aeruginosa*, it possesses two siderophores known as Pyoverdine (PVD) and Pyochelin (PCL). PVD is considered the major siderophore since it has higher affinity for iron than PCL[36]. In this context, siderophores can be used as cooperative molecules, in which every bacteria cell is benefited from them, or as competitive agents. The last scenario is common in iron-limited environments in which siderophores are used to lock iron avoiding its uptake by other bacteria and host cells[40]. Besides, apart from its role as key nutrient, PVD has a dual role during *P. aeruginosa* infections, being a essential component for biofilm development[24] and acting as signaling molecule for the production of exotoxin A and endoproteinase PrpL VFs[41-42].

1.3.1.3.2.3 Rhamnolipids

Rhamnolipids are rhamnose-containing glycolipidic compounds that show different relevant functions regarding *P. aeruginosa* pathogenicity. The most important are:

- Dispersion of biofilms from other bacteria such as *Desulfovibrio vulgaris* and *S. aureus*[43].

- Preservation of the pores and channels between microcolonies enabling the passage of liquid and nutrients within mature biofilm[24].
- Cytotoxic and immunomodulatory effects on mammalian cells[44].
- During the colonization period, they potentially help in the adaptation process increasing surface activity, wetting ability, detergency, and other amphipathic-related characteristics[44-45].

1.4 Transition between acute and chronic infections

As above described, *P. aeruginosa* is equipped with an arsenal of different VFs that allow respiratory tract colonisation and injury especially during acute infections.

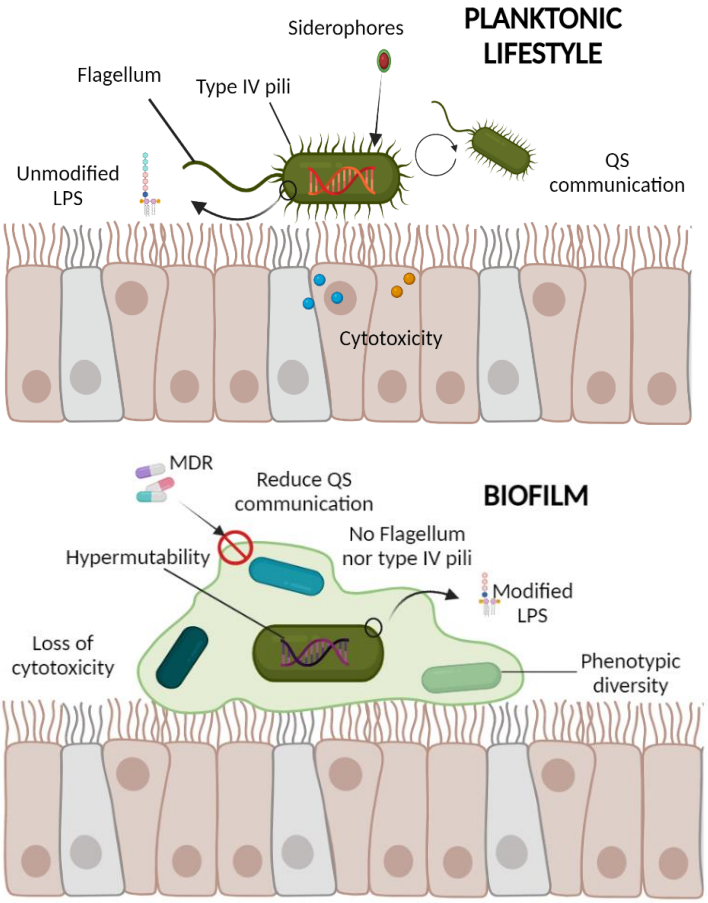

Figure 1. 6 *Representation of P. aeruginosa adaptation from a planktonic lifestyle (acute infection) to biofilm formation (chronic infection) in epithelial cells. In early stages, bacteria use different virulence factors that allow colonization and lung injury (up). P. aeruginosa undergo adaptative changes that enable establishment of long-term chronic infections (down). Adapted from Jurado-Martín et al.[36].*

Despite the host immune responses, *P. aeruginosa* has the ability of surviving for long period of times establishing chronic infections in the lungs of patients, which causes resistance processes and makes antibiotic therapies less effective[17, 36]. The adopted mucoid phenotype is characterized by the formation of biofilms and the downregulation of genes coding for VFs[46-48].

Therefore, it is essential to have appropriate diagnostic strategies to detect infections at early stages (acute infections) that will allow applying more specific antibiotic treatments preventing chronification of the infections and the appearance of resistant strains[49]. Figure 1. 6 shows the main differences between these two type of infections.

1.4.1 Biofilms

Biofilms are complex bacteria aggregates on surface embedded in a self-generated extracellular matrix that allow bacteria to survive under different unexpected environmental conditions[24]. The extracellular matrix is composed of three different exopolysaccharides (EPS) named Psl, Pel and alignate that contribute to biofilm formation and promote antibiotic tolerance by decreasing their difussion[16, 24, 45]; extracellular DNA (eDNA), which supports cellular organization and alignment via twitching motility[24]; and different proteins that help overcoming environmental stress, promote matrix stability, facilitate surface adherence and enhance interaction with other matrix molecules[24, 45].

P. aeruginosa biofilm formation process is divided into 4 different stages (see Figure 1. 7)[24, 36, 45]:

- Bacteria cells adhere to a surface making use of cell appendages (reversible attachment). At the same time, EPS biosynthesis starts.
- Bacterial cell attachment becomes irreversible and start to propagate into more structured architectures named microcolonies.
- Microcolonies develop into 3-dimensional mushroom shape structures (biofilm maturation).
- Part of the biofilm is dispersed. The dispersed cells undergo a transition to a planktonic lifestyle mode allowing the biofilm cycle to start again.

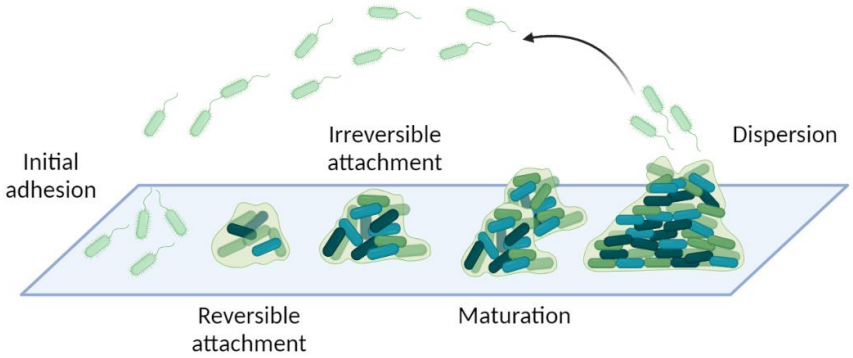

Figure 1. 7 *P. aeruginosa biofilm formation, maturation and dispersion.*

It has been documented that a bacterial communication mechanism known as Quorum Sensing (QS) controls the formation, maturation and dispersion of biofilms at different levels by releasing eDNA, maintaining biofilm channels and detaching biofilm cells[50-51]. Hence, QS has attracted attention as a promising target to develop diagnostic and therapeutic approaches[52-53].

1.5 Quorum sensing system

1.5.1 Quorum sensing system concept

QS is a bacterial mechanism by which individual bacteria communicate with each other allowing the activation and coordination of the expression of a myriad of genes related with pathogenicity and other physiological processes such as VF production, biofilm formation and sporulation[53]. Thus, bacteria produce and sense small signal molecules known as autoinducers (AI), which differ accordingly to the bacteria group[54]. In general, AIs can be classified as acylated homoserine lactones (AHLs), which are the most common AIs in gram negative bacteria; peptide signals, in gram positive bacteria; and autoinducer 2 (AI-2), found in both bacteria groups (see Figure 1. 8)[55]. Besides, some species of bacteria produce specific and unique AIs. Thus, *P. aeruginosa* bacterium produced Pseudomonas Quinolone Signal (PQS) and Integrated QS signal (IQS) AIs.

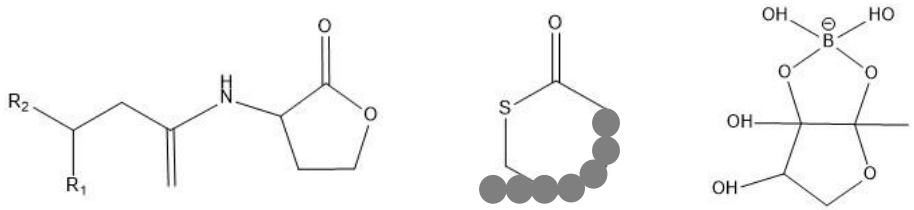

AHL **AI peptides** **AI-2**

Figure 1. 8 *Chemical structures of general AIs of different bacterial type. From left to right: general structure of AHLs, found in gram negative bacteria; general structure of AI peptides (grey spheres refer to amino acids), in gram positive bacteria; and general structure of AI-2, on both type of bacteria*.

The general mechanism of QS signalling is highly conserved among both gram positive and negative bacteria and can be summarized as follows. First, bacteria produce AIs through the action of the corresponding synthase enzymes. The secreted AIs can be freely diffuse through the bacterial membrane or, in contrast, by an active transport process. When an extracellular concentration threshold of AIs is reached, they are bound by their specific receptors, which can reside in the IM or in the cytoplasm. These receptors will activate the expression of a particular set of genes related with different biological processes[56].

1.5.2 Gram positive QS network: *Staphylococcus aureus* QS pathways

One of the most studied gram-positive bacterium regarding QS is the MDR *S. aureus*. As gram positive bacterium, *S. aureus* produces and releases small AI peptides (AIP) that act as signalling molecules to induce the expression of different genes related with pathogenicity[57].

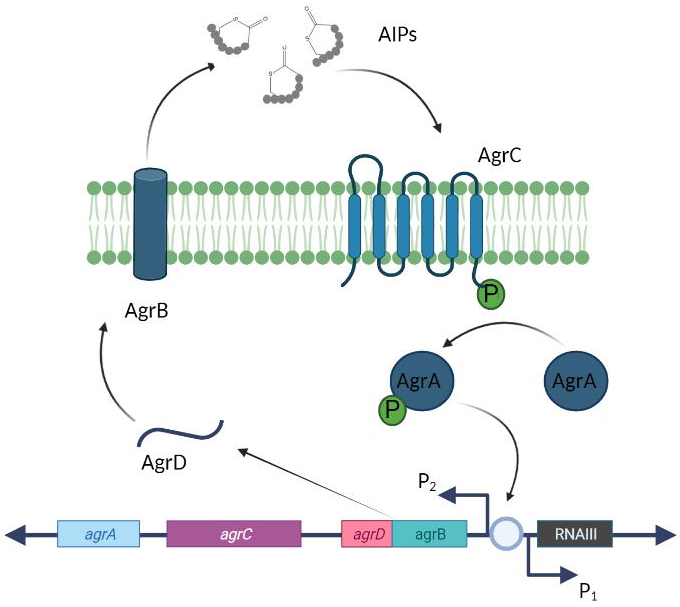

Figure 1. 9 *Schematic illustration of S. aureus accesory gene regulator (Agr) QS system. The agr locus contains two transcripts named ribonucleic acid III (RNAIII) and RNAII. RNAII is an operon that contains 4 genes, agrBDCA. These genes encode molecules required in the synthesis os AIPs. RNAIII transcripts a small RNA molecule which up-regulates extracellular VFs and down-regulates cell surface proteins.*

In this particular case, VFs expression in *S. aureus* is controlled by the accesory gene regulator (Agr) system. The components of this system are encoded in the *agrBDCA* operon, which encodes for an AgrC histidine kinase, its cognate receptor AgrA, an AgrB membrane protease and the precursor peptide of AIPs called AgrD[57-58]. As shown in Figure 1. 9., AgrB transforms AgrD precursor to mature AIP and exports it extracellularly. AIP is then recognized by AgrC which will phosphorylate AgrA in the citosol. Phosphorylated-AgrA binds to P2 and P3 promoters upregulating *agr* transcription. Then, VFs expression is activated and cell surface protein expression downregulated[58].

1.5.3 Gram negative QS network: *P. aeruginosa* QS pathways

To date, four different and interconnected QS systems have been described for *P. aeruginosa*: Las, Rhl, Pqs and Iqs systems[59-60](see Figure 1. 10).

The first two systems are LuxR-I systems, which means they produce and detect AHLs as signaling molecules. In this context, LasI and RhlI synthases are responsible for producing N-(3-

oxododecanoyl)-L-homoserine lactone (3oxoC_{12}-HSL) and N-butyryl-L-homoserine lactone (C_4-HSL) as AIs, respectively, which will be further detected by their corresponding cytosolic transcription factor LasR and RhlR. Both systems are responsible of producing different VFs and also inducing biofilm formation.

The third QS system, Pqs, is associated with 4-hydroxy-2-alkylquinoline (HAQ) signals named PQS and its precursor 2-heptyl-4-quinolone (HHQ). Both molecules activate the transcriptional regulator PqsR enhancing the expression of *pqsABCDE* operon, which triggers the production of several VFs and biofilm formation. Unlike Las and Rhl systems, which are common to other gram negative bacteria, Pqs system is more specific since HAQ have only been detected in *P. aeruginosa* and certain *Burkholderia* and *Alteromonas spp*[61]. This fact has point to HAQs value as specific biomarkers.

The fourth QS system is called Iqs and it is responsible of integrating Las system partially taking over its central role under phosphate depletion stress conditions. The AI of this system is IQS, which chemically stands for 2-(2-hydroxylphenyl)-thiazole-4-carbaldehyde; however, the receptor is still unknown.

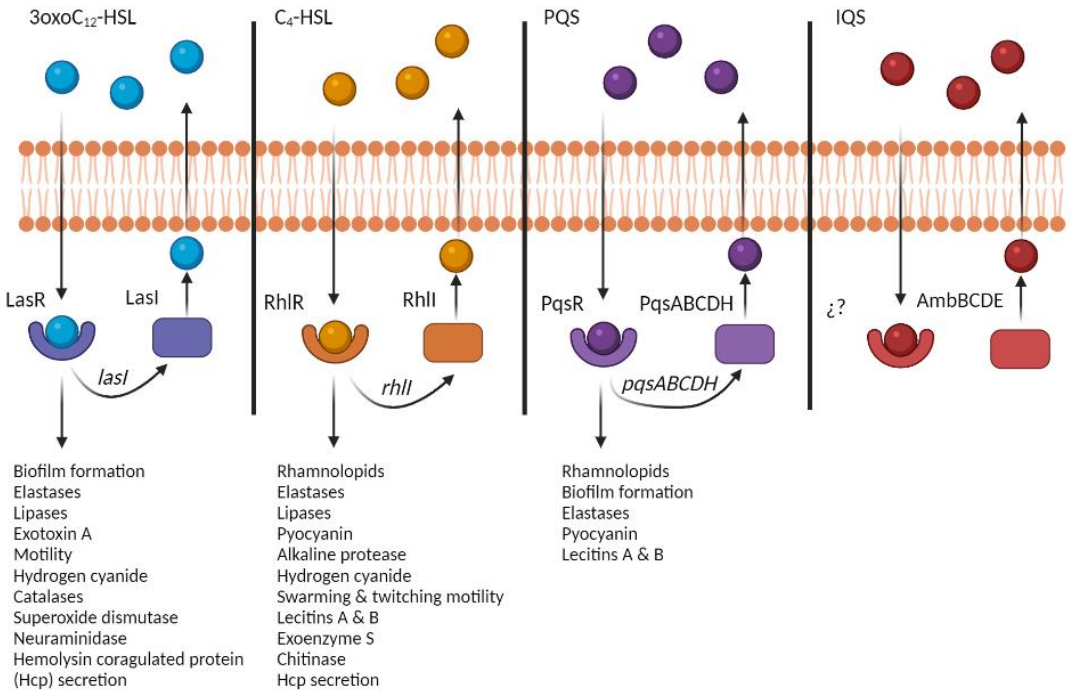

Figure 1. 10 *Schematic illustration of 4 QS pathways in P. aeruginosa bacterium and their main pathogenicity function. Abbreviations: 3oxoC_{12}-HSL, N-(3-oxododecanoyl)-L-homoserine lactone; C_4-HSL, N-butyryl-L-homoserine lactone; PQS, Pseudomonas quinolone signa; IQS, integrating quorum sensing signal.*

Apart from the four mentioned QS systems, recently the role of PqsE has also being discussed as a possible fifth QS system in *P. aeruginosa*. This enzyme, encoded in *pqsABCDE* operon for HAQ synthesis, is apparently crucial for the synthesis of pyocyanin (PYO), one of the main virulence factors in *P. aeruginosa*, activating Rhl system by a still not fully understood mechanism[62].

1.6 Pyocyanin virulence factor

1.6.1 Pyocyanin biosynthesis and production

PYO is a nitrogen-containing aromatic blue pigment belonging to the family of phenazines and one of the main VFs of *P. aeruginosa*[63-64]. Phenazines are aromatic, colored, secondary metabolites produced by fluorescent pseudomonads, streptomycetes and other few bacterial genera which possess antibiotic properties affecting different organisms such as fungi, bacteria and humans[65]. Besides, phenazines are involved in numerous bacterial processes, as biofilm formation, and can also act as cell signal molecules. The most studied phenazines producing bacteria are *P. fluorescens*, *P. chlororaphis*, *P. aureofaciens* and *P. aeruginosa*, which typically produce two or more phenazines (except for *P. fluorescens* that only produced one)[49].

In the case of *P. aeruginosa*, it produces 5 different phenazines being PYO the most important one as it is only produced by this bacterium[64]. As observed in Figure 1. 11, PYO biosynthesis is regulated by two almost identical operons (*phz1* and *phz2*) which encode 5 enzymes responsible of converting chrosimic acid to phenazine-1-carboxylic acid (PCA). PCA can be further transformed to 5-methylphenazine-1-carboxylic acid betaine by the action of PhzM enzyme to finally being converted to PYO by PhzS[66].

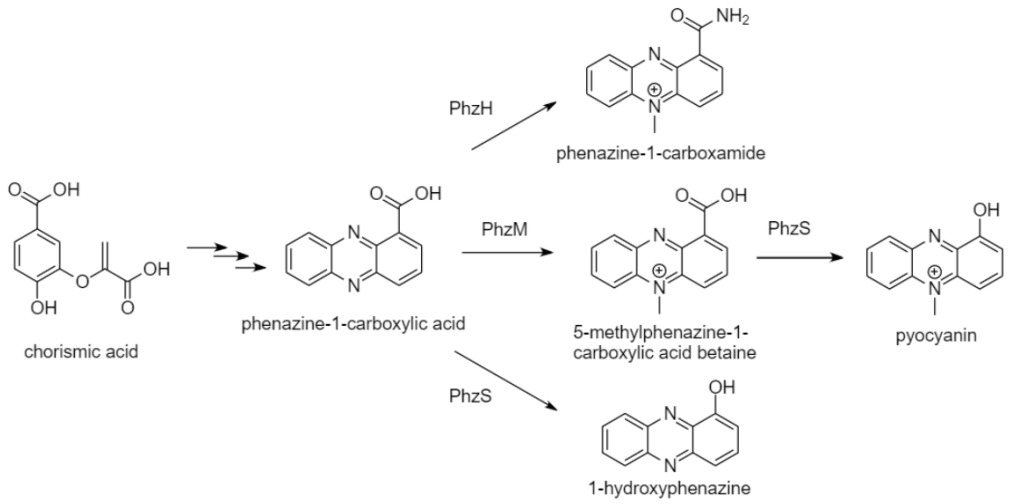

Figure 1. 11 *Biosynthetic pathways of P. aeruginosa phenazines. Adapted from Mavrodi et al.* [64].

The production of PYO is mainly controlled by QS along with small noncoding ribonucleic acids (sRNAs) and environmental factors[49]. Therefore, PYO is considered an effector molecule of QS system[67-68]. In fact, several studies have reported that PYO production is controlled by Las, Rhl and Pqs QS systems. In this sense, Higgins et al.[66] explained the role of LasR in the up-regulation of Rhl and Pqs systems which interact through RhlR and PqsE[69], respectively, to activate *phz1* and *phz2* operons. Besides, it has been documented that *P. aeruginosa lasR* mutant strains are able to produce PYO making use only of Rhl and Pqs systems[70]. In the same line, Lu et al.[71] demonstrated the role of PqsR, which increased PCA production by chromosomal inactivation of *pqsR*, resulting in the full inhibiton of PCA biosynthesis. In contrast, Sun et al.[72] showed that PCA production could be inhibited by the transcriptional regulator RsaL, which repressed Las and Pqs systems.

1.6.2 Cellular cytotoxicity and immunomodulatory effects of PYO

PYO exerts a large number of toxic effects in host cells[73] mainly due to its redox properties and its low molecular weight (210.23 g mol^{-1}), which allows it to penetrate cytoplasmic membranes[74]. Hence, it alters the homeostasis and physiology of the host by disrupting[73, 75-76]:

- energy metabolism by decreasing ATP and calcium levels.
- cellular respiration by decreasing glutathione and nicotinamide adenine dinucleotide phosphate (NADPH).
- redox equilibrium by enhancing the formation of reactive oxygen species (ROS). The increase of intracellular ROS induces oxidative stress on host cells causing free radical formation and damaging components of cells, specially the mitochondria[73, 77].
- mucociliary clearance *in vivo*[78].
- cell signalling pathways, which can result in the induction of premature senescence in human fibroblasts[79], neutrophil apoptosis[80-81] and some B cells, T cells and macrophages function inhibition[82-83].

Moreover, it has been reported that PYO has immunomodulatory effects on the host by modifying the production of cytokines (low molecular weight proteins secreted by immune cells in response to cellular damage)[84-85], imparing ciliary beat (defence mechanism of the respiratory tract against strange bodies)[86] and inhibiting nitric oxide production by macrophages and endothelial cells[87].

1.7 Diagnostic tools for detecting bacteria

The most common and gold standard technique used for detecting *P. aeruginosa* still consists on the use of culture plates inoculated with swab samples. However, this method is time consuming, taking between 24 and 48 h to obtain results, which usually implies a delay on the administration of the correct treatment aggravating the symptoms and/or increasing resistance problems[88]. Thus, the development of fast diagnostic tools could significantly improve the management of *P. aeruginosa* infections. In this sense, the identification of new biomarkers of infection has become an essential milestone. Table 1. 1 shows the most recent developed diagnostic techniques for the detection of *P. aeruginosa* bacterium and the corresponding biomarker of infection used. In general, these techniques can be classified in 4 different groups: spectroscopic, molecular biology based methodologies, electrochemical and immunochemical technologies. The presented techniques are validated in artificial media.

Table 1. 1 *Diagnostic techniques reported to detect P. aeruginosa bacterium based on different biomarkers of infection.*

General technique	Assay	Biomarker	Reference
Spectroscopic	Colorimetric biosensor based on magnetic nanoparticles (NP)	LasA	[89]
Spectroscopic	Fluorescence resonance energy transfer (FRET) labelled peptides with 3Glycine	LasA	[90]
Spectroscopic	Fluorescence vesicles affine to toxins	Toxins	[91]
Spectroscopic	FRET-based nanoprobe of Au-conjugated carbon dots	PYO	[92]
Spectroscopic	Surface-enhanced Raman spectroscopy (SERS) Solution phase using Ag sensor	PYO	[93]
Molecular Biology	Real time polymerase chain reaction (rtPCR)	*oprL*	[94]
Molecular Biology	TriplexPCR+agarelectrophoresis	*lasI, lasR, gyrB*	[95]
Molecular Biology	MagneticNP (MNP) +PCR	*gyrB*	[96]
Molecular Biology	GenomicDNA extracted using amino modified magnetic NPst+nestedPCR	*ecfX*	[97]
Molecular Biology	Polimerase spiral reaction	*toxA*	[98]
Electrochemical	Polianiline/AuNP-indium tin oxide electrode (cyclic voltammetry)	PYO	[99]
Electrochemical	Paper-based method	PYO	[100]
Electrochemical	Nanograss based sensor	PYO	[101]
Immunochemical	Enzyme-linked immunosorbent assay (ELISA)	PYO/1-OHphz	[102]
Immunochemical	ELISA	Antipseudomonas IgG	[103]

1.7.1 Analytical approaches for PYO detection

As previously explained, it has already been reported that PYO is secreted at high concentrations during early colonization to establish infection (acute infection), whereas during chronic infection its levels are downregulated together with other VFs and motility[46-48, 104]. Besides, PYO is a VF only secreted by *P. aeruginosa*. Therefore, all these facts position PYO as a very interesting biomarker to discern between both types of infections caused by *P. aeruginosa*.

The most commonly used analytical methods for PYO measurement are based on its unique characteristics. In this sense, absorbance methods exploit PYO optical properties at different pHs[92]. Besides, at pH 7, PYO solutions show a blue colour with different maximal absorption peaks. Thus, PYO is quantified in culture media at 690 nm[49]. However, PYO absorption spectrum varies according to the used solvent and is very sensitive to pH[105]. At the same time, PYO can be quantified using electrochemical methods[99-100, 106-111] due to its unique redox properties since, unlike other biologically relevant small molecules, it is oxidized at negative voltages (250 mV vs. Ag/AgCl reference). The main disadvantages of these type of methods are possible interferents with other molecules in the media and, in most of the cases, the need of sample pretreatments. Furthermore, SERS studies have also been used to measure PYO in different clinical samples[93, 112-114].

Despite showing limits of detection (LoD) in the low µM range, these techniques required pretreatment steps which lengthened the process. In general, all the mentioned methods are faster than the previously described gold-standard, nevertheless, most of them still require pre-treatment steps and trained people to perform the assay. Thus, more rapid, reliable, specific and sensitive techniques are required. In this context, immunochemical analytical methods are positioned as a good alternative since they can offer simple and low cost solutions to clinical diagnostic, they show low LoD and most of then do not require sample pretreatments. Furthermore, these methods are very specific since they are based on the interaction between an antigen and an antibody (Ab). Therefore, they are starting to be implemented in clinical laboratories[115-116]. Table 1. 2 presents the latest developed methods for PYO detection in clinical samples.

Table 1. 2 *Diagnostic methods used for PYO detection in clinical samples.*

Diagnostic method	LoD	Sample type	Reference
Carbon fiber electrochemical sensor	0.03 µM	Bacterial cultures	[106]
Amperometrical detection	125 nM	Artificial sputum samples	[107]
SERS + microfluid platform	0.5 µM	Saliva samples	[112]
Paper based electrochemical sensor (squared wave voltammetry)	95 nM	Bacteria cultures	[108]
Biodegradable gold coated Zein film SERS + AuNPs	25 µM	Spiked drinking water	[113]
Polyaniline/AuNP-indium tin oxide modified electrochemical sensor (squared wave voltammetry)	500 nM	50 samples corneal ulcers	[109]
SERS-active silicon nanowire matrix covered by bimetallic noble metal NP	15 µM	Artificial sputum	[114]
Thermosensive agar-based hydrogel+Au/Agnanoalloy (electrochemical)	0.04 µM	Whole blood and serum	[110]
Polianiline/AuNP-indium tin oxide electrode (cyclic voltammetry)	500 nM	*P. aeruginosa* cultures from pneumonia, corneal ulcers, urinary tract and wound infections	[99]
Electrochemical paper-based method	10 nM	Spiked human saliva and contamined surfaces	[100]
Nanograss based sensor	172 nM	Sputum obtained by endolaryngeal suction with hypertonic saline (HTS)	[117]
FRET-based nanoprobe of Au-conjugated carbon dots	3.04 nM	*P. aeruginosa* MTCC nº744	[92]
Electrochemical sensor based on AuNP functionalized reduced graphene oxide	0.27 µM 1.34 µM 2.3 µM	PBS media Spiked human saliva Spiked urine	[111]
Solution phase SERS using Ag sensor	23.1 µM	Spiked wound samples	[93]
ELISA method	0.60 nM	Spiked sputa	[102]

1.7.2 PYO levels in biological and clinical samples

Despite the fact that PYO can be considered a good biomarker of *P. aeruginosa* infections, few studies have reported PYO levels in clinical samples. Thus, the majority of the reported results are based on PYO measurements in *P. aeruginosa* clinical isolates, which relies on their culturing and further selectivity studies previous to PYO determination in culture media. Furthermore, the majority of the data has been obtained from respiratory tract infections.

Regarding lung infections, Wilson et al. [118] measured PYO in sputum for the first time in 1988 (n =13). Thus, after sample extraction and purification, PYO was analysed using high-performance liquid chromatography-ultraviolet (HPLC-UV) detecting PYO at levels ranging from 0.2 to 27.3 μg mL^{-1} (up to 100 μM). Furthermore, Hunter et al.[119] measured PYO and PCA in 45 sputum samples from CF patients by HPLC-UV showing a negative correlation between phenazines concentration and lung function. Nevertheless, this study is under revision given a technical problem regarding the use of an old HPLC system that lacked tandem mass spectrometry capability. Therefore, they assigned a specific chromatographic peak to phenazines overestimating their abundance when the peak represented other non-phenazine metabolite[120]. Since then, to our knowledge, no other work addressing direct measurement of PYO in sputum samples has been reported except the work presented by Alatraktchi et al.[117]. In fact, it was the first study that quantify PYO directly in sputum samples obtained by endolaryngeal suction with hypertonic saline (HTS) using electrochemical sensing. In this preliminary test, custom-made nanograss (NG) sensors were used to determine PYO concentration in the collected endolaryngeal suctions from 5 CF patients and compared with 16S rDNA PCR as reference method and the conventional gold standard based on bacterial culture. The low LoD (172 nM) shown by this technique allowed the direct quantification of PYO. Besides, PYO concentrations were higher in samples from early colonized patients (13.6 μM) than in samples from chronically infected patients (0.3 μM). In addition, these results were the same obtained using the reference method but differ from the gold standard. Thus, confirming the high rate of false negatives attributed to plate culture method.

The following examples are PYO measures from lung infection strains grown in culture media. In this context, Silva et al.[121] reported PYO levels of strains collected from lung, mouth, blood, rectum, tracheal aspirate, urine, venous catheter, pleural secretion, eschar samples from patients hospitalized in intensive care units of Brazilian hospitals during the period 1999-2010 (ATCC 27853 *P. aeruginosa* strain as control). After a culturing step, PYO was extracted following a chloroform extraction method. They found that all strains produced PYO, being the highest values in urine samples (around 90 μM) and the lowest in sputum samples (around 18 μM). Furthermore, Elliot et al.[122] used transparent carbon ultramicroelectrod arrays (T-CUAs) together with square-wave voltammetry to detect PYO on PA14 and PA11 (clinically relevant *P. aeruginosa* strain isolated from CF patients sputum sample) strains. The obtained PYO concentrations after 24 h incubation at 37 ºC were of 3 ±2 μM and 45 ±5 μM, respectively.

As previously mentioned, *P. aeruginosa* is also found in burn wounds, leading to severe disease states including sepsis[123]. In this context, Cruickshank and Lowbury[124] analysed a total of 5 burns

infected with *P. aeruginosa*. They used extraction and absorbance methods and found PYO levels up to 8.1 µM. In the same way, Khadim and Marjani[125] examined 22 isolates from burn infections to quantify PYO by spectroscopy. They detected PYO values of 10.85 µg mL^{-1}.

PYO levels have also been quantified on ear secretions and blood stream infections. Thus, Reimer et al. [126] collected ear secretions samples from 17 patients for culturing and analysing PYO content by HPLC-UV. They detected PYO concentrations ranging from 3 to 2714 nmol g^{-1}. Furthermore, Gupte et al. [127] analysed bacterial isolates from 75 patients suffering from *P. aeruginosa* blood stream intections using chloroform extraction-absorbance method. PYO levels higher than 80 µM were detected.

Therefore, the lack of rapid and effective diagnostic tools to detect *P. aeruginosa* at early stages of infection, where this pathogen is more susceptible to antibiotic treatments, has usually resulted in a delay of the administration of a proper treatment increasing the appearance of resistance processes. Thus, the identification of new biomarkers of infection is of crucial importance. In this context, the main QS-regulated VF of *P. aeruginosa*, PYO, can be a great biomarker candidate to differentiate between *P. aeruginosa* infections since it is only secreted by this bacterium, specially at early stages of infection. Therefore, this thesis aims to develop a fast, specific and sensitive ELISA to detect PYO in different biological and clinical samples and check its potential as biomarker of *P. aeruginosa* infections.

1.8 References

1. Organization, W. H. The top 10 causes of death. https://www.who.int/news-room/fact-sheets/detail/the-top-10-causes-of-death.
2. National Center for Chronic Disease Prevention and Health Promotion, D. o. P. H. COPD Death Rates in the United States. Centers for Disease Control and Prevention.
3. Organization, W. H. Tuberculosis. https://www.who.int/news-room/fact-sheets/detail/tuberculosis#:~:text=A%20total%20of%201.5%20million,with%20tuberculosis%20(TB)%20worldwide.
4. Deaths from tuberculosis INCREASED in 2020 for the primary time in 15 years. https://news.elegantsite.gr/deaths-from-tuberculosis-increased-in-2020-for-the-primary-time-in-15-years/.
5. Whooping cough — Level 3 cause. http://www.healthdata.org/results/gbd_summaries/2019/whooping-cough-level-3-cause.
6. Organization, W. H. Pneumonia. https://www.who.int/news-room/fact-sheets/detail/pneumonia.

7. Aslam, B.; Wang, W.; Arshad, M. I.; Khurshid, M.; Muzammil, S.; Rasool, M. H.; Nisar, M. A.; Alvi, R. F.; Aslam, M. A.; Qamar, M. U.; Salamat, M. K. F.; Baloch, Z., Antibiotic resistance: a rundown of a global crisis. *Infect Drug Resist* **2018,** *11*, 1645-1658.
8. Hutchings, M. I.; Truman, A. W.; Wilkinson, B., Antibiotics: past, present and future. *Curr Opin Microbiol* **2019,** *51*, 72-80.
9. Dietvorst, J.; Vilaplana, L.; Uria, N.; Marco, M.-P.; Muñoz-Berbel, X., Current and near-future technologies for antibiotic susceptibility testing and resistant bacteria detection. *TrAC Trends in Analytical Chemistry* **2020,** *127*, 115891.
10. Subramaniam, G.; Girish, M., Antibiotic Resistance - A Cause for Reemergence of Infections. *Indian J Pediatr* **2020,** *87* (11), 937-944.
11. Waglechner, N.; Wright, G. D., Antibiotic resistance: it's bad, but why isn't it worse? *BMC Biol* **2017,** *15* (1), 84.
12. Barrasa-Villar, J. I.; Aibar-Remon, C.; Prieto-Andres, P.; Mareca-Donate, R.; Moliner-Lahoz, J., Impact on Morbidity, Mortality, and Length of Stay of Hospital-Acquired Infections by Resistant Microorganisms. *Clin Infect Dis* **2017,** *65* (4), 644-652.
13. Miethke, M.; Pieroni, M.; Weber, T.; Bronstrup, M.; Hammann, P.; Halby, L.; Arimondo, P. B.; Glaser, P.; Aigle, B.; Bode, H. B.; Moreira, R.; Li, Y.; Luzhetskyy, A.; Medema, M. H.; Pernodet, J. L.; Stadler, M.; Tormo, J. R.; Genilloud, O.; Truman, A. W.; Weissman, K. J.; Takano, E.; Sabatini, S.; Stegmann, E.; Brotz-Oesterhelt, H.; Wohlleben, W.; Seemann, M.; Empting, M.; Hirsch, A. K. H.; Loretz, B.; Lehr, C. M.; Titz, A.; Herrmann, J.; Jaeger, T.; Alt, S.; Hesterkamp, T.; Winterhalter, M.; Schiefer, A.; Pfarr, K.; Hoerauf, A.; Graz, H.; Graz, M.; Lindvall, M.; Ramurthy, S.; Karlen, A.; van Dongen, M.; Petkovic, H.; Keller, A.; Peyrane, F.; Donadio, S.; Fraisse, L.; Piddock, L. J. V.; Gilbert, I. H.; Moser, H. E.; Muller, R., Towards the sustainable discovery and development of new antibiotics. *Nat Rev Chem* **2021**, 1-24.
14. Shore, C. K.; Coukell, A., Roadmap for antibiotic discovery. *Nat Microbiol* **2016,** *1* (6), 16083.
15. Laws, M.; Shaaban, A.; Rahman, K. M., Antibiotic resistance breakers: current approaches and future directions. *FEMS Microbiol Rev* **2019,** *43* (5), 490-516.
16. Azam, M. W.; Khan, A. U., Updates on the pathogenicity status of Pseudomonas aeruginosa. *Drug Discov Today* **2019,** *24* (1), 350-359.
17. Ruffin, M.; Brochiero, E., Repair Process Impairment by Pseudomonas aeruginosa in Epithelial Tissues: Major Features and Potential Therapeutic Avenues. *Front Cell Infect Microbiol* **2019,** *9*, 182.
18. Olejnickova, K.; Hola, V.; Ruzicka, F., Catheter-related infections caused by Pseudomonas aeruginosa: virulence factors involved and their relationships. *Pathog Dis* **2014,** *72* (2), 87-94.
19. Curran, C. S.; Bolig, T.; Torabi-Parizi, P., Mechanisms and Targeted Therapies for Pseudomonas aeruginosa Lung Infection. *Am J Respir Crit Care Med* **2018,** *197* (6), 708-727.
20. Pang, Z.; Raudonis, R.; Glick, B. R.; Lin, T. J.; Cheng, Z., Antibiotic resistance in Pseudomonas aeruginosa: mechanisms and alternative therapeutic strategies. *Biotechnol Adv* **2019,** *37* (1), 177-192.
21. Huemer, M.; Mairpady Shambat, S.; Brugger, S. D.; Zinkernagel, A. S., Antibiotic resistance and persistence-Implications for human health and treatment perspectives. *EMBO Rep* **2020,** *21* (12), e51034.

22. Poole, K., Efflux-mediated antimicrobial resistance. *J Antimicrob Chemother* **2005,** *56* (1), 20-51.
23. Lambert, P. A., Mechanisms of antibiotic resistance in Pseudomonas aeruginosa. *J R Soc Med* **2002,** *95 Suppl 41*, 22-6.
24. Thi, M. T. T.; Wibowo, D.; Rehm, B. H. A., Pseudomonas aeruginosa Biofilms. *Int J Mol Sci* **2020,** *21* (22).
25. Sonmezer, M. C.; Ertem, G.; Erdinc, F. S.; Kaya Kilic, E.; Tulek, N.; Adiloglu, A.; Hatipoglu, C., Evaluation of Risk Factors for Antibiotic Resistance in Patients with Nosocomial Infections Caused by Pseudomonas aeruginosa. *Can J Infect Dis Med Microbiol* **2016,** *2016*, 1321487.
26. Khan, H. A. A., A.; Mehboob, R. , Nosocomial infections: Epidemiology, prevention, control and surveillance. *Assian Pac J Trop Biomed* **2017,** *7* (5), 478-482.
27. Behzadi, P.; Barath, Z.; Gajdacs, M., It's Not Easy Being Green: A Narrative Review on the Microbiology, Virulence and Therapeutic Prospects of Multidrug-Resistant Pseudomonas aeruginosa. *Antibiotics (Basel)* **2021,** *10* (1).
28. Maurice, N. M.; Bedi, B.; Yuan, Z.; Goldberg, J. B.; Koval, M.; Hart, C. M.; Sadikot, R. T., Pseudomonas aeruginosa Induced Host Epithelial Cell Mitochondrial Dysfunction. *Sci Rep* **2019,** *9* (1), 11929.
29. Barr, H. L.; Halliday, N.; Camara, M.; Barrett, D. A.; Williams, P.; Forrester, D. L.; Simms, R.; Smyth, A. R.; Honeybourne, D.; Whitehouse, J. L.; Nash, E. F.; Dewar, J.; Clayton, A.; Knox, A. J.; Fogarty, A. W., Pseudomonas aeruginosa quorum sensing molecules correlate with clinical status in cystic fibrosis. *Eur Respir J* **2015,** *46* (4), 1046-54.
30. Andersen, D. H., CYSTIC FIBROSIS OF THE PANCREAS AND ITS RELATION TO CELIAC DISEASE. *Progress in Pediatrics* **1938**, 344-399.
31. Bergeron, C.; Cantin, A. M., Cystic Fibrosis: Pathophysiology of Lung Disease. *Semin Respir Crit Care Med* **2019,** *40* (6), 715-726.
32. Ratner, D.; Mueller, C., Immune responses in cystic fibrosis: are they intrinsically defective? *Am J Respir Cell Mol Biol* **2012,** *46* (6), 715-22.
33. Cohen, T. S.; Prince, A., Cystic fibrosis: a mucosal immunodeficiency syndrome. *Nat Med* **2012,** *18* (4), 509-19.
34. Bhagirath, A. Y.; Li, Y.; Somayajula, D.; Dadashi, M.; Badr, S.; Duan, K., Cystic fibrosis lung environment and Pseudomonas aeruginosa infection. *BMC Pulm Med* **2016,** *16* (1), 174.
35. Blanchard, A. C.; Waters, V. J., Microbiology of Cystic Fibrosis Airway Disease. *Semin Respir Crit Care Med* **2019,** *40* (6), 727-736.
36. Jurado-Martin, I.; Sainz-Mejias, M.; McClean, S., Pseudomonas aeruginosa: An Audacious Pathogen with an Adaptable Arsenal of Virulence Factors. *Int J Mol Sci* **2021,** *22* (6).
37. Green, E. R.; Mecsas, J., Bacterial Secretion Systems: An Overview. *Microbiol Spectr* **2016,** *4* (1).
38. Pena, R. T.; Blasco, L.; Ambroa, A.; Gonzalez-Pedrajo, B.; Fernandez-Garcia, L.; Lopez, M.; Bleriot, I.; Bou, G.; Garcia-Contreras, R.; Wood, T. K.; Tomas, M., Relationship Between Quorum Sensing and Secretion Systems. *Front Microbiol* **2019,** *10*, 1100.
39. Depluverez, S.; Devos, S.; Devreese, B., The Role of Bacterial Secretion Systems in the Virulence of Gram-Negative Airway Pathogens Associated with Cystic Fibrosis. *Front Microbiol* **2016,** *7*, 1336.

40. Kramer, J.; Ozkaya, O.; Kummerli, R., Bacterial siderophores in community and host interactions. *Nat Rev Microbiol* **2020,** *18* (3), 152-163.
41. Bonneau, A.; Roche, B.; Schalk, I. J., Iron acquisition in Pseudomonas aeruginosa by the siderophore pyoverdine: an intricate interacting network including periplasmic and membrane proteins. *Sci Rep* **2020,** *10* (1), 120.
42. Lamont, I. L. B., P. A.; Ochsner, U.; Vasil, A. I.; Vasil, M. L., Siderophore-mediated signaling regulates virulence factor production in Pseudomonas aeruginosa. *PNAS* **2002,** *99* (10), 7072-7077.
43. Wood, T. L.; Gong, T.; Zhu, L.; Miller, J.; Miller, D. S.; Yin, B.; Wood, T. K., Rhamnolipids from Pseudomonas aeruginosa disperse the biofilms of sulfate-reducing bacteria. *NPJ Biofilms Microbiomes* **2018,** *4*, 22.
44. Soberon-Chavez, G.; Lepine, F.; Deziel, E., Production of rhamnolipids by Pseudomonas aeruginosa. *Appl Microbiol Biotechnol* **2005,** *68* (6), 718-25.
45. Mann, E. E.; Wozniak, D. J., Pseudomonas biofilm matrix composition and niche biology. *FEMS Microbiol Rev* **2012,** *36* (4), 893-916.
46. Ryall, B.; Carrara, M.; Zlosnik, J. E.; Behrends, V.; Lee, X.; Wong, Z.; Lougheed, K. E.; Williams, H. D., The mucoid switch in Pseudomonas aeruginosa represses quorum sensing systems and leads to complex changes to stationary phase virulence factor regulation. *PLoS One* **2014,** *9* (5), e96166.
47. D'Argenio, D. A.; Wu, M.; Hoffman, L. R.; Kulasekara, H. D.; Deziel, E.; Smith, E. E.; Nguyen, H.; Ernst, R. K.; Larson Freeman, T. J.; Spencer, D. H.; Brittnacher, M.; Hayden, H. S.; Selgrade, S.; Klausen, M.; Goodlett, D. R.; Burns, J. L.; Ramsey, B. W.; Miller, S. I., Growth phenotypes of Pseudomonas aeruginosa lasR mutants adapted to the airways of cystic fibrosis patients. *Mol Microbiol* **2007,** *64* (2), 512-33.
48. Smith, E. E.; Buckley, D. G.; Wu, Z.; Saenphimmachak, C.; Hoffman, L. R.; D'Argenio, D. A.; Miller, S. I.; Ramsey, B. W.; Speert, D. P.; Moskowitz, S. M.; Burns, J. L.; Kaul, R.; Olson, M. V., Genetic adaptation by Pseudomonas aeruginosa to the airways of cystic fibrosis patients. *Proc Natl Acad Sci U S A* **2006,** *103* (22), 8487-92.
49. Vilaplana, L.; Marco, M. P., Phenazines as potential biomarkers of Pseudomonas aeruginosa infections: synthesis regulation, pathogenesis and analytical methods for their detection. *Anal Bioanal Chem* **2020,** *412* (24), 5897-5912.
50. Hurley, M. N.; Camara, M.; Smyth, A. R., Novel approaches to the treatment of Pseudomonas aeruginosa infections in cystic fibrosis. *Eur Respir J* **2012,** *40* (4), 1014-23.
51. Lee, K.; Yoon, S. S., Pseudomonas aeruginosa Biofilm, a Programmed Bacterial Life for Fitness. *J Microbiol Biotechnol* **2017,** *27* (6), 1053-1064.
52. Rehman, Z. U.; Leiknes, T., Quorum-Quenching Bacteria Isolated From Red Sea Sediments Reduce Biofilm Formation by Pseudomonas aeruginosa. *Front Microbiol* **2018,** *9*, 1354.
53. Fong, J.; Zhang, C.; Yang, R.; Boo, Z. Z.; Tan, S. K.; Nielsen, T. E.; Givskov, M.; Liu, X. W.; Bin, W.; Su, H.; Yang, L., Combination Therapy Strategy of Quorum Quenching Enzyme and Quorum Sensing Inhibitor in Suppressing Multiple Quorum Sensing Pathways of P. aeruginosa. *Sci Rep* **2018,** *8* (1), 1155.
54. Schutz, C.; Empting, M., Targeting the Pseudomonas quinolone signal quorum sensing system for the discovery of novel anti-infective pathoblockers. *Beilstein J Org Chem* **2018,** *14*, 2627-2645.

55. Jiang, Q.; Chen, J.; Yang, C.; Yin, Y.; Yao, K., Quorum Sensing: A Prospective Therapeutic Target for Bacterial Diseases. *Biomed Res Int* **2019,** *2019*, 2015978.
56. Scoffone, V. C.; Trespidi, G.; Chiarelli, L. R.; Barbieri, G.; Buroni, S., Quorum Sensing as Antivirulence Target in Cystic Fibrosis Pathogens. *Int J Mol Sci* **2019,** *20* (8).
57. Marroquin, S.; Gimza, B.; Tomlinson, B.; Stein, M.; Frey, A.; Keogh, R. A.; Zapf, R.; Todd, D. A.; Cech, N. B.; Carroll, R. K.; Shaw, L. N., MroQ Is a Novel Abi-Domain Protein That Influences Virulence Gene Expression in Staphylococcus aureus via Modulation of Agr Activity. *Infect Immun* **2019,** *87* (5).
58. Salam, A. M.; Quave, C. L., Targeting Virulence in Staphylococcus aureus by Chemical Inhibition of the Accessory Gene Regulator System In Vivo. *mSphere* **2018,** *3* (1).
59. Mukherjee, S.; Bassler, B. L., Bacterial quorum sensing in complex and dynamically changing environments. *Nat Rev Microbiol* **2019,** *17* (6), 371-382.
60. E, O. M.; Reen, F. J.; O'Gara, F.; McGlacken, G. P., Analogues of Pseudomonas aeruginosa signalling molecules to tackle infections. *Org Biomol Chem* **2018,** *16* (2), 169-179.
61. Lu, C.; Kirsch, B.; Zimmer, C.; de Jong, J. C.; Henn, C.; Maurer, C. K.; Musken, M.; Haussler, S.; Steinbach, A.; Hartmann, R. W., Discovery of antagonists of PqsR, a key player in 2-alkyl-4-quinolone-dependent quorum sensing in Pseudomonas aeruginosa. *Chem Biol* **2012,** *19* (3), 381-90.
62. García-Reyes, S.; Soberón-Chávez, G.; Cocotl-Yanez, M., The third quorum-sensing system of Pseudomonas aeruginosa: Pseudomonas quinolone signal and the enigmatic PqsE protein. *Journal of Medical Microbiology* **2020**.
63. Jayaseelan, S.; Ramaswamy, D.; Dharmaraj, S., Pyocyanin: production, applications, challenges and new insights. *World J Microbiol Biotechnol* **2014,** *30* (4), 1159-68.
64. Mavrodi, D. V.; Bonsall, R. F.; Delaney, S. M.; Soule, M. J.; Phillips, G.; Thomashow, L. S., Functional analysis of genes for biosynthesis of pyocyanin and phenazine-1-carboxamide from Pseudomonas aeruginosa PAO1. *J Bacteriol* **2001,** *183* (21), 6454-65.
65. Sun, S.; Zhou, L.; Jin, K.; Jiang, H.; He, Y. W., Quorum sensing systems differentially regulate the production of phenazine-1-carboxylic acid in the rhizobacterium Pseudomonas aeruginosa PA1201. *Sci Rep* **2016,** *6*, 30352.
66. Higgins, S.; Heeb, S.; Rampioni, G.; Fletcher, M. P.; Williams, P.; Camara, M., Differential Regulation of the Phenazine Biosynthetic Operons by Quorum Sensing in Pseudomonas aeruginosa PAO1-N. *Front Cell Infect Microbiol* **2018,** *8*, 252.
67. Dietrich, L. E.; Price-Whelan, A.; Petersen, A.; Whiteley, M.; Newman, D. K., The phenazine pyocyanin is a terminal signalling factor in the quorum sensing network of Pseudomonas aeruginosa. *Mol Microbiol* **2006,** *61* (5), 1308-21.
68. Castaneda-Tamez, P.; Ramirez-Peris, J.; Perez-Velazquez, J.; Kuttler, C.; Jalalimanesh, A.; Saucedo-Mora, M. A.; Jimenez-Cortes, J. G.; Maeda, T.; Gonzalez, Y.; Tomas, M.; Wood, T. K.; Garcia-Contreras, R., Pyocyanin Restricts Social Cheating in Pseudomonas aeruginosa. *Front Microbiol* **2018,** *9*, 1348.
69. Recinos, D. A.; Sekedat, M. D.; Hernandez, A.; Cohen, T. S.; Sakhtah, H.; Prince, A. S.; Price-Whelan, A.; Dietrich, L. E., Redundant phenazine operons in Pseudomonas aeruginosa exhibit environment-dependent expression and differential roles in pathogenicity. *Proc Natl Acad Sci U S A* **2012,** *109* (47), 19420-5.
70. Cabeen, M. T., Stationary phase-specific virulence factor overproduction by a lasR mutant of Pseudomonas aeruginosa. *PLoS One* **2014,** *9* (2), e88743.

71. Lu, J.; Huang, X.; Li, K.; Li, S.; Zhang, M.; Wang, Y.; Jiang, H.; Xu, Y., LysR family transcriptional regulator PqsR as repressor of pyoluteorin biosynthesis and activator of phenazine-1-carboxylic acid biosynthesis in Pseudomonas sp. M18. *J Biotechnol* **2009,** *143* (1), 1-9.
72. Sun, S.; Chen, B.; Jin, Z. J.; Zhou, L.; Fang, Y. L.; Thawai, C.; Rampioni, G.; He, Y. W., Characterization of the multiple molecular mechanisms underlying RsaL control of phenazine-1-carboxylic acid biosynthesis in the rhizosphere bacterium Pseudomonas aeruginosa PA1201. *Mol Microbiol* **2017,** *104* (6), 931-947.
73. Hall, S.; McDermott, C.; Anoopkumar-Dukie, S.; McFarland, A. J.; Forbes, A.; Perkins, A. V.; Davey, A. K.; Chess-Williams, R.; Kiefel, M. J.; Arora, D.; Grant, G. D., Cellular Effects of Pyocyanin, a Secreted Virulence Factor of Pseudomonas aeruginosa. *Toxins (Basel)* **2016,** *8* (8).
74. Marreiro de Sales-Neto, J.; Lima, E. A.; Cavalcante-Silva, L. H. A.; Vasconcelos, U.; Rodrigues-Mascarenhas, S., Anti-inflammatory potential of pyocyanin in LPS-stimulated murine macrophages. *Immunopharmacol Immunotoxicol* **2019,** *41* (1), 102-108.
75. Rada, B.; Leto, T. L., Pyocyanin effects on respiratory epithelium: relevance in Pseudomonas aeruginosa airway infections. *Trends Microbiol* **2013,** *21* (2), 73-81.
76. Rada, B.; Leto, T. L., Redox warfare between airway epithelial cells and Pseudomonas: dual oxidase versus pyocyanin. *Immunol Res* **2009,** *43* (1-3), 198-209.
77. Li, T.; Huang, X.; Yuan, Z.; Wang, L.; Chen, M.; Su, F.; Ling, X.; Piao, Z., Pyocyanin induces NK92 cell apoptosis via mitochondrial damage and elevated intracellular Ca(2). *Innate Immun* **2019,** *25* (1), 3-12.
78. Lau, G. W.; Hassett, D. J.; Ran, H.; Kong, F., The role of pyocyanin in Pseudomonas aeruginosa infection. *Trends Mol Med* **2004,** *10* (12), 599-606.
79. Muller, M.; Li, Z.; Maitz, P. K., Pseudomonas pyocyanin inhibits wound repair by inducing premature cellular senescence: role for p38 mitogen-activated protein kinase. *Burns* **2009,** *35* (4), 500-8.
80. Allen, L.; Dockrell, D. H.; Pattery, T.; Lee, D. G.; Cornelis, P.; Hellewell, P. G.; Whyte, M. K., Pyocyanin production by Pseudomonas aeruginosa induces neutrophil apoptosis and impairs neutrophil-mediated host defenses in vivo. *J Immunol* **2005,** *174* (6), 3643-9.
81. Manago, A.; Becker, K. A.; Carpinteiro, A.; Wilker, B.; Soddemann, M.; Seitz, A. P.; Edwards, M. J.; Grassme, H.; Szabo, I.; Gulbins, E., Pseudomonas aeruginosa pyocyanin induces neutrophil death via mitochondrial reactive oxygen species and mitochondrial acid sphingomyelinase. *Antioxid Redox Signal* **2015,** *22* (13), 1097-110.
82. Meirelles, L. A.; Newman, D. K., Both toxic and beneficial effects of pyocyanin contribute to the lifecycle of Pseudomonas aeruginosa. *Mol Microbiol* **2018,** *110* (6), 995-1010.
83. Moayedi, A.; Nowroozi, J.; Akhavan Sepahy, A., Cytotoxic effect of pyocyanin on human pancreatic cancer cell line (Panc-1). *Iran J Basic Med Sci* **2018,** *21* (8), 794-799.
84. Larian, N.; Ensor, M.; Thatcher, S. E.; English, V.; Morris, A. J.; Stromberg, A.; Cassis, L. A., Pseudomonas aeruginosa-derived pyocyanin reduces adipocyte differentiation, body weight, and fat mass as mechanisms contributing to septic cachexia. *Food Chem Toxicol* **2019,** *130*, 219-230.
85. Holdsworth, S. R.; Gan, P. Y., Cytokines: Names and Numbers You Should Care About. *Clin J Am Soc Nephrol* **2015,** *10* (12), 2243-54.

86. Kanthakumar, K.; Taylor, G. W.; Cundell, D. R.; Dowling, R. B.; Johnson, M.; Cole, P. J.; Wilson, R., The effect of bacterial toxins on levels of intracellular adenosine nucleotides and human ciliary beat frequency. *Pulm Pharmacol* **1996,** *9* (4), 223-30.
87. Shellito, J.; Nelson, S.; Sorensen, R. U., Effect of pyocyanine, a pigment of Pseudomonas aeruginosa, on production of reactive nitrogen intermediates by murine alveolar macrophages. *Infect Immun* **1992,** *60* (9), 3913-5.
88. Breuer, O.; Caudri, D.; Akesson, L.; Ranganathan, S.; Stick, S. M.; Schultz, A.; Arest, C. F., The clinical significance of oropharyngeal cultures in young children with cystic fibrosis. *Eur Respir J* **2018,** *51* (5).
89. Alhogail, S.; Suaifan, G.; Bikker, F. J.; Kaman, W. E.; Weber, K.; Cialla-May, D.; Popp, J.; Zourob, M. M., Rapid Colorimetric Detection of Pseudomonas aeruginosa in Clinical Isolates Using a Magnetic Nanoparticle Biosensor. *ACS Omega* **2019,** *4* (26), 21684-21688.
90. Kaman, W. E.; Arkoubi-El Arkoubi, N. E.; Roffel, S.; Endtz, H. P.; van Belkum, A.; Bikker, F. J.; Hays, J. P., Evaluation of a FRET-peptide substrate to predict virulence in Pseudomonas aeruginosa. *PLoS One* **2013,** *8* (11), e81428.
91. Thet, N. T.; Hong, S. H.; Marshall, S.; Laabei, M.; Toby, A.; Jenkins, A., Visible, colorimetric dissemination between pathogenic strains of Staphylococcus aureus and Pseudomonas aeruginosa using fluorescent dye containing lipid vesicles. *Biosens Bioelectron* **2013,** *41*, 538-43.
92. Sharma, C.; Shukla, A. K.; Acharya, A., Rational design of a FRET-based nanoprobe of gold-conjugated carbon dots for simultaneous monitoring and disruption of Pseudomonas aeruginosa biofilm through selective detection of virulence factor pyocyanin. *Environmental Science: Nano* **2021,** *8* (6), 1713-1728.
93. Tanaka, Y.; Khoo, E. H.; Salleh, N.; Teo, S. L.; Ow, S. Y.; Sutarlie, L.; Su, X., A portable SERS sensor for pyocyanin detection in simulated wound fluid and through swab sampling. *Analyst* **2021,** *146* (22), 6924-6934.
94. Feizabadi, M. M.; Majnooni, A.; Nomanpour, B.; Fatolahzadeh, B.; Raji, N.; Delfani, S.; Habibi, M.; Asadi, S.; Parvin, M., Direct detection of Pseudomonas aeruginosa from patients with healthcare associated pneumonia by real time PCR. *Infect Genet Evol* **2010,** *10* (8), 1247-51.
95. Aghamollaei, H.; Moghaddam, M. M.; Kooshki, H.; Heiat, M.; Mirnejad, R.; Barzi, N. S., Detection of Pseudomonas aeruginosa by a triplex polymerase chain reaction assay based on lasI/R and gyrB genes. *J Infect Public Health* **2015,** *8* (4), 314-22.
96. Tang, Y.; Zou, J.; Ma, C.; Ali, Z.; Li, Z.; Li, X.; Ma, N.; Mou, X.; Deng, Y.; Zhang, L.; Li, K.; Lu, G.; Yang, H.; He, N., Highly sensitive and rapid detection of Pseudomonas aeruginosa based on magnetic enrichment and magnetic separation. *Theranostics* **2013,** *3* (2), 85-92.
97. Tang, Y.; Ali, Z.; Zou, J.; Yang, K.; Mou, X.; Li, Z.; Deng, Y.; Lu, Z.; Ma, C.; Shah, M. A.; Elingarami, S.; Yang, H.; He, N., Detection of Pseudomonas aeruginosa based on magnetic enrichment and nested PCR. *J Nanosci Nanotechnol* **2014,** *14* (7), 4886-90.
98. Dong, D.; Zou, D.; Liu, H.; Yang, Z.; Huang, S.; Liu, N.; He, X.; Liu, W.; Huang, L., Rapid detection of Pseudomonas aeruginosa targeting the toxA gene in intensive care unit patients from Beijing, China. *Front Microbiol* **2015,** *6*, 1100.
99. Elkhawaga, A. A.; Khalifa, M. M.; El-Badawy, O.; Hassan, M. A.; El-Said, W. A., Rapid and highly sensitive detection of pyocyanin biomarker in different Pseudomonas aeruginosa infections using gold nanoparticles modified sensor. *PLoS One* **2019,** *14* (7), e0216438.

100. e Silva, R. F.; Longo Cesar Paixão, T. R.; Der Torossian Torres, M.; de Araujo, W. R., Simple and inexpensive electrochemical paper-based analytical device for sensitive detection of Pseudomonas aeruginosa. *Sensors and Actuators B: Chemical* **2020,** *308*, 127669.
101. Alatraktchi, F. A.; Svendsen, W. E.; Molin, S., Electrochemical Detection of Pyocyanin as a Biomarker for Pseudomonas aeruginosa: A Focused Review. *Sensors (Basel)* **2020,** *20* (18).
102. Pastells, C.; Pascual, N.; Sanchez-Baeza, F.; Marco, M. P., Immunochemical Determination of Pyocyanin and 1-Hydroxyphenazine as Potential Biomarkers of Pseudomonas aeruginosa Infections. *Anal Chem* **2016,** *88* (3), 1631-8.
103. Mauch, R. M.; Rossi, C. L.; Ribeiro, J. D.; Ribeiro, A. F.; Nolasco da Silva, M. T.; Levy, C. E., Assessment of IgG antibodies to Pseudomonas aeruginosa in patients with cystic fibrosis by an enzyme-linked immunosorbent assay (ELISA). *Diagn Pathol* **2014,** *9*, 158.
104. Mena, A.; Smith, E. E.; Burns, J. L.; Speert, D. P.; Moskowitz, S. M.; Perez, J. L.; Oliver, A., Genetic adaptation of Pseudomonas aeruginosa to the airways of cystic fibrosis patients is catalyzed by hypermutation. *J Bacteriol* **2008,** *190* (24), 7910-7.
105. Cheluvappa, R., Standardized chemical synthesis of Pseudomonas aeruginosa pyocyanin. *MethodsX* **2014,** *1*, 67-73.
106. Sharp, D.; Gladstone, P.; Smith, R. B.; Forsythe, S.; Davis, J., Approaching intelligent infection diagnostics: Carbon fibre sensor for electrochemical pyocyanin detection. *Bioelectrochemistry* **2010,** *77* (2), 114-9.
107. Alatraktchi, F. A.; Johansen, H. K.; Molin, S.; Svendsen, W. E., Electrochemical sensing of biomarker for diagnostics of bacteria-specific infections. *Nanomedicine (Lond)* **2016,** *11* (16), 2185-95.
108. Alatraktchi, F. A.; Noori, J. S.; Tanev, G. P.; Mortensen, J.; Dimaki, M.; Johansen, H. K.; Madsen, J.; Molin, S.; Svendsen, W. E., Paper-based sensors for rapid detection of virulence factor produced by Pseudomonas aeruginosa. *PLoS One* **2018,** *13* (3), e0194157.
109. Khalifa, M. M.; Elkhawaga, A. A.; Hassan, M. A.; Zahran, A. M.; Fathalla, A. M.; El-Said, W. A.; El-Badawy, O., Highly specific Electrochemical Sensing of Pseudomonas aeruginosa in patients suffering from corneal ulcers: A comparative study. *Sci Rep* **2019,** *9* (1), 18320.
110. Cernat, A.; Canciu, A.; Tertis, M.; Graur, F.; Cristea, C., Synergic action of thermosensitive hydrogel and Au/Ag nanoalloy for sensitive and selective detection of pyocyanin. *Anal Bioanal Chem* **2019,** *411* (17), 3829-3838.
111. Rashid, J. I. A.; Kannan, V.; Ahmad, M. H.; Mon, A. A.; Taufik, S.; Miskon, A.; Ong, K. K.; Yusof, N. A., An electrochemical sensor based on gold nanoparticles-functionalized reduced graphene oxide screen printed electrode for the detection of pyocyanin biomarker in Pseudomonas aeruginosa infection. *Mater Sci Eng C Mater Biol Appl* **2021,** *120*, 111625.
112. Zukovskaja, O.; Jahn, I. J.; Weber, K.; Cialla-May, D.; Popp, J., Detection of Pseudomonas aeruginosa Metabolite Pyocyanin in Water and Saliva by Employing the SERS Technique. *Sensors (Basel)* **2017,** *17* (8).
113. Jia, F.; Barber, E.; Turasan, H.; Seo, S.; Dai, R.; Liu, L.; Li, X.; Bhunia, A. K.; Kokini, J. L., Detection of Pyocyanin Using a New Biodegradable SERS Biosensor Fabricated Using Gold Coated Zein Nanostructures Further Decorated with Gold Nanoparticles. *J Agric Food Chem* **2019,** *67* (16), 4603-4610.
114. Zukovskaja, O.; Agafilushkina, S.; Sivakov, V.; Weber, K.; Cialla-May, D.; Osminkina, L.; Popp, J., Rapid detection of the bacterial biomarker pyocyanin in artificial sputum using a

SERS-active silicon nanowire matrix covered by bimetallic noble metal nanoparticles. *Talanta* **2019,** *202*, 171-177.

115. Zelini, P.; Fornara, C.; Furione, M.; Sarasini, A.; Klemens, J.; Arossa, A.; Spinillo, A.; Gerna, G.; Lilleri, D., Determination of anti-p52 IgM and anti-gB IgG by ELISA as a novel diagnostic tool for detection of early and late phase of primary human cytomegalovirus infections during pregnancy. *J Clin Virol* **2019,** *120*, 38-43.
116. Vatankhah, M.; Beheshti, N.; Mirkalantari, S.; Khoramabadi, N.; Aghababa, H.; Mahdavi, M., Recombinant Omp2b antigen-based ELISA is an efficient tool for specific serodiagnosis of animal brucellosis. *Braz J Microbiol* **2019,** *50* (4), 979-984.
117. Alatraktchi, F. A.; Dimaki, M.; Stovring, N.; Johansen, H. K.; Molin, S.; Svendsen, W. E., Nanograss sensor for selective detection of Pseudomonas aeruginosa by pyocyanin identification in airway samples. *Anal Biochem* **2020,** *593*, 113586.
118. Wilson, R.; Sykes, D. A.; Watson, D.; Rutman, A.; Taylor, G. W.; Cole, P. J., Measurement of Pseudomonas aeruginosa phenazine pigments in sputum and assessment of their contribution to sputum sol toxicity for respiratory epithelium. *Infect Immun* **1988,** *56* (9), 2515-7.
119. Hunter, R. C.; Klepac-Ceraj, V.; Lorenzi, M. M.; Grotzinger, H.; Martin, T. R.; Newman, D. K., Phenazine content in the cystic fibrosis respiratory tract negatively correlates with lung function and microbial complexity. *Am J Respir Cell Mol Biol* **2012,** *47* (6), 738-45.
120. Retraction: Phenazine Content in the Cystic Fibrosis Respiratory Tract Negatively correlates with Lung Function and Microbial Complexity. *Am. J. Respir. Cell Mol Biol* **2019,** *60* (1), 134.
121. Silva, L. V.; Galdino, A. C.; Nunes, A. P.; dos Santos, K. R.; Moreira, B. M.; Cacci, L. C.; Sodre, C. L.; Ziccardi, M.; Branquinha, M. H.; Santos, A. L., Virulence attributes in Brazilian clinical isolates of Pseudomonas aeruginosa. *Int J Med Microbiol* **2014,** *304* (8), 990-1000.
122. Elliott, J.; Simoska, O.; Karasik, S.; Shear, J. B.; Stevenson, K. J., Transparent Carbon Ultramicroelectrode Arrays for the Electrochemical Detection of a Bacterial Warfare Toxin, Pyocyanin. *Anal Chem* **2017,** *89* (12), 6285-6289.
123. Brandenburg, K. S.; Weaver, A. J., Jr.; Karna, S. L. R.; You, T.; Chen, P.; Stryk, S. V.; Qian, L.; Pineda, U.; Abercrombie, J. J.; Leung, K. P., Formation of Pseudomonas aeruginosa Biofilms in Full-thickness Scald Burn Wounds in Rats. *Sci Rep* **2019,** *9* (1), 13627.
124. Cruickshank, C. N.; Lowbury, E. J., The effect of pyocyanin on human skin cells and leucocytes. *Br J Exp Pathol* **1953,** *34* (6), 583-7.
125. Khadim, M. M. A. M., M. F., Pyocyanin and Biofilm Formation in Pseudomonas aeruginosa Isolated from Burn Infections in Baghdad, Iraq. *Jordan Journal of Biological Sciences* **2019,** *12* (1), 31-35.
126. Reimer, A.; Edvaller, B.; Johansson, B., Concentrations of the Pseudomonas aeruginosa toxin pyocyanin in human ear secretions. *Acta Otolaryngol Suppl* **2000,** *543*, 86-8.
127. Gupte, A.; Jyot, J.; Ravi, M.; Ramphal, R., High pyocyanin production and non-motility of Pseudomonas aeruginosa isolates are correlated with septic shock or death in bacteremic patients. *PLoS One* **2021,** *16* (6), e0253259.

Chapter 2

QS inhibition as a tool for controlling infectious diseases

The increase in multidrug resisant (MDR) bacteria and the ineffectiveness of antibiotics have aggravated the incidence of infectious diseases worldwide becoming one of the most important concerns on global health today. In this context, new techniques based on blocking or attenuating virulence pathways could position as a very interesting approach to battle against this threat. Thus, in this chapter strategies focused on inhibiting the conserved quorum sensing (QS) system are summarized highlighting the advantages and possible drawbacks of each approach and also presenting the possible future perspectives on this field.

In preparation

***Rodriguez-Urretavizcaya, B.**; Vilaplana, Ll.; Marco, M.P. Strategies for quorum sensing inhibition as a tool for controlling Pseudomonas aeruginosa infections. (2021).*

2.1 Introduction

Disruption of quorum sensing (QS) system appears as a promising strategy to overcome antibiotic resistance mainly due to its ability to regulate different important processes related to pathogenicity[1-2] without affecting bacterial viability, which will minimize the appearance of resistance processes[3-4]. Thus, in recent years, efforts have been focused on the development of molecules with the ability of interfering with one or more steps of the QS pathways. These molecules are known as quorum quenchers or QS inhibitors (QQ and QSI, respectively)[5] and can be of different chemical nature[5-6].

Given the structure of QS system, it can be blocked mainly at three different points of the route. Thus, the quenching strategies used are based on (Figure 2. 1)[7-8]:

A. disrupting autoinducer (AI) biosynthetic pathways**.**
B. preventing the binding of AI to its cognate receptor.
C. arresting or blocking different QS targets.

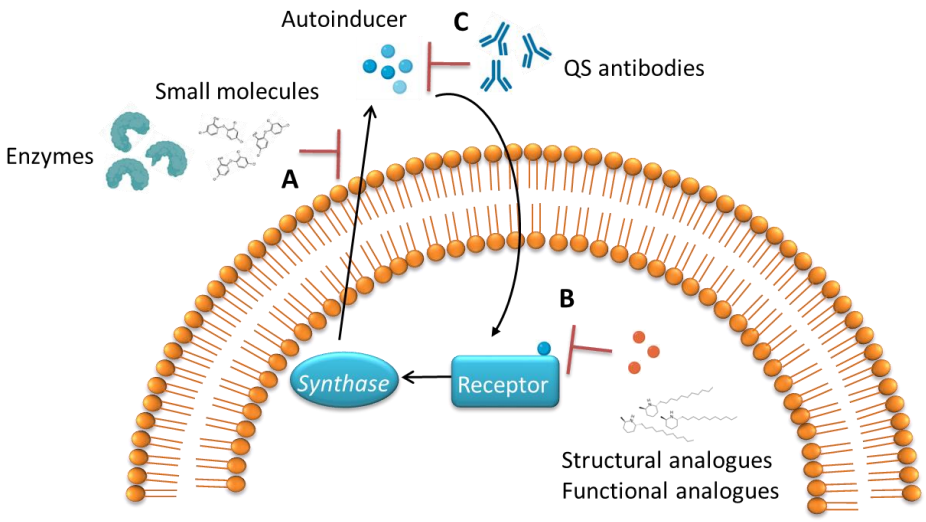

Figure 2. 1 *Different strategies used for disrupting QS. (A) Avoiding AI biosynthesis using enzymes or small molecules. (B) Preventing AI binding to its cognate receptor with structural and functional analogues. (C) Sequestering AI with scavengers (i.e. antibodies, cyclodextrins...).*

This chapter attempts to provide an overview and to discuss about the already reported strategies based on blocking different components of each of the *P. aeruginosa* QS systems: Iqs, Rhl, Las and Pqs.

2.2 Blocking *P. aeruginosa* QS systems

First, examples of QSIs of the least studied QS system, Iqs, will be presented. Then, QQ molecules against Las and Rhl systems will be analysed since both systems have similar mechanism based on the production and detection of acylated homoserine lactones (AHLs) AIs. Finally, inhibitor examples of the *P. aeruginosa* specific Pqs system will be given.

2.2.1 Iqs system

Due to the lack of information about the mechanism of action of this system and the unknown identification of its cognate receptor[9], B-11 Integrated Quorum Sensing (IQS) analogue is the only IQS inhibitor already reported for this system[10]. This molecule was obtained by reaction of thiazole-4-carboxylic acid with different linear alcohols. As illustrated in Figure 2. 2, B-11 keeps the same thizaole ring of IQS molecule which confers it with high anti-biofilm activity and, also, with the capacity of controlling *pqs* and *rhl* expression. This translates into a 30 % decrease in rhamnolipid levels (glycolipidic surface-active molecules involve in early stages of infection) resulting in virulence reduction. Nevertheless, as this QS system is only activated under phosphate depletion conditions, B-11 is only relevant disrupting QS in that situation.

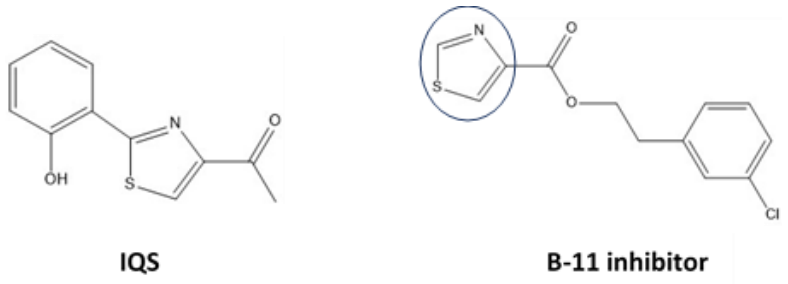

Figure 2. 2 *IQS structure (left) and B-11 inhibitor (right) structures. The thiazole ring is circled in blue and it confers the inhibition properties to the QSI.*

2.2.2 Rhl and Las system

Despite both Las and Rhl systems activate and modulate the expression of hundreds of specific genes related with virulence and biofilm formation[11], due to the hierarchical role of Las system, most QSIs target Las system rather than Rhl system. However, most inhibitors against Las act as "dual inhibitors" disrupting both systems since QS pathways are interconnected. In this section, examples of QSIs inhibiting AHLs and LuxR receptors are summarized as they are the most relevant examples already reported in this case[12]. The examples presented below have been classified according to the before mentioned classification of QS disrupting strategies (see Figure 2. 1). Therefore, first AI biosynthesis disruption examples based on AI degradation are explained

followed by AI-cognate receptor prevention (LuxR antagonists) and AHL capture using antibodies (Abs).

2.2.2.1 Autoinducers degradation

Lactonases, acylases and oxidoreductases are the most common QSIs for AHL degradation[13]. The first two type of enzymes induce the hydrolysis of the ester bond of the AHL ring (lactonolisys)[14] and the hydrolysis of the acyl-amide bond in a specific and irreversible manner[14], respectively. In contrast, oxidorreductases modify the chemical structure of the corresponding AI by catalysing its reduction or oxidation. The most recent examples of these type of enzymes are described below.

In this regard, Dong et al. [15] cloned and expressed the *AI inactivation* from *Kurthia huakui* LAM0618^T gene (*aiiK*) in *E. coli* to obtained a purified recombinant AiiK lactonase. This AiiK was found to reduce biofilm formation and pyocyanin (PYO) production on PAO1 strain 2-fold and 4-fold times, respectively. Besides, Wahjudi et al. [16] evaluated the acylation capacity of the PA0305 protein produced by *P. aeruginosa* due to its close similarity to HacB acylase from *Pseudomonas syringae*. Thus, they demonstrated that PA0305 was able to degrade AHLs with acyl side chains ranging in length from 6 to 14 C. Furthermore, the overexpression of *pa0305* gene resulted in a significant reduction after 5 h post-inoculation in LasB elastase and PYO production in PAO1 strain. In the case of oxidoreductases, Bijtenhoorn et al.[17] identified the first Nicotinamide Adenine Dinucleotide Phosphate (NADP)-dependent short chain dehydrogenase/reductase (SDR) with the ability of inactivating 3oxoC_{12}-HSL by transforming it to 3OHC_{12}-HSL. The gene encoding for this enzyme was named bpiB09 and was isolated from a soil metagenome. Together with this, BpiB09 also induced a reduction on PAO1 biofilm tichkness from 30-35 µm to 5 - 10 µm after 72 h and a decrease of around 75 % in PYO production. Table 2. 1 summarizes these and other relevant examples of QQ enzymes in *P. aeruginosa*. More examples are described by Fetzner et al.[18].

Table 2. 1 *Classification of some relevant examples of lactonases, acylases and oxidoreductases as QQs in P. aeruginosa.*

QQ enzyme	Target	Main effects	Reference
Lactonases			
AI inactivation A (AiiA)	Degradation of AHLs	Decreased pyocyanin (PYO) levels	[19]
PON1	Degradation of AHLs	Blocked biofilm formation	[20]
SsoPox	Degradation of AHLs	Decreased protease and PYO secretion and biofilm formation	[21]
SsoPox-1	Degradation of AHLs	Decreased LasB, PYO and biofilm formation	[22]
Aii810	Degradation of AHLs	Decreased virulence and biofilm formation. Degraded 3oxoC_{12}-HLS and C_4-HSL by 72.3 and 100 %	[23]
AiiK	Degradation of AHLs	Decreased PYO production and inhibited biofilm formation	[15]
Acylases			
AiiD	Hydrolize AHL amide	Decreased elastase and PYO secretion, among others	[24]
QuiP	Degradation of long chain AHLs (12-18)	Decreased accumulation of 3oxoC_{12}-HLS	[25]
HacB (PA0305)	Degradation of AHLs (6-14)	Decreased of LasB and PYO	[16]
Oxidoreductases			
BpiB09	Transformation of 3oxoC_{12}-HSL to 3OHC_{12}-HLS	Decreased biofilm thickness from 30-35 µm to 5-10 µm and, also, reduced PYO	[17]
CYP102A1	Oxidation of AHLs of lengths 12-18	Decreased QS activity	[26]

However, despite the promising results showed in Table 2. 1, QQ enzymes present some constraints related with their structural integrity when they reach the infection[27] site. This is caused by their susceptibility to proteolytic degradation[18] and the possible onset of a high immunogenic response due to their foreign nature[28].

An alternative strategy to prevent AHLs biosynthesis is the use of small molecules. In this direction, Hoang et al.[29] found that triclosan (5-chloro-2-(2,4-dichlorophenoxy)phenol) inhibits AHLs production in *P. aeruginosa* by decreasing the activity of enoyl-acyl carrier protein reductase (ENR), which controls the length of acyl chains. Further studies showed that subinhibitory concentrations of triclosan affected 44 % of the global gene transcription in *P. aeruginosa*, being the QS-regulated genes among the most strongly downregulated ones[30]. Related with these findings, it has been recently reported[31] a structure-based identification

study of *P. aeruginosa* QSIs built on studying a 3D structure of enoyl-(acyl-carrier-protein) reductase (FabI). Active site residues were identified from FabI-triclosan complex. With these studies eight lead-like molecules were identified which can be used as starting point compounds to develop new QSIs.

All these examples point the potential of this strategy regarding the development of new QSI through inhibition of AIs biosynthetic pathways. However, supressing AHL synthesis could also have negative consequences since not all processes controlled by these AIs contribute necessarily to bacterial pathogenesis.

2.2.2.2 LuxR antagonists

2.2.2.2.1 Structural analogues

A common approach for disrupting gram negative QS systems consists on blocking the cognate receptors with molecules showing a similar chemical structure compared with the corresponding AIs (analogues). This structural resemblance allows analogue binding to the receptor without triggering any effect but preventing the action of the native AI. Most AHL analogues are based on 3oxoC12-HSL acyl chain modifications given that the head group of this compound is required for interacting with LuxR. Therefore, modifications on the head group will result in analogues without the required capacity of binding to the corresponding LuxR receptor. Nevertheless, one example of AHL analogue with head modifications has been reported by O'Loughlin et al.[32] who synthesized a meta-bromo thiolactone (mBTL) (Figure 2. 3) molecule that acts as a potent dual inhibitor in *in vivo* conditions antagonizing/agonizing LasR and RhlR, respectively, and partially controlling virulence in wild type (WT) PA14 strain.

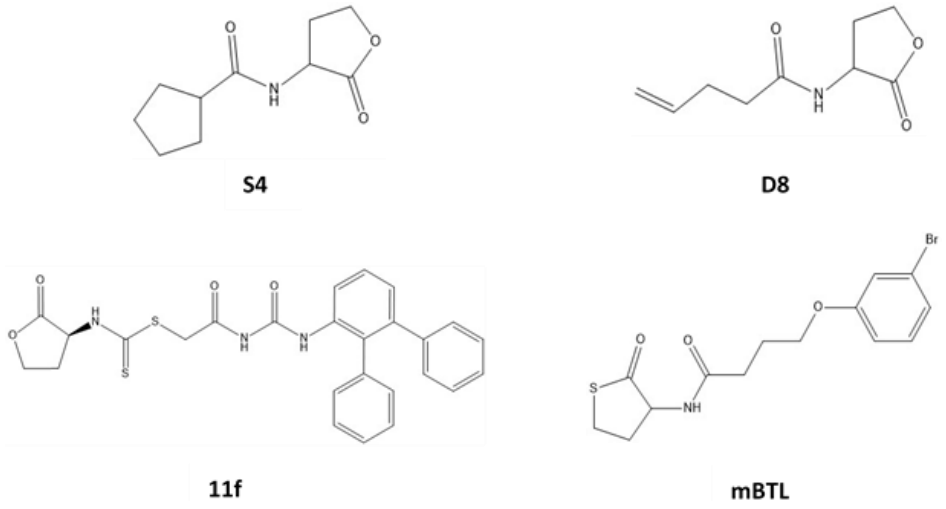

Figure 2. 3 *Chemical structures of AHL analogues D8, S4, 11f and meta-bromo-thiolactone (mBTL). S4 and D8 present short side chains (ciclopentane and 1-butene, respectively); 11f and mBTL, long side chains.*

Most 3oxoC_{12}-HSL analogues with acyl chain modifications behave as dual inhibitors due to the interconnection between QS systems[33]. In this sense, Welsh et al.[34] screened AHL analogues that targeted RhlR and found 2 short chain AHL analogues (D8 and S4) (Figure 2. 3) to be potent inhibitors of PYO production on bacterial cultures, decreasing by 84 and 88 % its levels, respectively. Moreover, these experiments showed a half maximal inhibitory concentration (IC_{50}) values of 9.9 and 6.8 μM for D8 and S4, which position them as very promising QS-based PYO inhibitors. In the same direction, Liu et al.[35] recently described a competitive AHL analogue named 11f inhibitor that presented a phenylurea group on its side chain (Figure 2. 3). This inhibitor was able of reducing PYO and rhamnolipid levels together with a reduction on biofilm formation on bacterial cultures by 30.3, 28.5 and 28.6 %, respectively.

A more recent approach regarding the use of AHL analogues focuses on targeting synthases instead of the cognate receptor. Thus, Shin et al.[36] have developed a set of AHL analogues against RhlI by modifying the acyl chain and the head group of the corresponding AHL. RhlI catalyses the acylation of S-adenosyl methionine (SAM) by C_4- acyl carrier protein (ACP) with the corresponding release of holo-ACP thiol and C_4-HSL synthesis. Therefore, the inhibitory activity of RhlI inhibitors was determined by measuring holo-ACP thiol content. Figure 2. 4 shows molecular features required for AHL analogues to be efficient RhlI inhibitors. All already reported inhibitors of this type showed IC_{50} at the μM range.

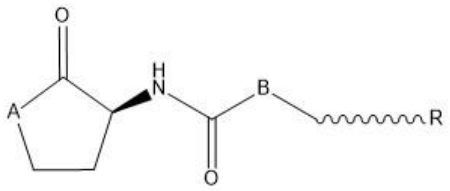

Figure 2. 4 *Molecular features of RhlI inhibitors based on AHL structure. A= S instead of O; B= CH_2; R= >C_{10}, aromatic and branched side chains. The preferable stereoisomer is D.*

2.2.2.2.2 Functional analogues

Unlike the already mentioned AHL analogues, most described functional analogues, which are structurally non-related with AHLs, are natural compounds. Thus, in 2008, Park et al.[37] described that Solenopsin A, a venom alkaloid from the fire ant *Solenopsis invicta*, inhibits Rhl system acting as C_4-HSL competitor. Moreover, 15 μmol L^{-1} of Solenopsin A decreased PYO levels and biofilm production by 40 and 50 %, respectively, when tested on different *P. aeruginosa* strain cultures. These results are remarkable due to the fact that very few inhibitors have been reported affecting directly the Rhl system.

Also, in this context, Vandeputte et al.[38] analyzed a group of flavonoids (polyphenolic plant and fungus secondary metabolites) according to their capacity of reducing 3oxoC_{12}-HSL and C_4-HSL production in PAO1 strain, achieved by inhibiting *lasR* and *rhlR* expression. They found that the compound naringenin, a flavonoid with a flavonone structural group, reduced PYO and elastase levels by 87 and 46 %, respectively, at 4 μM concentration. The presence of two hydroxyl groups, one at position 7 and the second one in the A-ring backbone, were required for LasR and RhlR inhibition[39]. Another compound that showed LasR inhibitory activity in PAO1 strain was found by Tan et al.[40] after screening a library of 3,040 natural compounds and their derivatives. Thus, they identified 5-imino-4,6-dihydro-3H-1,2,3-triazolo[5,4-*d*]-pyrimidin-7-one (G1) molecule for its ability to limit almost completely elastase production in PAO1 strain cultures when assayed at 50 and 100 μM concentrations. G1 also inhibited RhlR in LasR absence.

Other widely studied examples of natural QSIs are furanones from which even more active synthetic molecules have been produced. In this sense, Manefield et al.[41] demonstrated that halogenated furanones, isolated from the *Delisea pulchra* macroalga, prevented the binding of natural AHLs avoiding QS system signalling. These compounds present a similar structure to that of the natural AHL, but instead of the of homoserine-lactone ring, they have a furan ring. Nevertheless, halogenated furanones are extremely reactive and can be toxic to human cells limiting their potential use as QSIs. Hence, synthetic derivatives have been obtained to increase their QQ activity and decrease their toxic effect. In this sense, Wu et al.[42] studied C30 and C56 synthetic furanones in mice model with pulmonary infection caused by *P. aeruginosa*. The intravenous administration of both furanones facilitated the elimination of bacteria established in the lung reducing lung pathology and significantly increasing the survival time of mice.

2.2.2.3 QS antibodies

One of the most promising approaches to block QS system consists on using QQ Abs given their high specificity for the corresponding targets[2]. Moreover, Ab administration may preserve nonpathogenic gut microflora exerting less selective pressure for the appearance of resistance mechanisms[43] which places them as useful immunotherapeutic tools.

The highly conserved molecular scaffold and extracellular distribution of AHLs, place them as an ideal target for Ab-based therapy. In this direction, Kaufmann et al.[44] developed an anti 3oxoC_{12}-HSL monoclonal Ab (mAb), named RS2-1G9, with inhibitory effects on both PAO1 and on the double knockout PAO-JM2 (strain that lacks *rhlI* and *lasI*) cultures. The addition of RS2-1G9 mAb

reduced PYO levels by 80 and 30 % in both *P. aeruginosa* strains respectively, when administered at 7.8 µM[44-45]. Furthermore, Palliyil et al.[46] obtained a panel of sheep-mouse chimeric mAbs against AHLs by sheep immunization and recombinant Ab technology. These mAbs were first tested in *in vivo* conditions using the nematode worm *C. elegants* and, further, in a nonneutropenic lung model of mice infected with *P. aeruginosa* showing increasing survival rates when used at 500 nM concentration. In a similar vein, since natural Abs to 3oxoC_{12}-HSL are not produced by neither humans nor animals due to its low molecular weigth (300 Da), Miyairi et al.[47] immunized mice with acute *P. aeruginosa* lung infection with 3oxoC_{12}-HSL−bovine serum albumin (BSA) obtaining high titers of specific Abs against 3oxoC_{12}-HSL. Moreover, the presence of specific Abs was strongly correlated with mice survival. Indeed, control mice died by day 2 after bacteria administration while 36 % of the immunized mice rurvived to day 4.

Another common strategy consists in exploiting the catalytic activity of Abs. In this case, Abs are raised against haptens that mimic the transition state of a specific reaction and most of them are inspired on AHL degrading enzymes such as amidases and lactonases[2]. Lamo Marin et al. screened a panel of 17 catalytic Abs by testing their ability to block the signalling cascade of AHLs in PAO1 strain cultures and concluded that XYD-11G2 mAb (median lethal dosis; LD_{50} =23.6 µM) catalysed 3oxoC_{12}-HSL hydrolysis with moderate effectiveness, decreasing by 40 % PYO levels when tested at 10 µM[44, 48].

There are also Abs that specifically quench virulence factors (VFs) reducing and even avoiding pathogenesis processes caused by them[49]. KB001 (KaloBios) is an example of a pegylated mAb Fab fragment that targets PcrV secretion protein, which is located on the tip of the *P. aeruginosa* type 3 secretion system (T3SS). KB001 showed promising results when administered to mechanically ventilated subjects and also in patients suffering CF[49]. However, phase II clinical trials did not reach the required effectiveness criteria. In the same context, V2L2MD anti- PcrV mAb showed better *in vivo* protection levels than mAb166, the progenitor Ab of the clinical candidate KB001-A, since it exhibited a higher affinity towards PcrV[50].

Although the hierarchical Las system is positioned at the top of *P. aeruginosa* QS networks, it does not always play a crucial role in QS activity. This is the case of CF patients where Las pathway is often inactivated due to mutations in LasR. Therefore, since Las system may be nonessential in chronic infections, in these cases Pqs QS pathway and particularly PqsR molecule, appears as an interesting target due to its role in both chronic and acute infections[51].

2.2.3 Pqs QS system

Unlike Las and Rhl, Pqs system has been only described in *P. aeruginosa*, making its disruption more selective[52]. The general biosynthetic pathway of PQS and its precursor HHQ involves different enzymatic reactions including PqsA, PqsD, PqsH and PqsBC enzymes (see Figure 2. 5). The inhibition of these enzymes shows high impact in HHQ and PQS levels, finally causing QS disruption[53]. Thus, Pqs system blockage is mainly based on the inhibition of these enzymes.

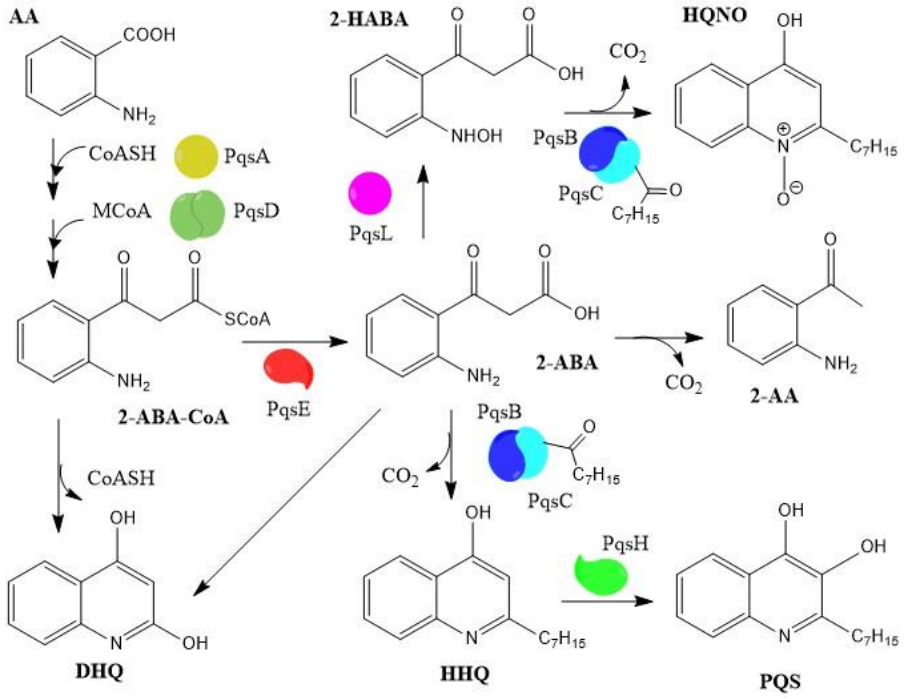

Figure 2. 5 *Biosynthetic pathway of Pqs QS system. AA = anthranilic acid; CoASH = Coenzyme A; MCoA = malonyl CoA; 2-ABA-CoA = 2'-aminobenzoylacetyl-CoA; DHQ = dihydroxyquinoline; 2-AA = 2'-aminoacetophenone; 2-HABA = 2'-hydroxylaminobenzoylacetate; HHQ = 4-hydroxy-2-heptylquinoline-N-oxide; PQS = P. aeruginosa Quinolone Signal. Adapted from Allegreta et al.* [53].

2.2.3.1 PqsA inhibition

Ji et al.[54] reported the design and synthesis of sulfonyladenosine anthranilyl-adenosine monophosphate (AMP) analogues (reaction intermediate) and identified anthranilyl-adeonsine-5'-O-monosulfamate (AMS) and sulfamide anthranilyl-5'-(aminodeoxy)adenosine-5'-N-monosulfamide (AMSN) as two potent PqsA inhibitors, affecting also HHQ and PQS biosynthesis. Anthranilyl-AMSN was the most potent inhibitor lowering HHQ and PQS levels by 90 and 92 %, respectively. However, those inhibitors showed limited permeability (2 -3 %), which made them less active, as demonstrated by accumulation studies carried out in PA14 cell cultures.

Another approach to inhibit PqsA was described by Pustelny et al.[55]. They studied the activity of 2,4-dioxygenase (Hod) enzyme due to the high similarity between its natural substrate and PQS. They elicited that Hod enzyme is able to catalyse the conversion of PQS to N-octanoylantranilic acid and carbon monoxide in PAO1 strain cultures reducing *pqsA* gene expression and PYO production by 70 and 60 %, respectively. Nevertheless, the efficiency of Hod was reduced by extracellular proteases.

2.2.3.2 PqsD inhibition

The first PqsD inhibitors were described by Storz et al.[56] based on acetyl coenzyme A (AcoA) molecule and its tetrahedral transition state. AcoA is the first substrate used by PqsD, which is further transformed to HHQ and/or PQS. Hence, they evaluated the inhibitory capacity of some of these analogues measuring HHQ and PQS levels by High Performance Liquid Chromatography – Mass Spectroscopy (HPLC-MS). They found some of these compounds to reduce HHQ and PQS levels by up to 77 and 42 % when used at 250 μM in PA14 bacterial cultures. Furthermore, biofilm formation was also reduced by 35 % using the same concentration. A year later, Sahner et al.[57] reported a PqsD covalent inhibitor corresponding to 5-aryl-ureidothiophene-2-carboxylix acid structure, which was identified by performing isothermal titration calorimetry and surface plasmon resonance (SPR) studies. Further introduction of amino acids at the ureido motif improved its permeability. Moreover, they analysed the activity of molecules with similar scaffold to the previously selected one and found that the most active inhibitor (ureidothiophene-2-carboxylic acid; IC_{50} =0.5 μM) had a phenylalanine substituent also at the ureido motif[58]. Therefore, they confirmed the relevance of substituents in this ureido part. All of these assays were performed in cell free systems, meaning they were tested in *in vitro* conditions using only cellular components. In contrast, none of these inhibitors were active in whole cell assays (PA14 cultures) mainly due to permeation and efflux problems.

Another important group of PqsD inhibitors focuses on 2-benzamidobenzoic acids (BB), which are β-ketoacyl-ACP synthase (FabH) inhibitors. Their relevance is mainly due to the structural similarity between PqsD and FabH. Thus, Weidel et al.[59] identified the first small molecules of this class and described that substituents at position 4 and 5 in the 2-aminobenzoic acid scaffold and the presence of a hydroxyl group at position 6 resulted in the most potent PqsD inhibitors reported. Moreover, Hinsberger et al.[60] analysed these inhibitors in an *in vitro* assay and modified some substituents with the aim of improving their effect. In this manner, they discovered a new BB analogue with a Cl group at position 3 that strongly inhibited PqsD (IC_{50} =6.2 μM).

Furthermore, the first dual PqsD/R inhibitor was designed by Thomann et al.[61] based on previous findings that showed that the combination of a PqsR antagonist and PqsD inhibitor synergically decreased PYO levels[32]. They synthesised a compound that shared the same scaffold as the above-mentioned BB analogue inhibitors, which consisted in a pyrimidine core with a triazole and a sulfone moiety. This dual inhibitor showed an IC_{50} of 15 and 21 μM for PqsR and PqsD respectively, and reduced PYO levels by 72 % when tested at 400 μM on bacterial cultures.

Finally, it is worth mentioning that PqsD inhibitors present some general deficiencies. They have low *in vivo* activity due to efflux mechanisms and some of them are not only specific for PqsD (moderate IC_{50}), showing inhibitory activity towards other enzymes that are critical for bacterial growth as is the case of RNA polimerase[62].

2.2.3.3 PqsR and PqsBC inhibition

The most common strategy for PqsR inhibition is the use of antagonists as they turn PqsR into more labile receptor[63]. Lesic et al.[64] are considered the pioneers to introduce PqsR inhibitors since they identified three halogenated AA analogues (precursor of 4-hydroxy-2-alkylquinolines; HAQs) which interfere with HAQ biosynthesis and repress PqsR dependent gene expression. Besides, these inhibitors reduced HHQ and PQS levels in *in vitro* and *in vivo* conditions. Their inhibitory effects were later confirmed by Starkey et al.[51] who developed a phenoxy BB derivative (M64) that decreased PYO levels (IC_{50} =300 nM) by increasing AA concentration in bacterial cultures. Moreover, its administration in combination with ciprofloxacin showed a synergistic effect increasing PA14 strain infected mice survival by 100 %. Moreover, Maura et al.[65] found that BB core inhibitors also inhibited PqsBC. Thus, they classified them in three different groups: specific PqsR inhibitors, potent PqsR/PqsBC dual inhibitors and dual inhibitors but showing a higher anti-PqsBC activity. The second group was the most promising one as it strongly blocked two different targets of the same pathway hindering the development of resistance processes. In the same direction, Kesarwani et al.[66] identified the volatile small molecule 2-AA that modulated PqsR activity and reduced PYO and pyoverdine (PVD) levels by 50 % (at 200 μM) in PA14 cells. In addition, Drees et al.[67] have found 2-AA to be a competitive inhibitor of PqsBC (IC_{50} =46 μM) which also inhibited HHQ levels (IC_{50} =319 μM) when tested in *in vivo* conditions using a *P. putida* strain that expressed constitutively the *pqsABCD* gene.

Another described PqsR inhibitor group focuses on HHQ analogues. In this sense, Lu et al.[52] synthesized 30 different HHQ analogues and identified a potent PqsR competitive antagonist

that reduced PYO levels in PA14 bacterial cultures by 74 % when assayed at 3 µM. This inhibitor had a *n*-C_7H_{15} substituent as side chain and a CF_3 substituent at position 6 of the carbocyclic ring. In order to increase the poor solubility of these analogues, further structural modifications were carried out[68], which enabled to conclude that substituents at position 3 and a carbonyl group at position 4 were required for the interaction with PqsR.

One of the most recent PqsR inhibitor examples has been described by Fang et al.[69] who showed QslA (QS LasR antiactivator that disrupts LasR dimerization) to bind to PqsR preventing its interaction with *phz1* cluster (responsible for phenazines biosynthesis), inhibiting phenazines and also HHQ and PQS production. Additional information can be found in Soheili et al.[70]. Figure 2. 6 shows the main chemical features of PqsR antagonists.

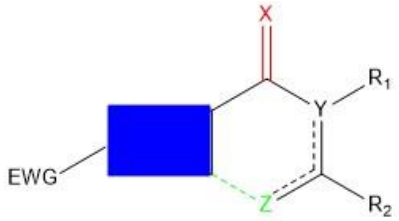

Figure 2. 6 *General structure of some PqsR antagonists. Scaffold that preferably possessed an electron withdrawing group (blue); electron withdrawing group (EWG); X = carbonyl or C=N (red); Z = N, O, NH attached to scaffold (green); Y = C, N; $R_{1,2}$ =H, alkyl(n-C_7H_{15}, n-C_9H_{19}) linker-aromatic group. Adapted from Soheili et al.*[70].

2.3 Concluding remarks

All the here presented results have showed the potential of disrupting *P. aeruginosa* QS system. Besides, the described QSIs have demonstrated high inhibition rates in *in vitro* contitions. However, only few QSIs have reached clinical stages probably due to their poor solubility and stability when used in *in vivo* conditions[71-73]. Furthermore, even though QSIs presumably do not trigger bacterial resistance, there are some evidences that could show the opposite. The first proof was reported by Defoirdt et al.[74] who demonstrated that QS genes highly differed between strains of the same *Vibrio* species and also between other pathogenic bacteria such as *P. aeruginosa* highlighting bacterial capacity to mutate and develop resistance. Later, Maeda et al.[75] identified a bromated furanone (C-30) (LasR inhibitor) that killed PA14 strain cultures by 5 fold in adenosine minimal medium (0.1 % w/v). In the same direction, Beckmann et al.[76] made use of Avida, a digital evolution platform that allowed organisms to interact between them and with the environment, and reported that some *P. aeruginosa* populations evolved resistance processes by activating the QS system at lower cell densities in comparison with parental strains.

In fact, bacteria can activate resistance to QS using different strategies[77] (for more examples read Kalia et al.[73]):

- Mutating LuxR-like receptors to enhance their affinity to AIs so that the required AI concentration threshold is decreased.
- Increasing AI production to ensure that this kind of molecules are always available to activate QS pathways.
- Synthesizing modified AIs in order to become less susceptible to different QSIs.

In this context, therapeutic Abs appear as a promising tool to fight these diseases due to their high specificity and affinity for the corresponding targets[73], which minimize the appearance of possible resistant processes and is also translated in fewer adverse effects. Indeed, it has been documented that the combination of pharmacological attributes of both Abs and antibiotics offers a great alternative to fight infectious diseases. In this sense, Mariathasan et al.[78] conjugated β-N-acetylglucosamine cell-wall teichoic acid (β-GlcNAc-WTA) Ab to 4-dimethylaminopiperidino-hydroxybenzoxazinorifamycin (rifalazil analogue) antibiotic through a MC-ValCit-PABQ linker (maleimide and caproic acid-valine citrulline- p-aminobenzyl quaternary ammonium salt) to effectively limit *S. aureus* infection in mice. The administration of a single dose of this conjugate (from 5 to 50 mg kg^{-1}) reduced *S. aureus* presence in mice kidneys in *in vivo* conditions. In the same context, Roy et al.[79] reduced biofilm thickness of PAO1 bacterial strain from 26 to 2 μm when an AI-2 analogue called phenyl-4,5-dihydroxy-2,3-pentanedione (DPD) was used along with gentamicin antibiotic at 100 μM and 5 μg mL^{-1} concentration, respectively, in *in vitro* conditions.

Other promising approaches are focused on developing nanostructures in order to improve the before-mentioned drawbacks of solubility and delivery[71]. In fact, the first *in vivo* anti-QS nanomaterial against *P. aeruginosa* was reported by Nafee et al.[80]. This nanomaterial contained solid lipid nanoparticles that improved antibacterial efectiveness while enhancing mucus penetration. Another new strategy used to avoid biofilm formation was described by Bassler and co-workers[81] who attached an anti-AI QSI of *S. aureus* to a polyethylene glycol surface, finding an 80 % reduction in biofilm coverage. This strategy could be developed for both gram positive and negative.

Nevertheless, due to the complexity of QS network, which makes its complete inhibition highly difficult, dual therapies are gaining relevance as they claim on inhibiting more than one QS

pathway or the same QS pathway at different levels. This can be achieved by using more than one QSI or a single compound that binds to different QS targets. An example of this was given by Golpasha et al[82] who studied the protective effect of a bivalent antigenic composition conjugate prepared with 3oxoC_{12}-HSL and PcvR (also known as antigen V, plays an important role in T3SS). They used that conjugate as a prophylactic vaccine and found that at 10 and 20 µg mouse^{-1} it increased mouse survival in 78 and 86 %, respectively inhibiting the spread of bacteria in skin and internal organs.

2.4 References

1. Fong, J.; Zhang, C.; Yang, R.; Boo, Z. Z.; Tan, S. K.; Nielsen, T. E.; Givskov, M.; Liu, X. W.; Bin, W.; Su, H.; Yang, L., Combination Therapy Strategy of Quorum Quenching Enzyme and Quorum Sensing Inhibitor in Suppressing Multiple Quorum Sensing Pathways of P. aeruginosa. *Sci Rep* **2018,** *8* (1), 1155.
2. Praneenararat, T.; Palmer, A. G.; Blackwell, H. E., Chemical methods to interrogate bacterial quorum sensing pathways. *Org Biomol Chem* **2012,** *10* (41), 8189-99.
3. Gamby, S.; Roy, V.; Guo, M.; Smith, J. A.; Wang, J.; Stewart, J. E.; Wang, X.; Bentley, W. E.; Sintim, H. O., Altering the communication networks of multispecies microbial systems using a diverse toolbox of AI-2 analogues. *ACS Chem Biol* **2012,** *7* (6), 1023-30.
4. Kapadnis, P. B.; Hall, E.; Ramstedt, M.; Galloway, W. R.; Welch, M.; Spring, D. R., Towards quorum-quenching catalytic antibodies. *Chem Commun (Camb)* **2009,** (5), 538-40.
5. Theuretzbacher, U.; Piddock, L. J. V., Non-traditional Antibacterial Therapeutic Options and Challenges. *Cell Host & Microbe* **2019,** *26* (1), 61-72.
6. Fleitas Martinez, O.; Cardoso, M. H.; Ribeiro, S. M.; Franco, O. L., Recent Advances in Anti-virulence Therapeutic Strategies With a Focus on Dismantling Bacterial Membrane Microdomains, Toxin Neutralization, Quorum-Sensing Interference and Biofilm Inhibition. *Front Cell Infect Microbiol* **2019,** *9*, 74.
7. Patel, B.; Kumari, S.; Banerjee, R.; Samanta, M.; Das, S., Disruption of the quorum sensing regulated pathogenic traits of the biofilm-forming fish pathogen Aeromonas hydrophila by tannic acid, a potent quorum quencher. *Biofouling* **2017,** *33* (7), 580-590.
8. Grandclement, C.; Tannieres, M.; Morera, S.; Dessaux, Y.; Faure, D., Quorum quenching: role in nature and applied developments. *FEMS Microbiol Rev* **2016,** *40* (1), 86-116.
9. Ó Muimhneacháin, E.; Reen, F. J.; O'Gara, F.; McGlacken, G. P., Analogues of Pseudomonas aeruginosa signalling molecules to tackle infections. *Organic & Biomolecular Chemistry* **2018,** *16* (2), 169-179.
10. Li, S.; Chen, S.; Fan, J.; Cao, Z.; Ouyang, W.; Tong, N.; Hu, X.; Hu, J.; Li, P.; Feng, Z.; Huang, X.; Li, Y.; Xie, M.; He, R.; Jian, J.; Wu, B.; Xu, C.; Wu, W.; Guo, J.; Lin, J.; Sun, P., Anti-biofilm effect of novel thiazole acid analogs against Pseudomonas aeruginosa through IQS pathways. *Eur J Med Chem* **2018,** *145*, 64-73.
11. Scoffone, V. C.; Trespidi, G.; Chiarelli, L. R.; Barbieri, G.; Buroni, S., Quorum Sensing as Antivirulence Target in Cystic Fibrosis Pathogens. *Int J Mol Sci* **2019,** *20* (8), 1838.

12. Chang, C. Y.; Krishnan, T.; Wang, H.; Chen, Y.; Yin, W. F.; Chong, Y. M.; Tan, L. Y.; Chong, T. M.; Chan, K. G., Non-antibiotic quorum sensing inhibitors acting against N-acyl homoserine lactone synthase as druggable target. *Sci Rep* **2014,** *4*, 7245.
13. LaSarre, B.; Federle, M. J., Exploiting quorum sensing to confuse bacterial pathogens. *Microbiol Mol Biol Rev* **2013,** *77* (1), 73-111.
14. Uroz, S.; Dessaux, Y.; Oger, P., Quorum sensing and quorum quenching: the yin and yang of bacterial communication. *Chembiochem* **2009,** *10* (2), 205-16.
15. Dong, W.; Zhu, J.; Guo, X.; Kong, D.; Zhang, Q.; Zhou, Y.; Liu, X.; Zhao, S.; Ruan, Z., Characterization of AiiK, an AHL lactonase, from Kurthia huakui LAM0618(T) and its application in quorum quenching on Pseudomonas aeruginosa PAO1. *Sci Rep* **2018,** *8* (1), 6013.
16. Wahjudi, M.; Papaioannou, E.; Hendrawati, O.; van Assen, A. H.; van Merkerk, R.; Cool, R. H.; Poelarends, G. J.; Quax, W. J., PA0305 of Pseudomonas aeruginosa is a quorum quenching acylhomoserine lactone acylase belonging to the Ntn hydrolase superfamily. *Microbiology* **2011,** *157* (Pt 7), 2042-55.
17. Bijtenhoorn, P.; Mayerhofer, H.; Muller-Dieckmann, J.; Utpatel, C.; Schipper, C.; Hornung, C.; Szesny, M.; Grond, S.; Thurmer, A.; Brzuszkiewicz, E.; Daniel, R.; Dierking, K.; Schulenburg, H.; Streit, W. R., A novel metagenomic short-chain dehydrogenase/reductase attenuates Pseudomonas aeruginosa biofilm formation and virulence on Caenorhabditis elegans. *PLoS One* **2011,** *6* (10), e26278.
18. Fetzner, S., Quorum quenching enzymes. *J Biotechnol* **2015,** *201*, 2-14.
19. Dong, Y. H.; Xu, J. L.; Li, X. Z.; Zhang, L. H., AiiA, an enzyme that inactivates the acylhomoserine lactone quorum-sensing signal and attenuates the virulence of Erwinia carotovora. *Proc Natl Acad Sci U S A* **2000,** *97* (7), 3526-31.
20. Ozer, E. A.; Pezzulo, A.; Shih, D. M.; Chun, C.; Furlong, C.; Lusis, A. J.; Greenberg, E. P.; Zabner, J., Human and murine paraoxonase 1 are host modulators of Pseudomonas aeruginosa quorum-sensing. *FEMS Microbiol Lett* **2005,** *253* (1), 29-37.
21. Guendouze, A.; Plener, L.; Bzdrenga, J.; Jacquet, P.; Remy, B.; Elias, M.; Lavigne, J. P.; Daude, D.; Chabriere, E., Effect of Quorum Quenching Lactonase in Clinical Isolates of Pseudomonas aeruginosa and Comparison with Quorum Sensing Inhibitors. *Front Microbiol* **2017,** *8*, 227.
22. Hraiech, S.; Hiblot, J.; Lafleur, J.; Lepidi, H.; Papazian, L.; Rolain, J. M.; Raoult, D.; Elias, M.; Silby, M. W.; Bzdrenga, J.; Bregeon, F.; Chabriere, E., Inhaled lactonase reduces Pseudomonas aeruginosa quorum sensing and mortality in rat pneumonia. *PLoS One* **2014,** *9* (10), e107125.
23. Fan, X.; Liang, M.; Wang, L.; Chen, R.; Li, H.; Liu, X., Aii810, a Novel Cold-Adapted N-Acylhomoserine Lactonase Discovered in a Metagenome, Can Strongly Attenuate Pseudomonas aeruginosa Virulence Factors and Biofilm Formation. *Front Microbiol* **2017,** *8*, 1950.
24. Federle, M. J.; Bassler, B. L., Interspecies communication in bacteria. *J Clin Invest* **2003,** *112* (9), 1291-9.
25. Huang, J. J.; Petersen, A.; Whiteley, M.; Leadbetter, J. R., Identification of QuiP, the product of gene PA1032, as the second acyl-homoserine lactone acylase of Pseudomonas aeruginosa PAO1. *Appl Environ Microbiol* **2006,** *72* (2), 1190-7.

26. Chowdhary, P. K.; Keshavan, N.; Nguyen, H. Q.; Peterson, J. A.; Gonzalez, J. E.; Haines, D. C., Bacillus megaterium CYP102A1 oxidation of acyl homoserine lactones and acyl homoserines. *Biochemistry* **2007,** *46* (50), 14429-37.
27. Smith, R. S.; Iglewski, B. H., Pseudomonas aeruginosa quorum sensing as a potential antimicrobial target. *J Clin Invest* **2003,** *112* (10), 1460-5.
28. Kaufmann, G. F.; Park, J.; Janda, K. D., Bacterial quorum sensing: a new target for anti-infective immunotherapy. *Expert Opin Biol Ther* **2008,** *8* (6), 719-24.
29. Hoang, T. T.; Schweizer, H. P., Characterization of Pseudomonas aeruginosa enoyl-acyl carrier protein reductase (FabI): a target for the antimicrobial triclosan and its role in acylated homoserine lactone synthesis. *J Bacteriol* **1999,** *181* (17), 5489-97.
30. Chuanchuen, R.; Schweizer, H. P., Global transcriptional responses to triclosan exposure in Pseudomonas aeruginosa. *International Journal of Antimicrobial Agents* **2012,** *40* (2), 114-122.
31. Kalia, M.; Yadav, V. K.; Singh, P. K.; Dohare, S.; Sharma, D.; Narvi, S. S.; Agarwal, V., Designing quorum sensing inhibitors of Pseudomonas aeruginosa utilizing FabI: an enzymic drug target from fatty acid synthesis pathway. *3 Biotech* **2019,** *9* (2).
32. O'Loughlin, C. T.; Miller, L. C.; Siryaporn, A.; Drescher, K.; Semmelhack, M. F.; Bassler, B. L., A quorum-sensing inhibitor blocks Pseudomonas aeruginosa virulence and biofilm formation. *Proc Natl Acad Sci U S A* **2013,** *110* (44), 17981-6.
33. Smith, K. M.; Bu, Y.; Suga, H., Induction and inhibition of Pseudomonas aeruginosa quorum sensing by synthetic autoinducer analogs. *Chem Biol* **2003,** *10* (1), 81-9.
34. Welsh, M. A.; Eibergen, N. R.; Moore, J. D.; Blackwell, H. E., Small molecule disruption of quorum sensing cross-regulation in pseudomonas aeruginosa causes major and unexpected alterations to virulence phenotypes. *J Am Chem Soc* **2015,** *137* (4), 1510-9.
35. Liu, H.; Gong, Q.; Luo, C.; Liang, Y.; Kong, X.; Wu, C.; Feng, P.; Wang, Q.; Zhang, H.; Wireko, M. A., Synthesis and Biological Evaluation of Novel L-Homoserine Lactone Analogs as Quorum Sensing Inhibitors of Pseudomonas aeruginosa. *Chem Pharm Bull (Tokyo)* **2019,** *67* (10), 1088-1098.
36. Shin, D.; Gorgulla, C.; Boursier, M. E.; Rexrode, N.; Brown, E. C.; Arthanari, H.; Blackwell, H. E.; Nagarajan, R., N-Acyl Homoserine Lactone Analog Modulators of the Pseudomonas aeruginosa Rhll Quorum Sensing Signal Synthase. *ACS Chem Biol* **2019,** *14* (10), 2305-2314.
37. Park, J.; Kaufmann, G. F.; Bowen, J. P.; Arbiser, J. L.; Janda, K. D., Solenopsin A, a venom alkaloid from the fire ant Solenopsis invicta, inhibits quorum-sensing signaling in Pseudomonas aeruginosa. *J Infect Dis* **2008,** *198* (8), 1198-201.
38. Vandeputte, O. M.; Kiendrebeogo, M.; Rasamiravaka, T.; Stevigny, C.; Duez, P.; Rajaonson, S.; Diallo, B.; Mol, A.; Baucher, M.; El Jaziri, M., The flavanone naringenin reduces the production of quorum sensing-controlled virulence factors in Pseudomonas aeruginosa PAO1. *Microbiology* **2011,** *157* (Pt 7), 2120-32.
39. Paczkowski, J. E.; Mukherjee, S.; McCready, A. R.; Cong, J.-P.; Aquino, C. J.; Kim, H.; Henke, B. R.; Smith, C. D.; Bassler, B. L., Flavonoids Suppress Pseudomonas aeruginosa Virulence through Allosteric Inhibition of Quorum-sensing Receptors. *Journal of Biological Chemistry* **2017,** *292* (10), 4064-4076.
40. Tan, S. Y.-Y.; Chua, S.-L.; Chen, Y.; Rice, S. A.; Kjelleberg, S.; Nielsen, T. E.; Yang, L.; Givskov, M., Identification of Five Structurally Unrelated Quorum-Sensing Inhibitors of

Pseudomonas aeruginosa from a Natural-Derivative Database. *Antimicrobial Agents and Chemotherapy* **2013,** *57* (11), 5629-5641.

41. Manefield, M. R., T. B.; Henzter, M.; Andersen, J. B .; Steinberg, P.; Kjelleberg, S.; Givskov, M., Halogenated furanones inhibit quorum sensing through accelerated LuxR turnover. *Microbiology* **2002,** *148*, 1119–1127.
42. Wu, H.; Song, Z.; Hentzer, M.; Andersen, J. B.; Molin, S.; Givskov, M.; Hoiby, N., Synthetic furanones inhibit quorum-sensing and enhance bacterial clearance in Pseudomonas aeruginosa lung infection in mice. *J Antimicrob Chemother* **2004,** *53* (6), 1054-61.
43. Pelfrene, E.; Mura, M.; Cavaleiro Sanches, A.; Cavaleri, M., Monoclonal antibodies as anti-infective products: a promising future? *Clin Microbiol Infect* **2018**.
44. Kaufmann, G. F.; Sartorio, R.; Lee, S. H.; Mee, J. M.; Altobell, L. J., 3rd; Kujawa, D. P.; Jeffries, E.; Clapham, B.; Meijler, M. M.; Janda, K. D., Antibody interference with N-acyl homoserine lactone-mediated bacterial quorum sensing. *J Am Chem Soc* **2006,** *128* (9), 2802-3.
45. Debler, E. W.; Kaufmann, G. F.; Kirchdoerfer, R. N.; Mee, J. M.; Janda, K. D.; Wilson, I. A., Crystal structures of a quorum-quenching antibody. *J Mol Biol* **2007,** *368* (5), 1392-402.
46. Palliyil, S. D., C.; Broadbent, I.; Charlton, K.; Porter, A. J., High-Sensitivity Monoclonal Antibodies Specific for Homoserine Lactones Protect Mice from Lethal Pseudomonas aeruginosa Infections. *Applied and Environmental Microbiology 80* (2), 462–469.
47. Miyairi, S.; Tateda, K.; Fuse, E. T.; Ueda, C.; Saito, H.; Takabatake, T.; Ishii, Y.; Horikawa, M.; Ishiguro, M.; Standiford, T. J.; Yamaguchi, K., Immunization with 3-oxododecanoyl-L-homoserine lactone-protein conjugate protects mice from lethal Pseudomonas aeruginosa lung infection. *J Med Microbiol* **2006,** *55* (Pt 10), 1381-1387.
48. De Lamo Marin, S.; Xu, Y.; Meijler, M. M.; Janda, K. D., Antibody catalyzed hydrolysis of a quorum sensing signal found in Gram-negative bacteria. *Bioorg Med Chem Lett* **2007,** *17* (6), 1549-52.
49. Francois, B.; Luyt, C. E.; Stover, C. K.; Brubaker, J. O.; Chastre, J.; Jafri, H. S., New Strategies Targeting Virulence Factors of Staphylococcus aureus and Pseudomonas aeruginosa. *Semin Respir Crit Care Med* **2017,** *38* (3), 346-358.
50. Warrener, P.; Varkey, R.; Bonnell, J. C.; DiGiandomenico, A.; Camara, M.; Cook, K.; Peng, L.; Zha, J.; Chowdury, P.; Sellman, B.; Stover, C. K., A novel anti-PcrV antibody providing enhanced protection against Pseudomonas aeruginosa in multiple animal infection models. *Antimicrob Agents Chemother* **2014,** *58* (8), 4384-91.
51. Starkey, M.; Lepine, F.; Maura, D.; Bandyopadhaya, A.; Lesic, B.; He, J.; Kitao, T.; Righi, V.; Milot, S.; Tzika, A.; Rahme, L., Identification of anti-virulence compounds that disrupt quorum-sensing regulated acute and persistent pathogenicity. *PLoS Pathog* **2014,** *10* (8), e1004321.
52. Lu, C.; Kirsch, B.; Zimmer, C.; de Jong, J. C.; Henn, C.; Maurer, C. K.; Musken, M.; Haussler, S.; Steinbach, A.; Hartmann, R. W., Discovery of antagonists of PqsR, a key player in 2-alkyl-4-quinolone-dependent quorum sensing in Pseudomonas aeruginosa. *Chem Biol* **2012,** *19* (3), 381-90.
53. Allegretta, G.; Maurer, C. K.; Eberhard, J.; Maura, D.; Hartmann, R. W.; Rahme, L.; Empting, M., In-depth Profiling of MvfR-Regulated Small Molecules in Pseudomonas aeruginosa after Quorum Sensing Inhibitor Treatment. *Front Microbiol* **2017,** *8*, 924.

54. Ji, C.; Sharma, I.; Pratihar, D.; Hudson, L. L.; Maura, D.; Guney, T.; Rahme, L. G.; Pesci, E. C.; Coleman, J. P.; Tan, D. S., Designed Small-Molecule Inhibitors of the Anthranilyl-CoA Synthetase PqsA Block Quinolone Biosynthesis in Pseudomonas aeruginosa. *ACS Chemical Biology* **2016,** *11* (11), 3061-3067.
55. Pustelny, C.; Albers, A.; Buldt-Karentzopoulos, K.; Parschat, K.; Chhabra, S. R.; Camara, M.; Williams, P.; Fetzner, S., Dioxygenase-mediated quenching of quinolone-dependent quorum sensing in Pseudomonas aeruginosa. *Chem Biol* **2009,** *16* (12), 1259-67.
56. Storz, M. P.; Maurer, C. K.; Zimmer, C.; Wagner, N.; Brengel, C.; de Jong, J. C.; Lucas, S.; Musken, M.; Haussler, S.; Steinbach, A.; Hartmann, R. W., Validation of PqsD as an anti-biofilm target in Pseudomonas aeruginosa by development of small-molecule inhibitors. *J Am Chem Soc* **2012,** *134* (39), 16143-6.
57. Sahner, J. H.; Brengel, C.; Storz, M. P.; Groh, M.; Plaza, A.; Muller, R.; Hartmann, R. W., Combining in silico and biophysical methods for the development of Pseudomonas aeruginosa quorum sensing inhibitors: an alternative approach for structure-based drug design. *J Med Chem* **2013,** *56* (21), 8656-64.
58. Sahner, J. H.; Empting, M.; Kamal, A.; Weidel, E.; Groh, M.; Borger, C.; Hartmann, R. W., Exploring the chemical space of ureidothiophene-2-carboxylic acids as inhibitors of the quorum sensing enzyme PqsD from Pseudomonas aeruginosa. *Eur J Med Chem* **2015,** *96*, 14-21.
59. Weidel, E.; de Jong, J. C.; Brengel, C.; Storz, M. P.; Braunshausen, A.; Negri, M.; Plaza, A.; Steinbach, A.; Muller, R.; Hartmann, R. W., Structure optimization of 2-benzamidobenzoic acids as PqsD inhibitors for Pseudomonas aeruginosa infections and elucidation of binding mode by SPR, STD NMR, and molecular docking. *J Med Chem* **2013,** *56* (15), 6146-55.
60. Hinsberger, S.; de Jong, J. C.; Groh, M.; Haupenthal, J.; Hartmann, R. W., Benzamidobenzoic acids as potent PqsD inhibitors for the treatment of Pseudomonas aeruginosa infections. *European Journal of Medicinal Chemistry* **2014,** *76*, 343-351.
61. Thomann, A.; de Mello Martins, A. G.; Brengel, C.; Empting, M.; Hartmann, R. W., Application of Dual Inhibition Concept within Looped Autoregulatory Systems toward Antivirulence Agents against Pseudomonas aeruginosa Infections. *ACS Chem Biol* **2016,** *11* (5), 1279-86.
62. Zhou, Z.; Ma, S., Recent Advances in the Discovery of PqsD Inhibitors as Antimicrobial Agents. *ChemMedChem* **2017,** *12* (6), 420-425.
63. Wysoczynski-Horita, C. L.; Boursier, M. E.; Hill, R.; Hansen, K.; Blackwell, H. E.; Churchill, M. E. A., Mechanism of agonism and antagonism of the Pseudomonas aeruginosa quorum sensing regulator QscR with non-native ligands. *Mol Microbiol* **2018,** *108* (3), 240-257.
64. Lesic, B.; Lepine, F.; Deziel, E.; Zhang, J.; Zhang, Q.; Padfield, K.; Castonguay, M. H.; Milot, S.; Stachel, S.; Tzika, A. A.; Tompkins, R. G.; Rahme, L. G., Inhibitors of pathogen intercellular signals as selective anti-infective compounds. *PLoS Pathog* **2007,** *3* (9), 1229-39.
65. Maura, D.; Drees, S. L.; Bandyopadhaya, A.; Kitao, T.; Negri, M.; Starkey, M.; Lesic, B.; Milot, S.; Deziel, E.; Zahler, R.; Pucci, M.; Felici, A.; Fetzner, S.; Lepine, F.; Rahme, L. G., Polypharmacology Approaches against the Pseudomonas aeruginosa MvfR Regulon and Their Application in Blocking Virulence and Antibiotic Tolerance. *ACS Chem Biol* **2017,** *12* (5), 1435-1443.

66. Kesarwani, M.; Hazan, R.; He, J.; Que, Y. A.; Apidianakis, Y.; Lesic, B.; Xiao, G.; Dekimpe, V.; Milot, S.; Deziel, E.; Lepine, F.; Rahme, L. G., A quorum sensing regulated small volatile molecule reduces acute virulence and promotes chronic infection phenotypes. *PLoS Pathog* **2011,** *7* (8), e1002192.
67. Drees, S. L.; Li, C.; Prasetya, F.; Saleem, M.; Dreveny, I.; Williams, P.; Hennecke, U.; Emsley, J.; Fetzner, S., PqsBC, a Condensing Enzyme in the Biosynthesis of the Pseudomonas aeruginosa Quinolone Signal: CRYSTAL STRUCTURE, INHIBITION, AND REACTION MECHANISM. *J Biol Chem* **2016,** *291* (13), 6610-24.
68. Lu, C.; Kirsch, B.; Maurer, C. K.; de Jong, J. C.; Braunshausen, A.; Steinbach, A.; Hartmann, R. W., Optimization of anti-virulence PqsR antagonists regarding aqueous solubility and biological properties resulting in new insights in structure-activity relationships. *Eur J Med Chem* **2014,** *79*, 173-83.
69. Fang, Y. L.; Chen, B.; Zhou, L.; Jin, Z. J.; Sun, S.; He, Y. W., The Anti-activator QslA Negatively Regulates Phenazine-1-Carboxylic Acid Biosynthesis by Interacting With the Quorum Sensing Regulator MvfR in the Rhizobacterium Pseudomonas aeruginosa Strain PA1201. *Front Microbiol* **2018,** *9*, 1584.
70. Soheili, V.; Tajani, A. S.; Ghodsi, R.; Bazzaz, B. S. F., Anti-PqsR compounds as next-generation antibacterial agents against Pseudomonas aeruginosa: A review. *European Journal of Medicinal Chemistry* **2019,** *172*, 26-35.
71. Singh, B. N.; Prateeksha; Upreti, D. K.; Singh, B. R.; Defoirdt, T.; Gupta, V. K.; De Souza, A. O.; Singh, H. B.; Barreira, J. C. M.; Ferreira, I. C. F. R.; Vahabi, K., Bactericidal, quorum quenching and anti-biofilm nanofactories: a new niche for nanotechnologists. *Critical Reviews in Biotechnology* **2017,** *37* (4), 525-540.
72. Remy, B.; Mion, S.; Plener, L.; Elias, M.; Chabriere, E.; Daude, D., Interference in Bacterial Quorum Sensing: A Biopharmaceutical Perspective. *Front Pharmacol* **2018,** *9*, 203.
73. Kalia, V. C.; Patel, S. K. S.; Kang, Y. C.; Lee, J.-K., Quorum sensing inhibitors as antipathogens: biotechnological applications. *Biotechnology Advances* **2019,** *37* (1), 68-90.
74. Defoirdt, T.; Boon, N.; Bossier, P., Can bacteria evolve resistance to quorum sensing disruption? *PLoS Pathog* **2010,** *6* (7), e1000989.
75. Maeda, T.; Garcia-Contreras, R.; Pu, M.; Sheng, L.; Garcia, L. R.; Tomas, M.; Wood, T. K., Quorum quenching quandary: resistance to antivirulence compounds. *ISME J* **2012,** *6* (3), 493-501.
76. Beckmann, B. E.; Knoester, D. B.; Connelly, B. D.; Waters, C. M.; McKinley, P. K., Evolution of resistance to quorum quenching in digital organisms. *Artif Life* **2012,** *18* (3), 291-310.
77. Garcia-Contreras, R.; Maeda, T.; Wood, T. K., Resistance to quorum-quenching compounds. *Appl Environ Microbiol* **2013,** *79* (22), 6840-6.
78. Mariathasan, S.; Tan, M. W., Antibody-Antibiotic Conjugates: A Novel Therapeutic Platform against Bacterial Infections. *Trends Mol Med* **2017,** *23* (2), 135-149.
79. Roy, V.; Meyer, M. T.; Smith, J. A.; Gamby, S.; Sintim, H. O.; Ghodssi, R.; Bentley, W. E., AI-2 analogs and antibiotics: a synergistic approach to reduce bacterial biofilms. *Appl Microbiol Biotechnol* **2013,** *97* (6), 2627-38.
80. Nafee, N.; Husari, A.; Maurer, C. K.; Lu, C.; de Rossi, C.; Steinbach, A.; Hartmann, R. W.; Lehr, C. M.; Schneider, M., Antibiotic-free nanotherapeutics: ultra-small, mucus-

penetrating solid lipid nanoparticles enhance the pulmonary delivery and anti-virulence efficacy of novel quorum sensing inhibitors. *J Control Release* **2014,** *192*, 131-40.

81. Kim, M. K.; Zhao, A.; Wang, A.; Brown, Z. Z.; Muir, T. W.; Stone, H. A.; Bassler, B. L., Surface-attached molecules control Staphylococcus aureus quorum sensing and biofilm development. *Nature Microbiology* **2017,** *2*, 17080.
82. Golpasha, I. D.; Mousavi, S. F.; Owlia, P.; Siadat, S. D.; Irani, S., Immunization with 3-oxododecanoyl-L-homoserine lactone-r-PcrV conjugate enhances survival of mice against lethal burn infections caused by Pseudomonas aeruginosa. *Bosn J Basic Med Sci* **2015,** *15* (2), 15-24.

Chapter 3

Research projects, objectives and thesis structure

3.1 Research projects

The presented thesis has been developed within the framework of 3 different research projects:

- **Immunochemical Diagnostic and Therapeutic Strategies based on the Quorum Sensing System (IMMUNO-QS project).** (ref # SAF2015-67476-R, 1/1/2016 - 30/6/2019, co-funded by "Ministerio de Economía y Competitividad (MINECO)" and "Fondo Europeo de Desarrollo Regional (FEDER)"). The main goals of the project were (A) the development of immunochemical methods to profile the expression of different QS signaling molecules as tools to investigate the mechanisms involved in the pathogenesis of *S. aureus* and *P. aeruginosa* evaluating their potential role as biomarkers of infection and (B) to assess the potential therapeutic value of the antibodies (Abs) produced against important molecules of the *P. aeruginosa* and *S. aureus* QS systems, as quorum quencher (QQ) agents. To accomplish these goals, specific Abs against QS signaling molecules of *S. aureus* (AIP-4 thiolactone form) and *P. aeruginosa* (HHQ and pyocyanin; PYO) were generated to develop QS single-analyte enzyme-linked immunosorbent assays (ELISAs) and a multiplexed microarray chip for QS profiling. In this sense, the potential of QS profiling to distinguish colonization *versus* infection was evaluated and, also, the generation of data regarding QS molecules levels on clinical samples from cystic fibrosis (CF) patients. Furthermore, the therapeutic value (QQ activity) of *P. aeruginosa* QS Abs on *in vitro* conditions was assessed.
- **Quorum Sensing as an alternative for the management of cystic fibrosis (QS4CF project).** (ref # RTI2018-096278-B-C21, 1/1/2019 - 30/6/2022, co-funded by "Ministerio de Ciencia, Innovación y Universidades (MICIU)" and FEDER). The objectives of this project were essentially the same of IMMUNO-QS project but adding new QS targets such as AIPs 1 to 3 of *S. aureus* and other alquilquinolones and IQS of *P. aeruginosa*. Besides, the preliminary results obtained in IMMUNO-QS proyect regarding the potential therapeutic role of the Ab produced against PYO on human macrophages in *in vitro* conditions were consolidated. In this context, the quenching capacity of other QS molecules were also assessed.
- **Quorum Sensing as potential biomarker targets to diagnose bacterial infections (QS-MOTION project).** (ref # FMTV3-201824-30-31, 11/7/2019 - 30/7/2022, funded by Fundació La Marató de TV3). This project was essentially focused on diagnosis purposes. The main goals were the development of immunochemical technologies to build up fast and accurate diagnosis methods to detect *S. aureus* and *P. aeruginosa* and to profile the expression of different QS signaling molecules. Thus, specific Abs against important QS

signaling molecules of *P. aeruginosa*, and *S. aureus* were generated to develop immunochemical analytical tools with very low limit of detection (LoD) (on the low nM range). That allowed their quantification on real clinical samples obtained from patients suffering lower respiratory tract infections assessing their potential value as biomarkers of infection. Moreover, the possibility to develop a multiplexed method for QS profiling was also investigated.

To ensure the translational character of the mentioned projects, the projects counted with the participation of:

- **Hospital Germans Trias i Pujol (HGTiP)**, Microbiology Laboratory (Badalona, Spain).
- **Hospital Universitari Vall d'Hebron (HUVH)**, Microbiology Laboratories and Respiratory Units of the Hospital Vall d'Hebrón (Barcelona, Spain).

3.2 General objectives

- Improvement of the efficiency of the diagnostic of infections caused by *P. aeruginosa* by the development of a monoclonal Ab (mAb)-based immunochemical assay to detect *P. aeruginosa* main virulence factor (VF), PYO. The assay has allowed the detection of PYO in bacterial isolates and clinical samples from patients infected with this pathogen helping in their diagnostic and stratification.
- Development of a new therapeutic strategy to figth *P. aeruginosa* infections based on the inhibition of QS mechanism using specific mAbs. In this sense, an *in vitro* system has been set up to study the effect of a mAb against a VF (PYO) and a mAb against a signalling molecule (PQS) on murine macrophages.

3.3 Thesis structure

The structure of this thesis follows the scheme detailed below:

- **Diagnostic chapters**:
    - *Chapter 4*: Production of a mAb against PYO and development of a specific ELISA to detect this VF.
    - *Chapter 5*: ELISA implementation for measuring PYO in bacterial isolates from patients infected with *P. aeruginosa* and evaluation of the potential of this VF as biomarker of *P. aeruginosa* infections with the aim of differentiating between chronic and acute infections.

- *Chapter 6*: ELISA implementation for measuring PYO on clinical samples from patients infected with *P. aeruginosa,* such as sputum and swab, and evaluation of its role as biomarker of *P. aeruginosa* infections.

- **Therapy chapters**:
  - *Chapter 7*: Analysis of PYO cytotoxicity and evaluation of PYO mAb as therapeutic agent in an an *in vitro* system based on different *hallmarks* of viability.
  - *Chapter 8*: Analysis of PQS cytotoxicity and evaluation of PQS mAb as therapeutic agent using the same above mentioned *in vitro* system.
- *Chapter 9*: Main conclusions of the thesis summarizing the contributions of each chapter and future experiments.
- *Annex*: General introduction to Cystic fibrosis transmembrane conductance regulator inhibitory factor (Cif) and implementation of an ELISA to detect this molecule on bacterial isolates from patients infected with *P. aeruginosa*. This part resulted from a collaboration with Dr. Natalia Vasylieva of Prof. Bruce D. Hammock Laboratory from the University of California Davis who developed both the ELISA and the Abs used (nanobodies).

Chapter 4

Development and optimization of an enzymatic immunoassay for pyocyanin detection

In this chapter, the production of a specific monoclonal antibody (mAb) against *P. aeruginosa* main virulence factor, pyocyanin (PYO), will be explained. This mAb has been used for developing an immunochemical assay for PYO detection which has been further optimized and characterized. Moreover, the robustness, the specificity, the sensitivity and accuracy of the assay have been analysed.

The work presented in this chapter is adapted from:

Rodriguez-Urretavizcaya, B.; Pascual, N.; Pastells, C.; Martin-Gomez, M.T.; Vilaplana Ll. and Marco, M.P. (2021). Diagnostic and Stratification of Pseudomonas aeruginosa Infected Patients by Immunochemical Quantitative Determination of Pyocyanin from Clinical Bacterial Isolates. *Front. Cell. Infect. Microbiol.* 11, 1-12. doi: 10.3389/fcimb.2021.786929

4.1 Introduction

Since the gold standard technique used for detecting *Pseudomonas aeruginosa* still consists on the use of culture plates inoculated with swab samples[1] and this method is time consuming (24 - 48 h), the development of fast diagnostic tools could significantly improve the management of *P. aeruginosa* infections allowing a rapid administration of the correct treatment and avoiding resistance problems[2]. Thus, the identification of new biomarkers of infection has become an essential milestone.

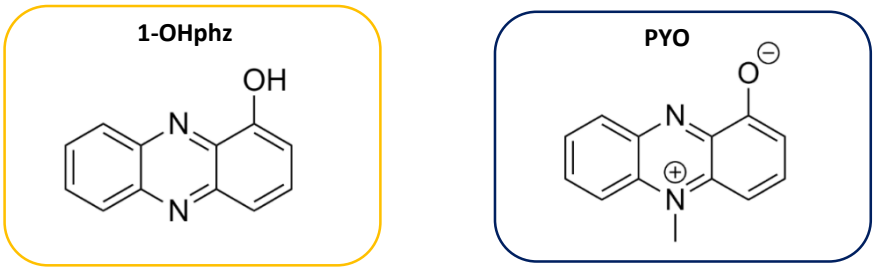

Figure 4. 1 *Chemical structures of 1-OHphz (yellow) and PYO (blue) phenazines. Both molecules are structurally similar having PYO molecule an extra methyl group in position 5.*

In this context, few years ago, our lab reported for the first time the development of a polyclonal antibody (pAb) and a microplate-based enzyme-linked immunosorbent assay (ELISA) for 1-hydroxyphenazine (1-OHphz) (As230/PC1-BSA), the main metabolite of pyocyanin (PYO) (see Figure 4. 1), with an excellent detectability (half maximal inhibitory concentration (IC_{50}) =0.53 nM)[3]. Due to the chemical difficulties with PYO stability, a 1-OHphz hapten was used to raise the antibodies (Abs) with the expectation that would also recognize PYO (Figure 4. 2). Besides the high structural similarities between PYO and 1-OHphz, PYO crossreacted only a 0.1 % (IC_{50} >800 nM). Thus, PYO quantification required its complete transformation to 1-OHphz prior the analysis, which was achieved by treating the samples with a strong base.

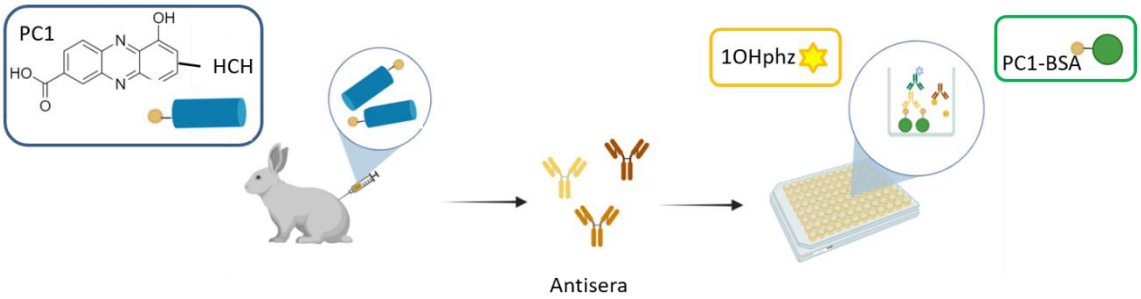

Figure 4. 2 *Polyclonal antibodies (pAbs) against 1-OHphz production. Rabits were immunized with PC1-Horseshoe-Crab Hemocyanin (HCH) bioconjugate as explained in Pastells et al.[3]. The obtained antisera were used to develop a competitive ELISA using PC1-bovine serum albumin (BSA) that allowed 1-OHphz quantification in the nM range.*

Aiming at simplifying the procedure, a high affinity monoclonal antibody (mAb) against PYO was obtained using the hybridoma technology, which allows selecting cell clones with tailored features based on a rational selective screening approach. With this objective, mice were immunized with PC1 (1-OHphz hapten) linked to Horseshoe-Crab Hemocyanin *(*HCH) (see Figure 4. 6 in Material & Methods). The hybridoma cells obtained after the fusion step were selectively screened after several cloning cycles performed to select those clones that best detected PYO on a competitive format, using both phenazines (PYO and 1-OHphz). Afterwards, bidimensional checkerboard experiments (2D-ELISAs) allowed to determine the most appropriate concentrations for the bioconjugate competitor PC1-BSA and each mAb clone to be tested on the competitive ELISAs.

4.2 Results & discussion

4.2.1 Development of the PYO ELISA assay

After obtaining and selecting the most specific mAbs against PYO, they were used to develop a highly sensitive ELISA. For the case of PYO, the preferred configuration was a competitive indirect ELISA since its low molecular weight (210.23 g mol^{-1}) impedes the simultaneous detection by more than one antibody (Ab) (the epitopes required for the recognition might be very close).

4.2.1.1 mAb screening and clone selection

The avidity of the obtained PYO mAbs for PC1-BSA conjugate and for PYO analyte will determine the competition, which was assessed by screening experiments were the absorbance of the assays in the presence and absence of the analyte was compared. Table 4. 1 shows the IC_{50} values of the selected clones for PYO and 1-OHphz using the developed ELISA. In all cases, final clones presented a better detectability for 1-OHphz than for PYO. While some of them (C.9.1.9.7.3.1.1. and C.9.1.7.2.1.2.1.) showed much higher affinity for 1-OHphz than for PYO (IC_{50} values for PYO ranging 15 - 20 nM), other clones (C.9.1.4.1.1.4.2. and C.9.1.4.1.1.4.4. C.9.1.9.1.1.2.2.) had more similar selectivities for both phenazines, with low IC_{50} values for PYO (< 2 nM). From these three best clones, C.9.1.9.1.1.2.2. (from now on PYO mAb122) was selected to quantify PYO as it showed better ELISA parameters such as slope and maximum absorbance (A_{max}) (-1.40 and 1.08, respectively).

Table 4. 1 *Half maximal inhibitory concentration (IC_{50}) of the selected mAb clones for PYO and 1-OHphz and when using the polyclonal antisera As230. The selected clone is highlighted in green (C.9.1.9.1.1.2.2.).*

Clone name[b]	IC_{50} (1-OHphz)/ nM[c]	IC_{50} (PYO)/ nM[d]	Relation [(IC_{50} (PYO)/ IC_{50} (1-OHphz)]
C.9.1.7.2.1.2.1	2.17	16.26	7.48
C.9.1.7.2.1.2.2	0.43	3.87	8.99
C.9.1.9.7.3.1.1	3.72	27.21	7.31
C.9.1.9.7.3.1.2	1.23	7.88	6.42
C.9.2.8.3.1.2.2	0.90	5.98	6.67
C.9.1.7.1.1.2.1	1.19	7.39	6.22
C.9.1.4.1.1.4.2	0.24	1.97	8.37
C.9.1.4.1.1.4.1	0.38	3.81	10.13
C.9.1.9.1.1.2.2	0.32	2.96	9.27
C.9.1.4.1.1.4.4	0.26	2.13	8.06
C.9.1.4.1.1.4.3	1.10	6.56	5.99
C.9.2.8.3.1.2.3	0.83	7.45	8.96
C.9.1.7.1.1.1.2	1.34	9.23	6.91
C.9.1.7.1.1.2.3	0.79	5.01	6.37
As 230[3]	0.62	> 800	1290.32

a Amax values were between 0.8 and 1.2.

b Antibody concentration used 0.008 µg mL^{-1} for PYO mAb122 and 1/6000 dilution for As230.

c,d Coating antigen concentration used 0.125 and 0.0625 µg mL^{-1} for PYO mAb/PC1-BSA and As230/PC1-BSA, respectively.

To perform these indirect competitive ELISAs, the appropriate dilutions of mAb and PC1-BSA coating antigen were established by carrying out 2D ELISAs[4]. These 2D experiments consisted on testing serial dilutions of PC1-BSA bioconjugate and several PYO mAb122 concentrations in order to select the optimal combination of them to achieve high absorbance values without reaching the saturation levels of the curve. In this manner, it was determined to use 0.125 µg mL^{-1} of coating antigen (PC1-BSA) and 0.008 µg mL^{-1} of PYO mAb122 concentrations.

The analytical parameters of the PYO mAb122/PC1-BSA ELISA are summarized in Table 4. 2. The low limit of detection (LoD) (0.07 nM) reached allowed considering the possibility to directly quantify PYO without the need to convert it to 1-OHphz.

Table 4. 2 *Analytical parameters of the PYO mAb122/PC1-BSA ELISA for PYO detection on assay buffer. The concentrations of the immunoreagents used were: PC1-BSA at 0.125 µg mL^{-1} and PYO mAb122 at 0.008 µg mL^{-1}. The data shown correspond to the average and standard deviation of the parameters of the calibration curves performed 3 different days using at least 3 well replicates per concentration (12 different concentrations).*

	PBST
A_{min}	0.07 ± 0.01
A_{max}	1.08 ± 0.09
Slope	-1.40 ± 0.49
IC_{50}/ nM	0.68 ± 0.10
Dynamic range/ nM	0.18 ± 0.08 and 2.18 ± 0.19
LoD/ nM	0.07 ± 0.04
R^2	0.99 ± 0.01

4.2.1.2 Physicochemical parameters optimization

The analytical parameters obtained for PYO mAb122/PC1-BSA ELISA showed a very low IC_{50} and optimals A_{max} and slope values (Table 4. 2). Thus, it was considered that it was not necessary to optimize all parameters that can influence the performance of this type of assay (preincubation time, competition time, % Tween 20, ionic strength) but only check the stability of the ELISA at pHs between 2.5 and 11.5 and when using different % of organic solvents.

4.2.1.2.1 pH optimization

Since it was aimed to measure PYO in clinical matrices such as sputum and the pH of these samples can vary[5], the robustness of the assay when changing the pH was evaluated. Therefore, the buffer of the assay (PBST) was prepared fixing the pH at different values ranging from 2.5 to 11.5 and the obtained ELISA parameters (slope, A_{max} and IC_{50}) were compared with those obtained when performing the assay at the pH considered in this case standard (7.5).

As illustrated in Figure 4. 3, no significant variation of the assay parameters was observed between pH 4.5 and 7.5 pointing to the robustness of the assay. Besides, the analytical parameters of PYO mAb122/PC1-BSA ELISA were slightly modified at pH values between 4 and 8, although the detectability was slightly better between pHs 6.5 and 7.5. Thus, the analysis of sputum samples, whose pHs vary from 5.5 to 8.3[5], should not interfere with PYO mAb/PC1-BSA ELISA performance.

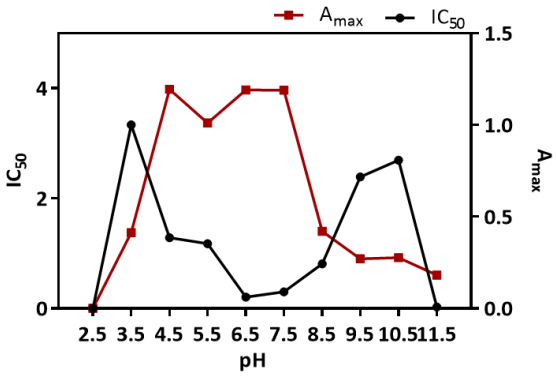

Figure 4. 3 *PYO mAb122/PC1-BSA ELISA performance in the pH optimization study. The selection of the most appropriate pH was based on the variations in A_{max} and IC_{50} values of the generated calibration curves providing better signal/noise ratio, detectability and sensitivity*.

4.2.1.2.2 Organic solvents analysis

As the analysis of clinical samples will probably involve a treatment step and this can result in the use of organic solvents, the stability of the ELISA at different %-s of organic solvents was analysed. Thus, PYO standard curves were prepared in different %-s of organic solvents in PBST (assay buffer) and compared with the control curve build in PBST. As shown in Figure 4. 4, the addition of methanol and acetonitrile did not produce a significant variation in IC_{50} and A_{max} parametres, although the IC_{50} slightly increased at acetonitrile concentrations > 20 % (from 8 to 11 nM in assay buffer vs 20 % acetonitrile). Furthermore, the presence of dimethylsulfoxide (DMSO) at concentrations between 1-5 % did not significantly vary the analytical parameters of the ELISA. In contrast, DMSO concentrations > 10 % increased the IC_{50} value of the assay (from 7 to 12 nM in assay buffer vs 20 % DMSO, respectively) while decreased the A_{max} (from 1.14 to 0.70 in assay buffer vs 20 % DMSO, respectively). A similar behaviour was observed when isopropanol was added. In this case, the studied analytical parameters remained constant at isopropanol concentrations between 2-10 % while the sensitivity was dramatically affected at concentrations > 20 % (IC_{50} value increased from 6 nM to 20 nM in 40 % isopropanol).

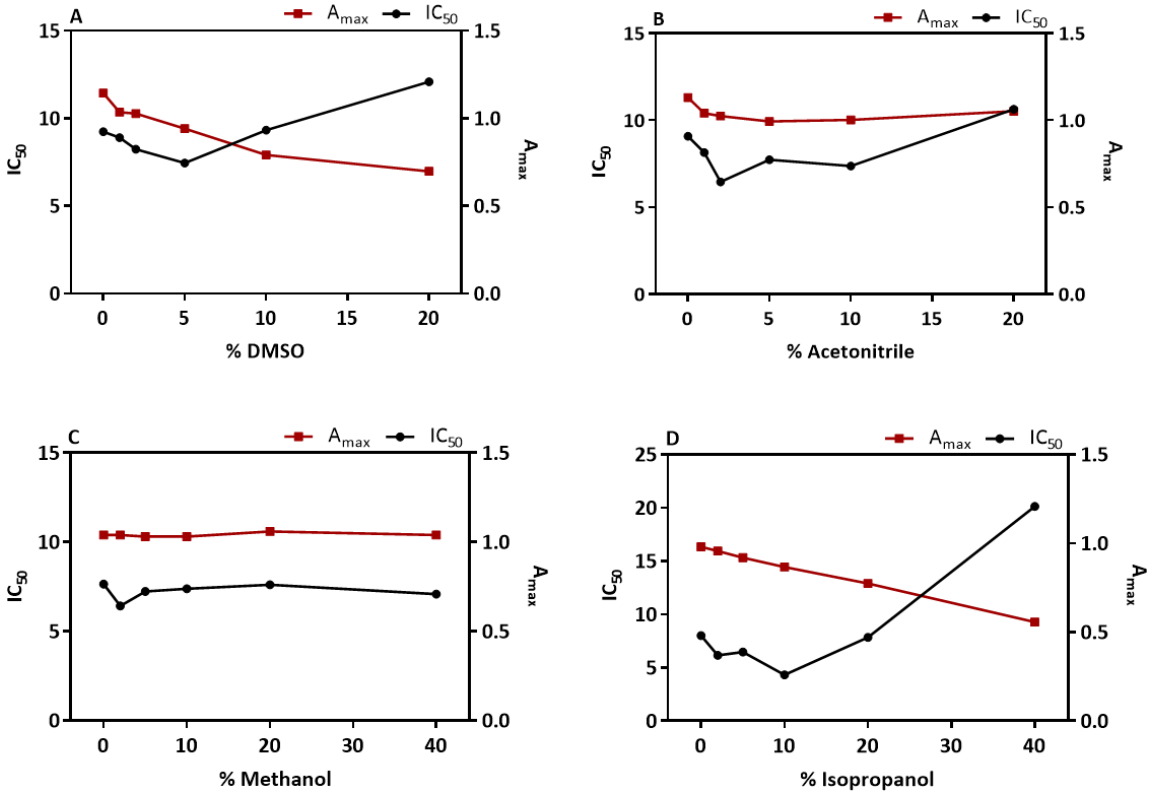

Figure 4. 4 *PYO mAb122/PC1-BSA ELISA performance at different % of organic solvent. PYO standard curves were prepared in different % of (A) DMSO (B) Acetonitrile (C) Methanol (D) Isopropanol. The selection of the most appropriate conditions was based on the variations in A_{max} and IC_{50} values of the generated calibration curves providing better signal/noise ratio, detectability and sensitivity.*

Taking into account all this data, general optimal conditions are described in Table 4. 3.

Table 4. 3 *Physicochemical parameters selected for performing optimal PYO mAb122/PC1-BSA ELISA run in assay buffer.*

	PYO mAb122/PC1-BSA
mAb concentration/ µg mL^{-1}	0.008
coating antigen/ µg mL^{-1}	0.125
pH	7.5
Organic solvents/ %	0
Competition time/ min	30
Preincubation time/ min	0
Conductivity/ mS cm^{-1}	15
Tween 20/ %	0.05

4.2.2 Specificity study

The specificity of the ELISA was assessed for both PYO and 1-OHphz due to their structural similarities (see Figure 4. 1). As expected, Figure 4. 5 illustrates that PYO mAb122/PC1-BSA ELISA recognized both phenazines with high affinity showing lower IC_{50} value for the last one (IC_{50}s

=0.32 vs 2.92 nM for 1-OHphz and PYO, respectively). However, it has been documented that 1-OHphz is found at much lower concentrations than PYO. In this sense, Wilson et al.[6] reported 9-fold times lower 1-OHphz levels than PYO concentration on sputa samples. Nevertheless, PYO concentrations have been expressed as PYO immunoreactivity equivalents (PYO IRequiv) to take this fact into consideration.

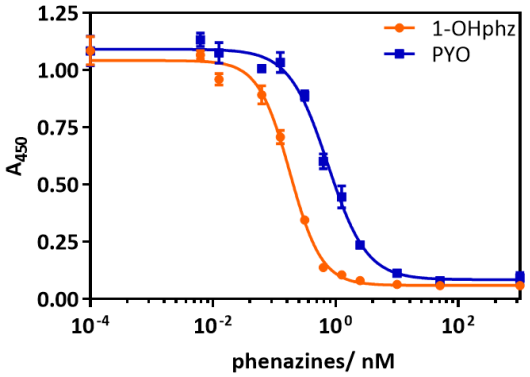

Figure 4. 5 *Cross-reactivity study using 1-OHphz and PYO metabolites in buffer under the aforementioned conditions for PYO mAb122/PC1-BSA ELISA. The obtained IC_{50} for 1-OHphz and PYO were 0.104 and 0.569 nM, respectively. Each calibration point was measured in triplicates on the same ELISA plate and the results show the average and standard deviation of analysis made on 3 different days.*

The most common used methods for PYO detection are based on its unique optical and electrical properties. Thus, PYO can be detected by absorbance at different wavelengths[7], SERS[8], ultraviolet visible (UV-Vis) or mass spectroscopy (MS)[6] and electrochemical systems[9-10], reaching LoDs in the low µM and in the high nM range. Nevertheless, the main drawbacks of some of these techniques are the lack of specificity, the long duration of the assay and the need of expensive equipments and time consuming pretreatment steps. In contrast, the developed PYO mAb122/PC1-BSA immunochemical assay has achieved a very low LoD (0.68 ±0.10 nM) and has not required any sophisticated equipment.

In this context, it has been previously reported a micro-plate ELISA (As230/PC1-BSA ELISA)[3] with a LoD of 0.01 nM able to detect PYO in less than 90 min. However, since this ELISA used a polyclonal antiserum (As230) which showed greater avidity for 1-OHphz than to PYO (IC_{50} values of 0.53 and > 800 nM for 1-OHphz and PYO, respectively), PYO quantification required its prior transformation to 1-OHphz. In contrast, the immunochemical strategy reported in this Chapter is the result of using the hybridoma technology to select mAb cell clones able to recognize PYO with a much higher affinity. In fact, the performance of selective cloning rounds has allowed to isolate 14 clones that were highly sensitive for PYO. Although all these clones detected 1-OHphz with higher avidity than PYO, 3 clones have shown similar IC_{50} for both phenazines. Hence, clone

C.9.1.9.1.1.2.2., named PYO mAb122, has been used to develop a sensitive immunochemical assay (PYO mAb/PC1-BSA ELISA) which has allowed to detect PYO in the low nM range (LoD =0.07 nM). Besides, since the LoD of the assay is lower than the reported PYO values on biological and clinical samples[10-11], PYO mAb/PC1-BSA ELISA will be used to determine PYO levels, first, on clinical isolates and, further, on clinical samples such as sputum and swab.

In addition, the ineffectiveness of classical antibiotics due to their innapropiate use has resulted in the rise of *P. aeruginosa* multidrug resistant (MDR) strains. Besides, in the last 30 years, no new antibiotics have been developed[12]. Therefore, new therapeutic techniques need to be developed. Among these emerging techniques, mAbs are gaining importance as a consequence of their high affinity and specificity[13-15], doubling in size its market in the last 5 years[16-17]. Thus, mAbs are increasingly being used in different human diseases such as infectious diseases; currently, 6 mAbs are approved by the US Food and Drug Administration (FDA) for this purpose[18-19]. Therefore, in this context, the here described PYO mAb122 will also be tested as a therapeutic agent, since it could minimize or even avoid the cytotoxic effects produced by PYO VF[11, 20] by specifically binding it.

4.3 Materials & methods

4.3.1 Buffers and chemical products

Phosphate-buffered saline (PBS) is 10 mM phosphate buffer with 0.8 % saline solution, adjusting the pH to 7.5. ***PBST (assay buffer)*** is PBS with 0.05 % Tween 20. 10XPBS is PBS 10 times concentrated. ***Coating buffer*** is 50 mM carbonate-bicarbonate buffer at pH 9.6. ***Citrate buffer*** is a 40 mM solution of sodium citrate at pH 5.5. ***The substrate solution*** contains 0.01 % 3,3',5,5'-tetramethylbenzidine (TMB) and 0.004 % H_2O_2 in citrate buffer.

PYO was obtained from Sigma-Aldrich Co (St. Louis, MO) and ***1-OHphz*** was synthesized following the procedures[21] described in Pastells et al.[3].

4.3.2. Synthesis processes

PC1 hapten and PC1-HCH conjugate. The synthesis of PC1 hapten and PC1-HCH conjugate were carried out by Carme Pastells and the procedure is explained in Pastells et al.[3].

PC1-BSA conjugate*.* PC1 was covalently attached to BSA (Sigma Aldrich) using the active ester (AE) method described by Pastells[3]. Thus, PC1 hapten (0.6 mg, 2.5 µmol) was reacted with

dicyclohexylcarbodiimide (DCC, 2.6 mg, 3 µmol) and N-hydroxysuccinimide (NHS; 0.72 mg, 3 µmol) in anhydrous dimethylformamide (DMF) (66.6 µl) under low stirring for 1 h at room temperature (RT). The suspension formed was centrifugation at 10,000 rpm for 10 min and the supernatant was added dropwise to a solution of BSA (10 mg) in borate buffer (1.93 mL). The mixture was stirred for 4 h at RT. Finally, the bioconjugate was purified by dialysis against 0.5 mM PBS (5 x 5 L) and Milli-Q water (1 x 5L dialyzed) and stored at -80 ºC. Hapten density was characterized by MALDI-TOF/TOF-MS.

4.3.3 Immunochemistry

4.3.3.1 Antibody production

All the here presented mAbs have been produced by the Custom Antibody Service (CAbS) Unit which belongs to CIBER in Bioengineering, Biomaterials and Nanomedicne (CIBER-BBN at the IQAC−CSIC).

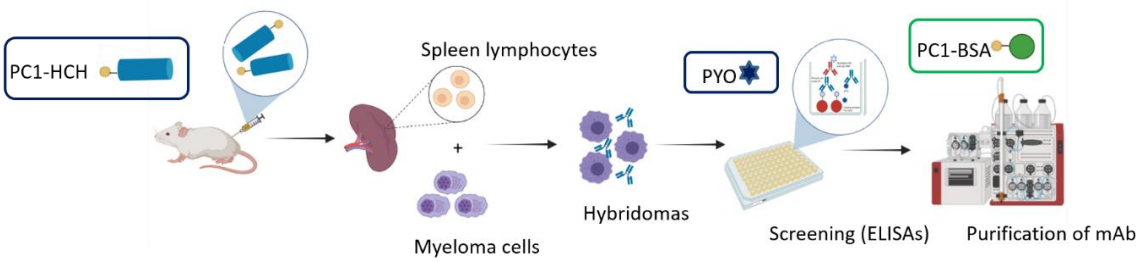

Figure 4. 6 *PYO mAb122 production. Mice were immunized using PC1-HCH bioconjugate. Spleen lymphocytes were fused with murine mieloma cells to obtain the corresponding hybridomas. The choosen hybridomas were cloned and used to produce mAbs. The selected mAbs were purified and used to develop a specific ELISA.*

BALB/c female mice (8-10 weeks old) were immunized with PC1-HCH (maleic acid (MA)). The first dose consisted of 100 µg of conjugate injected intraperitoneally as an emulsion of PBS and complete Freund's adjuvant. In addition, 3 booster injections were given at 3-week intervals using the same dose of immunogen emulsified in incomplete Freund's adjuvant. Mice selected as spleen donors for hybridoma production received a final injection of 100 µg of antigen in PBS 4 days prior to fusion.

P3-X63/Ag 8.653 murine myeloma cells (ATCC, Rockville, MD) were cultured in supplemented Dulbecco's Modified Eagle Medium (high-glucose DMEM with 2 mM alanylglutamine, 1 mM minimum nonessential amino acids, and 25 µg mL^{-1} gentamicin supplemented with 10% (v/v) fetal bovine serum (FBS)). Mouse spleen lymphocytes were fused with myeloma cells at a 4:1 ratio using PEG 1500 (Roche Applied Science, Mannheim, Germany) as a fusing agent. The fused

cells were cultured in 96-well culture plates at a density of 2 x 10^5 cells/100 µl of 15 % FBS supplemented DMEM per well. After 24h, hypoxanthine-aminopterin-thymidine (HAT) selection medium (10% FBS supplemented DMEM with 100 µM hypoxathine, 0.4 µM aminopterine, 16 µM thymidine, 2% Hybridoma Fusion and Cloning Supplement (HFCS, Roche)) was added (100 µl $well^{-1}$). Subsequently, 10 days after cell fusion, culture supernatants were screened by performing indirect ELISA assays, coating the corresponding plates with 1.0 µg mL^{-1} PC1-BSA conjugate, in order to select the hybridomas that were able to recognize PYO with high affinity. The chosen hybridomas were then cloned by the limiting dilution method using HAT medium without aminopterine (HT) medium, supplemented with 15% FBS and 1% HFCS. Finally, stable antibody-producing clones were expanded and cryopreserved in liquid nitrogen and the resulting supernatants containing mAbs were purified by protein G affinity chromatography (see Figure 4. 6). Afterward, 2D ELISAs were carried out for each purified mAb to determine the most appropriate PC1-BSA and mAb concentrations to be used on the competitive ELISA.

4.3.3.2 Competitive PYO ELISA

As illustrated in Figure 4. 7, PYO measurements were carried out using an indirect competitive ELISA, where the analyte (PYO; dark blue stars) competes with the hapten based on 1-OHphz molecule (PC1; light blue stars) for binding to the primary Ab (PYO mAb122).

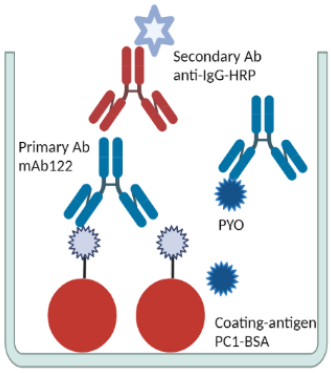

Figure 4. 7 *Schematic representation of an indirect competitive ELISA.*

Therefore, for PYO detection, microtiter plates were coated with PC1-BSA (0.125 µg mL^{-1} in coating buffer 100 µL $well^{-1}$) and incubated overnight at 4 ºC. Then, the plates were washed 4 times with PBST (4 × 300 µL) and serial dilutions of PYO (3200, 80, 3.2, 1.6, 0.64, 0.32, 0.032 and 0 nM in PBST) or the samples, diluted with the assay buffer, were added (50 µL $well^{-1}$) followed by the solution of the mAb122 (0.01575 µg mL^{-1} also in PBST, 50 µL $well^{-1}$). After 30 min incubation shaking at RT, the plates were washed as described above and the anti-IgG-HRP solution (1/2000 in PBST, 100 µL $well^{-1}$) was added, waiting an additional 30 min incubation

period. Subsequently, another cycle of washes was performed and the substrate solution was added (100 µL well^{-1}). Finally, the enzymatic reaction was stopped after 30 min at RT with 2 M H_2SO_4 (50 µL well^{-1}). The absorbances were measured at 450 nm.

4.4 Concluding remarks

- Immunization of mice with the same hapten described by Pastells et al.[3] and subsequent selective cloning rounds allowed the isolation of 14 mAbs showing high affinity for both PYO and 1-OHphz phenazines. From these 14 mAbs, clone 9.1.9.1.1.2.2. (PYO mAb122) has been selected since it showed low IC_{50} values for both 1-OHphz and PYO phenazines (0.104 and 0.569 nM, respectively).

- PYO mAb122 has been used to develop a highly sensitive immunochemical assay able to detect PYO in the low nM range (LoD =0.07 nM). The developed assay has shown excellent accuracy and robustness.

- Since the LoD of the developed assay is lower than reported PYO concentrations in biological and clinical samples[10-11], PYO mAb122/PC1-BSA ELISA will be implemented to directly measure PYO, first, in bacterial isolates from patients infected with *P. aeruginosa* and, later, in clinical samples from patients infected with *P. aeruginosa*, such as sputum and swab. Nevertheless, due to the specific interference caused by 1-OHphz, when measuring PYO, in these samples, PYO concentrations will be expressed as IRequiv of PYO.

4.5 References

1. Sismaet, H. J.; Pinto, A. J.; Goluch, E. D., Electrochemical sensors for identifying pyocyanin production in clinical Pseudomonas aeruginosa isolates. *Biosens Bioelectron* **2017,** *97*, 65-69.
2. Breuer, O.; Caudri, D.; Akesson, L.; Ranganathan, S.; Stick, S. M.; Schultz, A.; Arest, C. F., The clinical significance of oropharyngeal cultures in young children with cystic fibrosis. *Eur Respir J* **2018,** *51* (5).
3. Pastells, C.; Pascual, N.; Sanchez-Baeza, F.; Marco, M. P., Immunochemical Determination of Pyocyanin and 1-Hydroxyphenazine as Potential Biomarkers of Pseudomonas aeruginosa Infections. *Anal Chem* **2016,** *88* (3), 1631-8.
4. Ballesteros, B. B., D.; Camps, F.; Marco, M.-P., Preparation of antisera and development of a direct enzyme-linked immunosorbent assay for the determination of the antifouling agent Irgarol 1051. *Analytica Chimica Acta* **1997,** *347*, 139-147.

5. Fischer, H.; Widdicombe, J. H., Mechanisms of acid and base secretion by the airway epithelium. *J Membr Biol* **2006,** *211* (3), 139-50.
6. Wilson, R.; Sykes, D. A.; Watson, D.; Rutman, A.; Taylor, G. W.; Cole, P. J., Measurement of Pseudomonas aeruginosa phenazine pigments in sputum and assessment of their contribution to sputum sol toxicity for respiratory epithelium. *Infect Immun* **1988,** *56* (9), 2515-7.
7. Reszka, K. J.; O'Malley, Y.; McCormick, M. L.; Denning, G. M.; Britigan, B. E., Oxidation of pyocyanin, a cytotoxic product from Pseudomonas aeruginosa, by microperoxidase 11 and hydrogen peroxide. *Free Radic Biol Med* **2004,** *36* (11), 1448-59.
8. Polisetti, S.; Baig, N. F.; Morales-Soto, N.; Shrout, J. D.; Bohn, P. W., Spatial Mapping of Pyocyanin in Pseudomonas Aeruginosa Bacterial Communities Using Surface Enhanced Raman Scattering. *Appl Spectrosc* **2017,** *71* (2), 215-223.
9. Alatraktchi, F. A.; Noori, J. S.; Tanev, G. P.; Mortensen, J.; Dimaki, M.; Johansen, H. K.; Madsen, J.; Molin, S.; Svendsen, W. E., Paper-based sensors for rapid detection of virulence factor produced by Pseudomonas aeruginosa. *PLoS One* **2018,** *13* (3), e0194157.
10. Alatraktchi, F. A. a.; Svendsen, W. E.; Molin, S., Electrochemical Detection of Pyocyanin as a Biomarker for Pseudomonas aeruginosa: A Focused Review. *Sensors* **2020,** *20* (18), 5218.
11. Hall, S.; McDermott, C.; Anoopkumar-Dukie, S.; McFarland, A. J.; Forbes, A.; Perkins, A. V.; Davey, A. K.; Chess-Williams, R.; Kiefel, M. J.; Arora, D.; Grant, G. D., Cellular Effects of Pyocyanin, a Secreted Virulence Factor of Pseudomonas aeruginosa. *Toxins (Basel)* **2016,** *8* (8).
12. Shore, C. K.; Coukell, A., Roadmap for antibiotic discovery. *Nat Microbiol* **2016,** *1* (6), 16083.
13. Hunter, R. C.; Klepac-Ceraj, V.; Lorenzi, M. M.; Grotzinger, H.; Martin, T. R.; Newman, D. K., Phenazine content in the cystic fibrosis respiratory tract negatively correlates with lung function and microbial complexity. *Am J Respir Cell Mol Biol* **2012,** *47* (6), 738-45.
14. Ducancel, F.; Muller, B. H., Molecular engineering of antibodies for therapeutic and diagnostic purposes. *MAbs* **2012,** *4* (4), 445-57.
15. Khan, H. A.; Baig, F. K.; Mehboob, R., Nosocomial infections: Epidemiology, prevention, control and surveillance. *Asian Pacific Journal of Tropical Biomedicine* **2017,** *7* (5), 478-482.
16. Grilo, A. L.; Mantalaris, A., The Increasingly Human and Profitable Monoclonal Antibody Market. *Trends Biotechnol* **2019,** *37* (1), 9-16.
17. Mullard, A., FDA approves 100th monoclonal antibody product. *Nat Rev Drug Discov* **2021,** *20* (7), 491-495.
18. Lu, R. M.; Hwang, Y. C.; Liu, I. J.; Lee, C. C.; Tsai, H. Z.; Li, H. J.; Wu, H. C., Development of therapeutic antibodies for the treatment of diseases. *J Biomed Sci* **2020,** *27* (1), 1.
19. Dougan, M.; Nirula, A.; Azizad, M.; Mocherla, B.; Gottlieb, R. L.; Chen, P.; Hebert, C.; Perry, R.; Boscia, J.; Heller, B.; Morris, J.; Crystal, C.; Igbinadolor, A.; Huhn, G.; Cardona, J.; Shawa, I.; Kumar, P.; Adams, A. C.; Van Naarden, J.; Custer, K. L.; Durante, M.; Oakley, G.; Schade, A. E.; Holzer, T. R.; Ebert, P. J.; Higgs, R. E.; Kallewaard, N. L.; Sabo, J.; Patel, D. R.; Dabora, M. C.; Klekotka, P.; Shen, L.; Skovronsky, D. M.; Investigators, B.-. Bamlanivimab plus Etesevimab in Mild or Moderate Covid-19. *N Engl J Med* **2021,** *385* (15), 1382-1392.
20. Ran, H. H., D. J.; Lau, G. W., Human targets of Pseudomonas aeruginosa pyocyanin. *PNAS* **2003,** *100* (24), 14315–14320.

21. Vivian, D. L., The practical synthesis of 1-phenazinol. *Nature* **1956,** *178* (4536), 753.

Chapter 5

PYO as a good biomarker of acute and chronic *Pseudomonas aeruginosa* respiratory infections

In this chapter, the implementation of PYO mAb122/PC1-BSA ELISA to detect PYO in clinical bacterial isolates from patients infected with *Pseudomonas aeruginosa* is described. The optimized competitive assay has shown a very low limit of detection (LoD) in culture broth (0.15 nM) which has allowed PYO quantification in this type of samples. First, bacterial growth curves have been prepared to determine the kinetics of release of PYO by culturing different isolates obtained from infected patients. Thus, significant differences between clinical isolates obtained from patients with an acute or a chronic infection (~ 6000 nM vs ~ 8 nM of PYO content, respectively) have been found. Together with this data, 1-hydroxyphenazine (1-OHphz) levels have been also measured[1] since it is the main metabolite of PYO biosynthesis and its quantification could contribute to shed light about infection prognosis. Subsequently, these results have been confirmed by analysing PYO and 1-OHphz levels released of 37 clinical isolates obtained from infected patients at different stages. The results obtained have positioned PYO as a very useful biomarker to differentiate acute and chronic *P. aeruginosa* infections, which is not always obvious, and open the possibility to use such virulence factor (VF) also as biomarker for patient stratification and for an effective management of these kind of infections.

The work presented in this chapter is adapted from:

Rodriguez-Urretavizcaya, B.; Pascual, N.; Pastells, C.; Martin-Gomez, M.T.; Vilaplana Ll. and Marco, M.P. (2021). Diagnostic and Stratification of Pseudomonas aeruginosa Infected Patients by Immunochemical Quantitative Determination of Pyocyanin from Clinical Bacterial Isolates. *Front. Cell. Infect. Microbiol.* 11, 1-12. doi: 10.3389/fcimb.2021.786929

5.1 Introduction

As previously explained, usually *P. aeruginosa* infections are categorized as acute and chronic. Acute infections are associated with a planktonic lifestyle and they are frequent during early stages of infection. Besides, they show high virulence factor (VF) expression (as it is the case of pyocyanin (PYO)[2]) and, in general, are susceptible to antibiotics. In contrast, chronic infections are characterized for low VF levels[3-4] and are more resistant to antibiotics[5-11] mainly due to the formation of biofilms[7] and the generation of persister cell[8] (mucoid phenotype). Therefore, eradication therapies at early stages of the infection (acute infections) are recommended since at this stage bacterial strains are more susceptible to antibiotics, significantly improving the management of *P. aeruginosa* infections[12-16].

In this context, the identification of new biomarkers of infection has become an essential milestone. Thus, PYO, the main QS-regulated VF of *P. aeruginosa*, can be a great biomarker candidate to differentiate between *P. aeruginosa* acute and chronic infections since it is known to be secreted at higher concentrations during early stages of infection[3-4, 17-18] and it is specific of this bacterium[19-21].

Previously in our lab, As230/PC1-BSA ELISA was implemented to quantify 1-hydroxiphenazine (1-OHphz) and PYO in DKN263 (wild type) and DKN330 (*ΔphzA1-G1 ΔphzA2-G2,* the genes producing phenazines are mutated[21]) *P. aeruginosa* strains grown in Müeller Hinton (MH) media. Nevertheless, as explained in Chapter 4, PYO quantification required its transformation into 1-OHphz pior analysis. Therefore, in this chapter, PYO mAb122/PC1-BSA ELISA has been implemented to directly quantify PYO in culture broth of clinical isolates from patients infected with acute and chronic infections. Besides, this study has allowed to assess PYO potential as biomarker of infection and patient stratification.

5.2 Results & discussion

5.2.1 Implementation of PYO ELISA for the analysis of *P. aeruginosa* bacterial isolates on culture broth

PYO mAb122/PC1-BSA ELISA was first implemented for performing PYO measures in bacterial isolates from patients infected with *P. aeruginosa* since culture broth is an easier matrix to work with than matrices from clinical samples.

5.2.1.1 Matrix effect evaluation

The potential nonspecific interferences caused by the MH broth in the ELISA were initially assessed. For this purpose, calibration curves of PYO and 1-OHphz were prepared in MH diluted at different ratios with PBST (from 1/5 to 1/20) and measured with the corresponding ELISA to compare their performance with the calibration curves run in buffer (see Figure 5. 1).

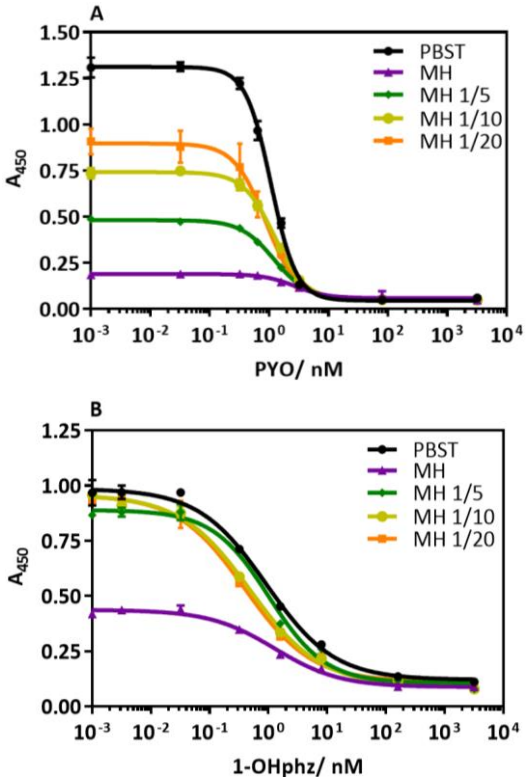

Figure 5. 1 *Matrix effect of the MH broth undiluted and dilute 5, 10 and 20 times with PBST on the performance of (A) PYO mAb122/PC1-BSA and (B) As230/PC1-BSA ELISA. The calibration curves were run using the conditions established for the assay in PBST. See Table 5. 1 and Table 5. 2 for analytical parameters of the standard curves in PBST and in 1/20 MH on PYO mAb122/PC1-BSA and in PBST and in 1/5 MH on As230/PC1-BSA ELISA. Each calibration point was measured in triplicates on the same ELISA plate and the results show the average and standard deviation of the assay carried out on 1 day.*

As shown in Figure 5. 1**,** the performance of PYO mAb122/PC1-BSA ELISA in MH broth after a just 1/5 dilution was similar to that in assay buffer (IC_{50} =1. 08 and 1.22 nM in PBST and 1/5 MH, respectively), although the signal was significantly decreased under these conditions (maximum absorbance (A_{max}) =1.31 and 0.48 in PBST and 1/5 MH dilution, respectively). Therefore, since PYO has always been found to be secreted at significant concentrations by cultured clinical isolates (in the µM range)[19] and the detectability achieved by this ELISA is well below these values, we decided to attempt measuring the samples using a 1/20 dilution of MH in PBST. In fact, Elliot et al.[22] detected PYO concentrations in the µM range when analysing PA14 and PA11 strains isolated from sputum samples of CF patients using an electrochemical method based on ultramicroelectrodes. Besides, Silva et al.[23] measured PYO levels up to 18 µM in *P. aeruginosa*

isolates from sputum samples using an extraction and spectroscopic method. In both cases, bacterial cultures were grown for 24 h.

As shown in Table 5. 1, the analytical parameters of the ELISA run in 1/20 MH seemed to be suitable for our purposes (IC_{50} =1.18 ± 0.24 nM, limit of detection (LoD) =0.15 ± 0.07 nM).

Table 5. 1 *Analytical parameters of the PYO mAb122/PC1-BSA ELISA for the detection of PYO in MH broth media diluted 20 times. Immunoreagent conditions were: 0.125 µg mL^{-1} for PC1-BSA and 0.008 µg mL^{-1} for PYO mAb122 in both cases. The data shown correspond to the average and standard deviation of of the parameters of the calibration curves performed 3 different days using at least 3 well replicates per concentration.*

	PBST	**1/20 MH**
A_{min}	0.07 ± 0.01	0.05 ± 0.01
A_{max}	1.08 ± 0.09	0.92 ± 0.14
Slope	-1.40 ± 0.49	-1.11 ± 0.21
IC_{50}/ nM	0.68 ± 0.10	1.18 ± 0.24
Dynamic range/ nM	0.18 ± 0.08 and 2.18 ± 0.19	0.32 ± 0.10 and 4.13 ± 1.35
LoD/ nM	0.07 ± 0.04	0.15 ± 0.07
R^2	0.99 ± 0.01	0.99 ± 0.01

Moreover, the reproducibility of the assay was demonstrated by measuring IC_{50}, slope and A_{max} values during a year (n =13). Thus, the obtained results followed a normal distribution (D'Agostino & Pearson normality test, Shapiro-Wilk normality test and KS normality test) showing values of (1.72 ±0.79 nM), (-1.28 ±0.27) and (0.97 ±0.29), respectively (see Figure 5. 2). Besides, the low variability of the assay was demonstrated through the low dispersion of the obtained results, which were concentrated around the mean value. In this sense, IC_{50} values only oscillated between 0.8 and 2.8; the slope between -0.9 and -1.7; and the A_{max} between 0.8 and 1.5 (outliers were not considered).

Accordingly, as illustrated in Figure 5. 1**,** the assay for 1-OHphz detection (As230/PC1-BSA ELISA) worked perfectly just diluting MH medium 5 times as the analytical parameters of the of As230/PC1-BSA ELISA obtained in this conditions compared to PBST were very similar (IC_{50} value of 0.93 and 1.02 nM and A_{max} of 0.99 and 0.89 in PBST and 1/5 MH dilution, respectively). However, as reported by Wilson et al.[24], 1-OHphz levels in sputa samples are 9-fold times lower than PYO. Therefore, unlike for PYO mAb122/PC1-BSA ELISA, it was decided to work at 1/5 dilution of MH in PBST. Table 5. 2 shows all the analytical parameters of the ELISA run in 1/5 MH dilution (IC_{50} =1.02 ±0.06 nM, LoD =0.10 nM).

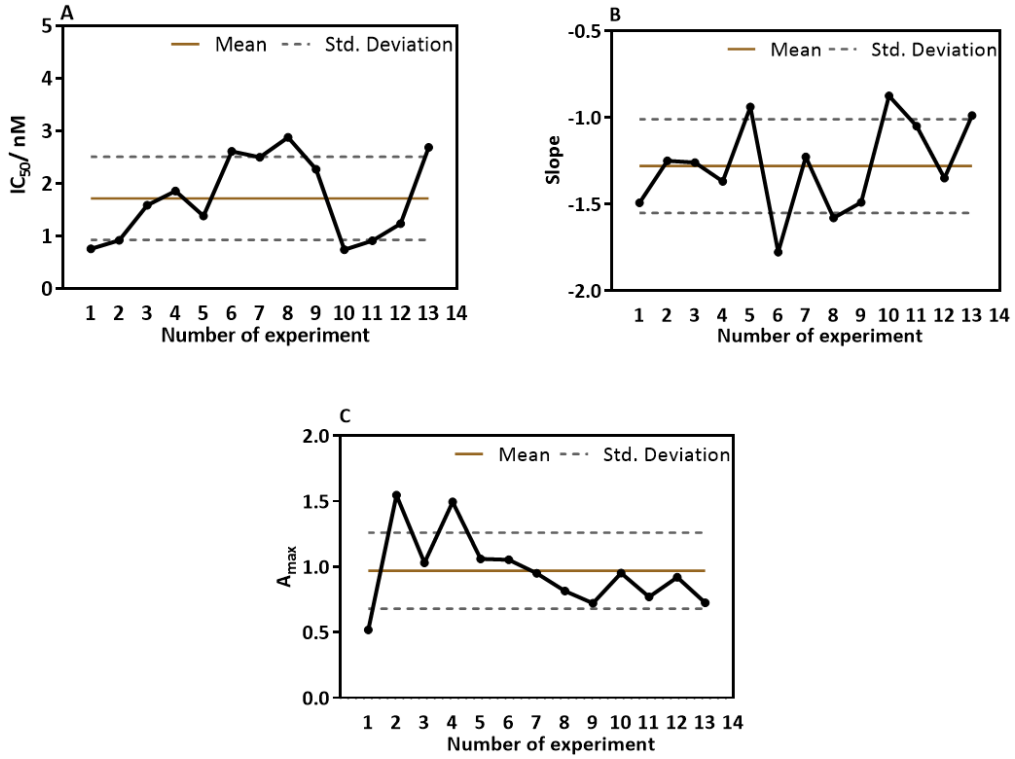

Figure 5. 2 *(A) IC_{50}, (B) slope and (C) A_{max} values of PYO mAb122/PC1-BSA ELISA. 13 identical experiments were run in 1/20 diluted MH media using PBST. Results are represented chronologically (in the same year).*

Table 5. 2 *Analytical parameters of As230/PC1-BSA ELISA in PBST and MH broth diluted 5 times. Inmunoreagent concentrations used were PC1-BSA at 0.0625 µg mL^{-1} and 1/6000 dilution of As230 in both cases. The data shown correspond to the average and standard deviation of the parameters of the calibration curves performed the same day using at least 3 well replicates per concentration.*

	PBST	**1/5 MH**
A_{min}	0.12 ± 0.02	0.11 ± 0.02
A_{max}	0.99 ± 0.02	0.89 ± 0.02
Slope	-0.75 ± 0.07	-0.90 ± 0.11
IC_{50}/ nM	0.93 ± 0.05	1.02 ± 0.06
Dynamic range/ nM	0.17 and 6.47	0.24 and 5.85
LoD/ nM	0.06	0.10
R^2	0.99 ± 0.03	0.99 ± 0.02

5.2.1.2 Accuracy studies

A set of blind samples were prepared by spiking MH culture medium diluted 20 times in PBST with different PYO concentrations (30, 15, 7.5, 3.75, 0.9375 nM) and measured with PYO mAb122/PC1-BSA ELISA. The obtained PYO values were compared with the spiked PYO concentrations. As it can be observed in Figure 5. 3, the coefficient of correlation between

concentrations of the blind spiked samples and the values measured with the ELISA was excellent (R^2 =0.997) and the slope of the linear regression was close to 1 (slope =1.08), showing almost a perfect match between spiked and measured concentration values.

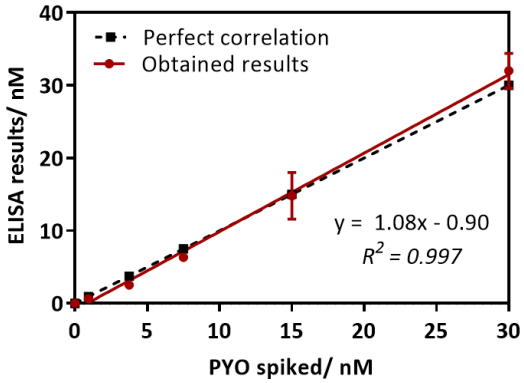

Figure 5. 3 *Results from the accuracy study using PYO mAb122/PC1-BSA ELISA. The graph shows the linear regression analysis of the MH media diluted 20 times spiked with different PYO concentrations ranging from 30 to 0 nM and the concentrations measured with the PYO mAb122/PC1-BSA ELISA. Assay was run in MH culture media diluted 20 times in PBST. Each calibration point was measured in triplicates on the same ELISA plate and the results show the average and standard deviation of the assay carried out on 3 different days.*

5.2.2 Growth curves and phenazines release profile of *P. aeruginosa* bacterial isolates

Bacterial growth curves were built up culturing clinical isolates from patients with acute and chronic infections. These measurements were important to compare growth dynamics of the different clinical isolates and also to determine the time required to detect these phenazines in the media using the ELISA developed. Thus, in total 5 *P. aeruginosa* isolates (using PAO1 as reference) were incubated in MH media to study their growth dynamics, through the measurement of culture turbidity (OD 600 nm) and colony forming units (CFUs) counting, and the production kinetics of both PYO and 1-OHphz phenazines.

Recently, our group has reported that the levels of released autoinducers (AIs) belonging to the Pqs QS system, such as Pseudomonas quinolone signal (PQS) and 2-Heptyl-4-quinolone (HHQ), by clinical isolates of *P. aeruginosa* were significantly different depending on the stage of the infection[25-26]. Thus, bacterial isolates from patients with acute infection presented quantifiable PQS levels after 5 h growth, while when these isolates belonged to patients with a chronic infection levels could only be quantified after more than 12 h growth, which was correlated to the virulence and behavior of *P. aeruginosa*. With this scenario, similar differences in terms of the release of a QS regulated VF such as PYO were expected.

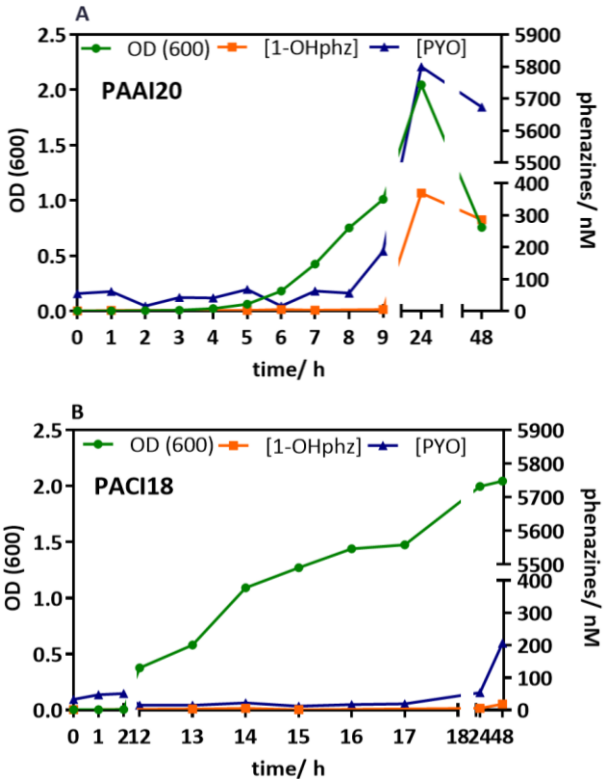

Figure 5. 4 *Growth curves and phenazines kinetics production of two P. aeruginosa isolates grown for 48 h (37 ºC, 500 rpm). The green line (OD 600) gives information about the bacterial growth. The blue and the yellow lines indicate IRequiv. of PYO and 1-OHphz production, respectively. Results obtained from (A) an isolate (PAAI20) of a patient undergoing an acute P. aeruginosa infection and (B) an isolate (PACI18) of a patient suffering chronic infection. Each data point was measured in triplicates on the same ELISA plate and the results show the average and standard deviation of the assay carried out on 1 day.*

Figure 5. 4 shows the growth curves obtained when analysing two representative bacterial isolates, PAACI18 and PAAI20, from patients with a chronic and an acute infection, respectively. As expected, a clear difference between them was observed. Thus, the PAAI20 isolate (acute infection) started its exponential growth phase after 6 h of incubation whereas PAACI18 (chronic infection) showed a longer lag phase initiating its exponential division at 12 h of incubation, in agreement with the behavior observed for the QS signaling molecules found for the same type of bacterial isolates. Furthermore, in the case of the isolate from acute infection, after reaching the maximum growth levels, the curve showed a very steep drop caused by the cytotoxic effect of PYO high levels (it should be noticed that after 24 h of incubation, bacterial cultures corresponding to isolates from acute infections show a clear blue color, see Figure 5. 5)[19, 27]. Focusing on CFUs counting, both isolates reached a plateau on the number of viable cells which was similar regarding the values obtained. Nevertheless, PAAI20 isolate yielded these maximum cell number levels at 8 h of incubation and, by contrast, PACI18 isolate hit this point after 15 h of culturing time (see Table 5. 3).

Table 5. 3 *Bacterial growth rates of P. aeruginosa bacterial isolates obtained from patients suffering acute or chronic infection, grown in MH media (n=3). Bacterial culture turbidity is determined measuring the optical density (OD) at 600 nm.*

Acute isolate PAAI20			**Chronic isolate PACI18**		
time/ h	***OD 600 nm[b]***	***Bact. Conc/CFU mL^{-1}***	***time/ h***	***OD 600 nm***	***Bact. Conc/CFU mL^{-1}***
0	0.003	3.0 x 10^5	0	0.003	3.1 x 10^5
1	0.004	4.0 x 10^5	1	0.003	6.1 x 10^5
2	0.005	1.6 x 10^6	2	0.006	1.9 x 10^6
3	0.009	3.9 x 10^6	12	0.376	3.3 x 10^9
4	0.023	3.0 x 10^7	13	0.581	1.9 x 10^9
5	0.063	6.8 x 10^7	14	1.091	1.5 x 10^9
6	0.183	3.7 x 10^8	15	1.270	2.4 x 10^{12}
7	0.427	5.2 x 10^{11}	16	1.440	2.2 x 10^{12}
8	0.754	1.4 x 10^{12}	17	1.475	1.0 x 10^{13}
9	1.012	5.2 x 10^{12}	24	1.996	5.2 x 10^{12}
24	2.046	1.3 x 10^{13}	48	2.045	3.9 x 10^{11}
48	0.747	2.3 x 10^{12}			

In addition, at the same time points, bacterial culture aliquots were also analysed to determine the pattern of phenazines production kinetics obtained by *P. aeruginosa* isolates from acute and chronic infections using PYO mAb122/PC1-BSA ELISA and As230/PC1-BSA[1] ELISA for PYO and 1-OHphz quantification, respectively. The results have been plotted in the same graphs of Figure 5. 4. As it can be observed, the release kinetics of the two studied phenazines were coherent with the results previously reported by Montagut et al.[25-26] for PQS and HHQ QS signaling molecules, who detected higher PQS and HHQ levels (in the low µM range) when analysing isolates with acute infections than isolates with chronic infections (in the low nM range). Thus, the bacterial isolate from the patient presenting an acute infection clearly showed much higher levels of both molecules (5800 nM for PYO and 370 nM for 1-OHphz at 24h) than the isolate obtained from a patient with a chronic infection (54 nM for PYO and 5 nM for 1-OHphz at 24 h). Focusing on the phenazine production kinetics patterns found, it remained constant when studying an isolate from a patients suffering a chronic infection, just slightly increasing for PYO after 48 h of culturing. In contrast, phenazine production profile corresponding to the isolate from a patient with an acute infection showed a marked increase in PYO levels after 9 h of incubation, which reached its maximum at 24 h. Furthermore, these levels were smoothly decreased after 48 h of culture predictably due to the effects of PYO itself on bacterial viability causing autolysis[28-29]. Besides, after 24 h of incubation, bacterial cultures corresponding to isolates from acute infections presented a clear blue color due to PYO production whereas isolates from chronic infections were colorless (see Figure 5. 5).

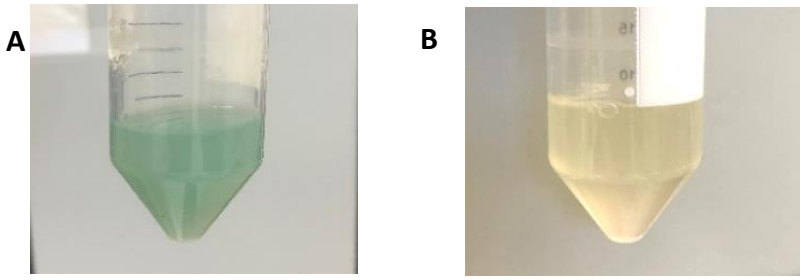

Figure 5. 5 *Bacterial isolates from patients infected with P. aeruginosa (A) chronic infection and (B) acute infection grown in MH media for 24 h at 37 ºC and 500 rpm.*

Moreover, in all cases, both phenazines showed the same secretion profile being the levels of the precursor 1-OHphz much lower than those quantified for the VF PYO. Thus, at the highest point of the growth curve of the clinical isolate from the patient with an acute infection, PYO reached values near 6000 nM, while the highest level of 1-OHphz achieved was around 400 nM.

At the light of these results, it was decided to confirm and expand these results by analysing 37 more bacterial isolates from patients with different respiratory infections at different stages and with distinct symptoms severity (see Table 5. 4). These clinical isolates were grown for 16 h to ensure measurements in case the isolates would belong to a patient with a chronic infection. As a reference control, the strain PAO1 was also cultured under the same conditions and the produced phenazines were also quantified.

Table 5. 4 *Clinical description of the 37 bacterial isolates from patients infected with P. aeruginosa that have been analysed.*

Nºpatient	Isolate Nb4D	Underlying clinical situation
1	PAAI1	Tracheobronchitis 3 weeks previously. Currently mild respiratory sumptoms attribited to another microorganism.
2	PAAI2	Critical intubated patient. Increase secretions during 24h. Desaturation and febricula without clear clinical signs of infection, no condensations
3	PAAI3	Typical catarrhal clinical picture during antibiotic-free interval. Clinically stable. Cystic fibrosis (CF). Intermittent colonization.
4	PAAI4	Increase secretions and cough. Renal transplant. Critical patient.
5	PAAI5	Pneumonia associated with mechanical ventilation. Critical patient.
6	PAAI6	Acute nosocomial infection
7	PAAI7	Tracheobronchitis due to *Pseudomonas* 1 week previously. Currently more viscous secretions. Critical patient.
8	PAAI8	Bronquitis due to *Pseudomonas*. Lung transplant recipient.
9	PAAI9	Asymptomatic, with few secretions. Lung transplant recipient.
20	PACI1	Clinical stability. Long-standing bronchiectasis.
21	PACI2	Broncorrhoea in previous weeks. Currently fine. Long-standing bronchiectasis.
22	PACI3	Clinical stability. Long-standing bronchiectasis.
23	PACI4	Creptinants without bronchospasm. Clinically stable. Long-standing bronchiectasis.
24	PACI5	Stable, good respiratory function (1.5 months later: reagudizationdue to sinusitis). CF plus chronic sinusitis.
25	PACI6	Severe CF respiratory function in decline. Monitoring outside Catalonia.
26	PACI7	Stable within gravity. Declining respiratory function. CF exacerbator.
27	PACI8	Catarrhal picture only with increased expectoration. Respiratory function in decline. CF.
-	PAO1[a]	Control strain.
10	PAAI10	*P. aeruginosa* bacteremia. Critical patient. Hematological.
11	PAAI11	Cytomegalovirus (CMV) pneumonitis superinfected with *P aeruginosa*.
12	PAAI12	Acute infection. Chronic obstructive pulmonary disease (COPD).
13	PAAI13	Cough, secretions, tachypnea and hypoxemia without fever or abnormal auscultation. It is treated and solved.
14	PAAI14	Catarrhal picture without obvious signs of infection. Lung transplant recipient.
15	PAAI15	Bronchoaspiration with few secretions. Good ventilation. Ictus. Critical patient.
16	PAAI16	Increased secretions, increased in inflammatory parameters. Critical patient.
17	PAAI17	Neumonia- Severe bronchospasm Severe COPD chronic, reagudize bronchitis phenotype.
18	PAAI18	CMV upturn in blood. Increased cough without expectoration or fever.
19	PAAI19	Acute infection.
28	PACI9	Chronic infection. Non-CF bronchiectasis.
29	PACI10	Apparently stable but severely impaired respiratory function. Severe COPD. Chronic bronchitis.
30	PACI11	Hemoptysis.
31	PACI12	Acute exacerbation (bronchitis). Severe exacerbating COPD.
32	PACI13	Long-standing bronchiectasis.
33	PACI14	Catarrhal episode without expectoration. CF.
34	PACI15	Lower respiratory tract infection not attributed to *Pseudomonas* (maybe viral). Long-standing bronchiectasis.
35	PACI16	Hemoptysis without respiratory symptoms. Respiratory function in decline. CF.
36	PACI17	Clinically stable. CF.
37	PACI18	Severe COPD. Viral infection 15 days before. Currently increasing cough, expectoration, dispnea and dysthermia. Long-standing bronchiectasis.

As shown in Figure 5. 6, the 37 studied bacterial isolates obtained from patients infected with *P. aeruginosa* acute and chronic infections could be classified in two groups according to their phenazines content. Thus, with few exceptions, which could be due to clinical casuistry, the levels of both PYO and 1-OHphz were remarkably higher in isolates from patients diagnosed with an acute infection: between 8000 - 300 nM and between 200 nM - 20 nM, respectively. On the contrary, these levels were much lower in the case of isolates obtained from patients suffering chronic infections which most values were found between 15 - 1 nM for PYO and between 4 nM - 1 nM for 1-OHphz (low nM range) (see Table 5. 5). Besides, for all clinical isolates it could be confirmed that PYO levels were higher than those of the precursor 1-OHphz. Therefore, all the data obtained has reinforced the hypothesis of PYO as a potential biomarker to discern between both types of infections caused by *P. aeruginosa.*

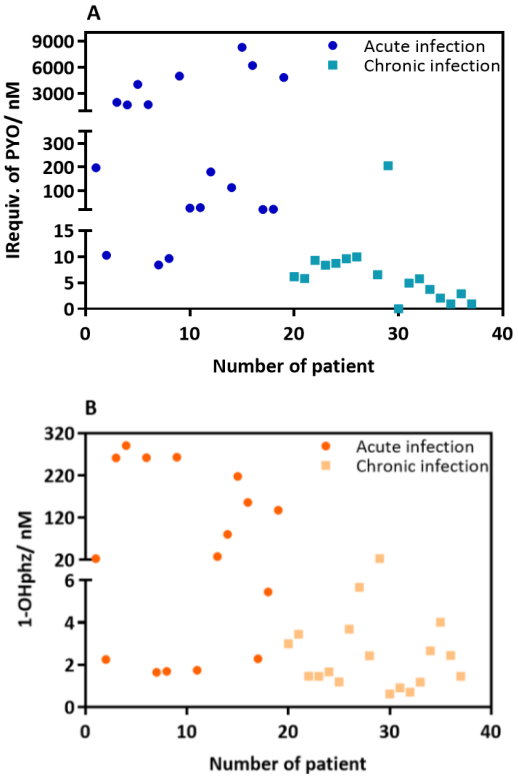

Figure 5. 6 *(A) PYO IRequiv. and (B) 1-OHphz levels (expressed in nM) found in the MH media where clinical bacterial isolates obtained from patients infected with P. aeruginosa were grown. Dark blue and yellow dots correspond to levels from isolates of patients with acute infections and light blue and yellow dots from patients with chronic infections. Each data point was measured in triplicates on the same ELISA plate and the results show the average and standard deviation of the assay carried out on 1 day. See Table 5. 4 for correspondence with the clinical record of the patient.*

Table 5. 5 *PYO and 1-OHphz concentrations measured in bacterial isolates from patients infected with P. aeruginosa. Bacterial isolates were grown for 16 h in MH media (n=3). Each isolate was measured in triplicates on the same ELISA plate and the results show the average and standard deviation of the assay carried out on 1 day PAAI = P. aeruginosa acute isolate; PACI= P. aeruginosa chronic isolate; n.d.= non detected.*

Number of patient	Isolate name	IRequiv. of PYO /nM	1-OHphz /nM
1	PAAI1	197.24 ± 4.57	22.75 ± 10.27
2	PAAI2	10.24 ± 4.16	2.25 ± 1.63
3	PAAI3	1959.42 ± 543.00	261.49 ± 47.72
4	PAAI4	1672.79 ± 4.47	290.60 ± 18.53
5	PAAI5	4022.66 ± 8.53	330.02 ± 24.17
6	PAAI6	1696.88 ± 42.66	261.92 ± 62.81
7	PAAI7	8.41 ± 2.94	1.65 ± 0.61
8	PAAI8	9.66 ± 0.70	1.69 ± 1.16
9	PAAI9	4970.63 ± 14.75	262.90 ± 55.41
20	PACI1	6.14 ± 1.99	3.00 ± 0.23
21	PACI2	5.82 ± 0.47	3.45 ± 1.16
22	PACI3	9.28 ± 2.35	1.46 ± 0.97
23	PACI4	8.37 ± 0.20	1.45 ± 0.96
24	PACI5	8.71 ± 3.54	1.67 ± 0.46
25	PACI6	9.60 ± 2.33	1.19 ± 0.44
26	PACI7	9.93 ± 1.40	3.69 ± 1.57
27	PACI8	15.60 ± 1.62	5.67 ± 1.32
-	PAO1	3535.12 ± 618.45	436.45 ± 41.38
10	PAAI10	27.18 ± 8.10	10.24 ± 1.89
11	PAAI11	29.02 ± 2.90	1.75 ± 0.93
12	PAAI12	179.26 ± 3.67	14.82 ± 2.50
13	PAAI13	510.57 ± 13.43	28.06 ± 0.51
14	PAAI14	106.54 ± 14.94	80.25 ± 5.62
15	PAAI15	8235.99 ± 993.75	217.65 ± 2.16
16	PAAI16	6195.56 ± 602.20	156.00 ± 13.06
17	PAAI17	22.34 ± 4.23	2.29 ± 1.14
18	PAAI18	22.14 ± 6.79	5.45 ± 0.96
19	PAAI19	4822.15 ± 241.55	137.61 ± 3.47
28	PACI9	6.55 ± 2.75	2.43 ± 0.00
29	PACI10	205.77 ± 5.13	23.09 ± 2.59
30	PACI11	*n.d.*	0.62 ± 0.30
31	PACI12	4.91 ±0.64	0.91 ± 0.35
32	PACI13	5.74 ± 0.70	0.71 ± 0.54
33	PACI14	3.73 ± 0.76	1.18 ± 0.34
34	PACI15	2.04 ± 0.11	2.67 ± 0.08
35	PACI16	0.96 ± 0.33	4.02 ± 0.42
36	PACI17	2.91 ± 0.60	2.45 ± 0.95
37	PACI18	0.93 ± 0.34	1.88 ± 0.07

Since bacterial cultures are confined systems where, in addition to the culture components, VFs, proteins and other bacterial exoproducts are released, these culture media could be considered as a quite complex sample. Thus, the preliminary data presented here, points out the possibility to use the reported PYO mAb122/PC1-BSA ELISA to diagnose *P. aeruginosa* infections in clinical samples and also to help to stratify patients according to the nature of their infection stage (acute or chronic) based on PYO content. In fact, given the high sensitivity of the assay (LoD =0.15 in 1/20 MH in PBST), further experiments will be aimed at directly measuring PYO levels in clinical samples (sputum and swab samples), which may open new avenues of knowledge such

as the possibility to predict exacerbations or to diagnose the infection at early stages of the diseases.

In the same vein, this will allow a better and continuous control of the development of *P. aeruginosa* infections improving patients' quality of life due to a faster initiation of more precise antibiotic treatment, reducing the appearance of antibiotic resistance processes. Moreover, this immunochemical approach could be used on different analytical configurations, such as point-of-care (PoC) immunosensor devices, to rapidly detect *P. aeruginosa* presence.

5.3 Materials & methods

5.3.1 Reagents

MH broth (Sigma Aldrich) was prepared diluting 21 g of the corresponding MH powder in 1 L of deionized water, as indicated by the manufacturer. The resulting liquid medium was subsequently autoclaved using a Presoclave II 75 (Selecta).

5.3.2 Clinical isolates samples

37 bacterial isolates collected at the Microbiology Department of the Vall d'Hebron University Hospital (VHUH, Barcelona, Spain) from patients diagnosed with *P. aeruginosa* acute or chronic infections (see Table 5. 4) were tested. Perfectly isolated colonies from primary cultures were selected and stored frozen in glycerol at -20 ºC until used. PAO1 strain (ATCC 15692) was used as reference strain.

5.3.3 Bacterial isolates analysis

5.3.3.1 Matrix effect study

Nonspecific interferences produced by bacterial isolates medium were analysed by preparing standard curves of PYO and 1-OHphz directly in MH broth diluted several times with PBST (0 and from 1/5 to 1/20) and measuring them with the PYO and 1-OHphz ELISAs, respectively, to assess the parallelism in respect to the calibrations curves prepared in the assay buffer.

5.3.3.2 Accuracy study

MH broth diluted 20 times in PBST was spiked at different PYO concentrations ranging from 30 nM to 0 nM (a total of 5 dilutions using a dilution factor of 2) and measured with PYO mAb122/PC1-BSA ELISA. The obtained results were compared with the spiked PYO values.

5.3.3.3 Bacterial isolates growth medium and inoculum preparation

Bacterial clinical isolate frozen stocks from patients with proven infection by *P. aeruginosa* were inoculated onto Columbia agar plates supplemented with 5 % sheep blood (Biomerieux Ref. 43041) and incubated overnight at 37 ºC. Next day, 4 or 5 colonies from each plated isolate were transferred using a sterile swab into 10 mL Falcon with 3 mL MH liquid media (initial suspension) and kept with gentle shaking (500 rpm) at 37 ºC. When turbidity reached values (measured as optical density (OD) at 600 nm) between 0.2-0.3 (equivalent to a McFarland turbidity containing approximately $1x10^8$ CFUs mL^{-1}), sample aliquots (10 µL) were taken and diluted in MH broth (10 mL) (t_0, start time point). The performance of these previous steps ensured that in all cases the starting material in terms of bacterial CFUs was similar for all isolate suspensions analysed. The prepared bacterial suspensions were then incubated at 37 ºC with gentle shaking (500 rpm) and aliquots were removed from each isolate tube at different time points to measure the OD (600) and phenazines content (see Figure 5. 7).

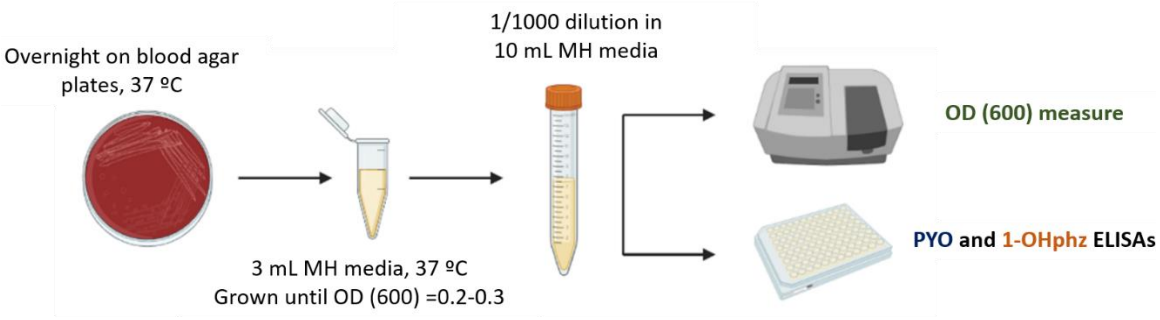

Figure 5. 7 *General protocol for building up bacterial growth curves and analysing phenazines production kinetics.*

5.3.3.4 Bacterial growth measurements and phenazines production kinetics

Bacterial suspension aliquots collected at different incubation times were used to plot bacterial growth curves and to build up PYO and 1-OHphz kinetic production curves. Bacterial growth studies were performed by measuring the turbidity at each time point of the broth culture aliquots. Turbidity correlates with cell density during the logarithmic growth phase and was measured as OD (600). In addition, CFUs were counted plating serial dilutions of each time point aliquot and counting the colonies after 24h incubation at 37 ºC.

The OD of each sample was measured at 600 nm at RT in a Multiskan GO spectrophotometer using High Precision Cell cuvette made of quartz (HellmaAnalytics) and CFUs were determined by carrying out serial 1:10 dilutions of each time point aliquot plating 10 µL on 5 % blood agar plates (37 ºC, 24 h). According to the OD (600) values measured, dilutions ranging from 1/10 to $1/10^8$ were prepared[30].

Collected bacterial time point aliquots were centrifuged (500 g, 5 min) for PYO mAb122/PC1-BSA and As230/PC1-BSA ELISAs measures. In the case of PYO, the resulting supernatants were diluted 20 times in assay buffer to avoid matrix effects, whereas, for 1-OHphz, 5 times in assay buffer[1].

5.4 Concluding remarks

- PYO mAb122/PC1-BSA and As230/PC1-BSA[1] ELISAs have been positively implemented to quantify PYO and 1-OHphz levels released by bacterial isolates obtained from patients infected with *P. aeruginosa*. In fact, matrix effect studies indicated that just diluting the isolate samples 20 times and 5 times in assay buffer, respectively, was enough to obtain correct measures.

- First, bacterial growth curves have been built up culturing clinical isolates from patients with acute and chronic infections to compare growth dynamics of the different clinical isolates. Thus, bacterial isolate from patient with acute infection started its exponential growth phase after 6 h of incubation whereas the isolate with chronic infection at 12 h of incubation.

- At the same time, phenazines production kinetics studies have also been assessed resulting in a much higher phenazine released levels in the bacterial isolate from the patient presenting an acute infection than isolate from the patient with a chronic infection (5800 nM for PYO and 370 nM for 1-OHphz vs 54 nM for PYO and 5 nM for 1-OHphz, respectively, at 24 h).

- The analysis of PYO and 1-OHphz phenazines levels of other 37 bacterial isolates from patients infected with *P. aeruginosa* confirmed the mentioned behaviour: bacterial isolates from patients with acute infections released higher concentrations of PYO and 1-OHphz than those with chronic infections (8000 – 300 nM vs 15 – 1 nM for PYO and (200 – 20 nM vs 4 – 1 nM for 1-OHphz, respectively).

- The obtained results position PYO as a good biomarker of infections caused by *P. aeruginosa* since PYO released is correlated with the type or stage of *P. aeruginosa* infection and this, in turn, should allow the stratification of patients with this type of infection.

5.5 References

1. Pastells, C.; Pascual, N.; Sanchez-Baeza, F.; Marco, M. P., Immunochemical Determination of Pyocyanin and 1-Hydroxyphenazine as Potential Biomarkers of Pseudomonas aeruginosa Infections. *Anal Chem* **2016,** *88* (3), 1631-8.
2. Chandler, C. E.; Horspool, A. M.; Hill, P. J.; Wozniak, D. J.; Schertzer, J. W.; Rasko, D. A.; Ernst, R. K., Genomic and Phenotypic Diversity among Ten Laboratory Isolates of Pseudomonas aeruginosa PAO1. *J Bacteriol* **2019,** *201* (5).
3. Mena, A.; Smith, E. E.; Burns, J. L.; Speert, D. P.; Moskowitz, S. M.; Perez, J. L.; Oliver, A., Genetic adaptation of Pseudomonas aeruginosa to the airways of cystic fibrosis patients is catalyzed by hypermutation. *J Bacteriol* **2008,** *190* (24), 7910-7.
4. D'Argenio, D. A.; Wu, M.; Hoffman, L. R.; Kulasekara, H. D.; Deziel, E.; Smith, E. E.; Nguyen, H.; Ernst, R. K.; Larson Freeman, T. J.; Spencer, D. H.; Brittnacher, M.; Hayden, H. S.; Selgrade, S.; Klausen, M.; Goodlett, D. R.; Burns, J. L.; Ramsey, B. W.; Miller, S. I., Growth phenotypes of Pseudomonas aeruginosa lasR mutants adapted to the airways of cystic fibrosis patients. *Mol Microbiol* **2007,** *64* (2), 512-33.
5. Klockgether, J.; Cramer, N.; Wiehlmann, L.; Davenport, C. F.; Tummler, B., Pseudomonas aeruginosa Genomic Structure and Diversity. *Front Microbiol* **2011,** *2*, 150.
6. Breidenstein, E. B.; de la Fuente-Nunez, C.; Hancock, R. E., Pseudomonas aeruginosa: all roads lead to resistance. *Trends Microbiol* **2011,** *19* (8), 419-26.
7. Heacock-Kang, Y.; Sun, Z.; Zarzycki-Siek, J.; McMillan, I. A.; Norris, M. H.; Bluhm, A. P.; Cabanas, D.; Fogen, D.; Vo, H.; Donachie, S. P.; Borlee, B. R.; Sibley, C. D.; Lewenza, S.; Schurr, M. J.; Schweizer, H. P.; Hoang, T. T., Spatial transcriptomes within the Pseudomonas aeruginosa biofilm architecture. *Mol Microbiol* **2017,** *106* (6), 976-985.
8. Van den Bergh, B.; Fauvart, M.; Michiels, J., Formation, physiology, ecology, evolution and clinical importance of bacterial persisters. *FEMS Microbiol Rev* **2017,** *41* (3), 219-251.
9. Taylor, P. K.; Yeung, A. T.; Hancock, R. E., Antibiotic resistance in Pseudomonas aeruginosa biofilms: towards the development of novel anti-biofilm therapies. *J Biotechnol* **2014,** *191*, 121-30.
10. Valentini, M.; Gonzalez, D.; Mavridou, D. A.; Filloux, A., Lifestyle transitions and adaptive pathogenesis of Pseudomonas aeruginosa. *Curr Opin Microbiol* **2018,** *41*, 15-20.
11. Lozano, C.; Azcona-Gutierrez, J. M.; Van Bambeke, F.; Saenz, Y., Great phenotypic and genetic variation among successive chronic Pseudomonas aeruginosa from a cystic fibrosis patient. *PLoS One* **2018,** *13* (9), e0204167.
12. Park, S. Y.; Park, H. J.; Moon, S. M.; Park, K. H.; Chong, Y. P.; Kim, M. N.; Kim, S. H.; Lee, S. O.; Kim, Y. S.; Woo, J. H.; Choi, S. H., Impact of adequate empirical combination therapy on mortality from bacteremic Pseudomonas aeruginosa pneumonia. *BMC Infect Dis* **2012,** *12*, 308.
13. Boucher, H. W.; Talbot, G. H.; Bradley, J. S.; Edwards, J. E.; Gilbert, D.; Rice, L. B.; Scheld, M.; Spellberg, B.; Bartlett, J., Bad bugs, no drugs: no ESKAPE! An update from the Infectious Diseases Society of America. *Clin Infect Dis* **2009,** *48* (1), 1-12.
14. Hirsch, E. B.; Tam, V. H., Impact of multidrug-resistant Pseudomonas aeruginosa infection on patient outcomes. *Expert Rev Pharmacoecon Outcomes Res* **2010,** *10* (4), 441-51.

15. Pang, Z.; Raudonis, R.; Glick, B. R.; Lin, T. J.; Cheng, Z., Antibiotic resistance in Pseudomonas aeruginosa: mechanisms and alternative therapeutic strategies. *Biotechnol Adv* **2019,** *37* (1), 177-192.
16. Zegans, M. E.; Becker, H. I.; Budzik, J.; O'Toole, G., The role of bacterial biofilms in ocular infections. *DNA Cell Biol* **2002,** *21* (5-6), 415-20.
17. Ryall, B.; Carrara, M.; Zlosnik, J. E.; Behrends, V.; Lee, X.; Wong, Z.; Lougheed, K. E.; Williams, H. D., The mucoid switch in Pseudomonas aeruginosa represses quorum sensing systems and leads to complex changes to stationary phase virulence factor regulation. *PLoS One* **2014,** *9* (5), e96166.
18. Smith, E. E.; Buckley, D. G.; Wu, Z.; Saenphimmachak, C.; Hoffman, L. R.; D'Argenio, D. A.; Miller, S. I.; Ramsey, B. W.; Speert, D. P.; Moskowitz, S. M.; Burns, J. L.; Kaul, R.; Olson, M. V., Genetic adaptation by Pseudomonas aeruginosa to the airways of cystic fibrosis patients. *Proc Natl Acad Sci U S A* **2006,** *103* (22), 8487-92.
19. Hall, S.; McDermott, C.; Anoopkumar-Dukie, S.; McFarland, A. J.; Forbes, A.; Perkins, A. V.; Davey, A. K.; Chess-Williams, R.; Kiefel, M. J.; Arora, D.; Grant, G. D., Cellular Effects of Pyocyanin, a Secreted Virulence Factor of Pseudomonas aeruginosa. *Toxins (Basel)* **2016,** *8* (8).
20. Jayaseelan, S.; Ramaswamy, D.; Dharmaraj, S., Pyocyanin: production, applications, challenges and new insights. *World J Microbiol Biotechnol* **2014,** *30* (4), 1159-68.
21. Dietrich, L. E.; Price-Whelan, A.; Petersen, A.; Whiteley, M.; Newman, D. K., The phenazine pyocyanin is a terminal signalling factor in the quorum sensing network of Pseudomonas aeruginosa. *Mol Microbiol* **2006,** *61* (5), 1308-21.
22. Elliott, J.; Simoska, O.; Karasik, S.; Shear, J. B.; Stevenson, K. J., Transparent Carbon Ultramicroelectrode Arrays for the Electrochemical Detection of a Bacterial Warfare Toxin, Pyocyanin. *Anal Chem* **2017,** *89* (12), 6285-6289.
23. Silva, L. V.; Galdino, A. C.; Nunes, A. P.; dos Santos, K. R.; Moreira, B. M.; Cacci, L. C.; Sodre, C. L.; Ziccardi, M.; Branquinha, M. H.; Santos, A. L., Virulence attributes in Brazilian clinical isolates of Pseudomonas aeruginosa. *Int J Med Microbiol* **2014,** *304* (8), 990-1000.
24. Wilson, R.; Sykes, D. A.; Watson, D.; Rutman, A.; Taylor, G. W.; Cole, P. J., Measurement of Pseudomonas aeruginosa phenazine pigments in sputum and assessment of their contribution to sputum sol toxicity for respiratory epithelium. *Infect Immun* **1988,** *56* (9), 2515-7.
25. Montagut, E. J.; Martin-Gomez, M. T.; Marco, M. P., An Immunochemical Approach to Quantify and Assess the Potential Value of the Pseudomonas Quinolone Signal as a Biomarker of Infection. *Anal Chem* **2021,** *93* (11), 4859-4866.
26. Montagut, E. J.; Vilaplana, L.; Martin-Gomez, M. T.; Marco, M. P., High-Throughput Immunochemical Method to Assess the 2-Heptyl-4-quinolone Quorum Sensing Molecule as a Potential Biomarker of Pseudomonas aeruginosa Infections. *ACS Infect Dis* **2020,** *6* (12), 3237-3246.
27. D'Argenio, D. A.; Calfee, M. W.; Rainey, P. B.; Pesci, E. C., Autolysis and autoaggregation in Pseudomonas aeruginosa colony morphology mutants. *J Bacteriol* **2002,** *184* (23), 6481-9.
28. Meirelles, L. A.; Newman, D. K., Both toxic and beneficial effects of pyocyanin contribute to the lifecycle of Pseudomonas aeruginosa. *Mol Microbiol* **2018,** *110* (6), 995-1010.

29. Ahmed, S.; Rudden, M.; Smyth, T. J.; Dooley, J. S. G.; Marchant, R.; Banat, I. M., Natural quorum sensing inhibitors effectively downregulate gene expression of Pseudomonas aeruginosa virulence factors. *Appl Microbiol Biotechnol* **2019,** *103* (8), 3521-3535.
30. Sarkar, S.; Lund, S. P.; Vyzasatya, R.; Vanguri, P.; Elliott, J. T.; Plant, A. L.; Lin-Gibson, S., Evaluating the quality of a cell counting measurement process via a dilution series experimental design. *Cytotherapy* **2017,** *19* (12), 1509-1521.

Chapter 6

Pyocyanin detection on clinical matrices: sputum and swab samples

In this chapter, the implementation of PYO detection assay (PYO mAb122/PC1-BSA ELISA) to detect this virulence factor (VF) on swab and sputum clinical samples from patients infected with *P. aeruginosa* is explained. With this aim, different sample treatments, matrix effect studies and accuracy studies are presented. Finally, PYO levels in sputum and swab samples from patients testing positive for *P. aeruginosa* are analysed.

6.1 Introduction

Chronic infections occuring in the lungs of patients with cystic fibrosis (CF) are one of the most notorious infections caused by *P. aeruginosa*[1]. As previously explained, CF patients are characterized by an abnormal mucus layer in the upper airways and bronchi. These chronic infections patients go through characteristic periods of stability and sporadic and repeated episodes of acute infections named exacerbations[2-3]. During exacerbations periods, there is a worsening of the infection affecting the respiratory tract and patients expectorate sputum, a complex mixture of saliva and mucus composed of mucin, aminoacids, lipdis and micronutrients, whose composition varies according to the patient[1, 4-5]. In the same vein, other patients suffering from chronic infections, such as non–cystic fibrosis borchiectasis (NCFB) and chronic obstructive pulmonary disease (COPD), also exhibit these acute episodes. In fact, infectious exacerbations are the most important cause of mortality in COPD, being *P. aeruginosa* the leading causative of these episodes[6]. Furthermore, *P. aeruginosa* is a common bacterium colonizing the airway of patients with NCFB, inducing persistent production of sputum which results in the rapid decline of lung infection[7-8]. Hence, early identification of these exacerbations is crucial to promp adecuate treatmens and to prevent a worsening of the pulmonary function.

In general, sputum is classified in 4 types according to its aspect/morphology: purulent, mucoid, bloody and serous[9]. From these four types, the first three are the most common ones. As illustrated in Figure 6. 1, mucoid sputum is clear, grey or white; purulent sputum, yellow or green and thicker than the others; and bloody sputum, reddish.

Figure 6. 1 *General morphology of different type of sputum samples. From left to right muocid, purulent and bloody sputum*.

Sputum samples have been widely used as non-invasive diagnostic technique to analyse lower respiratory tract infections although potentially less representative of the deep lung as compared with bronchoalveolar lavage (BAL) [10-11]. Furthermore, collection of sputum samples for microbiological surveillance is crucial in the routine of patients suffering chronic lung

infections[6-7, 12] as the medical history of these patients is marked by the before mentioned frequent exacerbation periods[13]. In the case of children, oropharyngeal swabs are collected and analysed due to the inability of children to expectorate sputum[14]. The main inconveniences of using these swabs are the less bacterial yield (*P. aeruginosa* colonized the lower-respiratory tract) and the higher levels of microbial diversity and organisms found in the upper-respiratory tract in contrast to the loswer-respiratory tract[15].

As explained in Chapter 1, *P. aeruginosa* chronic infections are characterized by the formation of biofilms (mucoid phenotype) and the downregulation of genes coding for virulence factors (VFs)[16]. In contrast, during acute infections, *P. aeruginosa* up-regulated the expression of an arsenal of different VFs. Thus, since exacerbations are episodes of acute infections, VFs could be used as valuable biomarkers to predict exacerbation periods.

In this context, Wilson et al. [17] measured PYO in sputum for the first time in 1988 using high-performance liquid chromatography-ultraviolet (HPLC-UV) detecting levels up to 100 µM[18]. Furthermore, Hunter et al.[19] measured PYO and phenazine-1-carboxylic acid (PCA) in 45 sputum samples from CF patients using the same technique. However, this study is under revision as they assigned a specific chromatographic peak to phenazines overestimating their abundance[20]. Since then, to our knowledge, there is only one work that has quantified PYO directly in sputum samples[21]. This preliminary study used custom-made nanograss (NG) sensors to directly measure PYO from sputum samples obtained by endolaryngeal suction with hypertonic saline (HTS). In total, 5 sputum samples from CF patients were analysed finding higher PYO concentrations in samples from early colonized patients compared to samples from chronically infected patients (13.6 µM vs 0.3 µM, respectively). Thus, in this chapter, the direct measure of PYO in sputum and swabs samples from patients testing positive for *P. aeruginosa* using the developed PYO mAb122/PC1-BSA ELISA is intended.

6.2 Results & discussion

6.2.1 PYO measures on sputum samples

Before explaining the implementation of the developed PYO mAb122/PC1-BSA ELISA to directly measure PYO in sputum samples, it has to be highlited that the immunoreagent concentrations used to carry out these experiments were slightly modified since a new batch of PYO mAb122 was used. Thus, bidimensional (2D) experiments were performed again in order to select the appropiate PYO mAb122 and PC1-BSA coating antigen concentrations for performing the ELISA

(data not shown). The selected concentrations were 0.2 and 0.025 µg mL^{-1} for PYO mAb122 and PC1-BSA, respectively. Table 6. 1 shows the analytical parameters of the PYO mAb122/PC1-BSA ELISA with these new concentrations.

Table 6. 1 *Analytical parameters of the PYO mAb122/PC1-BSA ELISA for the detection of PYO on assay buffer. The immunoreagents concentrations used were: PC1-BSA at 0.2 µg mL^{-1} and PYO mAb122 at 0.025 µg mL^{-1}. The data shown correspond to the average and standard deviation of the parameters of the calibration curves performed 3 different days using at least 3 well replicates per concentration.*

	PBST
A_{min}	0.04 ±0.01
A_{max}	1.10 ±0.03
Slope	-1.53 ±0.17
IC_{50}/ nM	6.14 ±0.88
Dynamic range/ nM	2.11 ±0.39 and 14.39 ±1.11
LoD/ nM	0.99 ±0.14
R^2	0.99 ±0.00

Furthermore, as previously explained in Chapter 4, PYO concentrations were expressed as PYO immunoreactivity equivalents (PYO IRequiv) to take the high sensitivity of PYO mAb122/PC1-BSA for both 1-OHphz and PYO into consideration.

6.2.1.1 Implementation of PYO ELISA for the analysis of sputum samples

Since sputum is an heterogeneous viscous sample formed by a mixture of saliva and mucus, it needs to be solubilized and homogenized prior to its analysis. Thus, a wide variety of protocols to treat sputum can be found on the literature, most of which are based on the use of mucolytic agents to disrupt this mucus[22]. Among the variety of existing agents, dithiothreitol (DTT)[11, 22-24] and N-Acetyl-L-Cysteine (NAC)[25-26] are most widely used. These agents contain a sulfhydryl group that cleaves disulphide bonds of proteins forming the mucus (mucoproteins) decreasing sputum viscosity[22]. Besides, as demonstrated by Cleland[27], DTT is the strongest reagent for breaking down disulphide bonds probably due to the fact that DTT is a dithiol whereas NAC, a monothiol. Moreover, after sputum samples are treated with solutions of these mucolytic agents, they are generally filtrated and centrifugated to remove possible small particulate material that has not been properly dissolved. Aditionally, in some cases, samples are also heated and/or enzymatically treated. Thus, Arias-Bouda et al.[25] described a protocol for treating sputum samples based on the use of NAC as mucolytic agent, the posterior addition of proteinase K to the mixture to digest other existing proteins, the heating of the sample (50 ºC, 6 h) to deactivate proteinase K and, finally, the centrifugation (12,000 g) of the solution. In addition, Peter et al.[28] used a protocol to treat sputum samples that consisted, first, in the addition of a solution of DTT

to the sputum sample and further filtration by centrifugation. Then, the sample was heated (95 ºC, 30 mins) and centrifugated (12,500 rpm).

In this context, the here studied sputum samples were first treated assessing a protocol based on the use of DTT mucolytic agent.

6.2.1.1.1 PYO measures on sputum samples treated with DTT

Previously in our lab, a DTT treatment protocol was developed for quantifying PYO and 1-hydroxyphenazine (1-OHphz) phenazines in sputum samples from patients infected with *P. aeruginosa*[29]. This protocol consisted in the addition of a solution of 0.1 % of DTT in 10 mM PBS to sputum samples (600 µL for 150 mg of sputum) to disrupt the mucus and posterior dilution in 10 mM PBS (600 µL) with the aim of minimizing the matrix effect. Finally, the solution was filtrated by centrifugation (4,000 g, 10 mins) to remove any possible particle that were not properly dissolved. Nevertheless, Pastells et al. were not able to detect phenazines in the analysed sputum samples probably due to an innapropiate storage of the samples, which could result in the degradation of these phenazines. Furthermore, another explanation for these results could be that the phenazines concentration found in the studied samples were below the limit of detection (LoD) of the used As230/PC1-BSA ELISA.

Therefore, a slightly modified version of the explained DTT protocol was used to treat the here studied sputum samples. Thus, an extra centrifugation step was added before the filtration step with the aim of removing impurities that had not been previously resuspended and that could later obstruct the filter (the whole protocol is described Figure 6. 11). The studied sputum samples were collected by the group of M.- Teresa Martin (Microbiology Department, Vall d'Hebron University Hospital (VHUH)) and analysed using the previously developed PYO mAb122/PC1-BSA ELISA.

6.2.1.1.1.1 Matrix effect evaluation

As explained above, the analysis of sputum samples from patients infected with *P. aeruginosa* required matrix effect studies since sputum matrix is highly complex. Due to the heterogenicity of sputum samples, a pool of 14 sputum samples (5 mucoid, 7 purulent and 2 bloody) from patients testing negative for *P. aeruginosa* (blank samples) were treated with DTT according to the protocol explained in Figure 6. 11. First, each sputum sample was treated individually and, then, the 14 treated sputum samples were mixed and homogeneized. This pool had a final

concentration of 125 mg mL^{-1} as each 150 mg of untreated weight sputum was diluted in a final volume of 1.2 mL. Thus, PYO standards were prepared in different dilutions of 125 mg mL^{-1} sputum (termed sputum in Figure 6. 2, red color) in PBS buffer (1/2, 1/5, 1/10 and 1/20). The obtained curves were compared with a control curve performed in PBST.

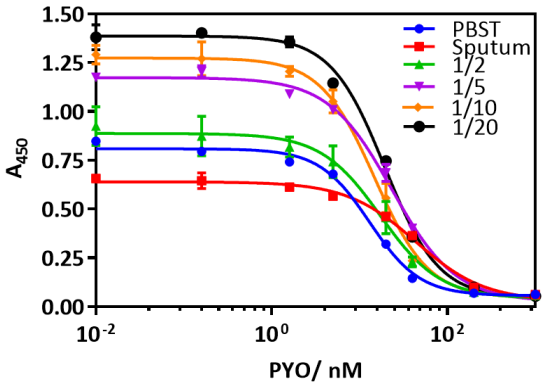

Figure 6. 2 *Matrix effect of the DTT treated sputum undiluted (125 mg mL^{-1}; red) and diluted 2 (green), 5 (purple), 10 (orange) and 20 (black) times in PBST on the performance of PYO mAb122/PC1-BSA ELISA. The calibration curves were run using the conditions established for the assay in PBST (see Table 6. 1). Each calibration point was measured in duplicates on the same ELISA plate and the results show the average and standard deviation of the assay carried out on 1 day.*

As shown in Figure 6. 2, the obtained calibration curve corresponding to 62.5 mg mL^{-1} sputum concentration (1/2 dilution, green color) was similar to the control curve (blue color). In fact, the analytical parameters of these curves did not vary signficantly (see Table 6. 2): maximun absorbance (A_{max}) of 0.81 and 0.89 and half maximal inhibitory concentration (IC_{50}) of 13.04 and 17.38 nM, for the control and 1/2 sputum dilution curves, respectively. Thus, this data indicated that the levels of PYO in sputum could be measured by diluting DTT treated samples by a factor of 2.

Table 6. 2 *Analytical parameters of the PYO mAb122/PC1-BSA ELISA for the detection of PYO on assay buffer (control) and undiluted and diluted DTT-treated sputum. Sputum refers to 125 mg mL^{-1} concentration. The data shown correspond to the average and standard deviation of the parameters of the calibration curves performed 1 day using at least 3 well replicates per concentration.*

	PBST	Sputum	1/2	1/5	1/10	1/20
A_{max}	0.81 ±0.01	0.64 ±0.01	0.89 ±0.03	1.17 ±0.02	1.27 ±0.02	1.39 ±0.02
A_{min}	0.06 ±0.02	0.03 ±0.02	0.04 ±0.04	0.03 ±0.02	0.05 ±0.03	0.04 ±0.03
Slope	-1.52 ±0.15	-1.11 ±0.14	-1.28 ±0.25	-1.20 ±0.10	-1.41 ±0.15	-1.42 ±0.14
Dynamic range/ nM	4.30 to 30.36	10.18 to 117.84	4.77 to 45.89	6.35 to 65.24	5.25 to 38.43	6.94 to 49.79
IC_{50} / nM	13.04 ±0.03	43.49 ±0.05	17.38 ±0.07	23.41 ±0.03	14.88 ±0.04	19.40 ±0.03
LoD/ nM	1.93	4.17	1.97	2.79	2.79	3.74
R^2	0.99	0.99	0.98	0.99	0.99	0.96

6.2.1.1.1.2 Recovery study

After performing the above explained matrix effect studies, recovery experiments were carried out. These recovery studies consisted in the addition of a known amount of analyte to a sample to determine what percentage of the added concentration is detected. Thus, 4 sputum samples (2 purulent, 1 mucoid, 1 bloody) from *P. aeruginosa* uninfected patients were selected and spiked with 10 nM of PYO before starting DTT treatment. Then, these sputum samples were treated following the protocol explained above and PYO levels were measured using the optimized PYO mAb122/PC1-BSA ELISA. At the same time, a non-spiked sputum sample was used as negative control.

All the studied sputum samples showed PYO levels below the LoD of the assay except for the purulent samples. Nevertheless, these purulent samples presented a matrix effect as the non-spiked sample showed PYO levels between 10 – 13 nM instead of 0 nM (data not shown). Therefore, since the final appearance of the DTT treated sputum samples was cloudy, an additional ultracentrifugation step was added to the DTT protocol after the filtration step with the aim of removing possible small particulate material coming from the sample. The ultracentrifugation was performed in Amicon® Ultra-0.5 Centrifual Filter tubes (30 mins at 12,000 g). Thus, 3 sputum samples (1 purulent, 1 mucoid and 1 bloody) from *P. aeruginosa* unifected patients were spiked with 10 nM of PYO before starting the treatment and after the ultracentrifugation step (***Figure 6. 3*** shows the aspect of the tubes after ultracentrifugation) and PYO levels were measured using PYO mAb122/PC1-BSA ELISA. In this case, all samples showed undetectable PYO concentrations (all below the LoD, data not shown).

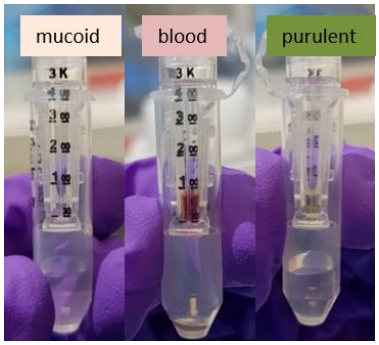

Figure 6. 3 *Aspect of the different types of sputum samples after the ultracentrifugation step performed at 12000 g for 30 mins.*

In this context, recovery studies were performed spiking a purulent sputum sample (*P. aeruginosa* sputum 522; PASP522) from a *P. aeruginosa* uninfected patient with 10 nM of PYO before and after the ultracentrifugation step (positive control) to analyse whether PYO was lost during this step. At the same time, a non-spiked sample was used as negative control. Again, the

sputum sample spiked prior to ultracentrifugation step showed undetectable levels of PYO, probably due to its precipitation together with proteins present in the sputum sample. Besides, even when the sputum sample was spiked after ultracentrifugation, PYO levels were very low (2.07 ±0.42 nM, 20 % recovery). Therefore, this result indicated that the matrix effect problem was not resolved. In consequence, based on the obtained results, another sputum treatment was tried.

6.2.1.1.2 PYO measures on lyophylized sputum samples

With the aim of avoiding heterogeneity problems coming from the sample and reducing the number of steps in the sputum treatment, sputum was lyophylized for 48 h (sputum morphology after lyophilization is shown in Figure 6. 4) and resuspended in 10 mM PBS. Besides, since liphylization consists in the removal of water from the sample by sublimation, this treatment could improve sample solubility. Finally, to prevent any possible particle in suspension, samples were further sonicated for 10 mins (see Figure 6. 12).

Figure 6. 4 *Sputum sample morphology after 48 h lyophilization.*

6.2.1.1.2.1 Matrix effect evaluation

Due to the different nature of each sputum type (purulent, mucoid and bloody), matrix effect studies were performed individually. Thus, each blank sputum sample was lyophilized and resuspended in 10 mM PBS to a final concentration of 2.5 mg mL^{-1} (stock solution). This concentration is refered to the weigth of the lyophilized sputum. From this stock solution, different sputum dilutions were prepared being 1 mg mL^{-1} of lyphylized sputum in PBS the most concentrated one (red color). Thus, PYO standards were prepared in different dilutions of 1 mg mL^{-1} sputum in PBS buffer (see Figure 6. 13). In total, 9 dilutions from 1/2 to 1/512 were prpepared using a dilution factor of 2 (all data not shown).

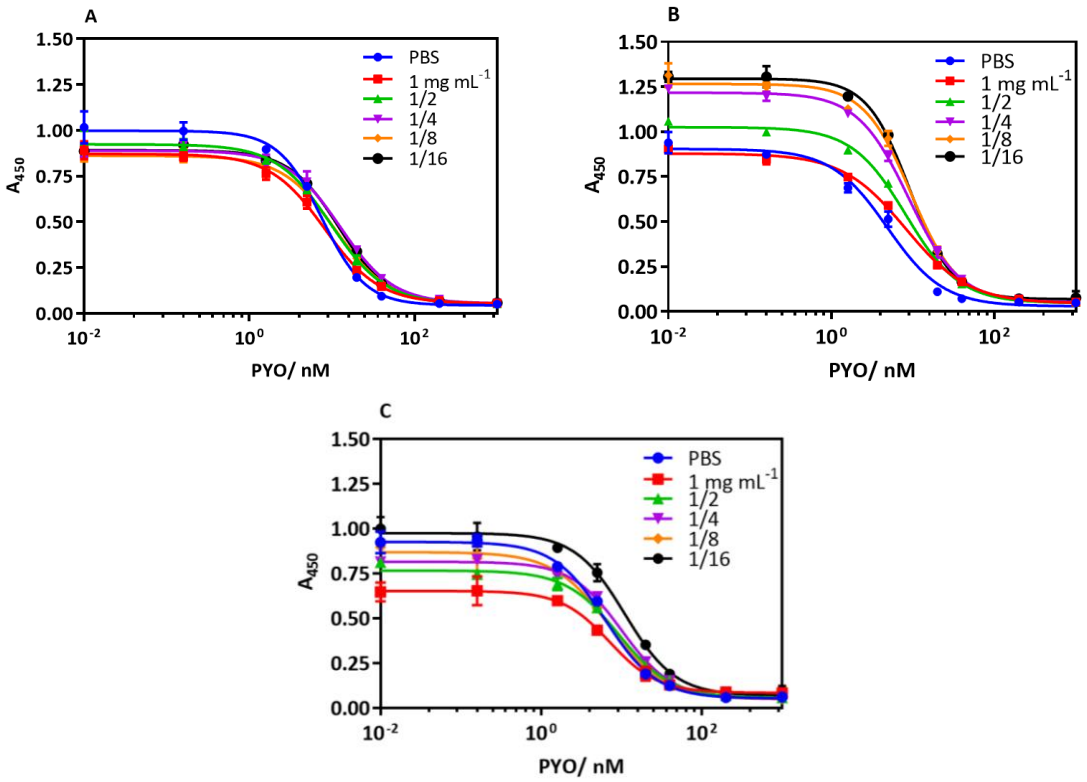

Figure 6. 5 *Matrix effect studied of each lyophylized sputum type (1 mg mL^{-1}) diluted 2, 4, 8 and 16 times with 10 mM PBS on the performance of PYO mAb122/PC1-BSA ELISA. (A) Purulent sputum. (B) Mucoid sputum. (C) Bloody sputum. The calibration curves were run using the conditions established for the assay in PBS (see Table 6. 1). Each calibration point was measured in duplicates on the same ELISA plate and the results show the average and standard deviation of the assay carried out on 1 day.*

As illustrated in Figure 6. 5, the calibration curves obtained when working at any purulent sputum dilution in PBS were similar meaning there was no matrix effect. Thus, it was decided to work with the most concentrated dilution (1 mg mL^{-1}; red color) in order to ensure PYO detection (IC_{50} of 8.19 nM and 7.56 nM and A_{max} of 0.91 and 0.88 in 1 mg mL^{-1} sputum and PBST, respectively). In contrast, in the case of the mucoid sputum, an unusual matrix effect was observed. In fact, the matrix effect was more evident as the dilution factor increase until a 1/128 dilution (data not shown). Therefore, with the aim of avoiding detection problems and being able to detect the majority of the studied sputum samples, the less diluted mucoid sputum concentration was selected to measured PYO (IC_{50} of 8.15 nM and 4.88 nM and A_{max} of 0.87 and 0.90 for 1 mg mL^{-1} sputum and PBS, respectively). Finally, as expected in this sort of matrix effect studies, the dilution of the bloody sputum matrix reduces its effect, being more notorious in the case of 1 mg mL^{-1} sputum concentration. Following the same criteria explained above, the analysis of these type of sputum samples was performed at 0.5 mg mL^{-1} bloody sputum in PBS as being the less diluted concentration of sputum showing similar a PYO mAb122/PC1-BSA ELISA performance compared to the control (IC_{50} =9.20 nM and 7.13 nM in 0.5 mg mL^{-1} sputum and

PBS, respectively), although the signal was decreased under these conditions (A_{max} =0.77 and 0.93 in 0.5 mg mL^{-1} sputum and PBS, respectively).

6.2.1.1.2.2 Accuracy study

A set of blind lyophilized sputum samples were spiked at several PYO concentrations (ranging from 20 nM to 0 nM) and measured by PYO mAb122/PC1-BSA ELISA. Thus, the obtained PYO values were compared with the initially spiked PYO concentrations. These experiments were carried out individually for each of the sputum types (purulent, mucoid and bloody) taken into consideration the corresponding matrix effect. Besides, this assay was performed on three different days.

As illustrated in Figure 6. 6, the correlation coefficients between concentrations of the spiked samples and the obtained values using ELISA were excellent for the three type of sputum since they were closed to the value of 1 (R^2 = 0.9897, 0.9810 and 0.9852 for purulent, mucoid and bloody sputum, respectively). Moreover, the slope of the linear regression was close to 1 (slope =1.132, 0.8476 and 0.9684 for purulent, mucoid and bloody sputum, respectively).

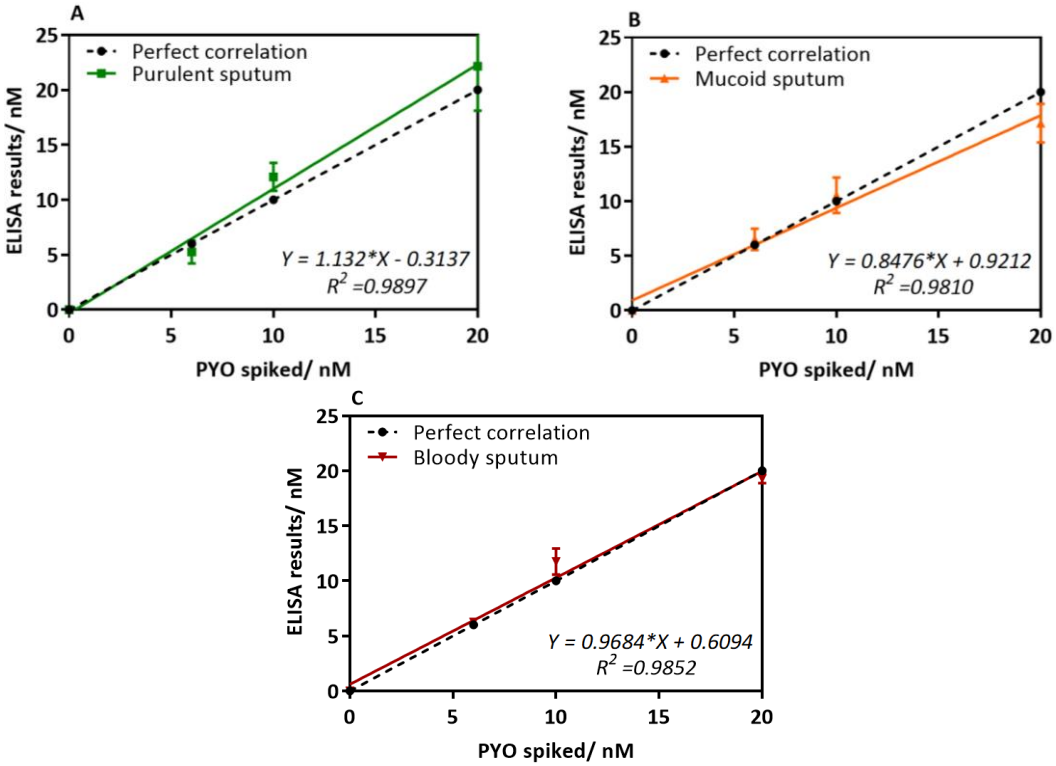

Figure 6. 6 *Results from the accuracy study using PYO mAb122/PC1-BSA ELISA. The graph shows the linear regression analysis of the (A) purulent (B) mucoid and (C) bloody sputum spiked with different PYO concentrations and the concentrations measured with the PYO mAb122/PC1-BSA ELISA. Assays were run in 1 mg mL^{-1} of purulent and mucoid sputum on assay buffer and 0.5 mg mL^{-1} of the bloody sputum on assay buffer. Each calibration point was measured in triplicates on the same ELISA plate and the results show the average and standard deviation of the analysis carried out on 3 different days.*

6.2.1.2 PYO quantification of lyophilized sputum samples from *P. aeruginosa* infected patients

Once PYO mAb122/PC1-BSA ELISA was implemented to measure PYO using lyophilization treatment, 2 mucoid (PASP179 and PASP772) and 2 purulent (PASP844 and PASP568) sputum samples from patients infected with *P. aeruginosa* were analysed. To ensure a correct PYO quantification, two positive controls and a negative control (blank sample) for each sputum type were used. The positive controls were prepared by spiking two blank samples with 20 and 5 nM PYO.

Table 6. 3 *IRequiv. of PYO values directly obtained from lyophylized sputum samples from P. aeruginosa infected patients performing PYO mAb122/PC1-BSA ELISA (Raw data) and by substrating the corresponding blank value (-blank). For both sputum types two positive controls (blank sputum sample spiked with 20 and 5 nM of PYO) and a negative control (blank sample) were measured. Each sample was measured in triplicates on the same ELISA plate and the results show the average and standard deviation of 1 experiment. PASP= P. aeruginosa sputum*

	IRequiv. of PYO/ nM (raw data)	**IRequiv. of PYO/ nM (-blank)**
Mucoid sputum		
Spiked 20 nM	23.17 ±1.25	21.38
Spiked 5 nM	6.73 ±0.18	4.94
Blank	1.79 ±0.32	0
PASP179	5.14 ±0.36	3.35
PASP772	3.70 ±0.22	1.91
Purulent sputum		
Spiked 20 nM	26.78 ±1.00	23.89
Spiked 5 nM	10.30 ±0.56	7.41
Blank	2.89 ±0.56	0
PASP844	4.36 ±0.43	1.47
PASP568	*n.d.*	*n.d.*

As expected from the accuracy studies, the recovery of the spiked PYO samples was around 100 %, which allowed a fiable measurement of PYO in sputum samples from *P. aeruginosa* infected patients. Therefore, as shown in Table 6. 3, PYO mAb122/PC1-BSA ELISA allowed PYO quantification on the mentioned sputum samples on the low nM range. Due to the the complexity and heterogeneity nature of these clinical samples, only few studies regarding the detection of PYO in sputum can be found on the literature[17, 19, 21]. Thus, the majority of the work is focused on the analysis of PYO in artificial sputum or sputum samples testing negative for *P. aeruginosa*[29-31]. The first study to detect PYO on sputum samples was performed in 1988 by Wilson et al.[17], measuring PYO levels up to 100 µM using HPLC-UV technique. Moreover, Hunter et al.[19] measured PYO and PCA phenazines sputum samples using the same technique but the

study was later under revision as they overestimated their abundance[20]. The most recent work which quantifies PYO directly in sputum samples was carried out by Alatraktchi et al. in 2020[21]. This study used NG to determine PYO concentration in sputum samples collected by endolaryngeal suction with HTS from 5 CF patients. The low LoD (172 nM) of this technique allowed the direct quantification of PYO in both samples from early colonized patients (13.6 µM) and in samples from chronically infected patients (0.3 µM). Therefore, since PYO mAb122/PC1-BSA ELISA showed a lower LoD (around 8 nM) than the one reported above, the low or even undetectable PYO levels obtained when measuring lyophylized sputum samples (see Table 6. 3) are due to a matrix effect.

In the light of these results, other sputum treatments are being studied with the aim of minimizing the observed matrix effect. Furthermore, a general protocol to treat any type sputum samples should be studied to avoid errors coming from the visual selection of the sputum type. Thus, given the complex composition of sputum (mucin, aminoacids, lipdis and micronutrients), protocols based on the additional use of enzymes such as proteinase K[25] and DNAses[32-34] could help to disrupt other components of the matrix reducing more the viscosity of the sputum and homogeneizing the sample.

Nevertheless, in the hypothetical case that non of these treatments allow PYO quantification on sputum samples, further experiments will be carried out regarding the analysis of bacterial isolates from patients infected with *P. aeruginosa* to optimize this method. In fact, in the majority of the reported studies, PYO is measured in bacterial cultures from *P. aeruginosa* strains isolated from sputum samples. In this vein, Silva et al.[35] grew *P. aeruginosa* isolates from sputum samples on culture medium for 24 h detecting PYO levels up to 18 µM using an extraction and spectroscopic method. Besides, Elliot et al.[36] used an electrochemical method based on ultramicroelectrodes to measure PYO in PA14 and PA11 strains isolated from sputum samples of CF patients. In this case, bacterial isolates were grown 24 h detecting PYO concentrations of 3 and 45 µM, respectively. Therefore, based on the results obtained in Chapter 5, these results will be expanded by analysing a higher number of isolates from patients infected with *P. aeruginosa.* At the same time, together with PYO quantification, other QS molecules will be measured with the aim of providing to clinicians additional information useful in the decision-making process for the management of these type of infections.

6.2.2 PYO measures on swab samples

6.2.2.1 Implementation of PYO ELISA for the analysis of swab samples

Since, as explained before, children are not able to expectorate sputum, oropharyngeal swabs were analysed with the aim of measuring PYO in these patients[14]. Therefore, the group of M.-Teresa Martin (Microbiology Department, VHUH) collected swab samples from children infected with *P. aeruginosa* using a specific collection and transport method named ESwab™ (see Material & Methods)[37].

6.2.2.1.1 Matrix effect evaluation

The used medium for swab collection and storage is composed of a high concentration of different salts (sodium chloride, potassium chloride, calcium chloride, magnesium chloride, monopotassium phosphate, disodium phosphate and sodium thioglycollate) that can interfere with the optimal performance of PYO mAb122/PC1-BSA ELISA. With the aim of studying this possible interference, PYO standards (1000, 200, 40, 20, 5, 1.6, 0.16 and 0 nM) were prepared diluting the swab medium with 10 mM PBST to reach different dilution factors (2, 5, 10 and 20).

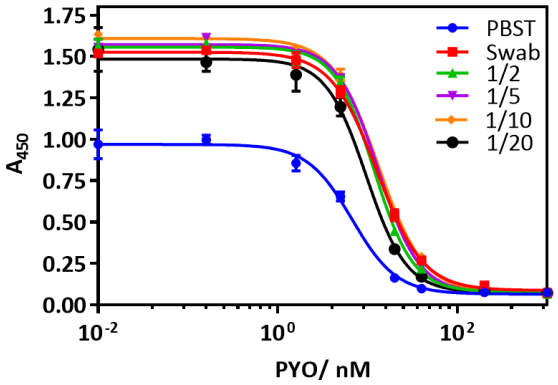

Figure 6. 7 *Matrix effect of the swab medium undiluted and diluted 2, 5, 10 and 20 times with 10 mM PBST on the performance of PYO mAb122/PC1-BSA ELISA. The calibration curves were run using the conditions established for the assay in PBST (see Table 6. 1). Each calibration point was measured in triplicates on the same ELISA plate and the results show the average and standard deviation of the assay carried out on 1 day.*

As illustrated in Figure 6. 7, all PYO standards prepared in different dilutions of swab medium behaved identically showing all of them higher absorbance values compared with PYO calibration curve in 10 mM PBST. Thus, the observed matrix effect was the same for all calibration curves prepared in swab medium. With the aim of disminishing the A_{max} so that the ELISA parameters resembled to the ones performed in assay buffer, the concentration of PYO mAb122 was decreased. Therefore, different PYO mAb122 concentrations were studied (data not shown) and 0.05 µg mL^{-1} was the selected one to analyse swab samples from pediatric patients infected with *P. aeruginosa.* As illustrated in Figure 6. 8, PYO standards prepared in

undiluted swab medium and PBST were similar as the analytical parameters of both calibration curves did not vary signficantly: A_{max} of 0.87 and 0.95 and IC_{50} 2.23 and 3.46 nM, respectively. Thus, it was decided to prepare PYO standard curve directly in swab medium using 0.05 µg mL^{-1} concentration of PYO mAb122.

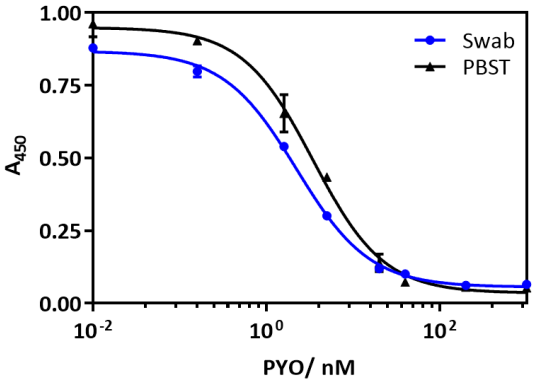

Figure 6. 8 *Matrix effect study of the swab medium on the performance of PYO mAb122/PC1-BSA ELISA. The calibration curve prepared with swab medium (blue) was performed using the conditions established for the assay in PBST but using 1/4 diluted PYO mAb122 concentration (0.05 µg mL^{-1}). Each calibration point was measured in triplicates on the same ELISA plate and the results show the average and standard deviation of the assay carried out on 1 day.*

6.2.2.1.2 Accuracy study

A set of blind samples were prepared by spiking swab medium with 300, 150, 60, 15, 7.5, 3.75, 1.875, 0.9375 and 0.1875 nM PYO concentrations. Figure 6. 9 shows the average of results measured on triplicates on three different days. The correlation coefficient obtained when comparing concentrations of the spiked samples against the values obtained with the ELISA was excellent (R^2 = 1) and the slope of the linear regression was close to 1 (slope =1.019).

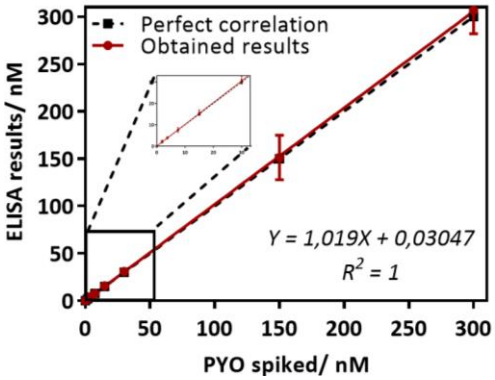

Figure 6. 9 *Results from the accuracy study using PYO mAb122/PC1-BSA ELISA. The graph shows the linear regression analysis of the swab medium spiked with different PYO concentrations ranging from 0 to 300 nM and the concentrations measured with the PYO mAb122/PC1-BSA ELISA. Assay was run in swab medium using a PYO mAb122 concentration of 0.05 µg mL^{-1}. Each calibration point was measured in triplicates on the same ELISA plate and the results show the average and standard deviation of analysis made on 3 different days.*

6.2.2.2 PYO quantification of swab samples from *P. aeruginosa* infected patients

17 swab samples from pediatric patients infected with *P. aeruginosa* (Figure 6. 10) were measured for PYO detection performing PYO mAb122/PC1-BSA ELISA. In this case, as previously described, PYO standard curve was prepared directly in swab medium using a four time diluted PYO mAb122 concentration (0.05 µg mL^{-1}).

Figure 6. 10 *Pictures of the P. aeruginosa positive swab samples obtained from Vall d'Hebron hospital.*

According to the obtained results, PYO content in the analysed swab samples was undetectable or detected in very low levels (around 1-3 nM) except in one sample whose concentration was of 12 nM (Table 6. 4).

Table 6. 4 *IRequiv. of PYO values directly obtained from swab samples from P. aeruginosa infected patients performing PYO mAb122/PC1-BSA ELISA. PYO calibration curve was run on swab medium using PYO mAb122 concentration of 0.05 µg mL^{-1}. Each sample was measured in triplicates on the same ELISA plate and the results show the average and standard deviation of 1 experiment. PASW= P. aeruginosa swab*

Swab reference	IRequiv. of PYO/ nM
PASW5840	1.78 ±0.04
PASW8820	1.76 ±0.25
PASW4881	12.25 ±0.94
PASW2789	2.81 ±0.00
PASW0904	3.16 ±0.21
PASW3406	0.59 ±0.15
PASW2904	*n.d.*
PASW5412	*n.d.*
PASW9495	*n.d.*
PASW6419	*n.d.*
PASW0349	*n.d.*
PASW5834	*n.d.*
PASW0056	*n.d.*
PASW1651	*n.d.*
PASW7775	*n.d.*
PASW7552	*n.d.*
PASW5503	5.36 ±0.04

These values are coherent since *P. aeruginosa* content on swab samples is always lower compared to sputum samples[15]. In this vein, Zemanick et al.[38] analysed oropharyngeal swab, spontaneously expectorated sputum, induced sputum and saliva samples from 16 CF patients (from 8 to 21 years) and, in most of the cases, bacterial concentration was higher in the lower airway in comparison with the upper airway. Therefore, the analysis of swab sample did not allow to determine differences between the studied samples due to the low PYO content detected.

6.3 Materials & methods

6.3.1 Reagents

The used reagents have been described in 5.3.1 section.

6.3.2 Sputum and swab samples

Sputum samples were collected by the group of M.- Teresa Martin (Microbiology Department, VHUH, Barcelona, Spain) from adult patients diagnosed with *P. aeruginosa* acute and chronic infections. Sputum samples were kept in 2 mL cryotubes and were stored at – 40 ºC until use.

Swab samples were collected by the group of M.- Teresa Martin (Microbiology Department, VHUH, Barcelona, Spain) from pediatric patients diagnosed with *P. aeruginosa* acute and chronic infections. The collection of swab samples was performed using a specific collection and transport method named ESwab™ (Copan's Liquid Amies Elution Swab). This system combines a flocked swab with 1 mL of collection liquid in a plastic, screw cap tube which allows to elute up to 90 % of bacteria in the corresponding liquid medium[37]. Swab samples were stored at – 40 ºC until use.

6.3.3 Sputum analysis

6.3.3.1 DTT treatment

General protocol using the detergent DTT. DTT is considered the strongest mucolytic agent that cleaves disulphide bonds of mucoproteins which form sputum. Thus, DTT was added to the studied sputum samples with the aim of breaking these bonds and homogenizing sputum samples. As illustrated in Figure 6. 11, the protocol started eliminating particulate matter from sputum samples, such as food particles and bacterial debris. Therefore, sputum was added to a Petri dish and, visually, these particles were removed using the tip of a pipette. Then, sputum was weighted using a precision balance (OHAUS) and treated with 0.2 % DTT (Sigma Aldrich) in

10 mM PBS (150 mg of weighted sputum with 300 µL of DTT solution). The solution was vortexed vigorously for 30 mins and further diluted with 10 mM PBS (300 µL). The mixture was vortexed vigorously for another 10 mins. Afterwards, with the aim of minimizing the matrix effect, the treated sample was diluted again in 10 mM PBS (600 µL). Then, the sample was centrifuged in a MicroStar12 centrifuge (VWR) (20 mins at 10,000 g) to get rid of possible particles that had not been resuspended and the supernatant was filtered by centrifugation using a 2 mL 0.45 µm nylon Spin-X Centrifuge Tube Filter (Sigma Aldrich) (10 mins at 4,000 g). The filtrate was collected and stored at - 40 ºC until use.

Modified protocol using the detergent DTT. Since the appearance of the DTT treated sputum samples was cloudy and the results obtained using the above mentioned DTT protocol indicated the presence of matrix effect, an additional ultracentrifugation step was added after the final filtration step to remove possible small particulate material coming from the sample.

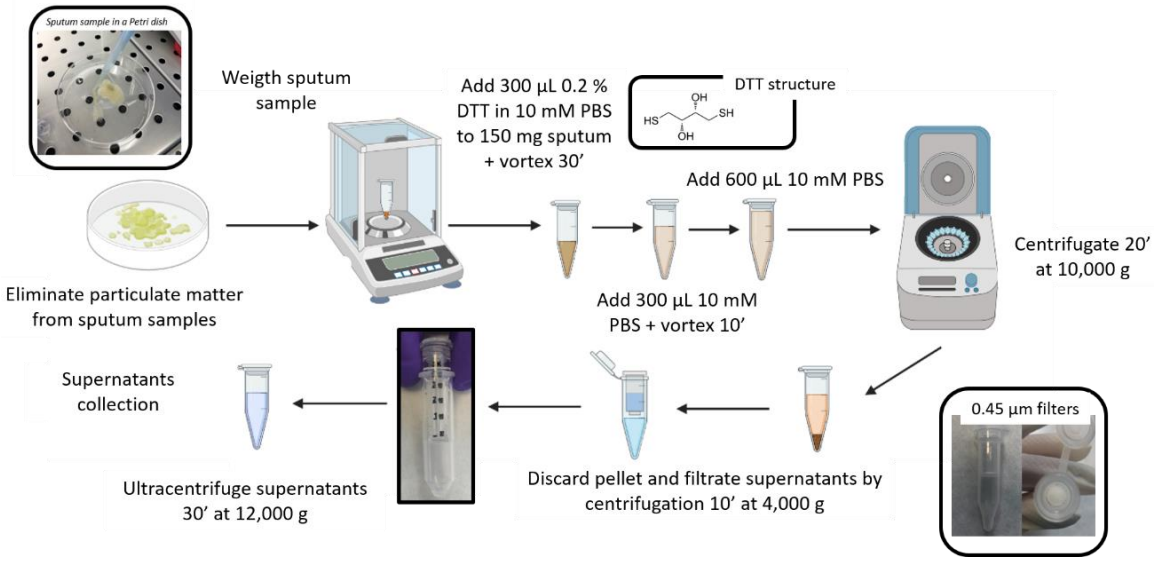

Figure 6. 11 *Protocol based on the use of the reducing agent dithiotheitrol (DTT) adding an extra ultracentrifugation step.*

6.3.3.2 Lyophylization treatment

Sputum samples from patients infected and not infected with *P. aeruginosa* were lyophilized according to the protocol shown in Figure 6. 12. Thus, after particulate matter from the sputum samples were removed, sputum samples were weighted on an Amicon® Ultra-0.5 Centrifual Filter (Sigma Aldrich) in order to avoid any loosing of sputum during the treatment procedure. Then, samples were lyophylized in a Lyoquest -85 PLUS Freeze Dryer (Telstar) (0.1 - 0.025 mbar and -80 ºC) for 48 h. Once lyophilized, sputum samples were weighted again to determine the amount of water lost during lyophylization process and diluted in 10 mM PBS to a final concentration of 2.5 mg mL^{-1}. The solution was sonicated using an Ultrasonic Unit FB

15054 (Fisher Scientific) (10 mins) in order to avoid any particle in suspension. The final stock was aliquoted in 1.5 mL volume and store at -40 ºC until use.

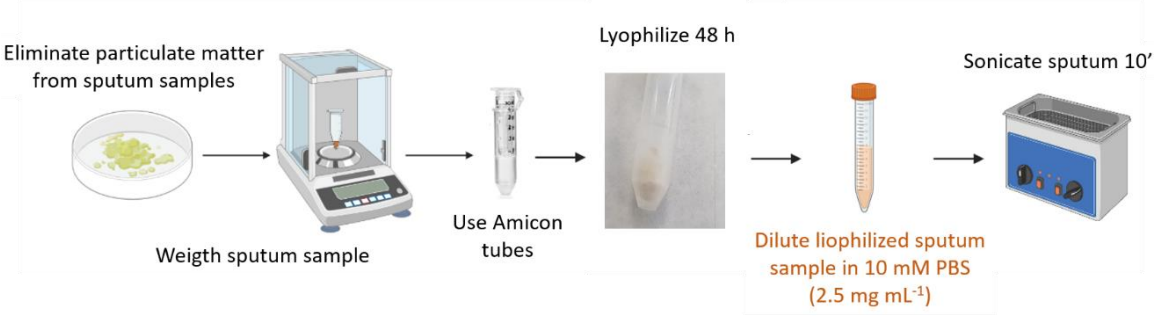

Figure 6. 12 *Sputum treatment protocol based on lyophilization process. After lyophylization, sputum stock solutions of 2.5 mg mL^{-1} concentration were prepared by diluting sputum sample in 10 mM PBS.*

6.3.3.3 Matrix effect studies

With the aim of evaluating whether the sputum medium interfere unspecifically with the performance of PYO mAb122/PC-BSA ELISA, matrix effect studies were assessed with DTT treated sputum samples and with lyophilized sputum samples.

DTT treated sputum samples. PYO standards curves were prepared in different dilutions of a pull of 14 sputum samples, which were previously mixed and homogeinized after being treated individually following DTT protocol. Thus, the obtained treated sputum mixture (125 mg mL^{-1} concentration; 150 mg of sputum sample diluted in a total volume of 1.2 mL) was diluted 2, 5, 10 and 20 times in PBS buffer. The obtained curves were compared with a control curve performed in PBS. The matrix dilution producing the most similar ELISA parameters compared with the ones obtained for the assay performed in assay buffer (IC_{50}, slope and A_{max}) was selected.

Lyophilized sputum samples. PYO standard curves were built in different dilutions of the lyophilized sputum from a concentration of 1 mg mL^{-1} of 10 mM PBS. This initial concentration was obtained by adding 2.25 mL of 10 mM PBS to the already prepared sputum stock of 2.5 mg mL^{-1} (see Figure 6. 12). From this initial 1 mg mL^{-1} concentration of sputum, a total of 9 dilutions were prepared carrying out serial dilutions using a dilution factor of 2 (from 1/2 to 1/512, see Figure 6. 13). These curves were run in parallel and compared with the control standard curve prepared in PBS. The matrix dilution producing the most similar ELISA parameters compared with the ones obtained for the assay performed in assay buffer (IC_{50}, slope and A_{max}) was selected. Due to the different nature of sputum samples, matrix effect were carried out for each sputum type individually (purulent, mucoid and bloody).

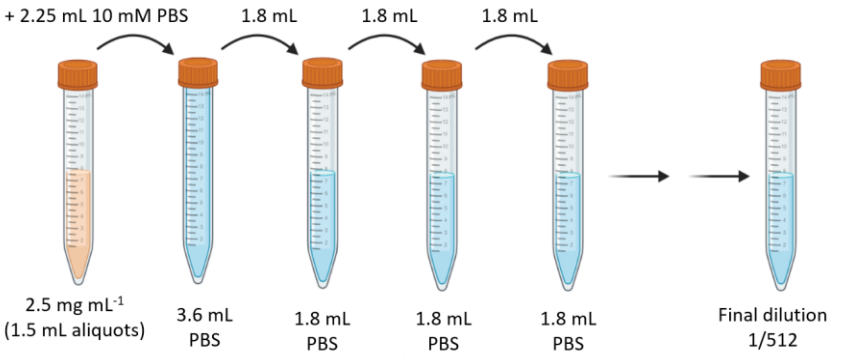

Figure 6. 13 *Preparation of lyophilized sputum dilutions for matrix effect evaluation. After adding 2.25 mL of 10 mM PBS to the initial lyophilized sputum stock of 2.5 mg mL^{-1} (1.5 mL aliquot) prepared following the protocol illustrated in Figure 6. 12, 1/2 serial dilutions were carried out until reaching a 1/512 dilution. These dilutions were used to performed the corresponding PYO satandard curves.*

6.3.3.4 Recovery and accuracy studies

Recovery studies. Sputum samples were spiked with PYO (10 nM) before carrying out DTT treatment protocol to determine the percentage of the added analyte concentration detected after performing this treatment. PYO levels were measured using PYO mAb122/PC1-BSA ELISA. Furthermore, these experiments were also carried out when the ultracentrifugation step was added to DTT protocol. Thus, sputum samples were spiked with PYO (10 nM) before and after they were ultracentrifugated and PYO concentration was measured using PYO mAb122/PC1-BSA ELISA. In all cases, the determined PYO values were compared with the initially added concentration (10 nM).

Accuracy studies. Since DTT treatment showed matrix effect problems and low recovery percentages, accuracy studies were only performed for lyophilized sputum samples. Furthermore, these experiments were carried out for each sputum type individually (purulent, mucoid and bloody). Therefore, blind lyophilized sputum samples were spiked at several PYO concentrations (ranging from 20 nM to 0 nM) and PYO levels were measured performing PYO mAb122/PC1-BSA ELISA taken into consideration the corresponding matrix effect for each sputum type. The obtained PYO values were compared with the spiked PYO concentration.

6.3.4 Swab analysis

6.3.4.1 Matrix effect studies

The potential nonspecific interferences from swab medium (Copan's Liquid Amies Elution Swab) were evaluated since this medium contains high concentrations of different salts (sodium chloride, potassium chloride, calcium chloride, magnesium chloride, monopotassium phosphate, disodium phosphate and sodium thioglycollate). Thus, PYO standard curves (1000,

200, 40, 20, 5, 1.6, 0.16 and 0 nM) were prepared in swab medium and in swab medium diluted 2, 5, 10 and 20 times in 10 mM PBST. The obtained curves were compared with the one performed in PBST.

6.3.4.2 Accuracy study

Blind swab samples were spiked at different PYO concentrations ranging from 300 to 0 nM (300, 150, 60, 15, 7.5, 3.75, 1.875, 0.9375 and 0.1875 nM) and measured performing PYO mAb122/PC1-BSA ELISA. The obtained results were compared with the spiked PYO values.

6.4 Concluding remarks

- PYO mAb122/PC1-BSA ELISA has been intended to be implemented for PYO quantification in clinical samples such as sputum and swabs. For its implementation, matrix effect studies have been carried out indicating the need of performing a previous treatment step in the case of sputum sample. With this aim, different sample treatment protocols have been studied: DTT treatment and lyophilization treatment.

- The treatment of sputum samples with DTT has not allowed PYO quantification as it presented issues with the matrix and recovery studies. Thus, with the aim of removing possible small particulate material coming from the sample that could interfere with the assay, an additional ultracentrifugation step was added to the DTT protocol. Nevertheless, in all the cases, PYO levels were below the LoD of the assay.

- In contrast, lyophilization has seemed to be the most appropriate treatment as demonstrated by the lower matrix effect shown for the three type of sputum (purulent, mucoid and bloody) at concentrations below 1 mg mL^{-1}. However, when analysing PYO levels in sputum samples from patients infected with *P. aeruginosa,* they were very low or even undetectable (below the LoD of the assay). Furthermore, since the LoD of PYO mAb122/PC1-BSA ELISA was lower than the reported LoD from other techniques used to directly measure PYO in sputa samples[21], these negative results were probably due to an unresolved matrix effect problem. Therefore, other sputum treatments, such as the additional use of proteinase K, are being studied with the aim of minimizing the observed matrix effect.

- The measure of PYO on swab samples from children infected with *P. aeruginosa* has been carried out directly without the need of any previous treatment nor dilution and performing PYO standard in swab medium using 0.05 µg mL^{-1} of PYO mAb122. From a total of 17 analysed swab samples, 7 showed low levels of PYO, whereas undetectable PYO concentrations were measured in the other 10 samples. These results are coherent with reported studies that showed that bacterial concentration in the upper airways is lower than in the lower airways[38].

6.5 References

1. Palmer, K. L.; Mashburn, L. M.; Singh, P. K.; Whiteley, M., Cystic fibrosis sputum supports growth and cues key aspects of Pseudomonas aeruginosa physiology. *J Bacteriol* **2005,** *187* (15), 5267-77.
2. Smyth, A. R.; Bell, S. C.; Bojcin, S.; Bryon, M.; Duff, A.; Flume, P.; Kashirskaya, N.; Munck, A.; Ratjen, F.; Schwarzenberg, S. J.; Sermet-Gaudelus, I.; Southern, K. W.; Taccetti, G.; Ullrich, G.; Wolfe, S.; European Cystic Fibrosis, S., European Cystic Fibrosis Society Standards of Care: Best Practice guidelines. *J Cyst Fibros* **2014,** *13 Suppl 1*, S23-42.
3. Ma, J. T.; Tang, C.; Kang, L.; Voynow, J. A.; Rubin, B. K., Cystic Fibrosis Sputum Rheology Correlates With Both Acute and Longitudinal Changes in Lung Function. *Chest* **2018,** *154* (2), 370-377.
4. Sanders, N. N.; De Smedt, S. C.; Van Rompaey, E.; Simoens, P.; De Baets, F.; Demeester, J., Cystic fibrosis sputum: a barrier to the transport of nanospheres. *Am J Respir Crit Care Med* **2000,** *162* (5), 1905-11.
5. Neve, R. L. P., V. V., Artificial Sputum Medium Formulation Impacts Pseudomonas aeruginosa Phenotype and Chemotype. *BioRxiv* **2021**.
6. Gallego, M. P., X.; Espasa, M.; Castañer, E.; Solé, M.; Suárez D.; Monsó, E.; Montón, C., Pseudomonas aeruginosa isolates in severe chronic obstructive pulmonary disease: characterization and risk factors. *BMC Pulmonary Medicine* **2014,** *14* (103), 2-12.
7. Ramsey, K. A.; Chen, A. C. H.; Radicioni, G.; Lourie, R.; Martin, M.; Broomfield, A.; Sheng, Y. H.; Hasnain, S. Z.; Radford-Smith, G.; Simms, L. A.; Burr, L.; Thornton, D. J.; Bowler, S. D.; Livengood, S.; Ceppe, A.; Knowles, M. R.; Noone, P. G., Sr.; Donaldson, S. H.; Hill, D. B.; Ehre, C.; Button, B.; Alexis, N. E.; Kesimer, M.; Boucher, R. C.; McGuckin, M. A., Airway Mucus Hyperconcentration in Non-Cystic Fibrosis Bronchiectasis. *Am J Respir Crit Care Med* **2020,** *201* (6), 661-670.
8. Kwok, W. C.; Ho, J. C. M.; Tam, T. C. C.; Ip, M. S. M.; Lam, D. C. L., Risk factors for Pseudomonas aeruginosa colonization in non-cystic fibrosis bronchiectasis and clinical implications. *Respir Res* **2021,** *22* (1), 132.
9. What is the significance of different sputum types? (accessed 2021/08/01).
10. Cuthbertson, L.; Rogers, G. B.; Walker, A. W.; Oliver, A.; Hafiz, T.; Hoffman, L. R.; Carroll, M. P.; Parkhill, J.; Bruce, K. D.; van der Gast, C. J., Time between collection and storage significantly influences bacterial sequence composition in sputum samples from cystic fibrosis respiratory infections. *J Clin Microbiol* **2014,** *52* (8), 3011-6.

11. Terranova, L.; Oriano, M.; Teri, A.; Ruggiero, L.; Tafuro, C.; Marchisio, P.; Gramegna, A.; Contarini, M.; Franceschi, E.; Sottotetti, S.; Cariani, L.; Bevivino, A.; Chalmers, J. D.; Aliberti, S.; Blasi, F., How to Process Sputum Samples and Extract Bacterial DNA for Microbiota Analysis. *Int J Mol Sci* **2018,** *19* (10).
12. Lenhart-Pendergrass, P. M.; Anthony, M.; Sariyska, S.; Andrews, A.; Scavezze, H.; Towler, E.; Martiniano, S. L.; Hoppe, J. E.; Zemanick, E. T., Detection of bacterial pathogens using home oropharyngeal swab collection in children with cystic fibrosis. *Pediatr Pulmonol* **2021,** *56* (7), 2043-2047.
13. Ma, Z.; Wang, T.; Li, Z.; Guo, X.; Tian, Y.; Li, Y.; Xiao, S., A novel biotinylated nanobody-based blocking ELISA for the rapid and sensitive clinical detection of porcine epidemic diarrhea virus. *J Nanobiotechnology* **2019,** *17* (1), 96.
14. Schultz, A.; Caudri, D., Cough swabs less useful but induced sputum very useful in symptomatic older children with cystic fibrosis. *Lancet Respir Med* **2018,** *6* (6), 410-411.
15. Goddard, A. F.; Staudinger, B. J.; Dowd, S. E.; Joshi-Datar, A.; Wolcott, R. D.; Aitken, M. L.; Fligner, C. L.; Singh, P. K., Direct sampling of cystic fibrosis lungs indicates that DNA-based analyses of upper-airway specimens can misrepresent lung microbiota. *Proc Natl Acad Sci U S A* **2012,** *109* (34), 13769-74.
16. Ryall, B.; Carrara, M.; Zlosnik, J. E.; Behrends, V.; Lee, X.; Wong, Z.; Lougheed, K. E.; Williams, H. D., The mucoid switch in Pseudomonas aeruginosa represses quorum sensing systems and leads to complex changes to stationary phase virulence factor regulation. *PLoS One* **2014,** *9* (5), e96166.
17. Wilson, R.; Sykes, D. A.; Watson, D.; Rutman, A.; Taylor, G. W.; Cole, P. J., Measurement of Pseudomonas aeruginosa phenazine pigments in sputum and assessment of their contribution to sputum sol toxicity for respiratory epithelium. *Infect Immun* **1988,** *56* (9), 2515-7.
18. WILSON, R. D. A. S., D.A.; WATSON, D.; A. RUTMAN, A.; TAYLOR, G.W.; COLE, P. J., Measurement of Pseudomonas aeruginosa Phenazine Pigments in Sputum and Assessment of Their Contribution to Sputum Sol Toxicity for Respiratory Epithelium. *INFECTION AND IMMUNITY* **1988,** *59* (9), 2515-2517.
19. Hunter, R. C.; Klepac-Ceraj, V.; Lorenzi, M. M.; Grotzinger, H.; Martin, T. R.; Newman, D. K., Phenazine content in the cystic fibrosis respiratory tract negatively correlates with lung function and microbial complexity. *Am J Respir Cell Mol Biol* **2012,** *47* (6), 738-45.
20. Retraction: Phenazine Content in the Cystic Fibrosis Respiratory Tract Negatively correlates with Lung Function and Microbial Complexity. *Am. J. Respir. Cell Mol Biol* **2019,** *60* (1), 134.
21. Alatraktchi, F. A.; Dimaki, M.; Stovring, N.; Johansen, H. K.; Molin, S.; Svendsen, W. E., Nanograss sensor for selective detection of Pseudomonas aeruginosa by pyocyanin identification in airway samples. *Anal Biochem* **2020,** *593*, 113586.
22. Saraswathy Veena, V.; Sara George, P.; Jayasree, K.; Sujathan, K., Comparative analysis of cell morphology in sputum samples homogenized with dithiothreitol, N-acetyl-L cysteine, Cytorich((R)) red preservative and in cellblock preparations to enhance the sensitivity of sputum cytology for the diagnosis of lung cancer. *Diagn Cytopathol* **2015,** *43* (7), 551-8.
23. Dicker, A. J.; Crichton, M. L.; Pumphrey, E. G.; Cassidy, A. J.; Suarez-Cuartin, G.; Sibila, O.; Furrie, E.; Fong, C. J.; Ibrahim, W.; Brady, G.; Einarsson, G. G.; Elborn, J. S.; Schembri, S.; Marshall, S. E.; Palmer, C. N. A.; Chalmers, J. D., Neutrophil extracellular traps are

associated with disease severity and microbiota diversity in patients with chronic obstructive pulmonary disease. *J Allergy Clin Immunol* **2018,** *141* (1), 117-127.

24. Woolhouse, I. S.; Bayley, D. L.; Stockley, R. A., Effect of sputum processing with dithiothreitol on the detection of inflammatory mediators in chronic bronchitis and bronchiectasis. *Thorax* **2002,** *57* (8), 667-71.
25. Arias-Bouda, L.-M.-P. N., L. N.; Ho, L. M.; Kuijper, S.; Jansen, H. M.; Kolk, A. H., Development of Antigen Detection Assay for Diagnosis of Tuberculosis Using Sputum Samples. *JOURNAL OF CLINICAL MICROBIOLOGY* **2000,** *38* (6), 2278–2283.
26. Sadowska, A. M., N-Acetylcysteine mucolysis in the management of chronic obstructive pulmonary disease. *Therapeutic Advances in Respiratory Disease* **2012,** *6* (3), 127-135.
27. Cleland, W. W., Dithiothreitol, a New Protective Reagent for Sh Groups. *Biochemistry* **1964,** *3*, 480-2.
28. Peter, J. G.; Cashmore, T. J.; Meldau, R.; Theron, G.; van Zyl-Smit, R.; Dheda, K., Diagnostic accuracy of induced sputum LAM ELISA for tuberculosis diagnosis in sputum-scarce patients. *Int J Tuberc Lung Dis* **2012,** *16* (8), 1108-12.
29. Pastells, C.; Pascual, N.; Sanchez-Baeza, F.; Marco, M. P., Immunochemical Determination of Pyocyanin and 1-Hydroxyphenazine as Potential Biomarkers of Pseudomonas aeruginosa Infections. *Anal Chem* **2016,** *88* (3), 1631-8.
30. Zukovskaja, O.; Agafilushkina, S.; Sivakov, V.; Weber, K.; Cialla-May, D.; Osminkina, L.; Popp, J., Rapid detection of the bacterial biomarker pyocyanin in artificial sputum using a SERS-active silicon nanowire matrix covered by bimetallic noble metal nanoparticles. *Talanta* **2019,** *202*, 171-177.
31. Rashid, J. I. A.; Kannan, V.; Ahmad, M. H.; Mon, A. A.; Taufik, S.; Miskon, A.; Ong, K. K.; Yusof, N. A., An electrochemical sensor based on gold nanoparticles-functionalized reduced graphene oxide screen printed electrode for the detection of pyocyanin biomarker in Pseudomonas aeruginosa infection. *Mater Sci Eng C Mater Biol Appl* **2021,** *120*, 111625.
32. Shak, S. C., D. J.; Hellmiss, R.; Marsters, S. A.; Baker, C. L., Recombinant human DNase I reduces the viscosity of cystic fibrosis sputum. *Proc. Nati. Acad. Sci. USA* **1990,** *87*, 9188-9192.
33. Cai, Y. C., K.; Gibson, P.; Henry, R., Comparison of Sputum Processing. *Pediatric Pulmonology* **1996,** *22*, 402-407.
34. Kim, J.-S. H., G. H.; Okamoto,K.; Rubin, B. K., Sputum Processing for Evaluation of In¯ammatory Mediators. *Pediatric Pulmonology* **2001,** *32*, 152-158.
35. Silva, L. V.; Galdino, A. C.; Nunes, A. P.; dos Santos, K. R.; Moreira, B. M.; Cacci, L. C.; Sodre, C. L.; Ziccardi, M.; Branquinha, M. H.; Santos, A. L., Virulence attributes in Brazilian clinical isolates of Pseudomonas aeruginosa. *Int J Med Microbiol* **2014,** *304* (8), 990-1000.
36. Elliott, J.; Simoska, O.; Karasik, S.; Shear, J. B.; Stevenson, K. J., Transparent Carbon Ultramicroelectrode Arrays for the Electrochemical Detection of a Bacterial Warfare Toxin, Pyocyanin. *Anal Chem* **2017,** *89* (12), 6285-6289.
37. ESwabTM. (accessed 2021/08/26).
38. Zemanick, E. T.; Wagner, B. D.; Robertson, C. E.; Stevens, M. J.; Szefler, S. J.; Accurso, F. J.; Sagel, S. D.; Harris, J. K., Assessment of airway microbiota and inflammation in cystic fibrosis using multiple sampling methods. *Ann Am Thorac Soc* **2015,** *12* (2), 221-9.

Chapter 7

Blocking pyocyanin with a specific mAb in *in vitro* conditions as a therapeutic tool for treating *P. aeruginosa* infections

In this chapter, the setting up of a cell culture based *in vitro* system to study the cytotoxicity of pyocyanin (PYO) and the protective effect of a previously developed specific monoclonal antibody (mAb) against this virulence factor (VF) (PYO mAb122) is described. In this sort of assays, murine alveolar macrophages (MH-S cell line) were treated with different PYO concentrations during an optimized period of time to determine the cytotoxic effect caused by PYO. With this aim, different cell viability hallmarks were assessed, which allowed to determine the median lethal dosis (LD_{50}) of this VF on MH-S cell viability. Subsequently, the protective effect of PYO mAb122 was also studied by testing its potential as quorum quencher (QQ) when cells were treated at a stoichiometric fixed PYO concentration corresponding to the LD_{50} value previously determined. The results obtained have showed a promising increase in the percentage of viable cells. Moreover, the potential of PYO mAb122 on blocking the dysregulation action of PYO on the host immune response has been analysed. For this purpose, the immunomodulatory effect of PYO and the addition of PYO mAb122 were studied on MH-S cells measuring different pro- and anti- inflammatory cytokines by ELISA.

In preparation

***Rodriguez-Urretavizcaya, B**.; Vilaplana, Ll.; Marco, M.P. Blocking Pyocyanin with a specific monoclonal antibody in vitro as a therapeutic tool for treating P. aeruginosa infections (2021)*

7.1 Introduction

Despite the rise of multidrug resistant (MDR) bacteria and the little effectiveness of the current antimicrobials, most therapeutic strategies used for treating any suspected case of *Pseudomonas aeruginosa* are still based on the administration of classical antibiotics, especially β-lactam antibiotics alone or in combination with other families of these type of drugs [1-4]. Thus, all these facts point to the need of developing novel and alternative effective therapies against *P. aeruginosa* infections.

Among the new emerging therapeutic techniques phage therapy, efflux bomb inhibitors, antimicrobial peptides and therapeutic monoclonal antibodies (mAbs) are the most promising ones[3]. In fact, focusing on therapeutic mAbs, since the first therapeutic mAb (Orthoclone OKT3) was approved by the US Food and Drug Administration (FDA) in 1986 to prevent kidney transplant rejection[5-6], the number of therapeutic mAbs approved has increased drastically to 79 in December 2019[7] and to 100 by 2021[8]. In fact, mAb market has doubled in size in the last years due to the appearance of fully human and bispecific mAbs[9]. Furthermore, from the total mAbs approximately 78 % are intended for cancer and autoimmune diseases[6]. However, mAbs are increasingly used in a broad range of human diseases such as asthma, psoriasis, arthritis and infectious diseases[7].

Regarding infectious diseases, the use of therapeutic mAbs has proven as a promising alternative since resistance can be diminished and even avoided due to their high specificity and affinity for the target, which decrease adverse effects[10-12]. Moreover, therapeutic mAbs have shown high stability in different conditions and low immunogenicity[13]. Hence, many companies are sponsoring clinical trials for more than 570 therapeutic mAbs from which 6 mAbs are currently approved by the US FDA for treating infectious diseases[7, 14]: raxibacumab and obiltoxaximab (for treatment of inhalational anthrax) , palivizumab (for prevention of respiratory syncytial virus), ibalizumab (for treatment of human immunodeficiency virus, HIV) and bamlanivimab and etesevimab (for prevention of COVID-19 in adults and pediatric patients).

Up to now, the main targets of mAbs against infectious diseases are virulence factors (VFs), toxins, surface proteins and polysaccharides[11, 15-17], most of which are known to be regulated by quorum sensing (QS)[18]. Thus, disruption of QS mechanisms has been explored as an attractive alternative to combat bacterial infections[19-20]. In this context, the main VF of *P. aeruginosa,* pyocyanin (PYO), can be considered a very interesting therapeutic target since it it is regulated

by QS[21], it is specific of *P. aeruginosa*[22] and it induces severe damage in different cell lines[23-27] through formation of reactive oxygen species (ROS)[28-29]. Furthermore, it increases pro-inflammatory cytokines *in vitro*[30] and decreases anti-inflammatory cytokines *in vivo*[31] (for more cytotoxicity effects see Chapter 1). In fact, antivirulence therapies have been developed against this VF. However, all of them inhibit PYO production indirectly by blocking or degrading autoinducers (AIs) or receptors of *P. aeruginosa* QS[32-34]. In this direction, Kaufmann et al.[20] developed a mAb against 3oxoC_{12}-HSL named RS2-1G9 that reduced PYO levels by 80 and 30 % in PAO1 and on the double knockout PAO-JM2 (strain that lacks *rhlI* and *lasI*) cultures[20, 35]. Another used strategy consisted in exploiting the catalytic activity of Abs. In this case, Lamo Marin et al. [36] screened a panel of 17 catalytic Abs raised against haptens that mimic transition states of AHL degrading enzymes such as amidases and lactonases reactions. They concluded that XYD-11G2 mAb (IC_{50} =23.6 µM) catalysed 3oxoC_{12}-HSL hydrolysis decreasing PYO content by 40 % in PAO1 culture[20, 37]. Also in this context, there are Abs that specifically quench cell-associated VF reducing and even avoiding pathogenesis[38]. KB001 (KaloBios) is a pegylated mAb Fab fragment that targets PcrV secretion protein (from the type 3 secretion system (T3SS) designed to treat ventilated subjects and CF patients[38]. Furthermore, V2L2MD anti-PcrV mAb provided better *in vivo* protection levels than the before mentioned[39].

This chapter reports the development of an *in vitro* system to test the cytotoxic effect of QS relevant molecules, such as PYO or Pseudomonas Quinolone Signal (PQS). In particular, Chapter 7 focuses in the cytotoxicity study of PYO, an effector molecule whose expression is controlled by QS system. Besides, the quenching effect of the previously developed PYO mAb122[40] as therapeutical agent is also evaluated using the same *in vitro* system and analyzing different cell viability hallmarks such as mitochondrial enzymatic activity, cell membrane integrity, esterase activity and cellular respiration[41]. For this purpose, cultures of MH-S macrophages were used since they showed high susceptibility to the effects produced by PYO. Subsequently, the immunomodulatory effect of PYO is evaluated using the same cell-based system by measuring the production of different pro- and anti- inflammatory cytokines (IL-8, IL-6, TNF-α and IL-13) by ELISA. Also, the effect of PYO mAb122 addition is assessed regarding the disruption of the immune host cell response, by comparing the cytokine levels of cells treated with PYO, cells treated with both PYO and PYO mAb122 and non-treated cells.

7.2 Results & discussion

7.2.1 Cytotoxicity evaluation of PYO on murine macrophages

PYO cytotoxicity was first evaluated in *in vitro* conditions on two murine macrophage lines (MH-S and Raw 264.7 cells) to analyse their sensistivity and select the most sensitive one. Besides, with the aim of determining the timing required for PYO to exert its cytotoxic effect on these cell lines, cells were treated with different concentrations of PYO during 24, 48 and 72 h and PYO cytotoxicity was studied using AlamarBlue reagent. According to PYO levels found in different biological samples such as ear secretion (up to 2.8 µM)[42], sputum (up to 100 µM)[43] and wounds (8.1 µM)[44], PYO concentrations ranging from 100 to 0 µM were selected for determining the corresponding median lethal dosis (LD_{50}) value. Based on the obtained results, MH-S and Raw 264.7 cells were grown for 72 h since it was the period of time required for PYO to exert clearly its effect when working with the concentrations already mentioned. In fact, at 24 and 48 h the difference in viability of cells treated with the highest and lowest PYO concentrations was not significant, which resulted in very similar fluorescence values (data not shown). Furthermore, at 72 h, the LD_{50} of PYO on Raw 264.7 cells was an order of magnitude greater than on MH-S (see Figure 7. 1). Hence, MH-S cell line was selected to perform PYO cytotoxicity studies.

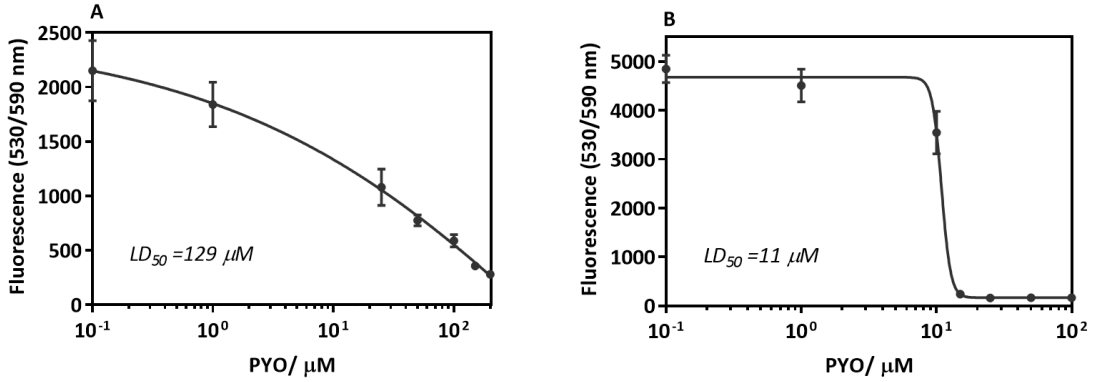

Figure 7. 1 *PYO cytotoxicity curves obtained using AlamarBlue reagent for (A) Raw 264.7 cells and (B) MH-S cells. The assay was performed in in vitro conditions during 3 days testing concentrations of PYO ranging from 100 to 0 µM (100-50-25-15-10-1-0 µM), corresponding to the Standard Curve. Results are expressed in fluorescence values at 530/590 nm. Each calibration point was measured in triplicates on the same culture plate and the results show the average and standard deviation of the assay carried out on one day.*

7.2.1.1 Murine alveolar macrophage cell line

Thus, as illustrated in Figure 7. 1, due to the higher susceptibility shown by MH-S cell line compared to Raw 264.7 cell line (LD_{50} =11 µM vs 129 µM), MH-S cells were selected to perform PYO cytotoxicity studies. With this purpose, PYO cytotoxic effect on MH-S cells was studied analysing three different hallmarks of cell viability (see Material and Methods):

- mitochondrial enzymatic activity (AlamarBlue reagent).

- esterase activity and membrane integrity (LIVE/DEAD dual staining).
- cell respiration (Luminescent adenosine triphosphate (ATP) Detection).

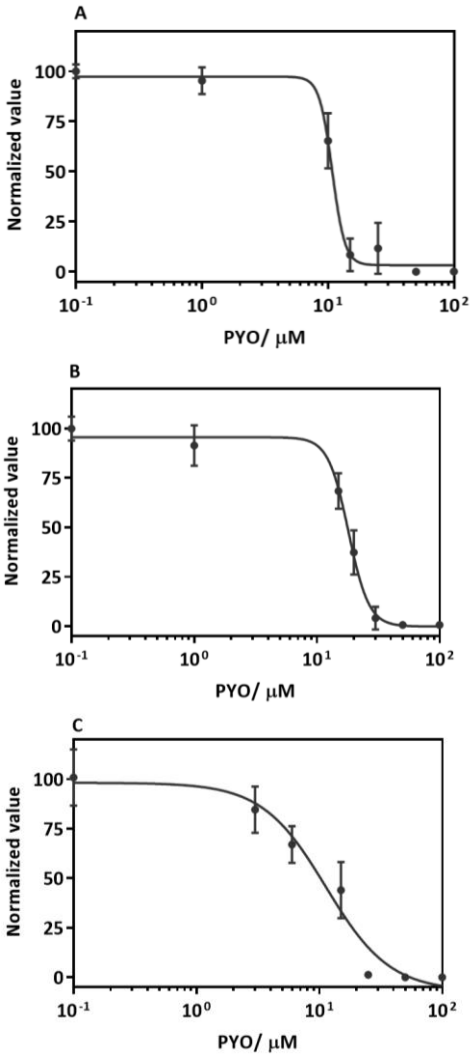

Max	97.39 ± 2.20
Min	3.32 ± 1.93
Slope	-8.54 ± 1.70
LD_{50}/ µM	10.80 ± 1.02
Dynamic range/ µM	7.63 ± 2.76 and 15.91 ± 4.06
LoD/ µM	5.97 ± 3.39
R^2	0.98 ± 0.01

Max	95.57 ± 1.79
Min	-0.10 ± 1.69
Slope	-5.23 ± 0.63
LD_{50}/ µM	18.10 ± 4.18
Dynamic range/ µM	13.74 ± 0.99 and 21.27 ± 2.97
LoD/ µM	11.42 ± 1.94
R^2	0.98 ± 0.01

Max	98.21 ± 4.34
Min	-6.97 ± 4.90
Slope	-1.67 ± 0.28
LD_{50}/ µM	11.31 ± 1.12
Dynamic range/ µM	7.24 ± 5.06 and 18.89 ± 0.69
LoD/ µM	4.77 ± 3.70
R^2	0.95 ± 0.04

Figure 7. 2 *PYO cytotoxicity curves and the corresponding analytical parameters. The graphs show the results obtained with: (A) AlamarBlue (AB), (B) LIVE/DEAD dual staining and (C) Luminescent ATP Detection assay. Assays were performed in in vitro conditions with MH-S cells during 3 days testing concentrations of PYO ranging from 100 to 0 µM (100-50-25-15-10-1-0 µM, 100-50-30-20-15-1-0 µM and 100-50-25-15-6-3-0 µM, respectively). Each calibration point was measured in triplicates on the same culture plate and the results show the average and standard deviation of the assay carried out on 3-4 different days. The obtained results were normalized according to the viability value of non-treated cells as it was considered to be equivalent to 100 % viability.*

For all studied hallmarks, MH-S cells were cultured at an optimal seeding density of 1 x10^5 cells mL^{-1} and treated with PYO concentrations ranging from 100 to 0 µM (standard curve) for 72 h according to the perform assay: 100-50-25-15-10-1-0 µM for AlamarBlue reagent, 100-50-30-20-15-1-0 µM for LIVE/DEAD dual staining and 100-50-25-15-6-3-0 µM for Luminescent ATP Detection. At the same time, non-treated MH-S cells were used as 100 % viability control and the obtained results were normalized in accordance with this value.

Figure 7. 2 shows the obtained LD_{50}-s values for PYO on MH-S cells according to the viability parameter measured, which varies from 10 to 20 µM. Besides, it is interesting to point out that PYO triggered the highest impact when focusing on mitochondrial enzymatic activity and cell respiration, as demonstrated by showing lower LD_{50} values in these cases (11 µM) compared with that for membrane integrity and esterase activity (18 µM). That could be explained due to PYO ability to increase ROS formation[28-29].

Furthermore, these LD_{50} values were coherent with previously reported values obtained when working with other cell lines (see Table 7. 1). Thus, Muller et al. [45] treated human skin fibroblasts with different PYO concentrations (50-0 µM) for 24 h obtaining a LD_{50} value of around 10 µM using CellTiter-Glo luminescent Cell Viability Assay kit , which measures ATP production. In the same line, O'Malley et al.[46] determined the LD_{50} of PYO on human alveolar type II cell line A549 based on two hallmarks of viability: mitochondrial activity and cell respiration. With this purpose, they used 3-(4,5-dimethylthiazol-2-yl)-2,5-diphenyltetrazolium bromide (MTT) assay and a luciferase-luciferine assay, respectively. The obtained LD_{50} values were 30 µM when analysing mitochondrial activity after 48 h, whereas the same LD_{50} value was observed after only 24 h based on cell respiration hallmark. Furthermore, Moayedi et al.[28] evaluated PYO cytotoxicity on a human pancreatic cancer cell line (Panc-1) using 2,3-Bis-(2-Methoxy-4-Nitro-5-Sulfophenyl)-2H-Tetrazolium-5-Carboxanilide (XTT) viability assay. After 24 h, the LD_{50} of PYO on Panc-1 cell line was around 45 µM. Finally, Mohammed et al.[47] obtained a LD_{50} value of 32 µM when they treated hepatocellular carcinoma human (HepG2) cells with PYO for 72 h using the neutral red dye assay, which is based on lysosomes activity.

Table 7. 1 *Reported LD_{50} values for PYO on different cell lines and the used viability assay. MTT =3-(4,5-dimethylthiazol-2-yl)-2,5-diphenyltetrazolium bromide; XTT =2,3-Bis-(2-Methoxy-4-Nitro-5-Sulfophenyl)-2H-Tetrazolium-5-Carboxanilide*

Cell line	LD_{50}	Viability assay	Reference
Human skin fibroblasts	10 µM (24 h)	CellTiter-Glo luminescent Cell Viability Assay kit	45
Human pancreatic cancer cell line (Panc-1)	45 µM (24 h)	XTT assay	28
Hepatocellular carcinoma human (HepG2)	32 µM (72 h)	Neutral red dye	47
The human alveolar type II cell line A549	30 µM (48 h) 30 µM (24 h)	MTT assay Luciferine-luciferase	46

7.2.2 Protective effect evaluation of PYO mAb122 on MH-S cell line

Once the LD_{50} of PYO on MH-S cells was determined, the potential protective effect of the previously developed PYO mAb122[40] was evaluated. With this aim, MH-S cells were first treated with a bivalent stoichiometric concentration of PYO mAb122 (assuming that each mAb binds two molecules of PYO), to ensure that the quencher was already in the host cells medium, and further with a LD_{50} concentration of PYO.

Before assessing the protective effect of PYO mAb122 on MH-S cells, the stability of this immunoreactive was studied since the assay protocol involved keeping the cells with PYO and/or PYO mAb122 for 3 days at 37 ºC and 5 % CO_2. Thus, MH-S cells were treated with a bivalent stoichiometric LD_{50} concentration and half of the LD_{50} concentration of PYO mAb122 for 3 days at the above mentioned conditions (see Figure 7. 9). Furthermore, a non-treated cell control and PYO standard curve were used to ensure a correct performance of the assay. After this time, treated cell culture supernatants were collected and used to assess PYO mAb122/PC1-BSA ELISA (conditions of the assay are explained in Chapter 4). As illustrated in Figure 7. 3, two PYO standard curves were built using PYO mAb122 corresponding to the LD_{50} value (middle blue) and to half of the LD_{50} (light blue) and performing PYO mAb122/PC1-BSA ELISA. These curves were compared with a control curve obtained using a non-cultured PYO mAb122, whose activity was known not to be modified (dark blue). The stability of PYO mAb122 was demonstrated since the obtained analytical parametres of the ELISA for the three curves were not significantly different: A_{450} values of 1.07, 1.03 and 1.09 and IC_{50} values of 4.75 nM, 5.22 nM and 4.86 nM for the control, LD_{50} and half LD_{50}, respectively.

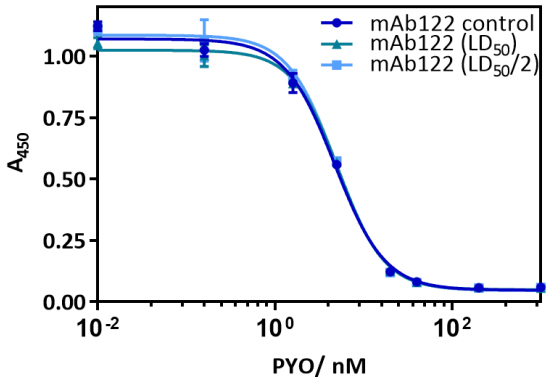

Figure 7. 3 *Stability studies of PYO mAb122 using PYO mAb122/PC1-BSA ELISA. PYO mAb122 was added to MH-S cells stoichiometrically at the LD_{50} (middle blue) and half of the LD_{50} concentration (light blue) and incubated for 3 days at 37 ºC and 5 % CO_2 in RPMI media. Cell culture supernatants were used to perform PYO mAb122/PC1-BSA ELISA at a final concentration of 0.008 µg mL^{-1} for PYO mAb122 (standard conditions). The obtained IC_{50}-s were of 5.22 and 4.86 nM, respectively (control IC_{50} value 4.75 nM). Each calibration point was measured in triplicates on the same ELISA plate and the results show the average and standard deviation of the assay carried out on 1 day.*

Once the stability of PYO mAb122 was confirmed, the possible quenching capability of PYO mAb122 regarding PYO cytotoxicity was evaluated assessing the same viability assays previously used to determine PYO cytotoxicity. Thus, three different characteristic features of viable cells were studied to confirm the protective effect of PYO mAb122: mitochondrial enzymatic activity, esterase activity and membrane integrity and cell respiration. Each assay was performed in triplicates and repeated 3-4 different days.

Another important issue to take into account when carrying out these sort of assays was to ensure that PYO mAb122 did not exert any cytotoxic effect by itself when administered on MH-S cells. Therefore, a control with cells only treated with this immunoreagent was performed. The corresponding viability percentage was compared with that obtained from non-treated MH-S cells (considered as 100 % of viability). This control was necessary since the previous use of polyclonal antibodies (pAbs) showed a cytotoxic effect on MH-S cells (data not shown). This is mainly due to the production protocol of pAbs which includes many steps that are performed without sterility, facilitating the accumulation of endotoxins that are difficult to eliminate. In contrast, mAbs are obtained with the use of cell culture techniques which diminishes the probability of forming these endotoxins.

Mitochondria are cytosolic organelles crucial in cell metabolism that play an important role in cellular energetics and in regulation of several forms of cell death, being the main source of intracellular ROS generation[48]. In the case of PYO, as explained before, it exerts most of its cytotoxic effects through ROS formation[49]. Therefore, mitochondrial enzymatic activity was considered an excellent cell viability hallmark to study. First of all viability of MH-S cells was checked using AlamarBlue reagent that relies on the reduction of resazurin to resorufin by mitochondrial diaphorase enzyme[50] of viable cells. The fluorescence signal obtained corresponds to the number of viable cells. As illustrated in Figure 7. 4A, the percentage of viable cells increased in a 4.34-fold when a bivalent stoichiometric concentration of PYO mAb122 was added to MH-S cells treated with 15 µM of PYO (LD_{50}) ($p < 0.0001$). Thus, PYO mAb122 exerted a protective effect on MH-S cells. Furthermore, PYO mAb122 addition *per se* did not cause any cytotoxic effect on MH-S cells as the percentage of viable cells remained the same as the one obtained for non-treated cells ($p = 0.5404$).

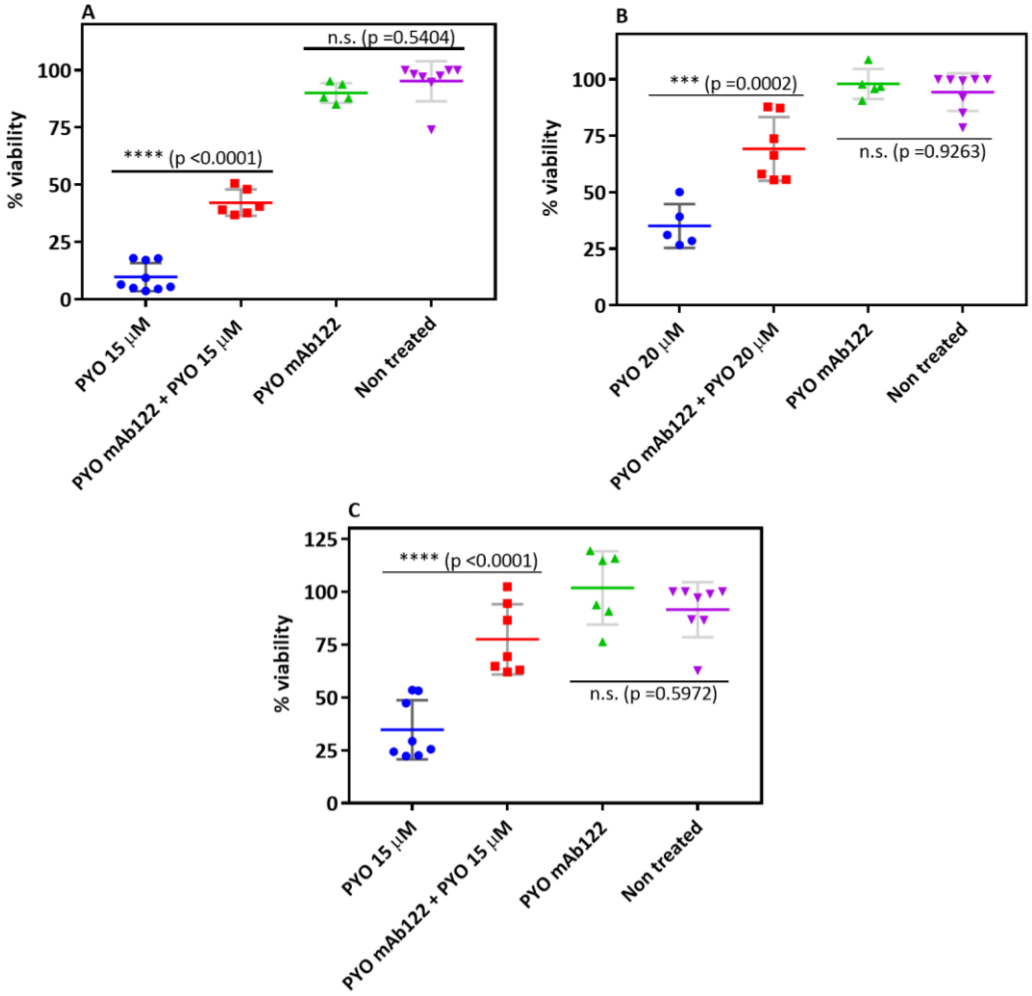

Figure 7. 4 *Protective effect of PYO mAb122 on MH-S cells. MH-S cells were treated with 15 µM of PYO (blue), PYO mAb122 plus 15 µM of PYO (red) and with PYO mAb122 (green) for 3 days at 37 ºC and 5 %CO_2. Non-treated MH-S cells (purple) were used as 100 % viability control. After this period of time, viability was measured using (A) AlamarBlue (AB), (B) LIVE/DEAD dual staining and (C) Luminescent ATP Detection assay. Viability of cells treated with PYO LD_{50} concentration (blue) were compared with viability of cells treated with a stoichiometric mAb concentration plus the same PYO concentration (red) in order to evaluate the protective effect of the mAb. The results shown correspond to the average and standard deviations of the analysis made by duplicates on the same culture plate on 3-4 different days. The obtained results were normalized according to the viability value of non-treated cells. P values were obtained performing a Tukey's multiple comparisons test.*

This mAb quenching effect was also confirmed by performing LIVE/DEAD dual staining experiments. This method uses acetoxymethyl calcein (Ca-AM) and propidium iodide (PI) biomarkers to discriminate between live and dead cells based on membrane integrity and esterase activity. An intact cytoplasmatic membrane and intracellular esterase activity are both characteristics of living cells. Hence, in this case, living cells uptake the non-fluorescence dye Ca-AM and transform it to Ca by the action of intracellular esterases. The produced Ca gives an intense green signal at 490/515 nm, which is proportional to the number of viable cells. On the

contrary, dead cells, which lack membrane integrity, are stained by the fluorescent DNA intercalator PI emitting a red fluorescence signal at 535/617 nm (see Material and Methods).

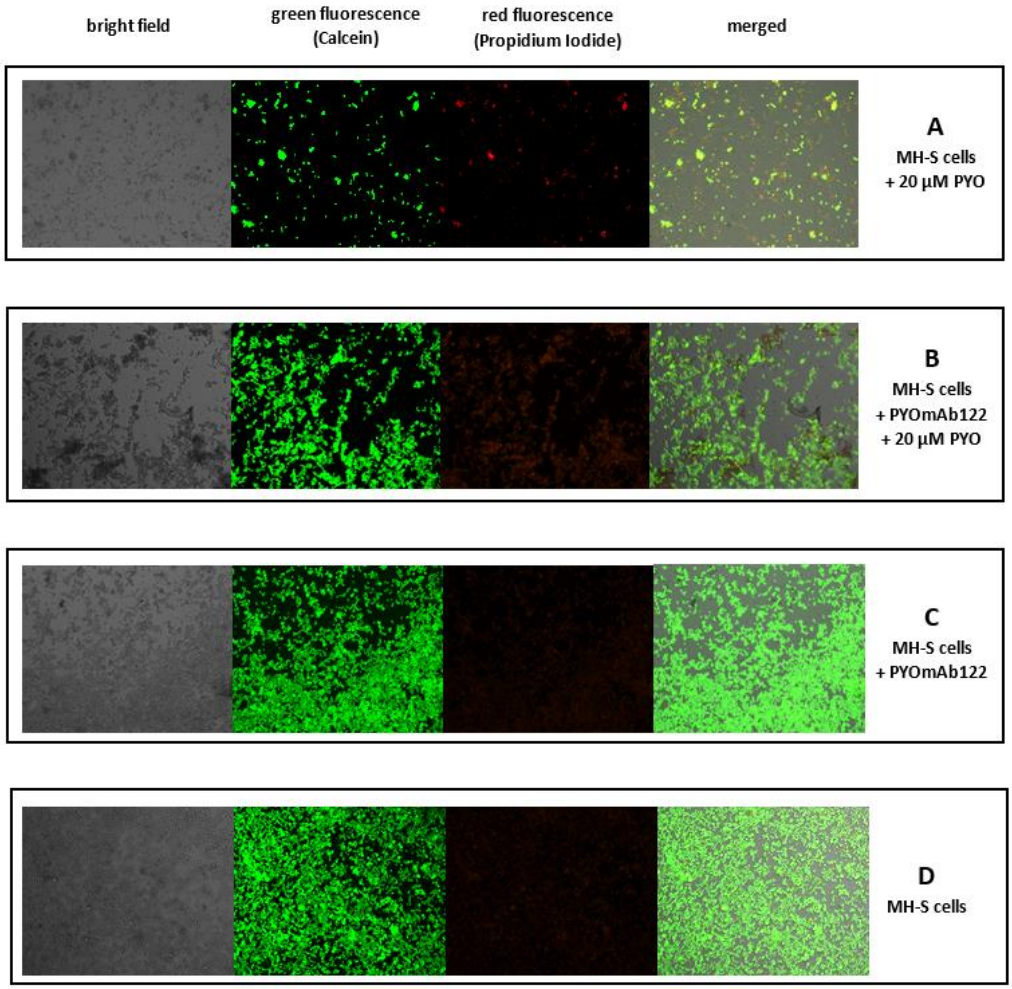

Figure 7. 5 *LIVE/DEAD dual staining of MH-S cells treated with (A) 20 µM of PYO, (B) PYO mAb122 plus 20 µM of PYO, (C) only PYO mAb122 and (D) without PYO nor PYO mAb122. MH-S cells were grown at 37 ºC and 5 % CO_2 at a seeding density of 1 x 10^5 cells mL^{-1} for 3 days. After that time, cells were exposed to a mixture of 4 µM acetoxymethyl Calcein (Ca-AM) and propidium iodide (PI) for 1 h at room temperature (RT). Ca-AM penetrates membranes of live cells and, once inside the citoplasm, it is converted to Ca by the action of esterases. Ca stains nucleic acids of live cells producing a green fluorescence signal at 490/515 nm. In contrast, PI stains nucleic acids of died cells emitting red fluorescence at 535/617 nm. Fluorescence has been monitored with a fluorescence microscope at 20-fold magnification.*

Figure 7. 4B shows how the addition of PYO mAb122 to MH-S cells treated with 20 µM of PYO (LD_{50}) increases in a 97 % the percentage of viable cells (p =0.0002). The results obtained also endorse the fact that PYO mAb122 does not exert any cytotoxic effect on MH-S cells by itself as the obtained viability value was not significantly different to that of non-treated MH-S cells (p =0.9263). Furthermore, the increase on cell viability levels and the nontoxic effect caused by the administration of PYO mAb122 could also be observed under the fluorescence microscope (see Figure 7. 5), where cell density is directly proportional to cell viability. In this sense, when cells were treated with low concentrations of PYO, the percentage of living cells increased. In

consequence, since a higher number of cells uptaked Ca-AM and transformed it to Ca, a stronger green fluorescence signal was emitted. In contrast, when cells were treated with higher PYO concentrations, the number of dead cells increased. Therefore, as the number of cells stained by PI was higher, a more intense red fluorescence signal was measured. Thus, when comparing wells with cells treated with 20 µM PYO plus or minus PYO mAb122 a clear increased in green fluorescence was observed with the presence of PYO mAb122. Furthermore, the nontoxic effect of PYO mAb122 was noticed since the intensity of the green fluorescence in both PYO mAb122 treated cells and non-treated cells was equal.

Another essential process of all viable cells is the cellular respiration. For this reason, the levels of intracellular ATP were also analysed. In fact, ATP is the main product synthesized by viable cells through aerobic respiration to obtain energy[51]. Therefore, Figure 7. 4C shows the protective effect of PYO mAb122 on the ATP produced by MH-S cells. The addition of PYO mAb122 to MH-S cells treated with 15 µM of PYO was translated on a 123 % increase of cellular viability ($p < 0.0001$). Moreover, just the addition of PYO mAb122 on MH-S cells did not cause any cytotoxic effect, reaching cellular viability levels similar to non-treated MH-S cells ($p = 0.5972$).

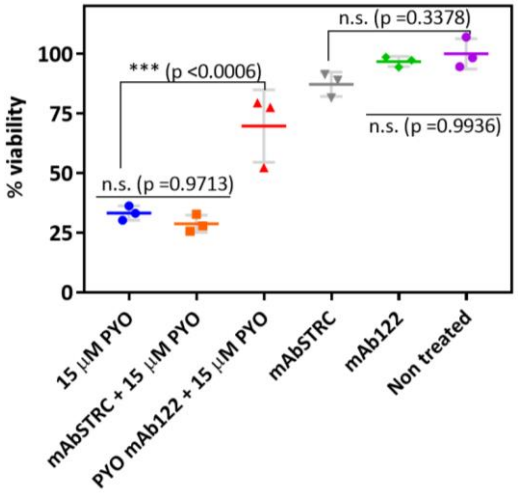

Figure 7. 6 *Specificity studies of PYO mAb122 effect on MH-S cells. MH-S cells were treated with 15 µM PYO (blue), a non specific mAb against streptomycin (STRC) antibiotic plus 15 µM PYO (orange), PYO mAb122 plus 15 µM PYO (red), just mAbSTRC (grey) and just PYO mAb122 (green) for 3 days at 37 ºC and 5 % CO_2. Non-treated MH-S cells (purple) were used as 100 % viability control. After that time, AlamarBlue (AB) viability assay was performed. The results shown correspond to the average and standard deviation of the analysis made by triplicates on the same culture plate on 1 day. Values were normalized according to the viability value of non-treated cells. P values were obtained performing a Tukey's multiple comparisons test.*

To validate that the obtained protective effect of PYO mAb122 was caused by its ability to specifically recognize and block PYO, the effect of an unrelated mAb was analysed following the same assay protocol (see Material & methods). In this case, the mAb used to perform these

experiments was a mAb specific for the antibiotic streptomycin (STRC), which is used to treat tuberculosis [52]. Figure 7. 6 shows that mAbSTRC did not exert any protection effect on MH-S cells as cell viability of MH-S cells treated with 15 µM PYO (blue) was the same of that of cells treated with an stoichiometric mAbSTRC concentration plus 15 µM PYO (orange) ($p = 0.9713$). At the same time, mAbSTRC immunoreagent *per se* did not cause any cytotoxicity to MH-S cells (grey) as no significant differences were observed when compared with non-treated cells (purple) ($p = 0.3378$). PYO mAb122 results were used as control to ensure a correct performance of the assay.

In the light of the obtained results, once the quenching effect of PYO mAb122 has been demonstrataed in *in vitro* conditions, the next step will be to analyse the bacterial response to PYO mAb122 in order to study QS systems regulation. Besides, since the complexity of this interconnected QS network makes its complete inhibition highly complicated, the use of dual therapies could also be a promising alternative to analyse as they inhibit more than one QS pathways or the same QS pathway at different levels. This can be achieved by using more than one quorum sensing inhibitor (QSI) or a single compound that binds to different QS targets. Furthermore, before carrying out *in vivo* experiments, co-culture systems will be developed to study the bacteria-host cell interaction at the QS level.

7.2.3 Immunomodulatory effect studies of PYO and PYO mAb122 on MH-S cells

It has been reported that both VFs and AIs, apart from producing cytotoxic effects on host cells, they also modulate their immune response by affecting the production of different cytokines. In fact, it is known that PQS modifies IL-6[53-54], IL-8[54] and IL-12[55] pro-inflammatory cytokines levels in *in vitro* conditions and PYO produces an inflammatory effect on airway epithelial cells[56] by increasing pro-inflammatory cytokines[23, 57] and decreasing anti-inflammatory cytokines[31]. Specifically, previous *in vitro* studies identified PYO to stimulate IL-8 expression in a concentration-dependent manner duplicating its levels at concentrations as low as 5 µM after 24 h exposure on human airway epithelial cells[57]. In the same vein, Chai et al.[58] demonstrated that U937 human monocyte model cells treated with 25 µM of PYO increased 3 times the secretion of IL-8 after 2 h. Other pro-inflammatory cytokines, such as IL-6[30] and TNF-α, are also released in the presence of PYO as confirmed by Rada et al.[23]. In fact, the addition of 8 µM of PYO concentration to tracheobronchiolar epithelial (TBEC) cells resulted in a 7-and 4-fold increase in IL-6 and TNF-α transcriptional levels, respectively, after 48 h exposure as demonstrated using a specific human whole genome microarray. Furthermore, this increase was also analysed by real time polymerase chain reaction (rtPCR) finding that IL-6 and TNF-α

messenger RNA (mRNA) levels were increased 391 and 26-fold times. Regarding anti-inflammatory cytokines, Larian et al.[31] demonstrated that PYO decreased IL-13 levels in mice. In this sense, mice were treated with increasing doses of PYO (2, 6, 19, and 50 mg kg^{-1}) by intraperitoneal injection. After 24 h from the last PYO dosage, they found that IL-13 levels in plasma decreased significantly ($p < 0.05$), which could contribute to *P. aeruginosa* survival. Therefore, the immunomodulatory capacity shown by PYO and other QS molecules increases their interest as therapeutic targets. Besides, the use of specific mAb against these molecules could be valuable to avoid modifications on cell immune respone.

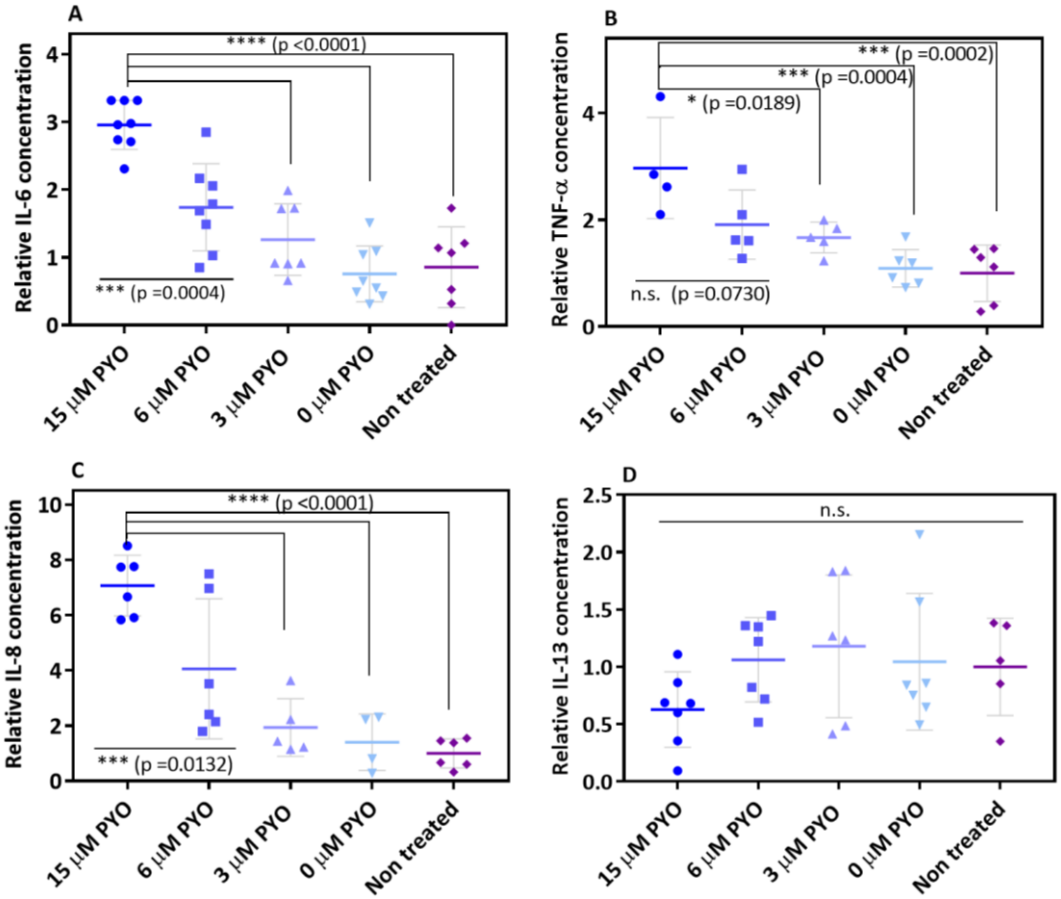

Figure 7. 7 *(A) IL-6, (B) TNF-α, (C) IL-8 and (D) IL-13 levels of MH-S cell supernatants treated with/without different PYO concentrations during 3 days at 37 ºC and 5 % CO_2 using ELISA. 15 µM corresponds to the LD_{50} of PYO on MH-S cells. The results shown correspond to the average and standard deviation of the analysis made at least by duplicates on the same plate on 3 different days. Values are expressed as fold changes relative to non-treated control (purple). P values were obtained carrying out Tukey's multiple comparisons tests.*

In this context, little is known about PYO immunomodulatory effect on macrophages. Thus, with the aim of analysing the immunomodulatory effect of PYO and the potential capacity of PYO mAb122 to avoid this effect on MH-S macrophages, cells were treated with different PYO and PYO mAb122 concentrations for 3 days at 37 ºC and 5 % CO_2. After this time, cell supernatants

were collected and IL-6, IL-8, TNF-α and IL-13 cytokines were measured by performing the corresponding ELISA (see Material & Methods). With this purpose, first, IL-6, IL-8 and TNF-α pro-inflammatory cytokines and IL-13 anti-inflammatory cytokine levels produced by non-treated MH-S cells were analysed (basal levels) since macrophages are one of the main producers of these molecules[59-61]. Then, the inflammatory response of MH-S cells to different PYO concentrations (15, 6 and 3 µM) was studied by measuring the same mentioned cytokines. As illustrated in Figure 7. 7, PYO induced a dose-dependent increment of IL-6, TNF-α and IL-8 pro-inflammatory cytokines basal levels (basal levels of 8, 112 and 1 pg mL^{-1}, respectively). Besides, an immunomodulatory effect was only observed when cells were treated at the LD_{50} concentration (15 µM). In contrast, IL-13 levels were not significantly affected at any studied PYO concentrations (basal level of 6 pg mL^{-1}). Therefore, PYO was only able to modify pro-inflammatory cytokines on MH-S cells.

With the aim of capturing PYO and trying to minimize the inflammatory response of MH-S cells due to PYO treatment at 15 µM, PYO mAb122 was added to cells at the required concentration considering a bivalent stoichiometry between mAb and PYO as explained before. Thus, MH-S cells were treated with 15 µM PYO plus or minus PYO mAb122 for 3 days at 37 ºC and 5 % CO_2. Cell supernatants were then collected and used to quantify the above mentioned cytokines. Figure 7. 8 shows that the addition of PYO mAb122 to cells treated with 15 µM PYO did not minimize the proinflammatory response of MH-S cells provoked by the effect of this VF. In contrast, TNF-α was significantly increased in the presence of PYO mAb122 ($p < 0.0001$). Besides, IL-13 anti-inflammatory cytokine level of PYO-treated cells was slightly increase in the presence of PYO mAb122 ($p = 0.0073$).

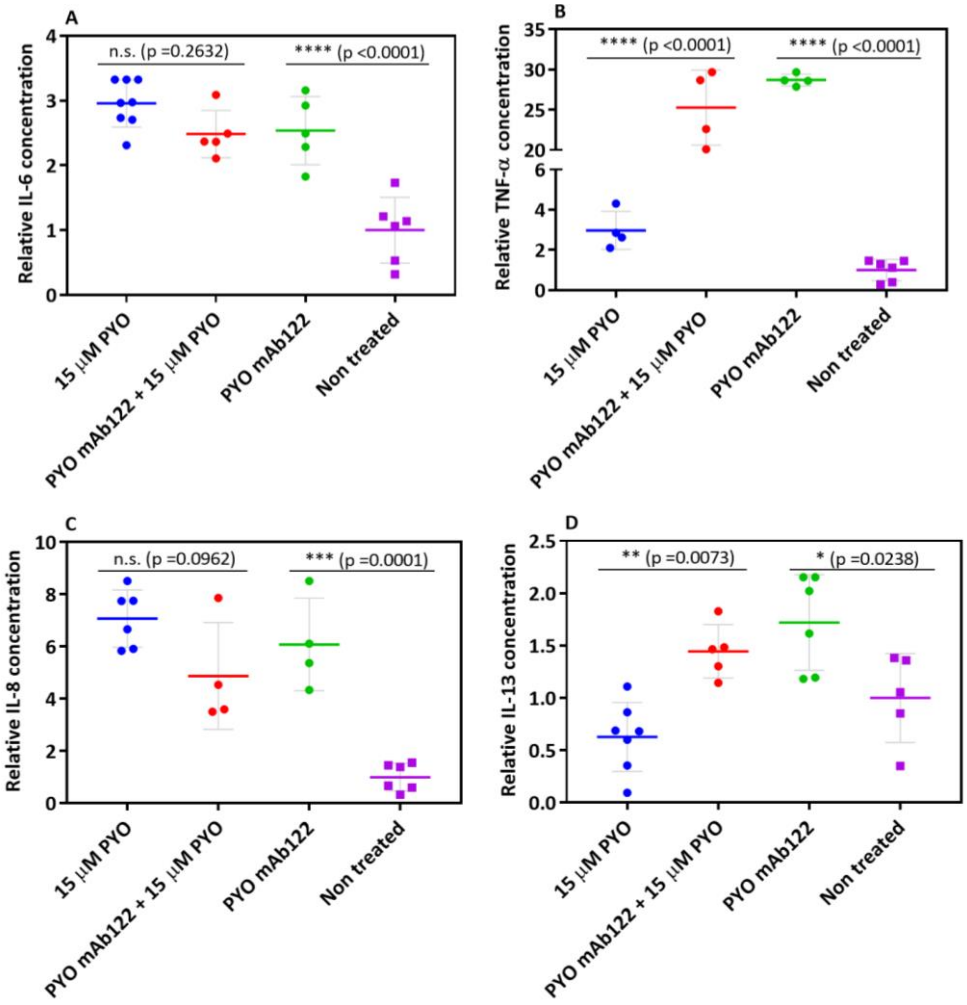

Figure 7. 8 *(A) IL-6, (B) TNF-α, (C) IL-8 and (D) IL-13 levels of MH-S cell supernatants treated with 15 µM PYO (blue), PYO mAb122 plus 15 µM PYO (red) and just PYO mAb122 (green) for 3 days at 37 ºC and 5 %CO_2 using the corresponding ELISA. Non-treated MH-S cells (purple) were used to determine cytokines' basal levels. 15 µM corresponds to the LD_{50} of PYO on MH-S cells. The results shown correspond to the average and standard deviation of the analysis made at least by duplicates on the same plate on 3 different days. Values are expressed as fold changes relative to non-treated control (purple). P values were obtained carrying out Tukey's multiple comparisons tests.*

Conversely, treatment with just PYO mAb122 caused an increase on IL-6, IL-8 and TNF-α pro-inflammatory cytokines production compared with the levels found in non-treated cells. This effect was more pronounced in the case of TNF-α, where the addition of PYO mAb122 to MH-S cells sharply increased TNF-α basal levels (28-fold; p <0.0001). Besides, the presence of PYO mAb122 itself increased 1.72-fold times IL-13 levels from non-treated MH-S cells. The increment of these cytokines can be attributed to a frequent inflammatory response of the cellular immune system called cytokine-release syndrome (CRS)[62]. CRS is considered a common acute inflammatory syndrome in which macrophages and monocytes increase the production of some inflammatory cytokines in response to different factors[63-64]. Among these factor, it has been documented that the administration of most mAbs, such as Daclizumab and Alemtuzumab,

produce CRS within the first 2 to 48 h after *in vivo* mAb infusion and can encompass symptoms like fever, headache and nausea. The clinical effects of CRS can range from mild symptoms such as fever and myalgias, which are expected to have good prognosis and disappear with time[65], to severe symtoms such as vascular leak, pulmonary edema, hepatic failure, and even death[66]. The most common techniques employ to manage CRS consist in the use of cytokine inhibitors, corticosteroids, small molecule inhibitors and genetic engineering approaches[67]. For example, in chimeric antigen receptor (CAR) T-cell therapy dexamethasone and methylprednisolone corticosteroids are usually used at high dosage (up to 10 mg/kg/dosis) for a short period of time to abrogate CRS due to their anti-inflammatory and immunosupressant effects[68]. However, as a consequence of the broad immunosuppressive effects of corticosteroids, sometimes small molecules inhibitors such as Bruton's tyrosine kinase (BTK) inhibitors are used as an alternative strategy[67, 69]. In this context, a currently FDA-approved BTK inhibitor for the relapsing chronic lymphocytic leukemia and mantle cell lymphoma called Ibrutinib directly targets leukemic B cells reducing aberrant cytokine production, such as IL-6, by inducing BTK signaling. In this context, another possible strategy to avoid CRS can be the use of nanobodies (Nb) instead of mAbs since their smaller size (150 vs 12 kDa mAb vs nanobodies) might produce lower immunogenicity[70].

7.3 Materials & methods

7.3.1 Cell line models

7.3.1.1 Raw 264.7 cell line

Raw 264.7 cells (ATCC® TIB-71™), a murine cell line from Abelson leukemia virus-induced tumor, were cultured in adherence in Dulbecco's Modified Eagle's Medium (DMEM, Sigma Aldrich) supplemented with 10 % heat inactivated fetal bovine serum (FBS, Sigma Aldrich), MEM non-essential amino acid solution 100 X (Sigma Aldrich) and Antibiotic-Antimycotic 100X (Gibco™). Cells were incubated at 37 ºC and 5 % CO_2 in humidified atmosphere.

7.3.1.2 MH-S cell line

MH-S cells (CRL-2019) (kindly given by Dra. A Lacoma (HUGTP, Badalona, Spain)), a murine alveolar macrophage cell line, were cultured in adherence in Roswell Park Memorial Institute (RPMI1640) culture medium (Gibco™) supplemented with 10 % heat inactivated FBS (Sigma Aldrich), 1M HEPES buffer solution (Gibco™) and Antibiotic-Antimycotic 100X (Gibco™). Cells were incubated at 37 ºC and 5 % CO_2 in a humidified atmosphere.

7.3.2 *In vitro* assay protocols

7.3.2.1 PYO cytotoxicity evaluation assays

With the aim of testing the cytotoxicity effect of PYO, a cell culture based *in vitro* assay was set up. Thus, as illustrated in Figure 7. 9, MH-S cells were plated in 96-well plates according to the viability assay performed at a seeding density of 1 x 10^5 cells $well^{-1}$ in a final volume of 100 µL and incubated for 2 h in complete RPMI medium for cell adhesion. Then, non-adherent cells were removed and the seeded ones were further treated with different PYO (Sigma Aldrich) concentrations and incubated for 3 days in RPMI. PYO solution was prepared in DMSO (Sigma Aldrich). The different concentrations assayed, ranging from 100 to 0 µM, were prepared with a different dilution factor depending on the viability hallmark studied. Cell viability percentage and LD_{50} values were estimated according each viability assay manufacturer instructions. Furthermore, together with PYO standard, a non-treated MH-S cells control was required since it was considered as 100 % viability.

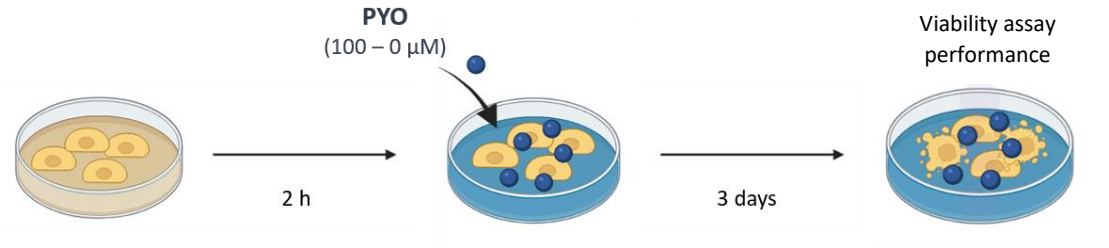

Figure 7. 9 *Schematic representation of the protocol followed to perform viability assays and determine PYO LD_{50} on MH-S cells.*

7.3.2.2 MAb protective effect evaluation

The protective effect of PYO mAb122 on MH-S cells was evaluated following broadly the same protocol explained above. Thus, first of all, cells were plated at a seeding density of 1 x 10^5 cells $well^{-1}$ in a final volume of 100 µL and incubated for 2 h for adhesion. After this time, non-adherent cells were removed. With the purpose of building PYO standard curve, seeded cells were treated with the same range of PYO concentration described in the previous section (100-0 µM). Indeed, this standard curve was necessary to ensure the correct performance of the assay, to check PYO cytotoxicity and to determine the LD_{50} of PYO on MH-S cell line for all viability hallmarks studied. At the same time, other cells were treated with PYO mAb122 to assess its protective effect on MH-S cells using the already obtained LD_{50} concentration value. In order to avoid PYO to exert its cytotoxic effects on cells, cells were first treated with a stoichometrycally equal concentration of PYO mAb122 (assuming that theoretically each specific mAb binds two PYO molecules) and, later, with a LD_{50} concentration of PYO (see Figure 7. 10).

After 3 days at 37 ºC and 5 % CO_2, viability assays were carried out to determine the percentage of protective effect exerted by the specific mAb. Thus, viability of cells treated with a LD_{50} concentration of PYO plus and minus PYO mAb122 was compared.

In all the performed assays, two controls were required: a non-treated cells control to use as 100 % viability value and a PYO mAb122-treated cells control to ensure the absence of cytotoxicity coming from the mAb.

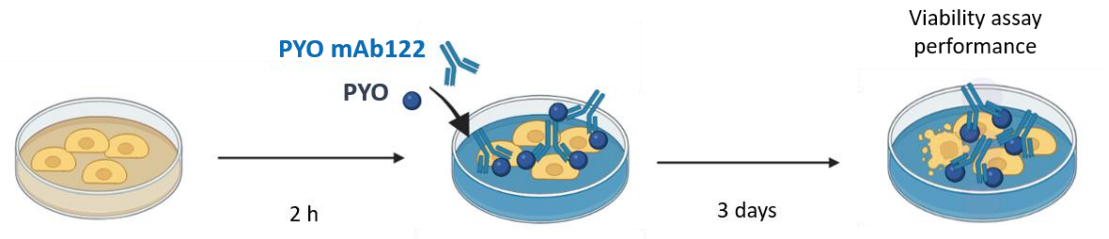

Figure 7. 10 *Schematic representation of the protocol followed to perform viability assays and determine the protective effect of the specific PYO mAb122 on MH-S cells (% protection).*

7.3.3 Viability assays

With the aim of determining the cytotoxic effect of PYO and further evaluate the protective effect of PYO mAb122 three different specific hallmarks of viable cells were studied: mitochondrial enzymatic activity, esterase activity and membrane integrity and cellular respiration. Thus, AlamarBlue (AB) Cell Viability Reagent (*Invitrogen™,* DAL1025) was used to study mitochondrial enzymatic activity, LIVE/DEAD dual staining (*Invitrogen™,* L3224) for esterase activity and membrane integrity and Luminescent ATP Detection Assay (*abcam*, ab113849) for cellular respiration.

7.3.3.1 Mitochondrial enzymatic activity

The AlamarBlue™ (AB) Cell Viability Reagent (*Invitrogen™,* DAL1025) allows the detection of viable cells trough cells metabolic function[71]. AB is a redox indicator based on the reduction of the blue and non-fluorescent resazurin to the pink and fluorescent resorufin[72]. Reduction of resazurin takes place intracellularly and involves mitochondrial reductases and other enzymes (Figure 7. 11)[71]. The quantity of the produced resorufin is proportional to the number of viable cells and it is quantified by fluorescence at an excitation/emission wavelength of 530/590 nm.

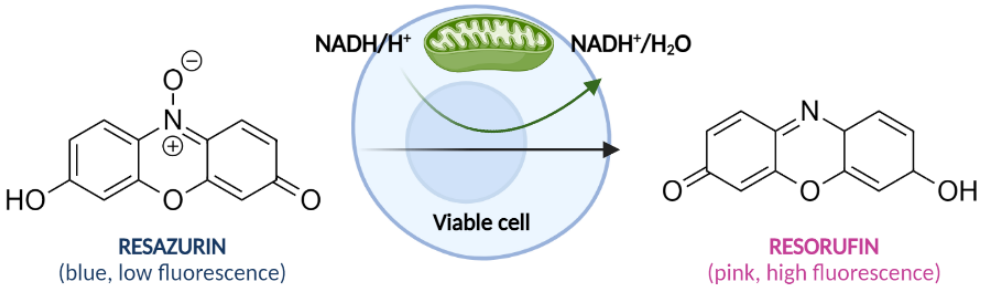

Figure 7. 11 *Resazurin molecule is used as an oxidation-reduction (redox) indicator which undergoes colorimetric change in response to cellular metabolic reduction. The reduced form resorufin is pink and highly fluorescent. The intensity of fluorescence produced is proportional to the number of living cells.*

The assay was carried out in Nunclon Delta treated 96-well flat bottom microwell plates (Thermofisher Scientific, 167008). After 3-day that the assay lasts, medium was removed, washed with 10 mM phosphate-buffered saline (PBS) (100 µL well^{-1}) and replaced with a solution of AB reagent 12 times diluted in RPMI (109 µL well^{-1}). The plate was then kept for 4 h at 37 ºC, shaking at 600 rpm. Finally, cell supernatants were diluted 10 times in PBS (100 µL well^{-1}) in a Nunc F96 microwell white polystyrene plate (Thermofisher Scientific, 236107) for fluorescence (F) lecture in a SPECTRAmax® GEMINI XS spectrofluorometer. Results were expressed as

$$\%\ \text{viability} = \frac{\text{F experimental cell sample}}{\text{F non treated cells}} \times 100$$

7.3.3.2 Cell membrane integrity and esterase activity

Esterase activity and plasma membrane integrity viability hallmarks were analysed using LIVE/DEAD™ dual staining (*Invitrogen™,* L3224) kit. This assay relies on the uptake of the non-fluorescent cell-permeant dye Ca-AM by living cells and the staining of dead cells by the fluorescent DNA intercalator PI. Ca-AM is hydrolyzed by intracellular esterases to Ca, which produces an intense green signal at 490/515 nm. In contrast, PI is able to reach the nucleus of dead cells due to the lack of cytoplasmatic membrane integrity emitting a red fluorescence signal at 535/617 nm (see Figure 7. 12).

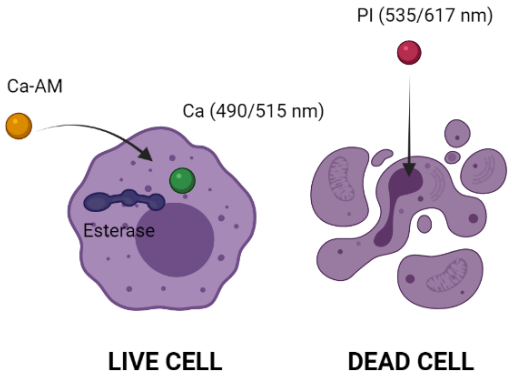

Figure 7. 12 *LIVE/DEAD™ dual staining assay discriminates live from dead cells by simultaneously staining with green fluorescence Ca (λ =490/515) to indicate esterase activity and red fluorescent PI (λ =535/617) to indicate loss of plasmatic membrane integrity (dead cells).*

The assay was performed in 96-well Nunclon Delta treated black/clear bottom microwell plates (Thermofisher Scientific, 137101). After 3 days, cells were washed with 10 mM PBS (100 µL well^{-1}) prior to the addition of a solution containing 4 µM Ca-AM and 4 µM PI diluted in 10 mM PBS (100 µL well^{-1}). Cells were then incubated 1 h at room temperature (RT) and finally F was read at 490/515 (for Ca) and 535/617 nm (for PI). Results were expressed as

$$\%\ \text{viability} = \frac{\text{F treated MH. S cells at } 490/515\ \text{nm} - \text{ F all dead cells at } 490/515\ \text{nm}}{\text{F all living cells at } 490/515\ \text{nm} - \text{ F all dead cells at } 490/515\ \text{nm}} \times 100$$

7.3.3.3 Cell respiration

The third studied hallmark of viability was focused on the production of ATP. ATP molecule is synthesized by viable cells through aerobic respiration to obtain energy. Thus, it is a good indicator of metabolically active cells[51]. The Luminescent ATP Detection Assay Kit (abcam, ab113849) was used to quantify ATP levels produced by MH-S cells (see Figure 7. 13).

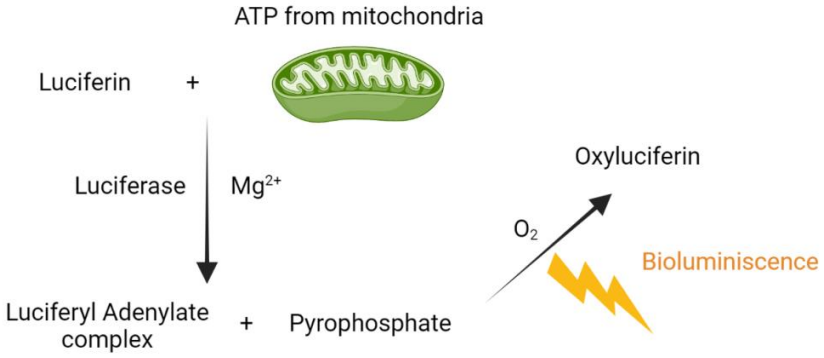

Figure 7. 13 *Luciferin reacts with intracellular ATP from live cells and, in presence of luciferase enzime and in aerobic conditions, it undergoes several transformations in which bioluminiscence is emitted.*

The assay was conducted according to manufacturer instructions in Nunclon Delta treated 96-well flat bottom microwell plates (Thermofisher Scientific, 167008). Briefly, after 3-day that the assay lasts, cell lysis was induced adding a detergent solution that contains ATPase inhibitors (50 µL well^{-1}) for 5 min at RT and shaking at 600 rpm. Then, a solution of the stable form of luciferase and luciferin substrate was added (50 µL well^{-1}) and incubated for another 5 min at RT and stirring at 600 rpm[73]. Finally, the plate was placed in the dark for 10 min and cell lysates (100 µL) were loaded in a 96 well white Microwell plate (Thermofisher Scientific, 236107) for bioluminescence lecture at 570 nm using a spectrophotometric plate reader Glomax multi detection system (Promega). Results were expressed as

$$\%\ \text{viability} = \frac{\text{bioluminiscence cell sample}}{\text{bioluminiscence non treated cells}} \times 100$$

7.3.4 PYO immunomodulatory effect study

The immunomodulatory effect of PYO on MH-S cells was assessed following the same protocol used to perform the viability assays. With this aim, cells were treated with 15, 6, 3 and 0 µM of PYO, with PYO mAb122 and with both PYO mAb122 and PYO. At the same time, non-treated cells were used as a control to obtain basal levels from all studied cytokines. After 3-day incubation at 37 ºC and 5 % CO_2, cell supernatants were collected for cytokines quantification (IL-6, IL-8, TNF-α and IL-13) using specific sandwich ELISAs. Supernatants were store at -20 ºC until analysis.

7.3.5 Cytokines immunoassays

The selected cytokines (IL-6, IL-8, TNF-α and IL-13) were determined by using commercially available ELISA kits (SinoBiological). Briefly, 96-well ELISA plates (Thermofisher Scientific) were coated with the corresponding capture mAb diluted in 10 mM PBS (100 µL well^{-1}) and incubated overnight (ON) at 4 ºC. Then, plates were washed three times with 0.05 % Tween 20 10 mM PBS (PBST) and blocked with 1 % bovine serum albumin (BSA) (*Thermofisher Scientific)* in 10 mM PBS (100 µL well^{-1}) for 30 min at RT shaking at 600 rpm. This washing step was repeated in between steps except before 4N H_2SO_4 addition. After the blocking step, cells supernatants and cytokine standards (prepared dilutions of the corresponding cytokine) were added (50 µL well^{-1}) and incubated for 2 h at RT. Cytokine standards were prepared in RPMI media to avoid the matrix effect observed which lowers the obtained absorbance compared to that of PBS (data not shown). Next, the corresponding detection mAb in 10 mM PBST was added (100 µL well^{-1}) and left for 1h shaking at 600 rpm. Finally, Ab binding was visualized by substrate solution

(tetramethylbenzidine and hydrogen peroxide solution) addition (100 µL $well^{-1}$). The reaction was stopped with 4N H_2SO_4 (50 µL $well^{-1}$) and the absorbance was measured at 450 nm.

7.4 Concluding remarks

- An *in vitro* system based on cell culture has been set up that allowed the study of the cytotoxic effects produced by different VFs and AIs and, at the same time, the evaluation of the protective effect of the corresponding specific mAbs.

- The protective effect of PYO mAb122 on MH-S cells has been evaluated by analysing three different viability hallmarks (mitochondrial enzymatic activity, cell respiration, membrane integrity and esterase activity):
    - An increase in cell viability has been observed when comparing the viability of PYO treated cells with cells treated with both PYO and PYO mAb122. These differences were statistically significant using Tukey's multiple comparisons test for all studied hallmarks ($p < 0.001$). In fact, the strongest effect was observed when evaluating mitochondrial enzymatic activity and cellular respiration compared with cell membrane integrity. Hence, PYO mAb122 exerted a protective effect (viability percentage ranges from around 50 to 75 %) on MH-S cells *in vitro* when focusing on different viability hallmarks.
    - The potential protective effect of PYO mAb122 was caused by its capacity to specifically recognize and capture PYO as demonstrated by the performed specificity studies. Indeed, the addition of a non specific mAb to MH-S cells did not avoid PYO cytotoxycity.
    - PYO mAb122 addition to MH-S cells has not exerted any cytotoxic effect on them as the percentage of viable cells matched with the viability level of non-treated cells (same behaviour for all studied hallmarks).

- The basal pro-inflammatory cytokines levels of MH-S cells increased with PYO concentration in a dose-dependent manner producing only a significant effect at the LD_{50} concentration. At the same time, the addition of PYO mAb122 to PYO-treated cells did not avoid the inflammatory response of MH-S cells provoke by PYO. Besides, pro-inflammatory cytokine levels from cells treated with both PYO mAb122 and PYO were similar to those from cell treated just with PYO mAb122. Therefore, PYO mAb122 by

itself induced this increase. This increment could be attributed to a frequent inflammatory response of the cellular immune system called CRS[62].

- In the case of IL-13 anti-inflammatory cytokine, the presence of PYO (at the studied concentrations) on MH-S cells did not significantly modify IL-13 levels. Furthermore, the addition of PYO mAb122 to cells treated with PYO induced IL-13 production on MH-S cells reaching the same levels of cells treated just with PYO mAb122.

7.5 References

1. Pang, Z.; Raudonis, R.; Glick, B. R.; Lin, T. J.; Cheng, Z., Antibiotic resistance in Pseudomonas aeruginosa: mechanisms and alternative therapeutic strategies. *Biotechnol Adv* **2019,** *37* (1), 177-192.
2. Chatterjee, M.; Anju, C. P.; Biswas, L.; Anil Kumar, V.; Gopi Mohan, C.; Biswas, R., Antibiotic resistance in Pseudomonas aeruginosa and alternative therapeutic options. *Int J Med Microbiol* **2016,** *306* (1), 48-58.
3. Behzadi, P.; Barath, Z.; Gajdacs, M., It's Not Easy Being Green: A Narrative Review on the Microbiology, Virulence and Therapeutic Prospects of Multidrug-Resistant Pseudomonas aeruginosa. *Antibiotics (Basel)* **2021,** *10* (1).
4. O'Donnell, J. N.; Bidell, M. R.; Lodise, T. P., Approach to the Treatment of Patients with Serious Multidrug-Resistant Pseudomonas aeruginosa Infections. *Pharmacotherapy* **2020,** *40* (9), 952-969.
5. Ecker, D. M.; Jones, S. D.; Levine, H. L., The therapeutic monoclonal antibody market. *MAbs* **2015,** *7* (1), 9-14.
6. Leavy, O., Therapeutic antibodies: past, present and future. *Nat Rev Immunol* **2010,** *10* (5), 297.
7. Lu, R. M.; Hwang, Y. C.; Liu, I. J.; Lee, C. C.; Tsai, H. Z.; Li, H. J.; Wu, H. C., Development of therapeutic antibodies for the treatment of diseases. *J Biomed Sci* **2020,** *27* (1), 1.
8. Mullard, A., FDA approves 100th monoclonal antibody product. *Nat Rev Drug Discov* **2021,** *20* (7), 491-495.
9. Grilo, A. L.; Mantalaris, A., The Increasingly Human and Profitable Monoclonal Antibody Market. *Trends Biotechnol* **2019,** *37* (1), 9-16.
10. Susilowati, H.; Artanto, S.; Yulianto, H. D. K.; Sosroseno, W.; Hutomo, S., The protective effects of antigen-specific IgY on pyocyanin-treated human lymphoma Raji cells. *F1000Res* **2019,** *8*, 1008.
11. Motley, M. P.; Banerjee, K.; Fries, B. C., Monoclonal antibody-based therapies for bacterial infections. *Curr Opin Infect Dis* **2019,** *32* (3), 210-216.
12. Suzuki, M.; Kato, C.; Kato, A., Therapeutic antibodies: their mechanisms of action and the pathological findings they induce in toxicity studies. *J Toxicol Pathol* **2015,** *28* (3), 133-9.
13. Ducancel, F.; Muller, B. H., Molecular engineering of antibodies for therapeutic and diagnostic purposes. *MAbs* **2012,** *4* (4), 445-57.
14. Dougan, M.; Nirula, A.; Azizad, M.; Mocherla, B.; Gottlieb, R. L.; Chen, P.; Hebert, C.; Perry, R.; Boscia, J.; Heller, B.; Morris, J.; Crystal, C.; Igbinadolor, A.; Huhn, G.; Cardona, J.; Shawa,

I.; Kumar, P.; Adams, A. C.; Van Naarden, J.; Custer, K. L.; Durante, M.; Oakley, G.; Schade, A. E.; Holzer, T. R.; Ebert, P. J.; Higgs, R. E.; Kallewaard, N. L.; Sabo, J.; Patel, D. R.; Dabora, M. C.; Klekotka, P.; Shen, L.; Skovronsky, D. M.; Investigators, B.-. Bamlanivimab plus Etesevimab in Mild or Moderate Covid-19. *N Engl J Med* **2021,** *385* (15), 1382-1392.

15. Wang-Lin, S. X.; Balthasar, J. P., Pharmacokinetic and Pharmacodynamic Considerations for the Use of Monoclonal Antibodies in the Treatment of Bacterial Infections. *Antibodies (Basel)* **2018,** *7* (1).
16. Doyle, C. R.; Moon, J. Y.; Daily, J. P.; Wang, T.; Pirofski, L. A., A Capsular Polysaccharide-Specific Antibody Alters Streptococcus pneumoniae Gene Expression during Nasopharyngeal Colonization of Mice. *Infect Immun* **2018,** *86* (7).
17. Visan, L.; Rouleau, N.; Proust, E.; Peyrot, L.; Donadieu, A.; Ochs, M., Antibodies to PcpA and PhtD protect mice against Streptococcus pneumoniae by a macrophage- and complement-dependent mechanism. *Hum Vaccin Immunother* **2018,** *14* (2), 489-494.
18. Rutherford, S. T.; Bassler, B. L., Bacterial quorum sensing: its role in virulence and possibilities for its control. *Cold Spring Harb Perspect Med* **2012,** *2* (11).
19. Reuter, K.; Steinbach, A.; Helms, V., Interfering with Bacterial Quorum Sensing. *Perspect Medicin Chem* **2016,** *8*, 1-15.
20. Kaufmann, G. F.; Sartorio, R.; Lee, S. H.; Mee, J. M.; Altobell, L. J., 3rd; Kujawa, D. P.; Jeffries, E.; Clapham, B.; Meijler, M. M.; Janda, K. D., Antibody interference with N-acyl homoserine lactone-mediated bacterial quorum sensing. *J Am Chem Soc* **2006,** *128* (9), 2802-3.
21. Castaneda-Tamez, P.; Ramirez-Peris, J.; Perez-Velazquez, J.; Kuttler, C.; Jalalimanesh, A.; Saucedo-Mora, M. A.; Jimenez-Cortes, J. G.; Maeda, T.; Gonzalez, Y.; Tomas, M.; Wood, T. K.; Garcia-Contreras, R., Pyocyanin Restricts Social Cheating in Pseudomonas aeruginosa. *Front Microbiol* **2018,** *9*, 1348.
22. Mavrodi, D. V.; Bonsall, R. F.; Delaney, S. M.; Soule, M. J.; Phillips, G.; Thomashow, L. S., Functional analysis of genes for biosynthesis of pyocyanin and phenazine-1-carboxamide from Pseudomonas aeruginosa PAO1. *J Bacteriol* **2001,** *183* (21), 6454-65.
23. Rada, B.; Gardina, P.; Myers, T. G.; Leto, T. L., Reactive oxygen species mediate inflammatory cytokine release and EGFR-dependent mucin secretion in airway epithelial cells exposed to Pseudomonas pyocyanin. *Mucosal Immunol* **2011,** *4* (2), 158-71.
24. Prince, L. R.; Bianchi, S. M.; Vaughan, K. M.; Bewley, M. A.; Marriott, H. M.; Walmsley, S. R.; Taylor, G. W.; Buttle, D. J.; Sabroe, I.; Dockrell, D. H.; Whyte, M. K., Subversion of a lysosomal pathway regulating neutrophil apoptosis by a major bacterial toxin, pyocyanin. *J Immunol* **2008,** *180* (5), 3502-11.
25. Usher, L. R.; Lawson, R. A.; Geary, I.; Taylor, C. J.; Bingle, C. D.; Taylor, G. W.; Whyte, M. K., Induction of neutrophil apoptosis by the Pseudomonas aeruginosa exotoxin pyocyanin: a potential mechanism of persistent infection. *J Immunol* **2002,** *168* (4), 1861-8.
26. Vilaplana, L.; Marco, M. P., Phenazines as potential biomarkers of Pseudomonas aeruginosa infections: synthesis regulation, pathogenesis and analytical methods for their detection. *Anal Bioanal Chem* **2020,** *412* (24), 5897-5912.
27. Hall, S.; McDermott, C.; Anoopkumar-Dukie, S.; McFarland, A. J.; Forbes, A.; Perkins, A. V.; Davey, A. K.; Chess-Williams, R.; Kiefel, M. J.; Arora, D.; Grant, G. D., Cellular Effects of Pyocyanin, a Secreted Virulence Factor of Pseudomonas aeruginosa. *Toxins (Basel)* **2016,** *8* (8).

28. Moayedi, A.; Nowroozi, J.; Akhavan Sepahy, A., Cytotoxic effect of pyocyanin on human pancreatic cancer cell line (Panc-1). *Iran J Basic Med Sci* **2018,** *21* (8), 794-799.
29. Rada, B.; Leto, T. L., Pyocyanin effects on respiratory epithelium: relevance in Pseudomonas aeruginosa airway infections. *Trends Microbiol* **2013,** *21* (2), 73-81.
30. Moura-Alves, P.; Puyskens, A.; Stinn, A.; Klemm, M.; Guhlich-Bornhof, U.; Dorhoi, A.; Furkert, J.; Kreuchwig, A.; Protze, J.; Lozza, L.; Pei, G.; Saikali, P.; Perdomo, C.; Mollenkopf, H. J.; Hurwitz, R.; Kirschhoefer, F.; Brenner-Weiss, G.; Weiner, J., 3rd; Oschkinat, H.; Kolbe, M.; Krause, G.; Kaufmann, S. H. E., Host monitoring of quorum sensing during Pseudomonas aeruginosa infection. *Science* **2019,** *366* (6472).
31. Larian, N.; Ensor, M.; Thatcher, S. E.; English, V.; Morris, A. J.; Stromberg, A.; Cassis, L. A., Pseudomonas aeruginosa-derived pyocyanin reduces adipocyte differentiation, body weight, and fat mass as mechanisms contributing to septic cachexia. *Food Chem Toxicol* **2019,** *130*, 219-230.
32. Welsh, M. A.; Eibergen, N. R.; Moore, J. D.; Blackwell, H. E., Small molecule disruption of quorum sensing cross-regulation in pseudomonas aeruginosa causes major and unexpected alterations to virulence phenotypes. *J Am Chem Soc* **2015,** *137* (4), 1510-9.
33. Miller, L. C.; O'Loughlin, C. T.; Zhang, Z.; Siryaporn, A.; Silpe, J. E.; Bassler, B. L.; Semmelhack, M. F., Development of potent inhibitors of pyocyanin production in Pseudomonas aeruginosa. *J Med Chem* **2015,** *58* (3), 1298-306.
34. Liu, H.; Gong, Q.; Luo, C.; Liang, Y.; Kong, X.; Wu, C.; Feng, P.; Wang, Q.; Zhang, H.; Wireko, M. A., Synthesis and Biological Evaluation of Novel L-Homoserine Lactone Analogs as Quorum Sensing Inhibitors of Pseudomonas aeruginosa. *Chem Pharm Bull (Tokyo)* **2019,** *67* (10), 1088-1098.
35. Debler, E. W.; Kaufmann, G. F.; Kirchdoerfer, R. N.; Mee, J. M.; Janda, K. D.; Wilson, I. A., Crystal structures of a quorum-quenching antibody. *J Mol Biol* **2007,** *368* (5), 1392-402.
36. Praneenararat, T.; Palmer, A. G.; Blackwell, H. E., Chemical methods to interrogate bacterial quorum sensing pathways. *Org Biomol Chem* **2012,** *10* (41), 8189-99.
37. De Lamo Marin, S.; Xu, Y.; Meijler, M. M.; Janda, K. D., Antibody catalyzed hydrolysis of a quorum sensing signal found in Gram-negative bacteria. *Bioorg Med Chem Lett* **2007,** *17* (6), 1549-52.
38. Francois, B.; Luyt, C. E.; Stover, C. K.; Brubaker, J. O.; Chastre, J.; Jafri, H. S., New Strategies Targeting Virulence Factors of Staphylococcus aureus and Pseudomonas aeruginosa. *Semin Respir Crit Care Med* **2017,** *38* (3), 346-358.
39. Warrener, P.; Varkey, R.; Bonnell, J. C.; DiGiandomenico, A.; Camara, M.; Cook, K.; Peng, L.; Zha, J.; Chowdury, P.; Sellman, B.; Stover, C. K., A novel anti-PcrV antibody providing enhanced protection against Pseudomonas aeruginosa in multiple animal infection models. *Antimicrob Agents Chemother* **2014,** *58* (8), 4384-91.
40. Rodriguez-Urretavizcaya, B. P., N.; Pastells, C.; Martin-Gomez, M.T.; Vilaplana, LL.; Marco, M.P, Diagnosis and Stratification of Pseudomonas aeruginosa Infected Patients by Immunochemical Quantitative Determination of Pyocyanin From Clinical Bacterial Isolates. *Front. Cell. Infect. Microbiol* **2021,** *11*, 1-12.
41. Maurice, N. M.; Bedi, B.; Yuan, Z.; Goldberg, J. B.; Koval, M.; Hart, C. M.; Sadikot, R. T., Pseudomonas aeruginosa Induced Host Epithelial Cell Mitochondrial Dysfunction. *Sci Rep* **2019,** *9* (1), 11929.

42. Reimer, A.; Edvaller, B.; Johansson, B., Concentrations of the Pseudomonas aeruginosa toxin pyocyanin in human ear secretions. *Acta Otolaryngol Suppl* **2000,** *543*, 86-8.
43. Wilson, R.; Sykes, D. A.; Watson, D.; Rutman, A.; Taylor, G. W.; Cole, P. J., Measurement of Pseudomonas aeruginosa phenazine pigments in sputum and assessment of their contribution to sputum sol toxicity for respiratory epithelium. *Infect Immun* **1988,** *56* (9), 2515-7.
44. Cruickshank, C. N.; Lowbury, E. J., The effect of pyocyanin on human skin cells and leucocytes. *Br J Exp Pathol* **1953,** *34* (6), 583-7.
45. Muller, M.; Li, Z.; Maitz, P. K., Pseudomonas pyocyanin inhibits wound repair by inducing premature cellular senescence: role for p38 mitogen-activated protein kinase. *Burns* **2009,** *35* (4), 500-8.
46. O'Malley, Y. Q. A., M. Y.; Mccormick, M. L.; Reszka, K . J.; Denning, G. M.; Britigan, B. E., Subcellular localization of Pseudomonas pyocyanin cytotoxicity in human lung epithelial cells. *Am J Physiol Lung Cell Mol Physiol* **2003,** *284*, L420–L430.
47. Mohammed, H. A. Y., H. S.; Mohammad, F. I., The Cytotoxicity Effect of Pyocyanin on Human Hepatocellular Carcinoma Cell Line (HepG2). *Iraqi Journal of Science* **2014,** *55* (2B), 668-674.
48. Vakifahmetoglu-Norberg, H.; Ouchida, A. T.; Norberg, E., The role of mitochondria in metabolism and cell death. *Biochem Biophys Res Commun* **2017,** *482* (3), 426-431.
49. Li, T.; Huang, X.; Yuan, Z.; Wang, L.; Chen, M.; Su, F.; Ling, X.; Piao, Z., Pyocyanin induces NK92 cell apoptosis via mitochondrial damage and elevated intracellular Ca(2). *Innate Immun* **2019,** *25* (1), 3-12.
50. Borra, R. C.; Lotufo, M. A.; Gagioti, S. M.; Barros Fde, M.; Andrade, P. M., A simple method to measure cell viability in proliferation and cytotoxicity assays. *Braz Oral Res* **2009,** *23* (3), 255-62.
51. Bonora, M.; Patergnani, S.; Rimessi, A.; De Marchi, E.; Suski, J. M.; Bononi, A.; Giorgi, C.; Marchi, S.; Missiroli, S.; Poletti, F.; Wieckowski, M. R.; Pinton, P., ATP synthesis and storage. *Purinergic Signal* **2012,** *8* (3), 343-57.
52. Rocha, D.; Magalhaes, C.; Ca, B.; Ramos, A.; Carvalho, T.; Comas, I.; Guimaraes, J. T.; Bastos, H. N.; Saraiva, M.; Osorio, N. S., Heterogeneous Streptomycin Resistance Level Among Mycobacterium tuberculosis Strains From the Same Transmission Cluster. *Front Microbiol* **2021,** *12*, 659545.
53. Kim, K.; Kim, Y. U.; Koh, B. H.; Hwang, S. S.; Kim, S. H.; Lepine, F.; Cho, Y. H.; Lee, G. R., HHQ and PQS, two Pseudomonas aeruginosa quorum-sensing molecules, down-regulate the innate immune responses through the nuclear factor-kappaB pathway. *Immunology* **2010,** *129* (4), 578-88.
54. Wardwell, P. R. W., D. R.; Garner, D. L.; Bader, R. A., Pseudomonas Quinolone Signal Modulates Cystic Fibrosis Epithelial Cell Response through the Toll- Like Receptor 4. *SOJ Immunology* **2015,** *3* (1).
55. Skindersoe, M. E.; Zeuthen, L. H.; Brix, S.; Fink, L. N.; Lazenby, J.; Whittall, C.; Williams, P.; Diggle, S. P.; Froekiaer, H.; Cooley, M.; Givskov, M., Pseudomonas aeruginosaquorum-sensing signal molecules interfere with dendritic cell-induced T-cell proliferation. *FEMS Immunology & Medical Microbiology* **2009,** *55* (3), 335-345.
56. Lau, G. W.; Hassett, D. J.; Ran, H.; Kong, F., The role of pyocyanin in Pseudomonas aeruginosa infection. *Trends Mol Med* **2004,** *10* (12), 599-606.

57. Denning, G. M.; Wollenweber, L. A.; Railsback, M. A.; Cox, C. D.; Stoll, L. L.; Britigan, B. E., Pseudomonas pyocyanin increases interleukin-8 expression by human airway epithelial cells. *Infect Immun* **1998,** *66* (12), 5777-84.
58. Chai, W.; Zhang, J.; Duan, Y.; Pan, D.; Liu, W.; Li, Y.; Yan, X.; Chen, B., Pseudomonas pyocyanin stimulates IL-8 expression through MAPK and NF-kappaB pathways in differentiated U937 cells. *BMC Microbiol* **2014,** *14*, 26.
59. Parameswaran, N.; Patial, S., Tumor necrosis factor-alpha signaling in macrophages. *Crit Rev Eukaryot Gene Expr* **2010,** *20* (2), 87-103.
60. Hancock, A.; Armstrong, L.; Gama, R.; Millar, A., Production of interleukin 13 by alveolar macrophages from normal and fibrotic lung. *Am J Respir Cell Mol Biol* **1998,** *18* (1), 60-5.
61. Arango Duque, G.; Descoteaux, A., Macrophage cytokines: involvement in immunity and infectious diseases. *Front Immunol* **2014,** *5*, 491.
62. Garcia Roche, A.; Diaz Lagares, C.; Elez, E.; Ferrer Roca, R., Cytokine release syndrome. Reviewing a new entity in the intensive care unit. *Med Intensiva* **2019,** *43* (8), 480-488.
63. Lee, D. W.; Gardner, R.; Porter, D. L.; Louis, C. U.; Ahmed, N.; Jensen, M.; Grupp, S. A.; Mackall, C. L., Current concepts in the diagnosis and management of cytokine release syndrome. *Blood* **2014,** *124* (2), 188-95.
64. Morris, E. C.; Neelapu, S. S.; Giavridis, T.; Sadelain, M., Cytokine release syndrome and associated neurotoxicity in cancer immunotherapy. *Nat Rev Immunol* **2021**.
65. Bugelski, P. J.; Achuthanandam, R.; Capocasale, R. J.; Treacy, G.; Bouman-Thio, E., Monoclonal antibody-induced cytokine-release syndrome. *Expert Rev Clin Immunol* **2009,** *5* (5), 499-521.
66. Riegler, L. L.; Jones, G. P.; Lee, D. W., Current approaches in the grading and management of cytokine release syndrome after chimeric antigen receptor T-cell therapy. *Ther Clin Risk Manag* **2019,** *15*, 323-335.
67. Khadka, R. H. S., R.; Kenderian, S. S.; Johnson, A. J., Management of cytokine release syndrome: an update on emerging antigen-specific T cell engaging immunotherapies. *Immunotherapy* **2019,** *11* (10), 851-857.
68. Liu, S.; Deng, B.; Yin, Z.; Pan, J.; Lin, Y.; Ling, Z.; Wu, T.; Chen, D.; Chang, A. H.; Gao, Z.; Song, Y.; Zhao, Y.; Tong, C., Corticosteroids do not influence the efficacy and kinetics of CAR-T cells for B-cell acute lymphoblastic leukemia. *Blood Cancer J* **2020,** *10* (2), 15.
69. Ruella, M.; Kenderian, S. S.; Shestova, O.; Klichinsky, M.; Melenhorst, J. J.; Wasik, M. A.; Lacey, S. F.; June, C. H.; Gill, S., Kinase inhibitor ibrutinib to prevent cytokine-release syndrome after anti-CD19 chimeric antigen receptor T cells for B-cell neoplasms. *Leukemia* **2017,** *31* (1), 246-248.
70. Salvador, J. P.; Vilaplana, L.; Marco, M. P., Nanobody: outstanding features for diagnostic and therapeutic applications. *Anal Bioanal Chem* **2019,** *411* (9), 1703-1713.
71. Rampersad, S. N., Multiple applications of Alamar Blue as an indicator of metabolic function and cellular health in cell viability bioassays. *Sensors (Basel)* **2012,** *12* (9), 12347-60.
72. Byth, H. A.; McHunu, B. I.; Dubery, I. A.; Bornman, L., Assessment of a simple, non-toxic Alamar blue cell survival assay to monitor tomato cell viability. *Phytochem Anal* **2001,** *12* (5), 340-6.
73. Riss, T. L. M., R. A.; Niles, A. L.; Duellman, S.; Benink, H. A.; Worzella, T. J.; Minor, L., Cell Viability Assays. In *Assay Guidance Manual*, Bethesda (MD), 2013.

Chapter 8

Use of a mAb against PQS for treating *Pseudomonas aeruginosa* infections *in vitro*

The previously set up cell cultured based system described in Chapter 7 has allowed to study the cytotoxic effect of pyocyanin (PYO) virulence factor (VF) and to further evaluate the protective effect of the corresponding specific monoclonal antibody (mAb) in *in vitro* conditions. Apart from quorum sensing (QS) effector molecules, this system can also be used to evaluate QS signalling molecules as is the case of autoinducers (AIs). Therefore, in this chapter, the same cell culture based *in vitro* system has been used to study Pseudomonas quinolone signal (PQS) since this AI is specific of *P. aeruginosa* bacterium and it has been reported that it also acts as virulence determinant by itself. Furthermore, the quenching effect of a specific mAb against PQS (mAb423) has been evaluated and compared with the protection obtained when blocking PYO VF. At the same time, since it has been documented that PQS modulates the immune response of different cell lines, the immunomodulatory effect of PQS has been analysed using the same *in vitro* system by measuring IL-6 pro-inflammatory and IL-13 anti-inflammatory cytokines. Besides, the potential use of PQS mAb423 to avoid the dysregulation action of PQS on MH-S cells has been evaluated.

In preparation

***Rodriguez-Urretavizcaya, B**.; Vilaplana Ll. and Marco, M.P. (2021). Use of a mAb against PQS for treating Pseudomonas aeruginosa infections in vitro*

8.1 Introduction

Pqs system involves a collection of alkylquinolones (AQs) such as Pseudomonas quinolone signal (PQS; the main signalling molecule of this system), 2-heptyl-4-quinolone (HHQ; PQS precursor), dihydroxyquinoline (DHQ)[1] and the corresponding N-oxides (AQNO), which appear to act mainly as virulence factor (VF) interacting with other pathogens such as *S. aureus*[2]. Furthermore, these AQs are obtained by the action of different enzymes named PqsA, PqsD, PqsR and PqsBC[3] (see Chapter 2). Therefore, the inhibition of these enzymes has an important impact on both PQS and HHQ levels[4]. In this sense, Ji et al.[5] identified two potent inhibitors against PqsA which decreased PQS production in PA14 bacterial cultures by 92 % when used at 1.5 mM. Besides, Sahner et al. [6] discovered structural analogues of acetyl coenzyme A (AcoA) molecule (PqsD substrate) that showed high affinity for PqsD enzyme (IC_{50} =0.5 µM). These inhibitors covalently bound to the active site of PqsD competing with AcoA and decreasing PQS production. Moreover, Fang et al.[7] described some recent PqsR inhibitor such as QslA (QS LasR antiactivator that disrupts LasR dimerization) which reduces PQS levels as well as HHQ and phenazines in bacterial cutures. In fact, the interaction of QslA with PqsR affects the binding of PqsR with *pqsA* and *phz1* promoters, which modulates PQS and HHQ production and phenazine-1-carboxylic acid (PCA) biosynthesis, respectively. However, most of these quorum quenchers (QQs) presented some deficiencies when tested in *in vivo* conditions due to the presence of efflux pumps and their moderate selectivity for the corresponding target, which resulted in the inhibition of other enzymes crucial for *P. aeruginosa* growth[8]. Therefore, the use of monoclonal antibodies (mAbs) against PQS can be a promising alternative to face these selectivity problems since they are very specific for its corresponding target avoiding the interaction with other molecules/enzymes.

In general terms, the most important functions of *P. aeruginosa* autoinducers (AIs) are VF production, biofilm formation and cell survival[9]. However, apart from these functions, it has been reported that N-(3-oxododecanoyl)-L-homoserine lactone (3oxoC_{12}-HSL)[10-15], PQS[10, 16-18], HHQ[10, 16, 19] and integrating QS system (IQS)[20] AIs can also act as virulence determinants affecting directly on the host. In contrast, it has been demonstrated that C_4-HSL did not exert any cytotoxic effects on cells[10, 21]. In this regard, aside from its role as AI and VF, PQS also triggers iron-starvation, regulating its acquisition[22], and stimulates outer membrane vesicles (OMVs) production[16]. Furthermore, PQS can also supress the host innate immune response by modulating IL-6[17, 23], TNF-α[17, 24], IL-8[23, 25] and IL-12[26] pro-inflammatory cytokines in a dose-dependent manner and according to the cell line.

In this context, based on the promising results obtained in Chapter 7 regarding the use of pyocyanin (PYO) mAb122 as therapeutic mAb to protect murine alveolar macrophages (MH-S) against PYO in *in vitro* conditions, the same *in vitro* system has been used to study the cytotoxic effect of PQS and to evaluate the quenching effect of a specific mAb against PQS (PQS mAb423). In this vein, the analysis of the inhibition of a signalling molecule specific for *P. aeruginosa* is of great interest since it is located on the top of the QS pathway. Subsequently, the immunomodulatory effect of PQS on MH-S cells and the evaluation of PQS mAb423 addition regarding the disruption of the immune response due to PQS treatment was assessed using the same cell culture based *in vitro* system. With this purpose, IL-6 pro-inflammatory cytokine and IL-13 anti-inflammatory cytokine levels were measured by enzyme-linked immunosorbent assay (ELISA).

8.2 Results & discussion

8.2.1 Cytotoxicity evaluation of PQS on murine macrophages

MH-S and Raw 264.7 murine macrophages were used to evaluate PQS cytotoxicity in *in vitro* conditions. First, the assay duration required for PQS to exert its cytotoxic effect on both cell lines was determined. With this purpose, cells were treated with different PQS concentrations during 24, 48 and 72 h and its cytotoxicity was determined using the AlamarBlue reagent. Based on PQS levels found in clinical isolates from patients infected with *P. aeruginosa* (16µM[27]) and in biological samples such as sputa (2 µM[28]), PQS concentrations rangind from 25 to 0 µM (25, 15, 6, 3 and 0 µM) were selected to determine PQS cytotoxicity kinetics.

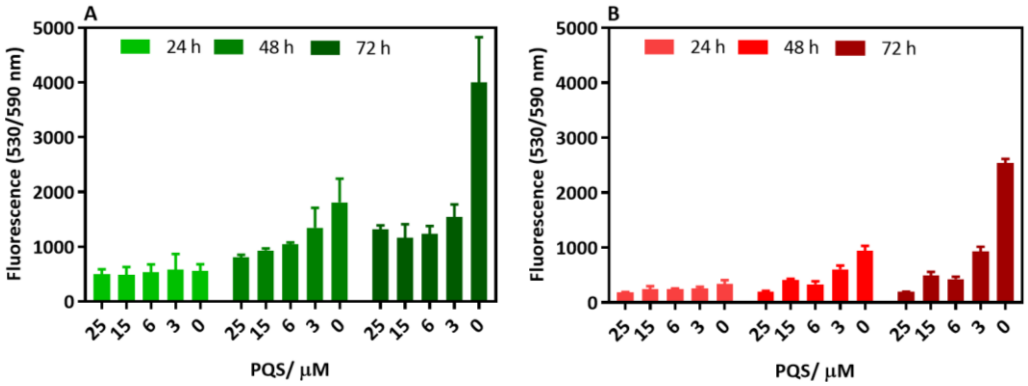

Figure 8. 1 *Kinetic studies for the analysis of PQS ytotoxicity on (A) MH-S and (B) and Raw 264.7 cell lines. Cells were treated with different PQS concentrations (25, 15, 6, 3 and 0 µM) for 24, 48 and 72 hours at 37 ºC and 5 % CO_2. PQS cytotoxicity was evaluated using AlamarBlue reagent. Results are expressed in fluorescence values at 530/590 nm. Each calibration point was measured in triplicates on the same culture plate and the results show the average and standard deviation of the assay carried out on 1 day.*

According to the obtained results, 72 h was selected as the time required to differentiate clearly viability levels between non-treated cells and PQS treated ones (see Figure 8. 1). Besides, regarding the effect of PQS in both tested cell lines at 72 h, as shown in Figure 8. 2, Raw 264.7 cells were not as susceptible as MH-S cells. In fact, at the studied PQS concentration range, no define curve was obtained when working with Raw 264.7 cells. In contrast, on MH-S cells, PQS showed a LD_{50} value around 2 µM.

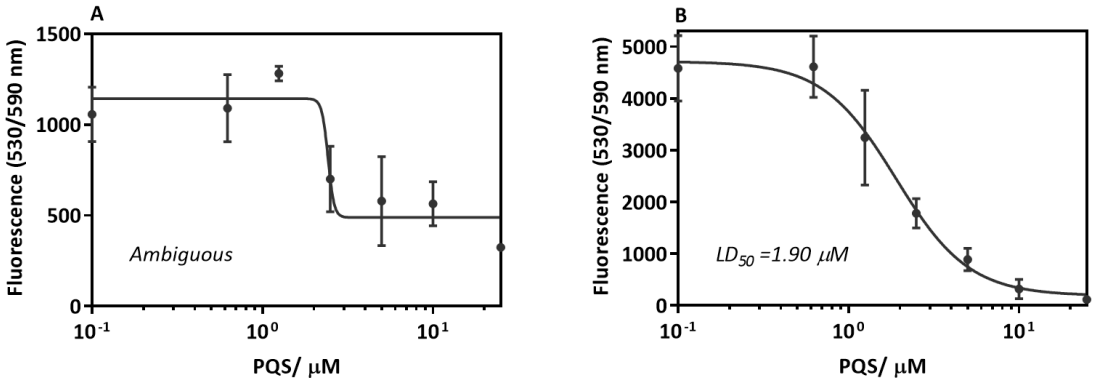

Figure 8. 2 *PQS cytotoxicity curves obtained using AlamarBlue reagent for (A) Raw 264.7 cells and (B) MH-S cells. The assay was performed in in vitro conditions during 3 days testing concentrations of PQS ranging from 25 to 0 µM (25-10-5-2.5-1.25-0.625-0 µM), corresponding to the Standard Curve. Results are expressed in fluorescence values at 530/590 nm. Each calibration point was measured in triplicates on the same culture plate and the results show the average and standard deviation of the assay carried out on 1 day.*

8.2.1.1 Murine alveolar macrophage cell line

Given the higher susceptibility shown by MH-S cells, MH-S cell line was selected to perform PQS cytotoxicity studies. With this aim, MH-S cells were cultured at a seeding density of 1 x10^5 cells mL^{-1} and treated with 25, 10, 5, 2.5, 1.25, 0.625 and 0 µM PQS concentrations (standard curve) for 72 h. PQS cytotoxic effect on MH-S cells was analysed studying the same three hallmarks of viability already used for PYO: mitochondrial enzymatic activity, esterase activity and membrane integrity and cell respiration. At the same time, non-treated MH-S cells were used as 100 % viability control. The obtained results were normalized according to this value.

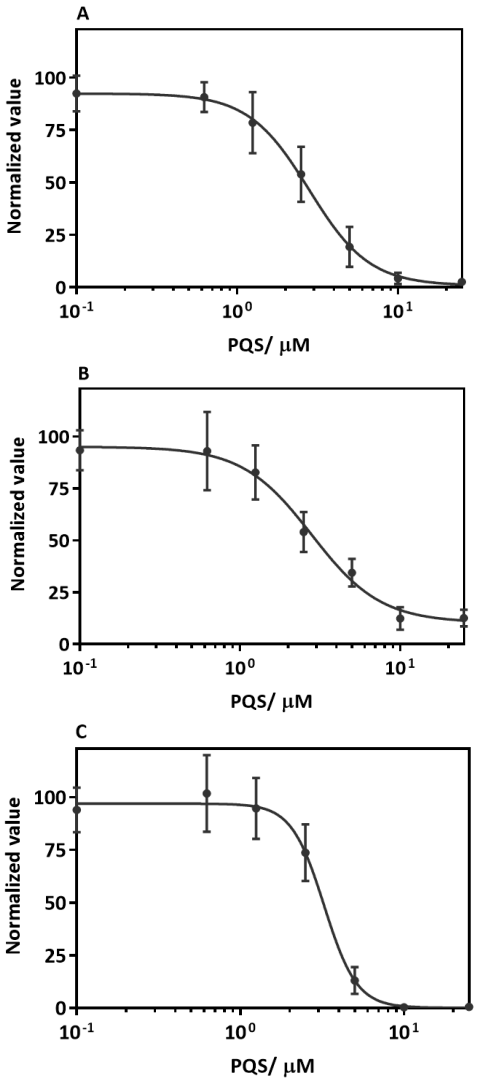

Max	96.91 ±2.18
Min	0.13 ±2.37
Slope	-4.35 ±0.58
LD_{50}/ µM	3.26 ±1.05
Dynamic range/ µM	2.36 ±0.45 and 4.48 ±0.50
LoD/ µM	1.45 ±0.64
R^2	0.97 ±0.02

Max	95.01 ±2.71
Min	10.34 ±3.19
Slope	-2.01 ±0.30
LD_{50}/ µM	2.80 ±1.09
Dynamic range/ µM	1.17 ±0.54 and 8.05 ±2.39
LoD/ µM	0.76 ±0.56
R^2	0.96 ±0.01

Max	92.39 ±2.24
Min	0.70 ±2.82
Slope	-2.31 ±0.28
LD_{50}/ µM	2.80 ±1.06
Dynamic range/ µM	1.32 ±0.52 and 4.85 ±1.39
LoD/ µM	0.72 ±0.47
R^2	0.97 ±0.02

Figure 8. 3 *PQS cytotoxicity curves and the corresponding analytical parameters. The graphs show the results obtained with: (A) AlamarBlue (AB), (B) LIVE/DEAD dual staining and (C) Luminescent ATP Detection assay. Assays were performed in in vitro conditions with MH-S cells during 3 days at 37 ºC and 5 % CO_2 testing concentrations of PQS ranging from 25 to 0 µM (25-10-5-2.5-125-0.625-0 µM). Each calibration point was measured in triplicates on the same culture plate and the results show the average and standard deviation of the assay carried out on 3 different days. The obtained results were normalized according to the viability value of non-treated cells as it was considered to be equivalent to 100 % viability.*

As shown in Figure 8. 3, the obtained LD_{50}-s for PQS on MH-S cells varied from 1 to 3 µM according to the cytotoxicity assay. These LD_{50} values are comparable with previously reported values obtained with other cell lines (see Table 8. 1). In this sense, Vrla et al.[16] treated TIB-67 mouse monocytes with various HHQ, HQNO and PQS concentrations (from 50 to 0 µM) for 48 h obtaining LD_{50} values of 10 µM for HHQ and HQNO and 1 µM for PQS based on mitochondrial enzymatic activity (MTT assay). Moreover, Kim et al.[17] analyzed PQS cytotoxicity on J774A.1 murine macrophage studying the same hallkmark of viability. Thus, macrophages were treated with PQS and HHQ for 24 h. After this time, cell viability was measured obtaining LD_{50} values for

both PQS and HHQ of around 4 µM. In the same line, Abdalla et al.[29] evaluated PQS cytototxicity on three different cell lines: lung A549, normal human epithelial cells (NHBE) and J774A.1 and THP1 macrophages cell lines. With this purpose, they studied cell viability based on the same mitochondrial enzymatic activity viability hallmark. All cell lines were treated with different PQS concentrations for 48 h obtaining LD_{50} values of around 39, 5, 19 and 14 µM, respectively. Therefore, NHBE cells were the most sensitive to PQS as demonstrated by the lowest LD_{50} value (5 µM).

Table 8. 1 *Reported LD_{50} values for PQS on different cell lines and the used viability assay. MTT =3-(4,5-dimethylthiazol-2-yl)-2,5-diphenyltetrazolium bromide*

Cell line	LD_{50}	Viability assay	Reference
TIB-67 mouse monocytes	1 µM	MTT	[16]
J774A.1 murine macrophage	4 µM	MTT	[17]
Lung A549	39 µM		
Normal human epithelial cells (NHBE)	5 µM	MTT	[18]
J774A.1 and THP1 macrophages	19 and 14 µM		

In this vein, the LD_{50} value of PQS on MH-S cells was lower than that previously obtained for PYO VF (LD_{50} between 11 and 20 µM). Thus, PQS AI showed higher cytotoxicity on MH-S cells than PYO.

8.2.2 Protective effect evaluation of PQS mAb423 on MH-S cell line

After studying the cytotoxic effect of PQS on MH-S cells, the quenching capacity of PQS mAb423 on MH-S cells was evaluated assesing the same type of assay used in Chapter 7. This mAb was selectively screened during several cloning cycles to specifically recognize PQS molecule (see Material & Methods). In fact, besides the great structural similarities with HHQ and HQNO, PQS crossreacted < 0.1 % in both cases (IC_{50} >1000 nM; data not shown).

Thus, since the assay protocol involved keeping MH-S cells with/without PQS and PQS mAb423 for 3 days at 37 ºC and 5 % CO_2, before assessing the protective effect of PQS mAb423 on MH-S cell line, its stability after this time at these conditions was analysed. For this purpose, MH-S cells were treated with PQS mAb423 at a bivalent stoichiometric LD_{50} concentration and half of the LD_{50} concentration for 3 days following the procedure shown in Figure 8. 12. Besides, to ensure a proper performance of the assay a non-treated cell control and PQS standard curve were used. After this time, cell supernatants treated with PQS mAb423 were collected to perform PQS mAb423/PQS-BSA ELISA (see Material & Methods). Thus, two PQS standard curves were

obtained using PQS mAb423 from cell supernatants corresponding to the LD_{50} (light orange) and to half of the LD_{50} (brown) and compared with a control curve obtained using a non-cultured PQS mAb423 (see Figure 8. 4). The obtained ELISA parametres for the three curves were similar demonstrating the stability of PQS mAb423: A_{450} values of 0.78, 0.70 and 0.70 and IC_{50} values of 7.16 nM, 10.11 nM and 11.00 nM for the control, LD_{50} and half LD_{50}, respectively.

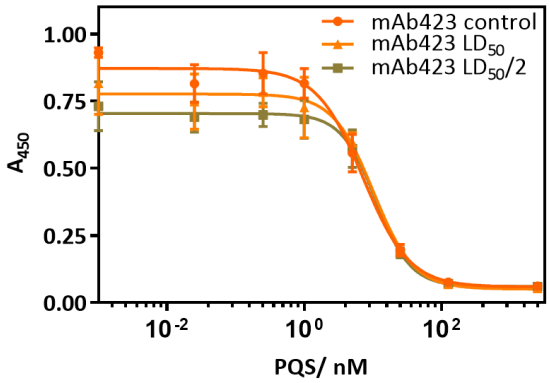

Figure 8. 4 *Stability studies of PQS mAb423 using PQS mAb423/PQS-BSA ELISA. PQS mAb423 was added to MH-S cells stoichiometrically at the LD_{50} (light orange) and half of the LD_{50} value (brown) and incubated for 3 days at 37 ºC and 5 % CO_2 in RPMI media. Cell culture supernatants were used to perform PQS mAb423/PQS-BSA ELISA at a final concentration of 0.1 µg mL^{-1} for PQS mAb423 (standard conditions, see Material & Methods). The obtained IC_{50}-s were of 10.11 and 11.00 nM, respectively (control IC_{50} value 7.16 nM). Each calibration point was measured in triplicates on the same ELISA plate and the results show the average and standard deviation of the assay carried out on 1 day.*

After confirming the stability of PQS mAb423 mAb at the assay conditions, its quenching effect was evaluated assessing the same viability assays previously used to study PQS cytotoxicity. With this purpose, MH-S cells were treated with both PQS mAb423 and PQS at the LD_{50} concentration. The required PQS mAb423 concentration was calculated considering a bivalent stoichiometric relation between mAb and PQS. Thus, the obtained viability was compared with the viability value of cells treated with just PQS at the LD_{50} concentration. At the same time, to ensure a correct performance of the assay and to determine the LD_{50} concentration of PQS, a PQS standard curve was built with the same PQS range of concentrations described in the previous section (25 - 0 µM). Moreover, a control with cells just treated with PQS mAb423 was required to confirm that the mAb by itself did not cause any cytotoxic effect on MH-S cells, as explained in Chapter 7. Besides, non-treated cells were used as 100 % viability control. Viability assays were carried out in triplicates on the same culture plate and repeated on 2-3 different days.

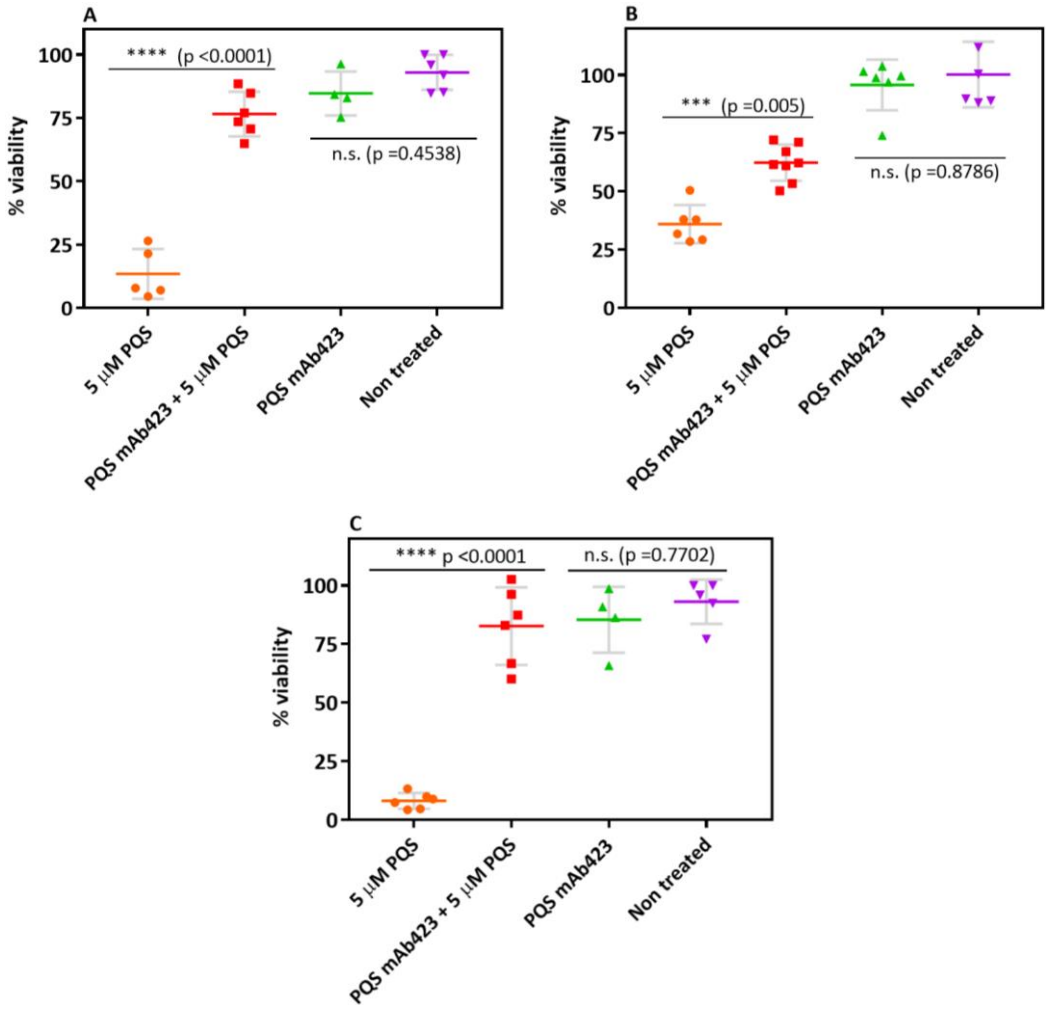

Figure 8. 5 *Protective effect of PQS mAb423 on MH-S cells. MH-S cells were treated with 5 µM of PQS (blue), PQS mAb423 plus 5 µM of PQS (red) and with just PQS mAb423 (green) for 3 days at 37 ºC and 5 % CO_2. Non-treated MH-S cells (purple) were used as 100 % viability control. After this period of time, viability was measured using (A) AlamarBlue (AB), (B) LIVE/DEAD dual staining and (C) Luminescent ATP Detection assay. Viability of cells treated with PQS LD_{50} concentration (orange) were compared with viability of cells treated with a stoichiometric mAb concentration plus the same PQS concentration (red) in order to evaluate the protective effect of the mAb. The results shown correspond to the average and standard deviations of the analysis made by duplicates on the same culture plate on 3-4 different days. The obtained results were normalized according to the viability value of non-treated cells viability. P values were obtained performing a Tukey's multiple comparisons test.*

The first viability hallmark analysed was the mitochondrial enzymatic activity. Mitochondria are cell organelles known to play an important role in obtaining energy for the cell. In fact, energy generation is obtained through the sequential transport of electrons from reduced nicotine adenine dinucleotide (NADH) to molecular oxygen, which produces ROS[30]. As mentioned before, PQS exerts its cytotoxic effects through ROS formation[22]. For this reason, the study of cell viability focusing on mitochondrial activity was considered of special interest. With this purpose, AlamarBlue reagent was used, in which MH-S cells viability is proportional to the obtained fluorescence at 530/590 nm corresponding to the reduction of resazurin by viable cells (see

Material & Methods). As previously explained, the protective effect of PQS mAb423 was evaluated comparing viability values of cells treated with a bivalent stoichiometric concentration of PQS mAb324 plus PQS at the LD_{50} concentration with cells treated with the same PQS concentration. Thus, Figure 8. 5A shows the quenching capacity of PQS mAb423 on MH-S cells as the percentage of viable cells increases a 5.7-fold reaching viability percentage values around 75 % ($p < 0.0001$). Accordingly, the non-cytotoxic effect of PQS mAb423 was verified comparing viability values of PQS treated MH-S cells with non-treated cells ($p = 0.4538$).

Moreover, the observed quenching effect was confirmed studying cell integrity and esterase activity (LIVE/DEAD™ dual staining) hallmarks in PQS treated MH-S cells together with PQS mAb423 addition. In this case, the emitted green fluorescence at 490/515 nm was proportional to the number of viable cells according to esterase activity, which transformed the non-fluorescent acetoxymethyl calcein (Ca-AM) to the fluorescence Ca. In contrast, dead cells lacking their membrane integrity were stained by the fluorescent DNA intercalator propidium iodide (PI) producing a red fluorescence signal at 535/617 nm (see Material & Methods).

Figure 8. 5B shows a significant 2.27-fold increase in viable cells when cells were treated with PQS mAb423 ($p = 0.0005$). Furthermore, just the addition of PQS mAb423 on MH-S cells did not cause any cytotoxic effect as there were not significant differences in viability levels compared with non-treated cells ($p = 0.8786$). The mentioned behaviours could also be observed under fluorescence microscope. As illustrated in Figure 8. 6, the presence of PQS mAb423 in MH-S cells treated with 5 µM PQS clearly increased green fluorescence while decreased red fluorescence. Thus, PQS mAb423 increased the number of viable cells minimizing the cytotoxic effect of PQS. Moreover, the nontoxic effect of PQS mAb423 was notice since the intensity of both green and red fluorescence in PQS mAb423 treated MH-S cells and non-treated MH-S cells was the same.

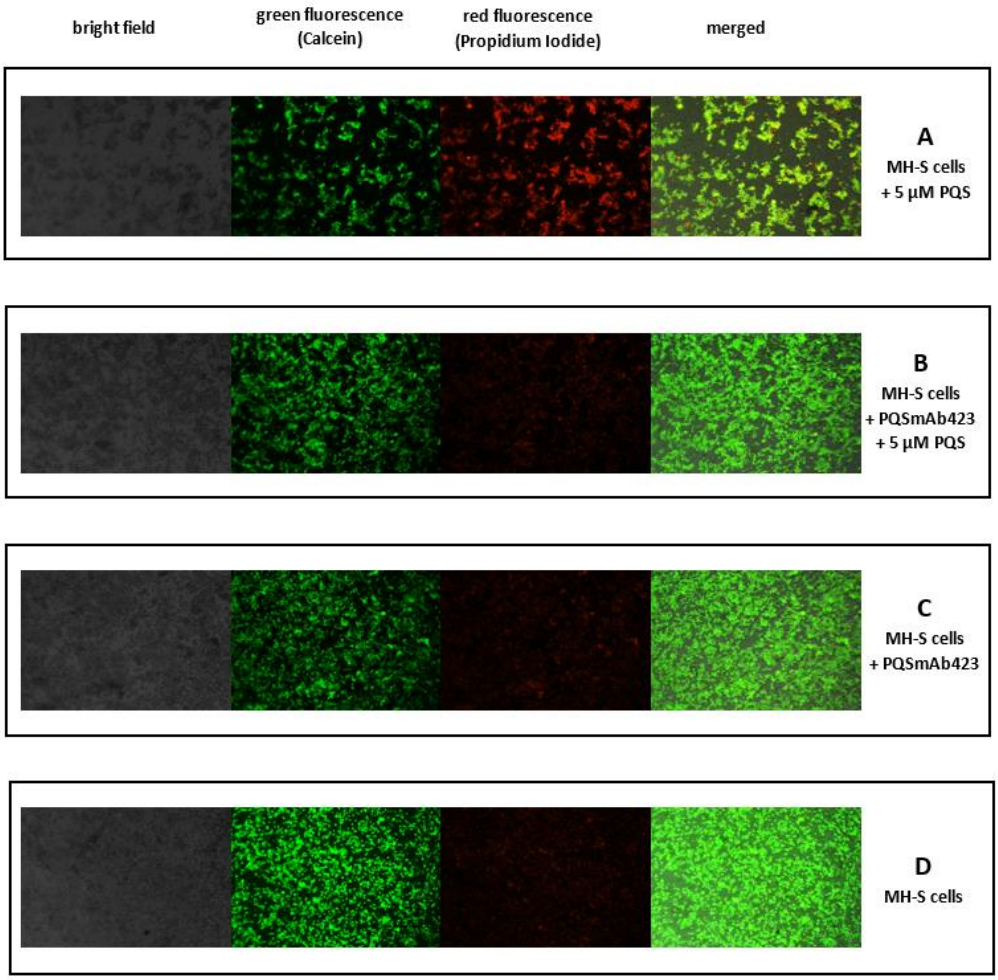

Figure 8. 6 *LIVE/DEAD dual staining of MH-S cells treated with (A) 5 µM of PQS, (B) PQS mAb423 plus 5 µM of PQS, (C) just PQS mAb423 and (D) without PQS nor PQS mAb423. MH-S cells were grown at 37 ºC and 5 % CO_2 at a seeding density of 1 x 10^5 cells mL^{-1} for 3 days. After that time, cells were exposed to a mixture of 4 µM acetoxymethyl Calcein (Ca-AM) and propidium iodide (PI) for 1 h at room temperature (RT). Ca-AM penetrates membranes of live cells and, once inside the citoplasm, it is converted to Ca by the action of esterases. Ca stains nucleic acids of live cells producing a green fluorescence signal at 490/515 nm. In contrast, PI stains nucleic acids of died cells emitting red fluorescence at 535/617 nm. Fluorescence has been monitored with a fluorescence microscope at 20-fold magnification.*

The last studied viability hallmark to evaluate PQS mAb423 protective effect was the production of intracellular ATP since it is the main product synthesized by viable cells through aerobic respiration[31] and it is proportional to the number of viable cells. As illustrated in Figure 8. 5C, the addition of PQS mAb423 to PQS treated MH-S cells significantly increased cell viability ($p < 0.0001$). In fact, PQS mAb423 triggered a cell protection reaching viability values similar to non-treated MH-S cells ($p = 0.4869$). Moreover, PQS mAb423 does not cause any cytotoxic effect on MH-S cells as the percentage of viable cells are similar to non-treated cells ($p = 0.7702$).

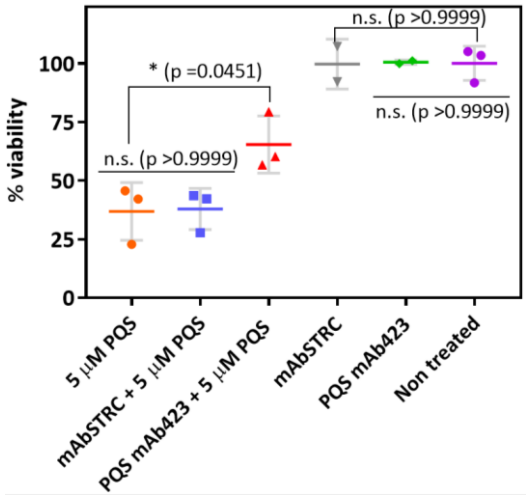

Figure 8. 7 *Specificity studies of PQS mAb423 effect on MH-S cells. MH-S cells were treated with 5 µM PQS (orange), a non specific mAb against streptomycin (STRC) antibiotic plus 5 µM PQS (blue), PQS mAb423 plus 5 µM PQS (red), just mAbSTRC (grey) and just PQS mAb423 (green). Non-treated MH-S cells (purple) were used as 100 % viability control. After that time, AlamarBlue (AB) viability assay was performed. The results shown correspond to the average and standard deviation of the analysis made by triplicates on the same culture plate on 1 day. Values were normalized according to the viability value of non-treated cells. P values were obtained performing a Tukey's multiple comparisons test.*

Finally, the specificity of PQS mAb423 for PQS was evaluated analysing the protective effect of streptomycin (STRC) mAb on MH-S cells since STRC is an unrelated target regarding PYO and PQS[32]. Figure 8. 7 shows that mAbSTRC did not exert any protection on MH-S cells as there was not significant differences on viability when comparing MH-S cells treated with 5 µM PQS (blue) with MH-S cells treated with both mAbSTRC and the same PQS concentration (orange) (p >0.9999). Futhermore, mAbSTRC itself did not cause any cytotoxicity to MH-S cells (grey) as no significant differences were observed compared with non treated cells (purple) (p >0.9999). Besides, PQS mAb423 was used as control to ensure a correct performance of the assay. Therefore, PQS mAb423 exerted its protection by specifically recognizing PQS.

Overall, PQS mAb423 showed the highest protection when analysing viability based on cell respiration and mitochondrial activity. This can be explained since PQS exerts its cytotoxicity through the formation of ROS species[22]. In fact, viability of PQS-treated MH-S cells increased with the presence of PQS mAb423 reaching values of 80 - 100 %. Furthermore, PQS mAb423 quenching effect seemed to be higher than that obtained with PYO mAb122 (50 - 75 % viability). Therefore, these results demonstrated that blocking an AI target could be even more effective than quenching an effector molecule, such as a VF. In this context, the observed therapeutical effect will be further confirm on bacterial cultures with the aim of analysing the bacterial response to PQS mAb423 addition regarding QS systems regulation. Nevertheless, as explained in Chapter 7, since the complexity of QS network makes its complete inhibition highly difficult,

dual therapies will be tried. In this case, PQS mAb423 could be used together with PYO mAb122 to inhibit *P. aeruginosa* Pqs QS system at two different levels. Finally, the protection effect of PQS mAb423 will be evaluated using an *in vivo* system.

8.2.3 Immunomodulatory effect studies of PQS and PQS mAb423 on MH-S cells

It has been documented that, apart from the cytotoxic effects produced on host cells, PQS has immunomodulatory effect on different cell lines, such as monocytes, macrophages and epithelial cells, by modulating IL-6, TNF-α, IL-8 and IL-12 pro-inflammatory cytokines levels[17, 23, 25]. Nevertheless, this modulatory effect varies according to the use PQS concentration, the time of exposure and the type of cell[23]. In this context, Kim et al.[17] studied the immunomodulatory effect of PQS and HHQ in *in vitro* conditions measuring TNF-α and IL-6 cytokines on extracts of bacterial culture supernatants from wild type (WT) PA14 strain and two *pqs* mutants of *P. aeruginosa* (*pqsA* and *pqsH*) by ELISA. This bacteria strains were grown overnight (ON), diluted to a final OD (600) of 0.02 and AQs were extracted using acidified ethyl acetate. First, they treated J774A.1 mouse monocytes with these extracts at different dilutions for 48 h and found *pqsA* strain to increase TNF-α and IL-6 production in more than 1000-fold times compared with WT strain (at 1/16X dilution). Therefore, they analysed the effect of adding 1 µM of PQS and HHQ to cells treated with extracts of culture supernatants from *pqsA* mutant at this dilution during 24 h. After this time, TNF-α and IL-6 levels were decreased in presence of PQS and HHQ from 450 pg mL^{-1} to 100 and 200 pg mL^{-1} and from 150 pg mL^{-1} to 70 and 80 pg mL^{-1}, respectively. In contrast, Wardwell et al.[23] treated IB3-1 cystic fibrosis (CF) airway epithelial cell line with 38 µM of PQS and observed a trend towards increase in IL-6 and IL-8 secretion. In the same vein, Wu et al.[25] stimulated primary tracheobronchial epithelial (hTBE) cells with *P. aeruginosa* culture filtrates for 24 h inducing a dose-dependent IL-8 increase reaching values of 20 ng mL^{-1}. However, after 24 h, IL-8 levels dreceased to control level values. Moreover, Skindersoe et al.[26] demonstrated that PQS caused a dose-dependent decrease of IL-12 pro-inflammatory cytokine on bone marrow-derived dendritic cells (BM-DCs). In fact, the addition of 20 µM of PQS lowered IL-12 basal levels from 1200 pg mL^{-1} to 600 pg mL^{-1} as measured by ELISA.

Thus, as previously explained in Chapter 7, the immunomodulatory effect produced by both PQS and PYO increases their interest as therapeutic targets. In fact, the use of specific mAbs against these QS molecules could inhibit virulence and, also, disrupted any modification from the immune response of the host. Therefore, the immunomodulatory effect of PQS and the potential capacity of PQS mAb423 to avoid this PQS effect on MH-S cells were evaluated by measuring a pro-inflammatory cytokine (IL-6) and an anti-inflammatory cytokine (IL-13). With

this purpose, first, basal levels of IL-6 and IL-13 cytokines produced by non-treated MH-S cells were analysed. Hence, cells were plated at a seeding density of 1 x 10^5 cells mL^{-1} and, after 3 days at 37 ºC and 5 % CO_2, cells supernatants were collected to measure cytokines by performing the corresponding ELISA. The basal levels of IL-6 and IL-13 cytokines on MH-S cells were of around 7 and 5 pg mL^{-1}. Then, the inflammatory response of MH-S cell line to PQS was studied by treating cells with different PQS concentrations (25, 10, 5, 2.5, 1.25, 0.625 and 0 µM) for 3 days at the same conditions. As illustrated in Figure 8. 8, PQS did not provoke any significant variations in neither IL-6 pro-inflammatory nor IL-13 anti-inflammatory cytokines compared with the non-treated cell levels. In consequence, since PQS did not have any immunomodulatory effect on MH-S cell line at the studied range of concentrations, the role of PQS mAb423 as possible therapeutic agent was not evaluated.

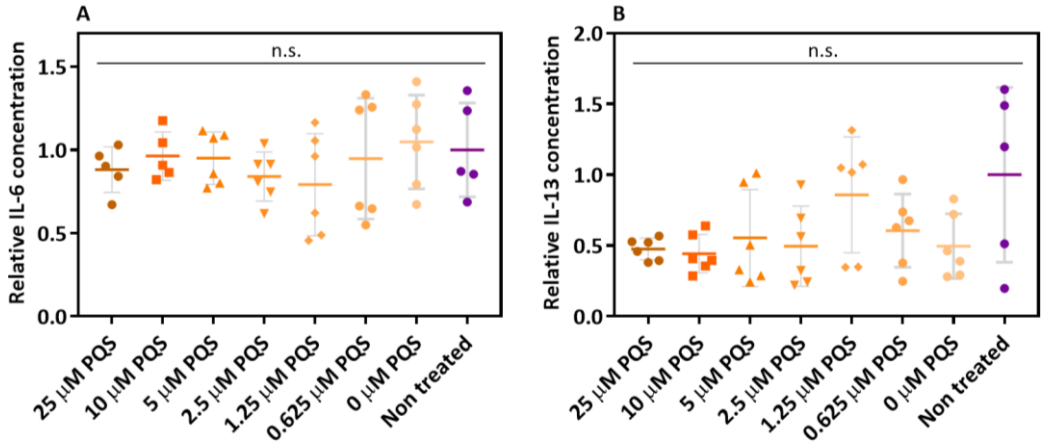

Figure 8. 8 *(A) IL-6 and (B) IL-13 levels of MH-S cells supernatants treated with/without different PQS concentrations during 3 days at 37 ºC and 5 % CO_2 using ELISA. 5 µM corresponds to the LD_{50} of PQS on MH-S cells. The results shown correspond to the average and standard deviation of the analysis made at least by duplicates on the same plate on 3 different days. Values are expressed as fold changes relative to non-treated control (purple). P values were obtained carrying out Tukey's multiple comparisons tests.*

In contrast, cells were only treated with PQS mAb423 with the aim of discarting the common cytokine release syndrome (CRS) produced by most mAbs (explained in Chapter 7). As illustrated in Figure 8. 9, unlike PYO mAb122, PQS mAb423 did not induce any IL-6 pro-inflammatory nor IL-13 anti-inflammatory cytokine levels variations compared with their basal levels at the used concentration. Thus, it seemed that PQS mAb423 did not provoke CRS syndrome. Nevertheless, the absence of CRS could be due to the lower mAb concentration used in the case of PQS mAb423 when treating MH-S cells.

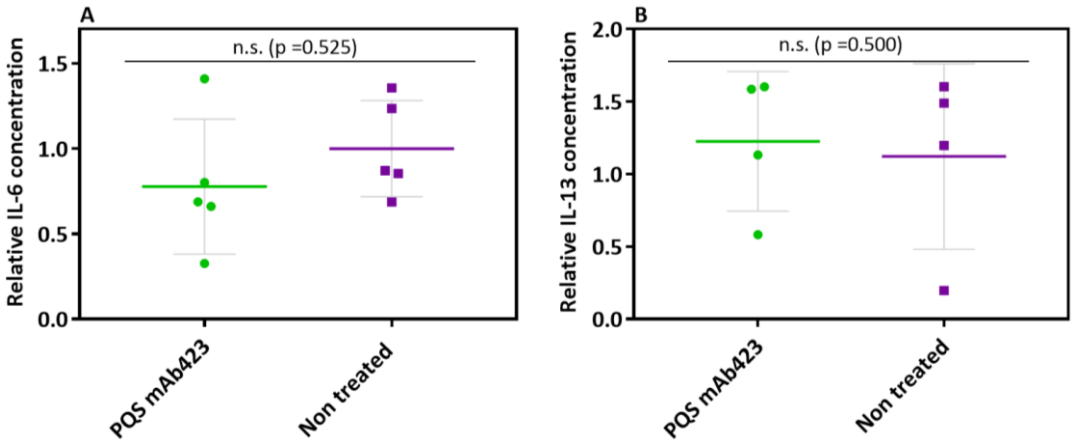

Figure 8. 9 *(A) IL-6 and (B) IL-13 levels of MH-S cells supernatants treated with a bivalent stoichiometric concentration of PQS mAb423 (green) and non treated (purple) for 3 days at 37 ºC and 5 % CO_2 using the corresponding ELISA. 5 µM corresponds to the LD_{50} of PQS on MH-S cells. The results shown correspond to the average and standard deviation of the analysis made at least by duplicates on the same plate on 3 different days. Values are expressed as fold changes relative to non-treated control. P values were obtained carrying out two-tailed Spearman correlation test.*

8.3 Materials & methods

8.3.1 Cell line models

The same Raw 264.7 cells (ATCC® TIB-71™) and MH-S cells (CRL-2019) macrophage cell lines described in the previous chapter 7 were used.

8.3.2 PQS mAb423 production

PQS mAb423 has been obtained by Raya et al. (*unpublished*) following the same protocol explained in Chapter 4 for PYO mAb122 with some modifications. Brieftly, mice were immunized using a KLH-PQS bioconjugate whose structure is illustrated in Figure 8. 10. Then, spleen lymphocytes were fused with murine myeloma cells to obtain the corresponding hybridomas, which were further cloned and used to produce estable mAbs. In fact, culture supernatants were screened by performing indirect ELISA assays in order to select the hybridomas that were able to recognize PQS with highest affinity.

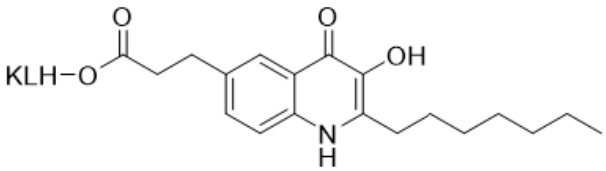

Figure 8. 10 *PQS-KLH bioconjugate structure used to immunize mice.*

8.3.3 PQS mAb423/PQS-BSA ELISA

The protocol followed to perform PQS mAb423/PQS-BSA ELISA was the same explained in Chapter 4 for PYO detection with some modifications regarding the coating and competition step (see Table 8. 2).

Table 8. 2 *Coating and competition step conditions and immunoreagent concentrations used for PQS mAb423/PQS-BSA ELISA.*

PQS-BSA/ µg mL^{-1}	0.5
PQS mAb423/ µg mL^{-1}	0.1
Buffer for the competition step	0.1 mM EDTA in PBST
Competition step conditions	30 mins at 37 ºC
PQS standard curve/ nM	2500-0 (dilution factor of 2)

8.3.4 *In vitro* assay protocols

8.3.4.1 PQS cytotoxicity evaluation assays

As shown in Figure 8. 11, MH-S and Raw 264.7 cells were plated in 96-well plates at a seeding density of 1 x 10^5 cells well^{-1} in a final volume of 100 µL and incubated for 2 h in complete RPMI and DMEM medium, respectively, for cell adhesion. Then, non-adherent cells were removed and the seeded ones were further treated with different PQS (Sigma Aldrich) concentrations during 3 days in the corresponding medium. PQS solutions were prepared in DMSO (Sigma Aldrich) ranging from 25 to 0 µM, with a 2.5 or 2 dilution factor. Cell viability percentage and LD_{50} values were estimated in all assays performed. Moreover, a non-treated MH-S cells control was required since it was considered as 100 % viability.

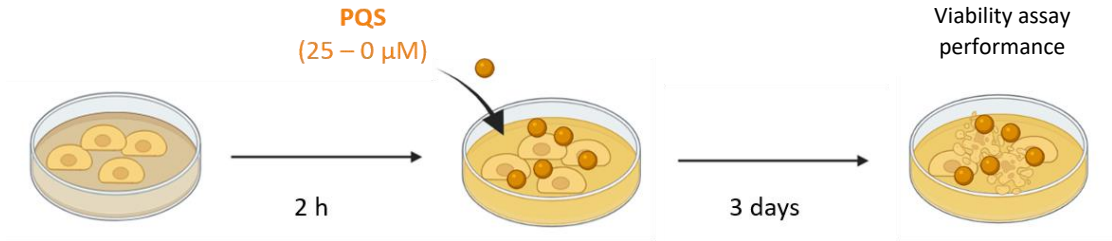

Figure 8. 11 *Schematic representation of the protocol followed to perform viability assays and determine PQS LD_{50} on MH-S cells.*

8.3.4.2 MAb protective effect evaluation

Following the same protocol explained above, the protective effect of PQS mAb423 on MH-S cells was evaluated. Thus, cells were plated at a seeding density of 1 x 10^5 cells well^{-1} in a final volume of 100 µL and incubated for 2 h for adhesion. Then, non-adherent cells were removed

and a standard curve for PQS was built (from 25 to 0 µM) to confirm a correct performance of the assay, to check PQS cytotoxicity and to determine PQS LD_{50} on MH-S cell line. Furthermore, with the aim of evaluating the protective effect of PQS mAb423, other cells were treated with a stoichometrycally equal concentration of PQS mAb423 considering that theoretically each specific mAb binds two PQS molecules. Therefore, to ensure that the quencher was already in the host cells medium, PQS mAb423 was added to MH-S cells prior to PQS treatment at the LD_{50} concentration (see Figure 8. 12). After 3 days at 37 ºC and 5 % CO_2, viability assays were carried out to determine the percentage of protective effect exerted by the specific mAb. In this sense, viability of cells treated with a LD_{50} concentration of PQS plus and minus PQS mAb423 was compared.

In all the performed assays, two controls were required: a non-treated cells control use as 100 % viability value and a PQS mAb423-treated cells control to ensure the absence of cytotoxicity coming from the mAb by itself.

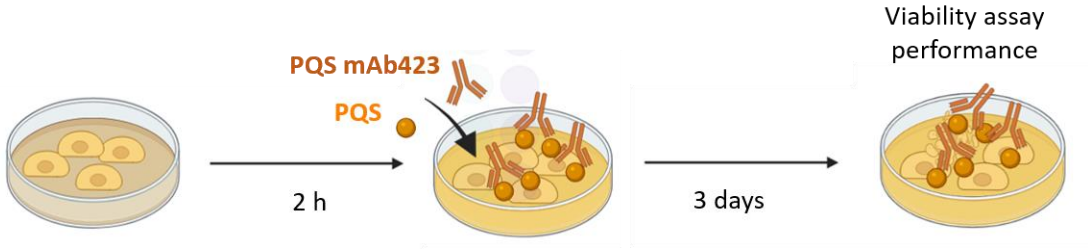

Figure 8. 12 *Schematic representation of the protocol followed to perform viability assays and determine the protective effect of the specific PQS mAb423 on MH-S cells (% protection).*

8.3.5 Viability assays

PQS cytotoxicity and PQS mAb423 protective effect were evaluated analysing three different viability hallmarks. Therefore, mitochondrial enzymatic activity, esterase activity and membrane integrity and cellular respiration were studied using AlamarBlue (AB) Cell Viability Reagent reagent (*Invitrogen™,* DAL1025), LIVE/DEAD dual staining (*Invitrogen™,* L3224) and Luminescent ATP Detection Assay (*abcam*, ab113849), respectively. All assays were performed following product manufacturer instructions, explained in detail in the previous chapter (Chapter 7).

8.3.6 PQS immunomodulatory effect study

With the aim of evaluating the immunomodulatory effect of PQS on MH-S cells, cells were treated with 25, 10, 5, 2.5, 1.25, 0.625 and 0 µM of PQS, with PQS mAb423 and with both PQS

mAb423 and PQS for 3 days at 37 ºC and 5 % CO_2. Besides, non-treated cells were used as a control to obtain basal levels from both studied cytokines. After 3 days, cell supernatants were collected to determine cytokines levels by assessing the corresponding specific ELISA. Supernatants were stored at -20 ºC until use.

8.3.7 Cytokines immunoassays

IL-6 and IL-13 cytokines were determined by ELISA using a commercially available kit (SinoBiological). The followed protocol is explained in detail in Chapter 7.

8.4 Concluding remarks

- The previously developed cell culture based *in vitro* system has been used to evaluate PQS cytotoxicity and the protective effect of a specific mAb against PQS (PQS mAb423).

- The protective effect of PQS mAb423 on MH-S cells has been assessed analysing mitochondrial enzymatic activity, cell respiration, membrane integrity and esterase activity hallmarks of viability.

    - A clear increase in cell viability has been observed when PQS mAb423 was added to PQS treated MH-S cells reaching viability values around 80 - 100 % when analysing cell respiration and mitochondrial enzymatic activity hallmarks. These results are coherent since PQS exerts its cytotoxicity through ROS production[22].
    - The potential quenching capacity of PQS mAb423 was achieved by its ability to specifically bind PQS. In fact, the use of a mAb against STRC, a non-related target regarding PQS, did not protect MH-S cells from PQS cytotoxic effect.
    - PQS mAb423 has not exerted any cytotoxic effect on MH-S cells as the obtained percentage of viability was not significantly different to that of non-treated cells.

- The addition of PQS concentrations (25-0 µM) to MH-S cells did not modify neither IL-6 pro-inflammatory nor IL-13 anti-inflammatory cytokines basal levels. Thus, since PQS did not exert any immunomodulatory effect on MH-S cells at this range of PQS concentrations, the role of PQS mAb423 in attenuating PQS immunomodulatory effect was not evaluated. However, the addition of just PQS mAb423 to MH-S cells was

evaluated. Thus, at the studied conditions, *a priori*, PQS mAb423 did not induce the common inflammatory response from the host immune system to most mAbs called CRS[33].

8.5 References

1. Gruber, J. D.; Chen, W.; Parnham, S.; Beauchesne, K.; Moeller, P.; Flume, P. A.; Zhang, Y. M., The role of 2,4-dihydroxyquinoline (DHQ) in Pseudomonas aeruginosa pathogenicity. *Peerj* **2016,** *4*.
2. Ritzmann, N. H.; Drees, S. L.; Fetzner, S., Signal Synthase-Type versus Catabolic Monooxygenases: Retracing 3-Hydroxylation of 2-Alkylquinolones and Their N-Oxides by Pseudomonas aeruginosa and Other Pulmonary Pathogens. *Applied and environmental microbiology* **2021,** *87* (6), e02241-20.
3. Heeb, S.; Fletcher, M. P.; Chhabra, S. R.; Diggle, S. P.; Williams, P.; Camara, M., Quinolones: from antibiotics to autoinducers. *FEMS Microbiol Rev* **2011,** *35* (2), 247-74.
4. Allegretta, G.; Maurer, C. K.; Eberhard, J.; Maura, D.; Hartmann, R. W.; Rahme, L.; Empting, M., In-depth Profiling of MvfR-Regulated Small Molecules in Pseudomonas aeruginosa after Quorum Sensing Inhibitor Treatment. *Front Microbiol* **2017,** *8*, 924.
5. Ji, C.; Sharma, I.; Pratihar, D.; Hudson, L. L.; Maura, D.; Guney, T.; Rahme, L. G.; Pesci, E. C.; Coleman, J. P.; Tan, D. S., Designed Small-Molecule Inhibitors of the Anthranilyl-CoA Synthetase PqsA Block Quinolone Biosynthesis in Pseudomonas aeruginosa. *ACS Chemical Biology* **2016,** *11* (11), 3061-3067.
6. Sahner, J. H.; Brengel, C.; Storz, M. P.; Groh, M.; Plaza, A.; Muller, R.; Hartmann, R. W., Combining in silico and biophysical methods for the development of Pseudomonas aeruginosa quorum sensing inhibitors: an alternative approach for structure-based drug design. *J Med Chem* **2013,** *56* (21), 8656-64.
7. Fang, Y. L.; Chen, B.; Zhou, L.; Jin, Z. J.; Sun, S.; He, Y. W., The Anti-activator QslA Negatively Regulates Phenazine-1-Carboxylic Acid Biosynthesis by Interacting With the Quorum Sensing Regulator MvfR in the Rhizobacterium Pseudomonas aeruginosa Strain PA1201. *Front Microbiol* **2018,** *9*, 1584.
8. Zhou, Z.; Ma, S., Recent Advances in the Discovery of PqsD Inhibitors as Antimicrobial Agents. *ChemMedChem* **2017,** *12* (6), 420-425.
9. Kumar, L.; Brenner, N.; Brice, J.; Klein-Seetharaman, J.; Sarkar, S. K., Cephalosporins Interfere With Quorum Sensing and Improve the Ability of Caenorhabditis elegans to Survive Pseudomonas aeruginosa Infection. *Front Microbiol* **2021,** *12*, 598498.
10. Holban, A. M.; Bleotu, C.; Chifiriuc, M. C.; Bezirtzoglou, E.; Lazar, V., Role of Pseudomonas aeruginosa quorum sensing (QS) molecules on the viability and cytokine profile of human mesenchymal stem cells. *Virulence* **2014,** *5* (2), 303-10.
11. Kravchenko, V. V.; Kaufmann, G. F.; Mathison, J. C.; Scott, D. A.; Katz, A. Z.; Wood, M. R.; Brogan, A. P.; Lehmann, M.; Mee, J. M.; Iwata, K.; Pan, Q.; Fearns, C.; Knaus, U. G.; Meijler, M. M.; Janda, K. D.; Ulevitch, R. J., N-(3-oxo-acyl)homoserine lactones signal cell activation through a mechanism distinct from the canonical pathogen-associated molecular pattern recognition receptor pathways. *J Biol Chem* **2006,** *281* (39), 28822-30.

12. Li, L.; Hooi, D.; Chhabra, S. R.; Pritchard, D.; Shaw, P. E., Bacterial N-acylhomoserine lactone-induced apoptosis in breast carcinoma cells correlated with down-modulation of STAT3. *Oncogene* **2004,** *23* (28), 4894-902.
13. Kumar, A. S.; Bryan, J. N.; Kumar, S. R., Bacterial quorum sensing molecule N-3-oxo-dodecanoyl-L-homoserine lactone causes direct cytotoxicity and reduced cell motility in human pancreatic carcinoma cells. *PLoS One* **2014,** *9* (9), e106480.
14. Jacobi, C. A.; Schiffner, F.; Henkel, M.; Waibel, M.; Stork, B.; Daubrawa, M.; Eberl, L.; Gregor, M.; Wesselborg, S., Effects of bacterial N-acyl homoserine lactones on human Jurkat T lymphocytes-OdDHL induces apoptosis via the mitochondrial pathway. *Int J Med Microbiol* **2009,** *299* (7), 509-19.
15. Shiner, E. K.; Terentyev, D.; Bryan, A.; Sennoune, S.; Martinez-Zaguilan, R.; Li, G.; Gyorke, S.; Williams, S. C.; Rumbaugh, K. P., Pseudomonas aeruginosa autoinducer modulates host cell responses through calcium signalling. *Cell Microbiol* **2006,** *8* (10), 1601-10.
16. Vrla, G. D.; Esposito, M.; Zhang, C.; Kang, Y.; Seyedsayamdost, M. R.; Gitai, Z., Cytotoxic alkyl-quinolones mediate surface-induced virulence in Pseudomonas aeruginosa. *PLoS Pathog* **2020,** *16* (9), e1008867.
17. Kim, K.; Kim, Y. U.; Koh, B. H.; Hwang, S. S.; Kim, S. H.; Lepine, F.; Cho, Y. H.; Lee, G. R., HHQ and PQS, two Pseudomonas aeruginosa quorum-sensing molecules, down-regulate the innate immune responses through the nuclear factor-kappaB pathway. *Immunology* **2010,** *129* (4), 578-88.
18. Abdalla, M. Y.; Hoke, T.; Seravalli, J.; Switzer, B. L.; Bavitz, M.; Fliege, J. D.; Murphy, P. J.; Britigan, B. E., Pseudomonas Quinolone Signal Induces Oxidative Stress and Inhibits Heme Oxygenase-1 Expression in Lung Epithelial Cells. *Infect Immun* **2017,** *85* (9).
19. Shashni, B.; Sharma, K.; Singh, R.; Sakharkar, K. R.; Dhillon, S. K.; Nagasaki, Y.; Sakharkar, M. K., Coffee component hydroxyl hydroquinone (HHQ) as a putative ligand for PPAR gamma and implications in breast cancer. *BMC Genomics* **2013,** *14 Suppl 5*, S6.
20. Wang, J.; Wang, C.; Yu, H. B.; Dela Ahator, S.; Wu, X.; Lv, S.; Zhang, L. H., Bacterial quorum-sensing signal IQS induces host cell apoptosis by targeting POT1-p53 signalling pathway. *Cell Microbiol* **2019,** *21* (10), e13076.
21. Tateda, K.; Ishii, Y.; Horikawa, M.; Matsumoto, T.; Miyairi, S.; Pechere, J. C.; Standiford, T. J.; Ishiguro, M.; Yamaguchi, K., The Pseudomonas aeruginosa autoinducer N-3-oxododecanoyl homoserine lactone accelerates apoptosis in macrophages and neutrophils. *Infect Immun* **2003,** *71* (10), 5785-93.
22. Pezzoni, M.; Meichtry, M.; Pizarro, R. A.; Costa, C. S., Role of the Pseudomonas quinolone signal (PQS) in sensitising Pseudomonas aeruginosa to UVA radiation. *J Photochem Photobiol B* **2015,** *142*, 129-40.
23. Wardwell, P. R. W., D. R.; Garner D.L.; Bader, R. A., Pseudomonas Quinolone Signal Modulates Cystic Fibrosis Epithelial Cell Response through the Toll-Like Receptor 4. *SOJ Immunology* **2015**.
24. Hooi, D. S.; Bycroft, B. W.; Chhabra, S. R.; Williams, P.; Pritchard, D. I., Differential immune modulatory activity of Pseudomonas aeruginosa quorum-sensing signal molecules. *Infect Immun* **2004,** *72* (11), 6463-70.
25. Wu, Q.; Lu, Z.; Verghese, M. W.; Randell, S. H., Airway epithelial cell tolerance to Pseudomonas aeruginosa. *Respir Res* **2005,** *6*, 26.

26. Skindersoe, M. E.; Zeuthen, L. H.; Brix, S.; Fink, L. N.; Lazenby, J.; Whittall, C.; Williams, P.; Diggle, S. P.; Froekiaer, H.; Cooley, M.; Givskov, M., Pseudomonas aeruginosa quorum-sensing signal molecules interfere with dendritic cell-induced T-cell proliferation. *FEMS Immunol Med Microbiol* **2009,** *55* (3), 335-45.
27. Lepine, F.; Deziel, E.; Milot, S.; Rahme, L. G., A stable isotope dilution assay for the quantification of the Pseudomonas quinolone signal in Pseudomonas aeruginosa cultures. *Biochim Biophys Acta* **2003,** *1622* (1), 36-41.
28. Collier, D. N.; Anderson, L.; McKnight, S. L.; Noah, T. L.; Knowles, M.; Boucher, R.; Schwab, U.; Gilligan, P.; Pesci, E. C., A bacterial cell to cell signal in the lungs of cystic fibrosis patients. *FEMS Microbiol Lett* **2002,** *215* (1), 41-6.
29. Abdalla, M. Y. H., T.; Seravalli, J.; Switzer, B. L.; Bavitz, M.; Fliege, J. D.; Murphy, P. J.; Britigan, B. E., Pseudomonas Quinolone Signal Induces Oxidative Stress and Inhibits Heme Oxygenase-1 Expression in Lung Epithelial Cells. *American Society for Microbiology. Infection and Immunity* **2017,** *85* (9).
30. Murphy, E.; Ardehali, H.; Balaban, R. S.; DiLisa, F.; Dorn, G. W., 2nd; Kitsis, R. N.; Otsu, K.; Ping, P.; Rizzuto, R.; Sack, M. N.; Wallace, D.; Youle, R. J.; American Heart Association Council on Basic Cardiovascular Sciences, C. o. C. C.; Council on Functional, G.; Translational, B., Mitochondrial Function, Biology, and Role in Disease: A Scientific Statement From the American Heart Association. *Circ Res* **2016,** *118* (12), 1960-91.
31. Bonora, M.; Patergnani, S.; Rimessi, A.; De Marchi, E.; Suski, J. M.; Bononi, A.; Giorgi, C.; Marchi, S.; Missiroli, S.; Poletti, F.; Wieckowski, M. R.; Pinton, P., ATP synthesis and storage. *Purinergic Signal* **2012,** *8* (3), 343-57.
32. Rocha, D.; Magalhaes, C.; Ca, B.; Ramos, A.; Carvalho, T.; Comas, I.; Guimaraes, J. T.; Bastos, H. N.; Saraiva, M.; Osorio, N. S., Heterogeneous Streptomycin Resistance Level Among Mycobacterium tuberculosis Strains From the Same Transmission Cluster. *Front Microbiol* **2021,** *12*, 659545.
33. Garcia Roche, A.; Diaz Lagares, C.; Elez, E.; Ferrer Roca, R., Cytokine release syndrome. Reviewing a new entity in the intensive care unit. *Med Intensiva* **2019,** *43* (8), 480-488.

Chapter 9

Conclusions and future perspectives of the thesis

9.1 General conclusions

9.1.1 Diagnostic chapters

A monoclonal antibody (mAb) showing high avidity for one of the main virulence factors (VFs) of *Pseudomonas aeruginosa* pyocyanin (PYO) (PYO mAb122) has been produced. This mAb can specifically detect PYO in the low nM range (limit of detection (LoD) =0.07 ± 0.04 on assay buffer) using a microplate-based indirect competitive enzyme-linked immunosorbent assay (ELISA). The developed ELISA (PYO mAb122/PC1-BSA ELISA) has shown excellent robustness and accuracy.

PYO mAb122/PC1-BSA ELISA has been implemented for performing PYO measurements in bacterial isolates from patients infected with *P. aeruginosa*. Matrix effect studies indicated that just diluting the isolate samples 20 times in assay buffer (LoDs of 0.15 ±0.07 nM) is enough to obtain correct measures.

Together with PYO detection assay, a polyclonal antibody-based ELISA (As230/PC1-BSA) previously developed for the detection of 1-hydroxyphenazine (1-OHphz), the precursor of PYO biosynthesis, have been used to perform measures on 37 bacterial isolates from patients infected with *P. aeruginosa.* A clear trend has been observed regarding phenazine levels. Thus, isolates from patients suffering an acute infection showed higher values than isolates from a chronic state of infection. These results position PYO as a good biomarker of *P. aeruginosa* infections and for patient stratification.

At the same time, the direct measure of PYO in clinical samples (sputum, swab) has been intended by using the developed PYO mAb122/PC1-BSA ELISA. For its implementation, matrix effect studies have been performed, indicating the need of carrying out a previous treatment step of the sample at least for sputum samples.

The treatment that has given the best results in the case of sputum samples was lyophilisation. In the case of swab samples, the direct measure rendered slight matrix effects. In any case, clinical sample measures will require further optimization since PYO concentrations measured were found in all cases below the LoD of the assay. In fact, these values did not allow to determine differences between samples from diferent infection types.

9.1.2 Therapy chapters

A cell-based *in vitro* assay has been developed allowing to test the cytotoxic effect of *P. aeruginosa* quorum sensing (QS) related molecules (PYO and Pseudomonas Quinolone Signal (PQS)) and also the protective effect of the corresponding specific mAbs regarding cellular viability. This assay uses the alveolar macrophage cell line MH-S and, for both tested QS targets, it requires a time duration of 72h.

The treatment of MH-S cells with PYO concentrations ranging from 100 to 0 µM during 72 h has allowed to determine the LD_{50} value, which was found to be between 11-18 µM depending on the viability hallmark studied. The lowest LD_{50} value was always determined when focusing on mitochrondial enzymatic activity and cell respiration.

The quenching ability of PYO mAb122 has been demonstrated in *in vitro* conditions studying three diferent characteristic traits of viable cells (mitochondrial enzymatic activity, membrane integrity and esterase activity and cell respiration). Furthermore, the protective effect of the mAb has been measured as percentatge of cellular viability, reaching levels between 50 - 75 %. This results point this mAb as a promising therapeutic agent to be tested in *in vivo* conditions.

The immunomodulatory effect of PYO has also been tested on MH-S macrophage cultures by measuring different cytokines using ELISA. The data obtained showed that PYO treatment increased IL-6, IL-8 and TNF-α pro-inflammatory cytokines when administered at the corresponding LD_{50} concentration. On the contrary, the levels of the anti-inflammatory cytokine IL-13 did not show any significant variation.

The addition of the specifc PYO mAb122 induced an important increase in all the mentioned pro-inflammatory cytokines on MH-S cells. In fact, IL-8 and IL-6 increase was similar to that observed in PYO-treated cells; however, TNF-α concentration raised 28-fold times compared with the same PYO-treated MH-S cells. This increment could be attributed to a frequent inflammatory response of the cellular immune system called cytokine-release syndrome (CRS).

The cytotoxic effect of a QS signaling molecule was also tested on MH-S cells since it has been reported that it also causes cellular damage. Thus, the cytotoxicity of PQS was assayed on MH-S cells treating them with concentrations ranging from 25 to 0 µM during 72 h. These assays allowed to determine the LD_{50} value, which was found to be between 1 - 3 µM depending on

the viability hallmark studied. The low LD_{50} value corroborated its toxic effect, in coherence with data reported in other cell lines.

The quenching ability of PQS mAb423 has been demonstrated in *in vitro* conditions studying the same three characteristic traits of viable cells. The potential therapeutic effect of this mAb has been measured as percentatge of cellular viability, reaching a complete protection (80 - 100 % viability). This results point that blocking an autoinducer (AI) target could be even more effective than quenching an effector molecule, such as a virulence factor (VF).

The immunomodulatory effect of PQS has also been tested on MH-S macrophage cultures. The results obtained showed that PQS did not induced any change on the studied cytokine levels (IL-6 and IL-13) when compared with the data obtained for non-treated cells. Moreover, the addition of the specifc PQS mAb423 was also studied in this context to determine if its presence also induced the CRS. Surprisingly, in this case CRS was not observed, which could be quite important for the possible use of this Ab as therapeutic agent.

9.2 Future perspectives

9.2.1 Diagnostic

Further investigations regarding the possibility to detect and monitor PYO levels in clinical samples are being studied. Thus, other sputum treatments that allow PYO detection without the need of diluting samples in excess are being investigated. This may open new avenues of knowledge such as the possibility to predict exacerbation periods or to diagnose the infection at early stages of the diseases reducing the morbidity and mortality of *P. aeruginosa* infected patients. In this vein, the detection of more than one QS molecules can be valuable to understand the stage of the disease and to provide patients with the most appropriate treatment strategy. Therefore, other specific mAbs against *P. aeruginosa* QS molecules are being produced with the aim of setting up the corresponding immunochemical approach. In fact, these mAbs and the immunochemical techniques explained in the thesis might be potentially used in combination to develop a multiplexed diagnostic technique able to measure simultaneously different QS molecules providing a potential characteristic signature of the stage of the infection or the prognostic of the pathology. Furthermore, this multiplexed microarray might reduce the analysis time and the volume of sample to be used.

In this context, the described immunochemical techniques could be used on different analytical configurations such as point-of-care (PoC) immunosensor devices due to the high versatility of Abs. Thus, this simple, rapid, portable and low-cost device, which are highly demanded in clinical diagnostics, might be a promising alternative for more rapid and efficient detection of biomarkers of *P. aeruginosa* infections.

9.2.2 Therapy

Further studies regarding the immunomodulatory effect of QS molecules and their corresponding mAbs on MH-S cell line need to be performed. With this purpose, first, a larger battery of cytokines in non-treated cells will be studied to obtain the basal cytokines profile of this cell line. Then, the same cytokines will be measured on cells treated with the QS molecule of interest at different concentrations and on cells treated with the corresponding quencher plus the QS molecule. The possibility of blocking the immunomodulatory effect of these QS molecues increases the interest of these mAbs as therapeutic agents and the interest of these QS molecules as therapeutic targets.

Based on the promising results obtained in *in vitro* conditions for both PYO mAb122 and PQS mAb423, the bacterial response to the addition of these mAbs will be analysed in order to study QS systems regulation. Furthermore, before carrying out *in vivo* experiments to ensure the observed quenching effect, co-culture systems will be developed where host cells will be incubated with bacterial culture supernatants in order to study the bacteria-host cell interaction at the QS level. Besides, since the complexity of QS network makes its complete inhibition highly complicated, the use of dual therapies might be of great interest as they aim to inhibit more than one QS pathway or the same QS pathway at different levels, which can be achieved by using more than one quorum sensing inhibitor (QSI) or a single compound that binds to different QS targets. In the same vein, another important aspect to take into consideration specially when working *in vivo* conditions will be the route of administration of these therapeutic mAbs. Thus, nebulization appears to be the most appropriate technique for mAb delivery into the lungs for respiratory infections treatment. Nevertheless, mAbs should be stable enough to prevent their degradation. Therefore, with this aim, the use of nanocarriers such as dendirmers to encapsulate these mAbs might overcome this problem.

ANNEX

Cystic fibrosis transmembrane conductance regulator inhibitory factor (Cif) detection on bacterial isolates from patients infected with *P. aeruginosa*

As a result of a collaboration with Bruce Hammock's group (University of California, Davis), which is a leading group in the immunochemistry fiel, and within the context of cystic fibrosis (CF), a collaboration was established for the detection of the cystic fibrosis transmembrane conductance regulator inhibitory factor (Cif) in clinical bacterial isolates from patients infected with *P. aeruginosa* since it was considered that, within the framework of the thesis, this could be really interesting and complementary to the previously obtained data. Therefore, in this annex, the implementation of the sandwich ELISA described by Vasylieva et al.[1] is explained.

A.1 Introduction

Cystic fibrosis transmembrane conductance regulator (CFTR) inhibitory factor (Cif) is another bacterial virulence factor (VF) secreted by *Pseudomonas aeruginosa* bacterium which catalyzes the hydrolysis of different epoxide compounds[2]. Besides, Cif molecule decreases CFTR-mediated chloride secretion through the apical membrane of human epithelial cells[3]. Chloride and bicarbonate secretion through CFTR channel are crucial for an adequate and efficient mucociliarity clearance in the airways[4]. Thus, as occurred in patients suffering from cystic fibrosis (CF) disease, whose *cftr* gene is mutated giving rise to a defective CFTR protein, this translates in the appearance of an abnormally tick and sticky mucus layer[5].

Furthermore, Cif VF is secreted via outer membrane vesicles (OMVs) and its general mechanism of action is illustrated in Figure A 1. In general, Cif inhibits the recycling of endocytic vesicles containing CFTR back to the plasma membrane, redirecting vesicles to the lysosome where CFTR is degraded by inactivating the host deubiquitination enzyme[2, 6]. Unlike other VFs, Cif is not regulated by the quorum sensing (QS) system.

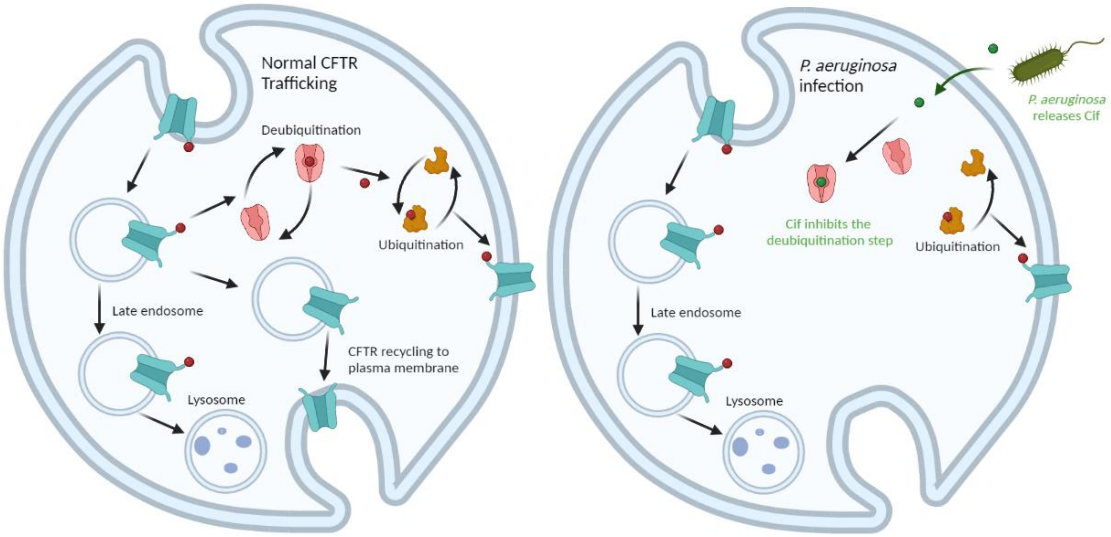

Figure A 1 *General mechanism of CFTR trafficking (left). Cif VF inhibits CFTR deubiquitination inducing CFTR lysosomal degradation and inhibiting CFTR containing vesicles recycling to plasma membrane (right).*

Nevertheless, together with PYO[4], *cif* expression is higher during early *P. aeruginosa* colonization and also on CF patients. In this sense, MacEachran et al.[7] demonstrated the presence of *cif* transcription in CF sputum, which contributed to the inhibition of CFTR expression facilitating biofilm formation on CF patients. Accordingly, it has also been reported CFTR function impairment in non-CF patients infected by *P. aeruginosa*[8].

In this context, the analysis of Cif levels in bacterial isolates from patients infected with *P. aeruginosa* (see Chapter 5) using a specific ELISA provided by Dr. Vasylieva of Prof. Bruce D. Hammock from the University of California Davis[1] was assessed. Unlike PYO detection, where a competitive ELISA was required due to its low molecular weight (210.23 g mol^{-1}); Cif determination was carried out using a sandwich ELISA due to its higher molecular weight (30 x 10^3 g mol^{-1} =30 KDa), which allowed its simultaneous recognizion by two Abs[7] (see Figure A 2).

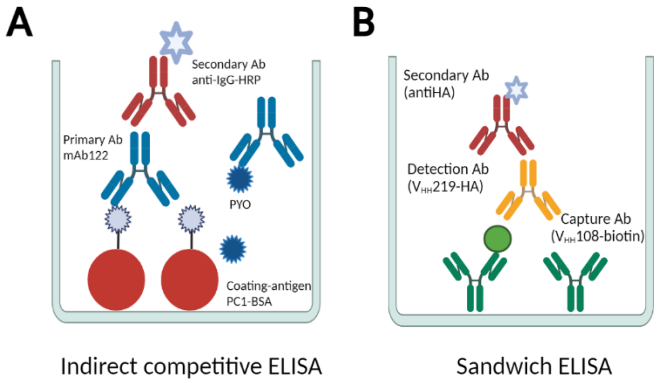

Figure A 2 *Comparison of an (A) indirect competitive ELISA and a (B) sandwich ELISA.*

In our particular case, the performed sandwich ELISA used two single domain Abs known as nanobodies (Nbs)[9]. Nbs are obtained from camelids and are heavy chain only Abs of around 12-14 kDa size[10]. As shown in Figure A 3, unlike conventional Abs that are composed of two identical light (V_L-C_L) and two identical heavy (V_H,$C_{H1,2,3}$) chains connected by disulphide bonds, camelid heavy chain Abs consist on just two identical heavy chains (V_{HH}-$C_{H2,3}$). The antigen-binding site is composed of a single variable domain named Nb[11].

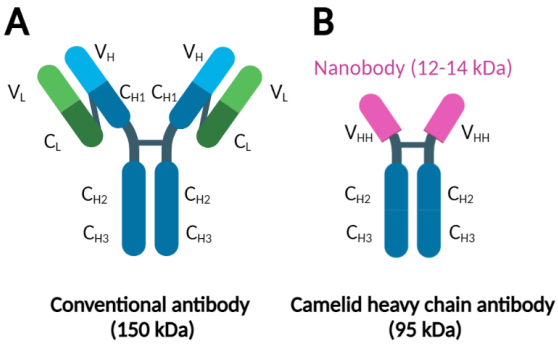

Figure A 3 *Graphical representation of different Ab structures. (A) Conventional Abs are composed of two identical heavy (variable,V_H, and constant, C_{H1-3}, domains) and light (variable,V_L, and constant, C_L, domains) chains Connected through disulfide bonds. The antigen-binding site consists of both V_H and V_L domains. (B) Camelid heavy chain Abs are composed of just two identical heavy chains (variable,V_H, and constant, C_{H2-3}, domains). The antigen-binding site consists of a single V_{HH} domain, also known as nanobody (purple).*

The main advantages of using Nbs lie on their higher stability when exposed to heat and solvents, higher solubility, higher tissue penetration, higher fast blood clearance and lower immunogenicity compared to conventional Abs[12-13]. Hence, they are becoming important as diagnostic[10] and therapeutic[11] tools.

Here, the provided CIF ELISA has been implemented to directly measure Cif in culture broth of clinical isolates without any previous treatment.

A.2 Results & discussion

A.2.1 Optimization of the CIF ELISA assay

Bruce Hammock's group (University of California, Davis) developed a sandwich ELISA assay for the detection of Cif (CIF ELISA). As all sandwich ELISAs, the general steps of the protocol consisted in the addition of a capture Ab, the analyte, the detection Ab and the labelled Ab (see Figure A 2). In this case, two Nbs were used as capure Ab (V_{HH}108-biotin) and detection Ab (V_{HH}219-HA). Thus, first, the correct performance and reproducibility of the assay was checked following the provided protocol. Then, given that our laboratory also has a lot of experience in immunoassays, the protocol was optimized with the aim of reducing the time duration of the assay and, further, to lower its limit of detection (LoD).

A.2.1.1 Incubation time studies

With the aim of reducing the time duration of the ELISA for Cif detection, the assay was performed using 60 (the stipulated time) and 30 min (the incubation time used in our lab) incubation times between steps. As demonstrated in Figure A 4, there were no significant differences between assays performed carrying out 60 mins incubation periods compared with the ones that used 30 mins incubations (IC_{50} values of 2.20 and 2.48 ng mL^{-1} and A_{max} of 1.38 and 1.18 for 60 and 30 mins, respectively) . Thus, on the light of these results the protocol explained by Vasylieva et al.[1] was carried out with 30 mins incubation times (see Material & Methods).

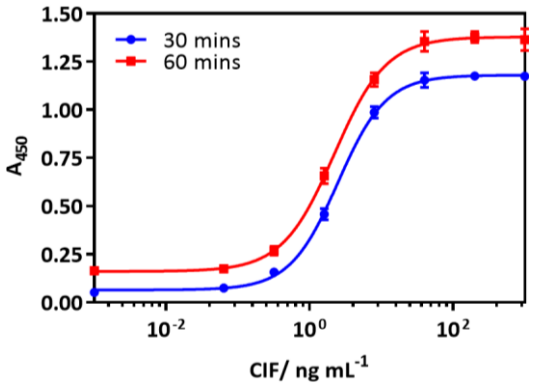

	30 mins	60 mins
A_{max}	1.18 ± 0.01	1.38 ± 0.01
A_{min}	0.06 ± 0.01	0.16 ± 0.01
Slope	1.30 ± 0.06	1.20 ± 0.07
IC_{50}/ ng mL^{-1}	2.48 ± 0.02	2.20 ± 0.02
Dynamic range/ ng mL^{-1}	0.81 and 7.03	0.70 and 7.03
LoD/ ng mL^{-1}	0.41	0.36
R^2	0.99	0.99

Figure A 4 *Incubation time analysis results and the corresponding analytical parameters. CIF ELISA was performed using 30 min (blue) and 60 min (red) incubations. Each calibration point was measured in triplicates on the same ELISA plate and the results show the average and standard deviation of the assay carried out on 1 day.*

A.2.1.1 Bidimensional experiments

With the purpose of optimizing the parameters of the assay when using 30 mins incubations, the appropiate Nbs concentrations required to perform the CIF ELISA at these conditions were established by carrying out bidimiensional (2D) checkerboard titration experiments. Thus, different capture-detection Nbs concentrations were tested (0.8 - 0 µg mL^{-1} and 0.2 - 0 µg mL^{-1}, respectively, using a dilution factor of 2) assaying three different Cif concentrations (1000, 500 and 100 ng mL^{-1}). Based on the obtained results shown in Figure A 5, 0.1 µg mL^{-1} of capture and detection Nbs were selected as the optimal combination to reach high absorbance values without reaching the saturation area of the curve.

The analytical parameters of the CIF ELISA using the above mentioned concentrations are summarized in Table A 1.

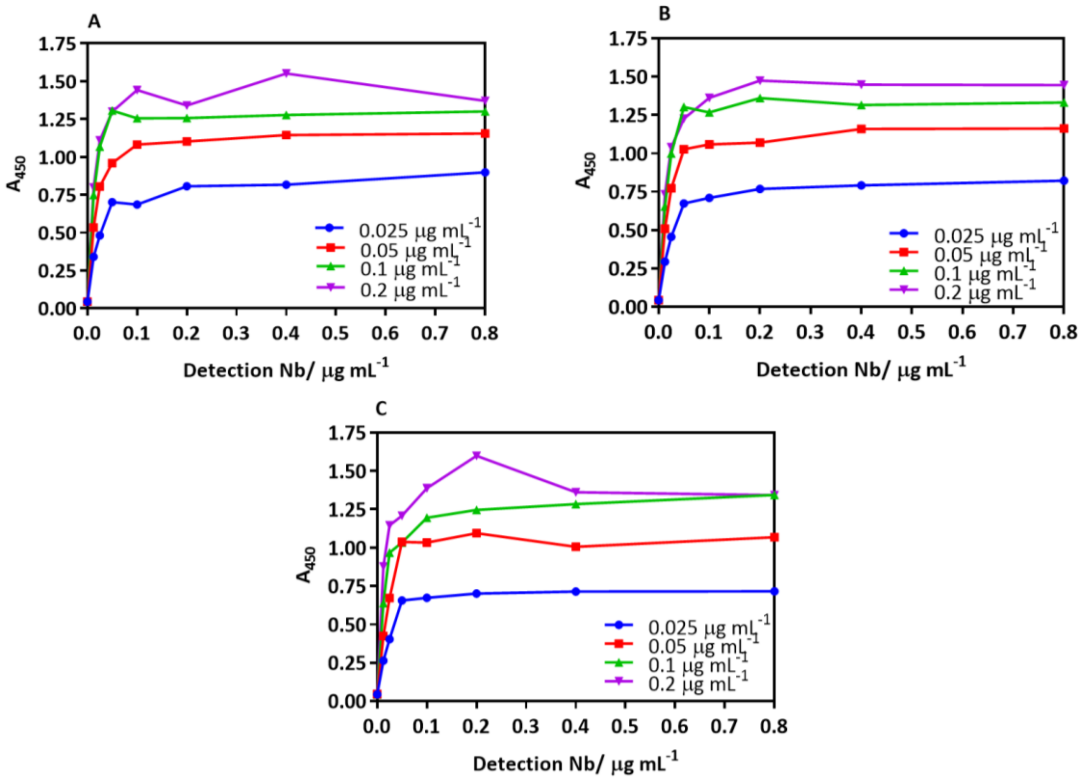

Figure A 5 *Bidimensional (2D) experiments for CIF ELISA using (A) 1000 (B) 500 and (C) 100 ng mL^{-1} concentrations of Cif. Detection and capture Nb concentrations ranging from 0.8-0 µg mL^{-1} and 0.2-0 µg mL^{-1}, respectively (dilution factor 2), were analysed. Each of the obtained curves corresponds to different capture Nb concentrations (purple, green, red and blue colors from highest to lowest capture Nb concentrations). Each calibration point was measured in triplicates on the same ELISA plate and the results show the average and standard deviation of the assay carried out on 1 day.*

Table A 1 *Analytical parameters of the CIF ELISA for Cif detection on assay buffer. Immunoreagents concentrations were: streptavidine at 10 µg mL^{-1}, V_{HH}108-biotin and V_{HH}219-HA at 0.1 µg mL^{-1} and antiHA secondary Ab at 1/3000 dilution. The data shown correspond to the average and standard deviation of the parameters of the calibration curves performed 3 different days using at least 3 well replicates per concentration (8 different concentrations).*

	PBST
A_{min}	0.05 ± 0.01
A_{max}	1.28 ± 0.07
Slope	1.04 ± 0.17
IC_{50}/ ng mL^{-1}	2.15 ± 0.42
Dynamic range/ ng mL^{-1}	0.61 ± 0.19 and 12.28 ± 6.62
LoD/ ng mL^{-1}	0.28 ± 0.11
R^2	0.99 ± 0.01

A.2.2 Implementation of CIF ELISA for the analysis of bacterial isolates

A.2.2.1 Matrix effect studies

Bacterial isolates from patients infected with *P. aeruginosa* required matrix effect studies since they were grown in Müeller Hinton (MH) medium. Therefore, with the aim of assessing if the medium interfered unspecifically with the performance of the ELISA, Cif standards were prepared in different dilutions of MH in PBS buffer (1/5, 1/10 and 1/20 dilutions).

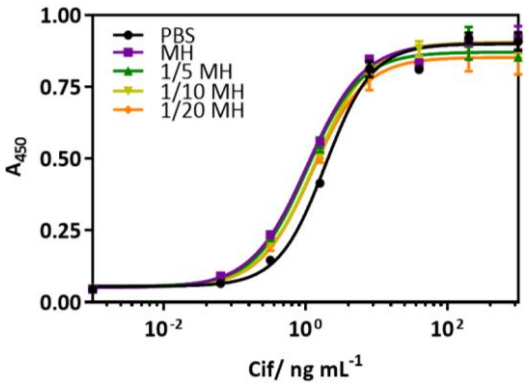

Figure A 6 *Matrix effect studies of the MH broth undiluted and diluted 5, 10 and 20 times with PBS buffer on the performance of CIF ELISA (see Table A 2). Each calibration point was measured in triplicates on the same ELISA plate and the results show the average and standard deviation of the assay carried out on 1 day.*

Table A 2 *Analytical parameters of the CIF ELISA for CIF detection on assay buffer and undiluted and diluted MH media. Immunoreagents concentrations were: streptavidine at 10 µg mL^{-1} and capture and detection Nb at 0.1 µg mL^{-1}. The data shown correspond to the average and standard deviation of the parameters of the calibration curves performed 3 different days using at least 3 well replicates per concentration.*

	PBS	MH	1/5 MH	1/10 MH	1/20 MH
A_{max}	0.90	0.90	0.87	0.91	0.85
A_{min}	0.06	0.05	0.06	0.05	0.05
Slope	1.31	1.10	1.17	1.14	1.18
Dynamic range/ ng mL^{-1}	0.65 to 6.35	0.30 to 4.17	0.33 to 4.01	0.39 to 4.66	0.37 to 4.07
IC_{50} / ng mL^{-1}	1.91	1.06	1.06	1.34	1.24
LoD/ ng mL^{-1}	0.33	0.14	0.16	0.18	0.18
R^2	0.99	0.99	0.99	1.00	0.99

As shown in Figure A 6, all CIF ELISA calibration curves obtained were similar at any MH dilution in PBS meaning there was no matrix effect. Furthermore, the analytical parameters of the diferent assays did not vary signficantly (see Table A 2). Therefore, since the expected Cif levels were low and MH media did not produce any matrix effect, bacterial isolates from *P. aeruginosa* infected patients were directly measured without any previous dilution.

A.2.3 Cif release profile of *P. aeruginosa* bacterial isolates

To determine the pattern of Cif production kinetics of *P. aeruginosa* isolates obtained from acute and chronic infections, bacterial isolates were grown on MH media as previously described for PYO detection in Chapter 5. Thus, bacterial isolates frozen stocks were inoculated onto blood agar plates ON and, after this time, a pre-culture with the ON grown colonies was prepared. When this pre-culture reached the desire turbidity, an aliquot was taken and diluted in MH media (final culture). Then, bacterial isolate culture aliquots were taken at different time points and analysed using CIF ELISA. Simultaneously, PYO was determined by PYO mAb122/PC1-BSA ELISA and used as a control to ensure a correct performance of the assay since PYO profiling was already studied (see Chapter 5). Therefore, a bacterial isolate from a patient with acute *P. aeruginosa* infection and another with a chronic infection were selected to investigate the kinetic release of Cif.

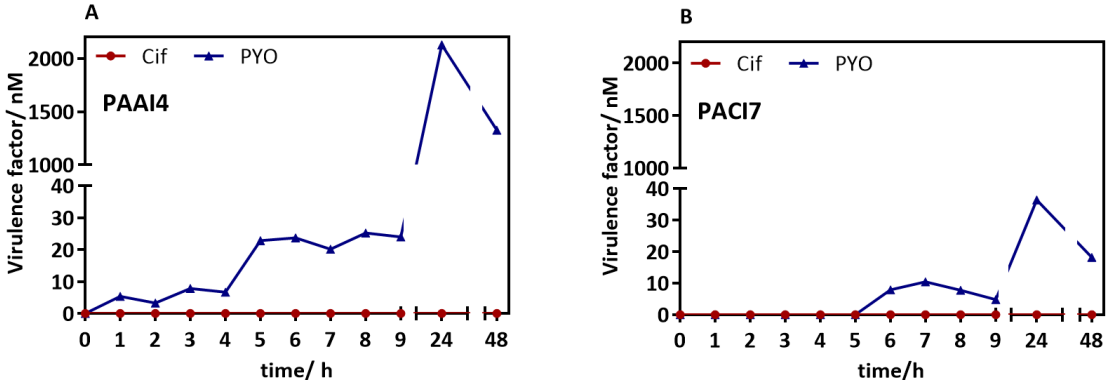

Figure A 7 *Cif and PYO kinetics production of two P. aeruginosa isolates grown for 48 h at 37ºC. The red and blue lines indicate Cif and PYO production, respectively. (A) Corresponds to the results obtained from an isolate of a patient undergoing an acute P. aeruginosa infection (PAAI4) and (B) from an isolate of a patient suffering chronic infection (PACI7).*

Figure A 7 shows the kinetic production of PYO and Cif obtained when analysing these two representative bacterial isolates (PAAI4 and PAACI7) from patients suffering an acute and a chronic *P. aeruginosa* infection, respectively. Unlike PYO mAb122/PC1-BSA ELISA, which allowed the measurement of PYO on the studied isolates, CIF ELISA did not allow the quantification of Cif molecule at any growing times. Since to our knowledge there are not previously reported Cif values on bacterial nor clinical samples from patients infected with *P. aeruginosa*, it could not be concluded whether the obtained results were because Cif levels were below the LoD of the ELISA or because Cif expression was not activated until *P. aeruginosa* interacts with the host cell.

Nevertheless, with the aim of confirming the obtained results, other 7 bacterial isolates from patients infected with *P. aeruginosa* were analysed using CIF ELISA. From these isolates, 6 corresponded to CF patients as, theorically, Cif expression is upregulated among these patients[7].

Table A 3 *IRequivPYO and Cif concentrations measured in bacterial isolates from patients infected with P. aeruginosa using PYO mAb122/PC1-BSA ELISA and CIF ELISA, respectively. Bacterial isolates were grown for 16 h in MH media. The data shown was measured in triplicates on the same ELISA plate and the results sho the average and standard deviation of the assay carried out on 1 day. PAAI =P. aeruginosa acute isolate; PACI =P. aeruginosa chronic isolate; <LoD =below limit of detection.*

Bacterial isolates	Cif/ nM	IRequivPYO/ nM
PACI12	<LoD	4.91 ±0.64
PAAI15	<LoD	8235.99 ±993.75
PACI5 (CF)	<LoD	8.71 ±3.54
PACI7 (CF)	<LoD	9.93 ±1.40
PACI14 (CF)	<LoD	3.73 ±0.76
PACI8 (CF)	<LoD	15.60 ±1.62
PACI16 (CF)	<LoD	0.96 ±0.33
PAO1	<LoD	3535.12 ±618.45

Table A 3 shows Cif and IRequivPYO levels found in the 7 bacterial isolates grown for 16 h (PAO1 strain as reference), based on previously obtained phenazine kinetics results. As expected, IRequivPYO concentrations were higher on isolates from patients with acute infection than in chronic ones. However, again, Cif concentrations were below the LoD of the used CIF ELISA.

In the light of the obtained results, gene expression experiments will be carried out to ensure that Cif is produced in these bacterial cultures. Thus, Cif production will be evaluated at a translational level by extracting the genetic material from the studied isolates. In the same vein, CIF ELISA will be also implemented to directly measure Cif in clinical samples, such as sputa, or, also, in a co-culture system.

A.3 Materials & Methods

A.3.1 Reagents

All the used reagents are explained in Material & Methods of Chapter 4 and 5.

A.3.2 Immunochemistry

The Nbs were obtained immunizing an alpaca with Cif protein (200 mg per injection) in complete Freund's adjuvant and boosted 4 times with the same dose in incomplete Freund's adjuvant. Blood was collected every two weeks to assess the antibody titer. Then, the mRNA was extracted and transcribed to cDNA which was used as template for PCR amplification of the VHH genes. Besides, a VHH phage-display library was created and screened to select the most specific Cif

clones. These clones were expressed and purified and their activity validated by ELISA. More information regarding Nbs production is described by Vasylieva et al.[1]. The here used Nbs were V_{HH}108-biotin as capture Nb and V_{HH}219-HA as detection Nb.

A.3.3 Clinical isolates samples

8 bacterial isolates collected at the Microbiology Department of the Vall d'Hebron University Hospital (VHUH, Barcelona, Spain) from patients diagnosed with *P. aeruginosa* acute or chronic infections were tested(see Table 5. 4 in Chapter 5). Perfectly isolated colonies from respiratory samples primary cultures were selected and stored frozen in glycerol at -20 ºC until used. PAO1 strain (ATCC 15692) was used as reference strain.

A.3.4 Bacterial isolates analysis

A.3.4.1 Bacterial isolates growth medium and inoculum preparation

Bacterial isolates frozen stocks were inoculated onto blood agar plates ON at 37 ºC and, after this time, a pre-culture with the ON grown colonies was prepared. Once turbidity reached an optical density (OD) at 600 nm value between 0.2-0.3, a sample aliquot was taken and diluted 1000 times in MH media. Then, bacterial isolate culture aliquots were taken at different time points and analysed using CIF ELISA. The procedures followed for these purposes are explained in detail in Chapter 5.

A.3.4.2 Cif and PYO production kinetics

Collected bacterial time point aliquots were centrifuged (500 g, 5 min) for PYO and Cif measures, which were performed carrying out PYO mAb122/PC1-BSA ELISA and CIF ELISA, respectively. To obtain correct measures, and according to the matrix effect studies, the resulting supernatants were diluted 20 times in assay buffer for PYO quantification and directly measured in the case of Cif.

A.3.5 CIF ELISA

The here explained protocol is based on Vasylieva et al.[1] but with some modifications, resulting from the optimization of the assay that have been carried out in our lab. Thus, for Cif detection, microtiter plates were coated with streptavidin (10 µg mL^{-1} in PBS 100 µL $well^{-1}$) and incubated for 1 h in agitation (600 rpm, RT). Then, a solution of 1 % w/v BSA in PBST was added to the plate (200 µL $well^{-1}$) and it was incubated ON at 4 ºC. Next day, plates were washed with PBST (4 × 300 µL). All the washing between ELISA steps were carried out the same way. Once washed, the

capture Nb solution (V_{HH}108-biotin; 0.1 µg mL^{-1} in PBS, 100 µL $well^{-1}$) was added and incubated for 30 min at RT. The next step consisted on the addition of serial dilutions of Cif (a total of 8 dilutions from 1000 nM to 0 nM in PBS using a dilution factor of 2) or the samples, diluted with the assay buffer (100 µL $well^{-1}$), waiting an additional 30 min incubation time lapse. Subsequently, the solution of detection Nb was added (V_{HH}219-HA; 0.1 µg mL^{-1} in PBS, 100 µL $well^{-1}$) and left other 30 min. Then, the anti-HA solution (1/3000 in PBST, 100 µL $well^{-1}$) was added and, after waiting an additional 30 min, the addition of the substrate solution (100 µL $well^{-1}$) was carried out. Finally, the enzymatic reaction was stopped after 30 min at RT by adding 2 M H_2SO_4 (50 µL $well^{-1}$). The absorbances were measured at 450 nm.

A.3.6 Implementation of CIF ELISA to the analysis of bacterial isolates

A.3.6.1 Matrix effect study

Nonspecific interferences produced by bacterial isolates medium were analysed by preparing standard curves of CIF in undiluted and diluted MH broth in PBST (1/5, 1/10 and 1/20 dilutions), and measuring them with CIF ELISA to assess the parallelism in respect to the calibration curve prepared in the assay buffer. The matrix dilution producing the most similar ELISA parameters compared with the one obtained for the assay performed in assay buffer (IC_{50}, slope and maximal absorbance) was selected.

A.4 Concluding remarks

- The direct detection of Cif molecule in bacterial isolates from *P. aeruginosa* infected patients has been intended by using a previously developed CIF ELISA[1]. With this purpose, the ELISA protocol has been first optimized to reduce the duration of the assay and to lower the LoD of the same. Besides, matrix effect studies have been performed indicating the possibility of directly measuring Cif in culture broth (LoD of around 1 ng mL^{-1}).
- The kinetics release of Cif in bacterial isolates from patients infected with acute and chronic infections has been investigated as previously done for PYO. In all the cases, the levels found were below the LoD of the assay. This fact was confirmed by analysing 7 more bacterial isolates and obtaining the same results. In consequence, other alternatives to measure Cif need to be studied. Simultaneously, PYO was measured and used as control. Again, PYO levels were higher in bacterial isolates with acute infections and lower in bacterial isolates with chronic infections.

A.5 References

1. Vasylieva, N.; Kitamura, S.; Dong, J.; Barnych, B.; Hvorecny, K. L.; Madden, D. R.; Gee, S. J.; Wolan, D. W.; Morisseau, C.; Hammock, B. D., Nanobody-based binding assay for the discovery of potent inhibitors of CFTR inhibitory factor (Cif). *Anal Chim Acta* **2019,** *1057*, 106-113.
2. Bomberger, J. M.; Ye, S.; Maceachran, D. P.; Koeppen, K.; Barnaby, R. L.; O'Toole, G. A.; Stanton, B. A., A Pseudomonas aeruginosa toxin that hijacks the host ubiquitin proteolytic system. *PLoS Pathog* **2011,** *7* (3), e1001325.
3. Bahl, C. D.; Morisseau, C.; Bomberger, J. M.; Stanton, B. A.; Hammock, B. D.; O'Toole, G. A.; Madden, D. R., Crystal structure of the cystic fibrosis transmembrane conductance regulator inhibitory factor Cif reveals novel active-site features of an epoxide hydrolase virulence factor. *J Bacteriol* **2010,** *192* (7), 1785-95.
4. Trinh, N. T.; Bilodeau, C.; Maille, E.; Ruffin, M.; Quintal, M. C.; Desrosiers, M. Y.; Rousseau, S.; Brochiero, E., Deleterious impact of Pseudomonas aeruginosa on cystic fibrosis transmembrane conductance regulator function and rescue in airway epithelial cells. *Eur Respir J* **2015,** *45* (6), 1590-602.
5. Kumar, S.; Tana, A.; Shankar, A., Cystic fibrosis--what are the prospects for a cure? *Eur J Intern Med* **2014,** *25* (9), 803-7.
6. Bomberger, J. M.; Ely, K. H.; Bangia, N.; Ye, S.; Green, K. A.; Green, W. R.; Enelow, R. I.; Stanton, B. A., Pseudomonas aeruginosa Cif protein enhances the ubiquitination and proteasomal degradation of the transporter associated with antigen processing (TAP) and reduces major histocompatibility complex (MHC) class I antigen presentation. *J Biol Chem* **2014,** *289* (1), 152-62.
7. MacEachran, D. P.; Ye, S.; Bomberger, J. M.; Hogan, D. A.; Swiatecka-Urban, A.; Stanton, B. A.; O'Toole, G. A., The Pseudomonas aeruginosa secreted protein PA2934 decreases apical membrane expression of the cystic fibrosis transmembrane conductance regulator. *Infect Immun* **2007,** *75* (8), 3902-12.
8. Swiatecka-Urban, A.; Moreau-Marquis, S.; Maceachran, D. P.; Connolly, J. P.; Stanton, C. R.; Su, J. R.; Barnaby, R.; O'Toole G, A.; Stanton, B. A., Pseudomonas aeruginosa inhibits endocytic recycling of CFTR in polarized human airway epithelial cells. *Am J Physiol Cell Physiol* **2006,** *290* (3), C862-72.
9. Beghein, E.; Gettemans, J., Nanobody Technology: A Versatile Toolkit for Microscopic Imaging, Protein-Protein Interaction Analysis, and Protein Function Exploration. *Front Immunol* **2017,** *8*, 771.
10. Muyldermans, S., Nanobodies: natural single-domain antibodies. *Annu Rev Biochem* **2013,** *82*, 775-97.
11. Jovcevska, I.; Muyldermans, S., The Therapeutic Potential of Nanobodies. *BioDrugs* **2020,** *34* (1), 11-26.
12. Bever, C. S.; Dong, J. X.; Vasylieva, N.; Barnych, B.; Cui, Y.; Xu, Z. L.; Hammock, B. D.; Gee, S. J., VHH antibodies: emerging reagents for the analysis of environmental chemicals. *Anal Bioanal Chem* **2016,** *408* (22), 5985-6002.
13. Salvador, J. P.; Vilaplana, L.; Marco, M. P., Nanobody: outstanding features for diagnostic and therapeutic applications. *Anal Bioanal Chem* **2019,** *411* (9), 1703-1713.